GEOLOGY AND GEOCHEMICAL INVESTIGATION OF THE PART OF USHIRI VALLEY, DISTRICT DIR, NORTHERN PAKISTAN

Thesis Submitted to The National Centre of Excellence in Geology
University of Peshawar in Partial Fulfilment of the Requirments for the
Degree of MASTER OF PHILOSOPHY

BY

IHTESHAMUL HAQ

NATIONAL CENTRE OF EXCELLENCE IN GEOLOGY

UNIVERSITY OF PESHAWAR

1999

بسم الله الرحمن الرحيم

IN THE NAME OF

ALLAH

THE MOST BENEFICENT
THE MOST MERCIFUL

AND HE IS ALONE THE HELPER

APPROVED BY

(Supervisor)
Dr. M. Tahir Shah
Associate Professor
NCE in Geology,
University of Peshawar

(External Examinar)
Dr. M. Rafiq
Professor
Geology Department,
University of Peshawar

(External Examinar)
Tariq Mahboob Khan
Principal Geologist
Atomic Energy Commission,
Issa Khel, Mian Wali

(Director)
NCE in Geology,
University of Peshawar

CONTENTS

CHAPTER - 8

LIST OF FIGURES

LIST OF TABLES

LIST OF PLATES

Acknowledgment

I am really indepted to my supervisor Dr. M. Tahir Shah, Associate Professor, NCE in Geology, University of Peshawar, whose supervison,guidance and continued support through out my research work, made it possible to achieve this goal.

I am also pleased to acknowledge the Director, NCE in Geology, University of Peshawar, for providing the financial support for the field work and laboratory facilities. Without his support it would not be possible for me to complete this research work.

My sincere thanks go to S.Hasan Gauhar, Director General; Arbab M. Sabir Hayat Deputy Director General and Rab Nawaz Khan, Director, Geological Survey of Pakistan, whose guidance and encouragement help me to enroll for the M.Phil. Degree Course.

I am extremely thankful to Dr. Muhammad Rafiq, Professor, Geology Department, University of Peahawar and Mr. Tariq Mahboob Khan, Principal Geologist, Pakistan Atomic Energy Commission, who have evaluated my thesis as external examiners. Their valuable suggestions made my thesis much improved.

I am very thankful to Ms. Shahina Zeb, Haleem, Amanullah Laghari, Aftab Gul and S. Faisal, M.Phil/ Ph.D scholars of NCE in Geology, University of Peshawar, for their nice company and cooperation during the completion of my thesis work.

Miss. Faridoon Sahar and Riaz Ahmed Durani, are also thanked for the partial drafting of this manscript and drafting of the geological figures respectively.

ABSTRACT

The study area is lying in the north-western portion of the Kohistan arc terrane. This terrane is bounded by two suture zones of regional extent at its northern and southern sides, believed to be formed by obliteration of ancient oceanic basin.The Kohistan arc consists of a series of east-west trending geological units, which are:

1) Jijal Ultramafic Complex, 2) Kamila Amphibolite, 3) Chilas Complex, 4) Chalt Volcanic Group, 5) Yasin Group and 6) Kohistan Batholith. This arc experienced its first collision at its northern margin with the Karakorum plate at 90-80 Ma, and its second collision at the sourthern margin during Early Eocene with the Indian plate.

Rocks of the area are distinguished into two main lithological units:
(1) Amphibolites and (2) Metadiorites/ Metagranodiorites. The amphibolites occupy the southern part of the studied area while metadiorite/ granodiorites are exposed in the northern part of the area. Both these rock units have intrusive contact and exhibit local faulting and shearing. The amphibolites also host small patches of gabbro-norites which are less metamorphosed. The amphibolites are generally massive but also exhibit banding at places. These amphibolites are intruded by quartz and quarrtzo-feldspathic veins espacially in areas where the shearing and faulting are intense. The amphibolites are also intruded by the metadiorite/granodiorite in the form of small plugs. The metadiorites/granodiorites are medium to coarse-grained, massive in character and have xenoliths of amphibolites. Copper mineralization in the form of dissiminated grains of tetrahydrite and chalcopyrite and supergene enrichment in the form of melachite and azurite occur within quartz veins in limited areas.

Petrographically the amphibolites are mainly composed of hornblende and plagioclase with subordinate amount of quartz and alkali feldspar. Biotite, muscovite, chlorite, epidote, apatite, sphene, rutile, calcite and opaque occur as accessories. The metagabbro-norites contain plagioclase, orthopyroxene and clinopyroxene as the dominant

mineral constituents. Quartz, sphene, apatite, chlorite, epidote and opaque are present as minor constituents. The metadiorite, quartz-diorite and metagranodiorite are dominantly composed of plagioclase with variable proportion of quartz and alkali feldspar. The other minor constituents include biotite, hornblende, muscovite, apatite, sphene, zircon, garnet and opaque.

Chemically the amphibolites and metagabbro-norites are comagmatic. Their chemical characteristics favour the igneous parentage (i.e.., host gabbro-norite) for the studied amphibolites. Both the amphibolites and gabbro-norites could be related to either Kamila amphibolites belt or Chilas Complex. The major and trace elements study of these rocks suggests that these are of calc-alkaline nature and are formed by the arc magma within the subduction related environment. The chemical characteristics of the granitoid rocks (metadiorite/granodiorite) suggest that these are comagmatic and have close affinity towards the calc-alkaline rocks, developed in island arc type of set up.

The mineralogical and geochemical studies of the stream sediments (both pan concentrate and -80 mesh) suggest that the area has no anomalous zone of base and precious metals which could be attributed to the specific mineralization in the area.

CHAPTER-1

INTRODUCTION

Location and Accessibility

The thesis area is covered by the Survey of Pakistan toposheet No.43-A\4 and is bounded by latitude 35° 8' to 35° 13' north and longitude 72° 6' to 72° 14' east. It lies in the central part of Dir District and is generally known as Ushiri valley. Umrale Khwar is the main stream flowing in the area from east to westwards and falling in the Panjkora river near Darora. The area is linked with Peshawar and Islamabad by a metalled road through the main pass of Malakand. The approach to the area is then made by the side road from main Dir-Chitral road near Darora.

Topography and Drainage

The area of study has moderate to high relief. The north-eastern, south-eastern and central part of the area has high relief where steep V-shaped valleys are formed. The north-western and south-western part, however, has moderate relief and, therefore, has little gentler valleys. The highest elevation is the Gorkoyoe Sar having a height of 11778 feet above sea level. The lowest part of the area is Jabai having an elevation of 4136 feet above sea level in the western part of the area. The area generally drains into the Umrale Khwar. Drainage is generally dendritic having a fine texture where most of the streams join each other at acute angle. Radial drainage pattern has also been present around high altitudes.

Vegetation

Vegetation comprises of pines, deodar, scrub, small to medium sized trees. Pines are generally covering the hills tops. The lower slopes are cleaned of bushes for making agriculture fields and fruit trees like walnut, mulberry, pear, apricot etc. are grown in the area. Walnut and pear are the main source of income of the people. The main crops of the area are maize, rice and barley. Poppies are still grown in certain places for illegal extraction of opium.

Climate

Climate of the area is marked by very cold winters and mild summers i.e. sub tropical in nature. The coldest months are December to February during which the temperature in certain localities fall to freezing point. The highest peaks and localities are generally covered with snow during the months of December to February every year. The area receives about 30 inches of rain, mainly in winters. Summers receive comparatively little rain.

Scope and Purpose of Investigation

The area of study is present within the Kohistan arc terrain and consists of a series of east-west trending geological units associated with two phases of post collisional plutonism (Zeitler, 1985; Treloar et al., 1989). Such type of magamatism demonstrates the existence of various types of mineral deposits, especially epithermal gold, porphyry type copper and volcanogenic massive sulfide (VMS) deposits (Agar, 1981; Coveney, 1981; Sillitoe, 1981, 1982; Franklin et al., 1981; Cox and Singer, 1986; Sawkins, 1990). The

existence of hydrothermal copper mineralization in Dir area (Shah 1991; Shah et al., 1997) indicates that the area has the capability to produce base and precious metal deposits. In view of the above mentioned facts the regional scale preliminary geochemical exploration in Dir area is necessary. The present study is a part of this senerio.

No detail geological and geochemical work has been carried out in the area of study. In order to achieve the above mentioned goals, the area needs to be properly investigated. For this purpose the following aims and objectives are proposed for the present study.

- To prepare the geological map of the area.
- To collect rocks and stream sediments (both pan concentrates and fine tractions) samples.
- To carry out petrographic studies of various rocks.
- To analyse various types of rocks for major and trace elements and to see their geochemical behaviour and tectonic studies.
- To prepare geochemical map of the area on the basis of stream sediment studies.
- To pin point zones of economic importance (if any) for further detail work.

Previous Work

Hyden (1915) has carried out preliminary geological work in district Dir which is the land mark for the subsequent geological work. Ahmad (1962), Khan and Saleemi (1972) and Arbab and Khan (1973) have carried out preliminary geological work in Barwa quadrangle, Kotegram and Akhagram quadrangle and Timargara quadrangle respectively of district Dir. They have also reported uneconomical copper mineralization in Barwa, Kambat and Ushiri areas. Corundum- bearing and related rocks arround Timargara have also been reported by Jan et al. (1969). Kakar et al. (1971) has prepared a geological map of the Jandul valley (area south-west of the thesis area) and also described in detail the geology of the area. Geology of Timargara and surrounding areas (areas south of the thesis area) of Dir district has been described by Chaudhary et al. (1974), Butt et al. (1980), Jan et al. (1983), Jan and Tahirkheli (1990), Shah, et al. (in press). Shah and Sarwar (in press) has also carried out stream sediments geochemical survey in Timargara and Jandul valley (Shah & Sarwar, 1998).

Dir and surrounding areas further north of the thesis area has been geologically investigated in detail by Tahirkheli (1979; 1982), Hamidullah et al. (1990), Shah and Hamidullah (1993), Shah et al. (1994) and Sullivan et al. (1993).

CHAPTER-2

REGIONAL GEOLOGY AND TECTONICS

There are three mountain chains in northern Pakistan which are named as Hindu Kush, Karakoram and Himalayas. The Kohistan arc occupies a transitional geographic position at the junction of these three mountain chains (Fig. 2.1). It has geological characteristics distinct from Hindukush, Karakoram and Himalaya and is, therefore, considered as a separate geographic and geologic domain.

The Himalayas and associated mountain ranges are formed as a result of collision (Himalayan orogeny) of Eurasian plate with a series of other continental plates separated from Gondwana. The Himalayan collision, in the NW Himalaya, was preceded by accretion of an intraoceanic island arc (i.e., the Kohistan arc terrane) at the southern margin of the Karakoram plate during Early Cretaceous (i.e, 100-80 ma) (Tahirkheli, 1983; Coward et al., 1986; Petterson and Windley, 1985). Himalayan orogeny started about 65 Ma ago when there was an initial contact of Indian plate with the southern margin of the Eurasian plate (KlootWijk et al., 1992). Nanga Parbat and the Kaghan regions of the Indian plate were the first to have collided with the Kohistan arc terrane about 60-65 Ma. The Himalayan collision is considered to have occurred during a wide spane of time (~20 Ma) and was not a short-lived event (Andrews & Speed, 1982; Albertsm & Degnan, 1993; Sullivan et al., 1993).

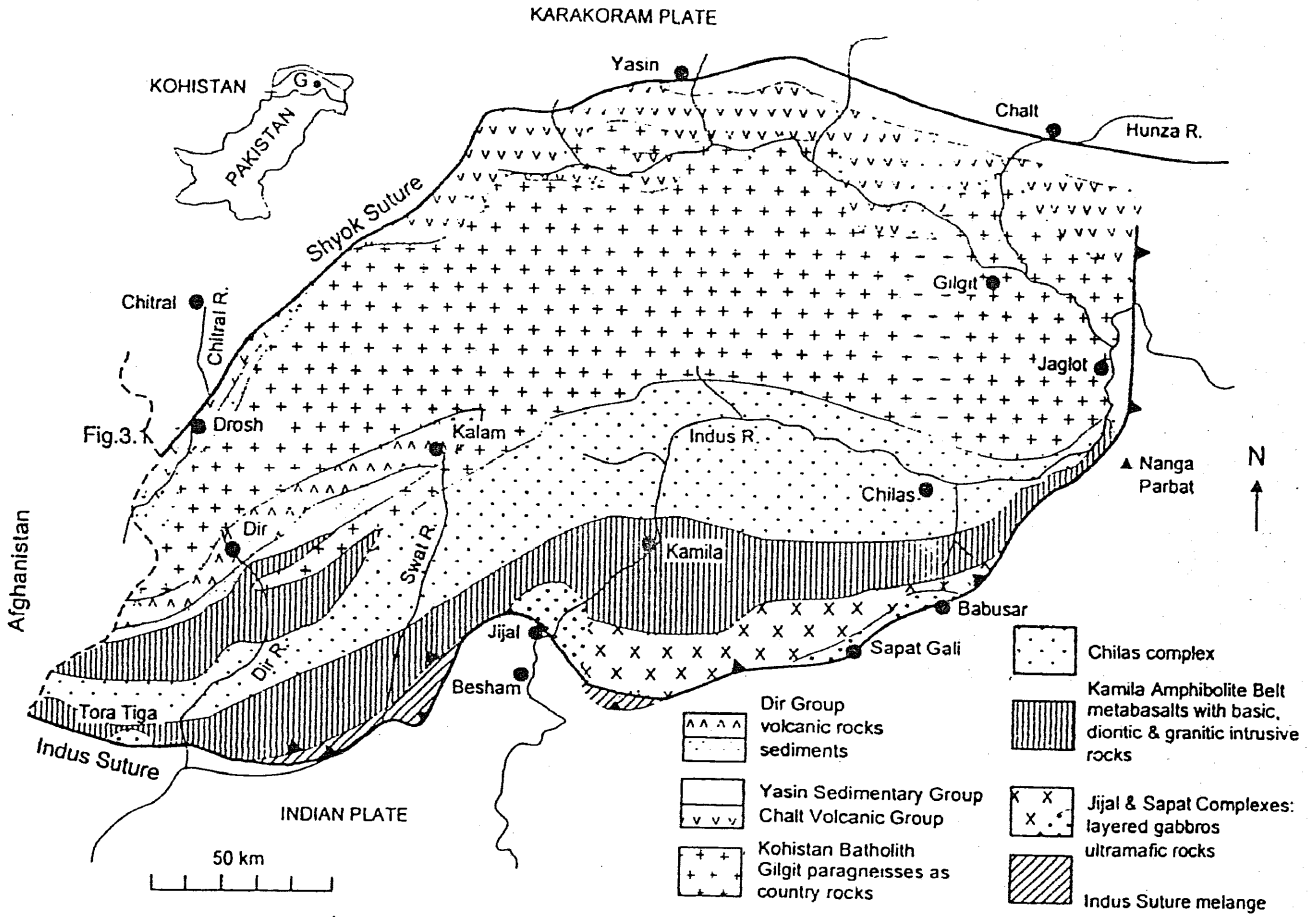

Fig.2.1. Regional geological map of Northern Pakistan, showing the location of the studied area.

The study area is lying within the north-western portion of the Kohistan arc terrane. Therefore, more detailed account of the regional geology and tectonics of the Kohistan arc terrane is discussed as follows:

KOHISTAN ARC TERRANE

The Kohistan arc terrane occupies the collision zone between the collided India and Karakoram plates (Fig. 2.1). It covers an area of about 36000sq.km in northern Pakistan. The Kohistan arc is a result of the Kohistan-Ladakh island arc and developed as a part of the northward subduction of Neotethyan oceanic lithosphere during Late Jurassic to Cretaceous times (Honegar et al, 1982; Tahirkheli and Jan 1979). The Kohistan arc is separated from the Ladakh arc by Nanga Parbat Haramosh dome formed only during the last 10 Ma (Zeitler et al., 1985). The Ladakh arc terrane to the east has remarkable lithological and geochemical resemblance with the Kohistan arc terrane suggesting their mutual continuity in the geological part. The Kohistan arc is separated from the Karakoram Plate in the north by Main-Karakoram Thrust (MKT), from Indian Plate in the south by Main Mantle Thrust (MMT) and from the Nanga Parbat massif in the east by the Raikot fault.

The MKT (also known as the northern suture; Pudsey, 1986 or Shyok suture; Searle, 1991) is about 4 km thick melange zone-comprising meter to hectometer scale blocks of limestone, marble, conglomerate, serpentinized metavolcanics and ultramafics set in a matrix of slates. MMT marks the subduction of Indian plate underneath the Kohistan arc terrane. The existence of major ophiolite (Arif and Jan, 1993) and glaucophane schists (Shams, 1980) suggest closure at the site of subduction zone in a major oceanic basin. It has sharp bend at the Jijal, where the ultramafics of the Kohistan terrane

are in direct contact with the gneisses of the Indian plate. Elsewhere, like in Mingora (Kazmi et al., 1984) and Allai (Shah and Majid, 1985), the MMT is represented by several hundreds of meters wide melange zone consists of ophiolite, ultramafics and gabbroic rocks, greenschists metavolcanics and glaucophane bearing pelitic melanges.

THE JIJAL COMPLEX: The Jijal complex is a tectonic wedge of ultramafic- mafic plutonic body in the north of MMT. It covers about 150 sq km area along the Indus river (Jan and Howie, 1981; Millar et. al., 1991). The Jijal complex is divided into 4 km thick lower part of layered ultramafics (i.e., diopsidites, harzburgites, dunites and websterites and about 7 km thick upper part of Garnet granulite. The Jijal ultramafic rocks have been derived from tholleiitic-basaltic magma in a magmatic chamber at the base of an intraoceanic island arc (Jan & Windley, 1990).

SPAT ULTRAMAFIC-MAFIC COMPLEX: Ultramafic and associated gabbroic rocks in the hanging wall of the MMT from Shergarh Sar (Shah & Majid, 1992), Babusar (Ahmad & Chaudhry; 1976) and Tora Tiga (Jan et al., 1983) are continuation of Spat complex.

This complex mainly comprises of stratiform ultramafic and gabbroic rocks in the Sapatgali area of Kaghan Kohistan (Jan et al., 1993). These rocks are metamorphosed from epidot-amphibolite to greenschist facies and lack garnet.

THE KAMILA AMPHIBOLITE BELT: This rock sequence occupy a considerable portion of the southern Kohistan arc and has the direct contact with the MMT in the eastern and western part of the Kohistan terrane. Kamila amphibolites included banded and homogeneous amphibolites,

hornblendites and hornblende schists, calc-silicates and quartzo-feldspathic intrusion (Jan, 1979; Jan, 1988; Shah et al., 1994). Two types of amphibolites are predominantly fine grained and medium-to-coarse grained (Khan et al., 1993). In the north the amphibolite belt is either undeformed or cut by narrow amphibolitic shear zone. The southern part of the amphibolite belt is marked by variably sheared rocks of the Kamila shear zone. The fine-grained amphibolites are metavolcanic in origin while the medium to coarse grained amphibolites are gabbroic in origin (Khan et al., 1993).

THE CHILAS COMPLEX: Chilas complex is a massive calc-alkaline gabbro-norite body which occasionally has spectacular igneous layering (Jan et al., 1984; Khan et al 1989). The complex is about 50 Km wide and is trending 300 km in east-west direction. It has southern contact with highly deformed metavolcanics and gabbros of the Kamila amphibolite and in the north with the schistose metavolcanics. It represents a higher level intrusion into the Kamila amphibolite belt and comprises ultramafics, anorthosites and gabbro-norites/hypersthene diorites. The intrusion has a typical calc-alkaline geochemistry (Khan et al., 1993).

THE KOHISTAN BATHOLITH: In the northern part of Kohistan terrane, a major belt of granitic rocks was identified by Tahirkheli and Jan (1979) and Jan et al. (1981). This belt was later termed as Kohistan Batholith by Petterson and Windly (1985) and Coward et al (1986). it is mainly comprised of calc-alkaline gabbro, diorite, granodiorite, granite plutons which intrude a predominantly metasedimentary sequence in the south and Chalt volcanics in the north. Three phases; 102 Ma trondhjemites/quartz diorites, 85-45 Ma old gabbros, diroites and granites and 33-28 Ma old leucogranites and pegmatites have been recognized by Petterson and Windley, (1985).

THE CHALT VOLCANICS: The Chalt volcancis extend from Hunza valley in the east towards Chitral in the west (Thairkheli, 1979; Coward et al., 1982; 1986; Pudse 1986). On the basis of geochemistry and facies analysis, Petterson et al. (1990) subdivided these volcanics into the Hunza valley volcanics in the east and western volcanics in the west. These volcanics are subduction-related high-Mg tholleiitic andesites, boninites, calc-alkaline andesites and dacite-rhyolite, metamorphosed to green schists facies (Ivanac et al. 1956; Petterson and Windly, 1985; Petterson et al. 1990).

YASIN GROUP METASEDIMENTS: The name Yasin Group was assigned by Ivanac et al. (1956) to sediments intercalated with volcanic suit of lavas, tuff and agglomerate. Tahirkheli (1979; 1982) has divided this group into sedimentary part which he termed the Yasin group and the volcanic part named as Rakaposhi volcanic group. Detail study of the Yasin Group was carried out by Pudsey et al. (1985), Pudsey (1986); suggested that the detrital sediments of the Yasin Group are of deep water origin, probably deposited in the back or intra arc basin.

DIR GROUP: This group comprises the assemblages of volcanoclastic sediments in the lower part and upper part is basaltic-andesite flows, ignimbirites and pyroclastic in nature. This Group has been divided into Barawal Banda Slate Formation (lower part) and Utror Volcanic Formation (upper part). These Formations are trending NE-SW for more than 120 km and about 15-20 km wide. The Barawal Banda Slate Formation is composed of basal conglomerate and breccia; stratified and graded pebbly sandstone, siltstone and mudstone with occasional thin beds of fossiliferous limestone of Late Paleocene to Early Eocene age. The Barawal Banda Slate Formation was deposited as a marine fore-arc sequence following collapse of the continental margin (Sullivan et al. 1993). The Utror Formation comprises of

volcanic breccia in the lower part, lava flows in the middle part and pyroclastic flows and ignimbrite in the upper part. These rocks are composed of basalt, basaltic-andesite, dacite, rhyolite and tuff of calc-alkaline nature (Shah and Hamidullah, 1993; Shah et al. 1994; Sullivan et al. 1993).

CHAPTER-3

LOCAL GEOLOGY

The thesis area (covering 110 sq.kms) is a part of the Kohistan arc terrane and is located just north of the Main Mantle Thrust (MMT). Two main units a) amphibolite and b) metadiorite/metagranodiorite are widely exposed in the area (Fig. 3.1). The former occupy the southern while the later covers, the northern part of the area.

The amphibolite and metadiorite/metagranodiorite have intrusive contact. Small plugs of the later are present within the former in the south-western part of the area. At places, these amphibolites also enclose small patches of gabbro-norites. However, small bodies of amphibolites are also enclosed within the metadiorite/ metagranodiorite in the north-western portion of the study area (Fig.3.1).

AMPHIBOLITE

Amphibolite is widely exposed in the southern parts of the study area (Fig. 3.1). It is medium-to coarse-grained, massive (banded at places) and foliated rock with greenish-grey to green colour on fresh surface and brownish green on weather surface. Foliations are generally striking EW to NW and dipping gentally (30' to 60') towards north and north-east respectively.These rocks are intruded by the metadiorite/metagranodiorite and exhibit chilling effects at the intrusive contact. Along this contact the amphibolite is relatively fine-grained (hornfelsic) and has high concentration of hornblende. At places the aplite dikes (>1m thick and >3m long) are also noticed within these amphibolites. These rocks are also sheared and attained schistocity along the shear zones where the micro veins of epidote are

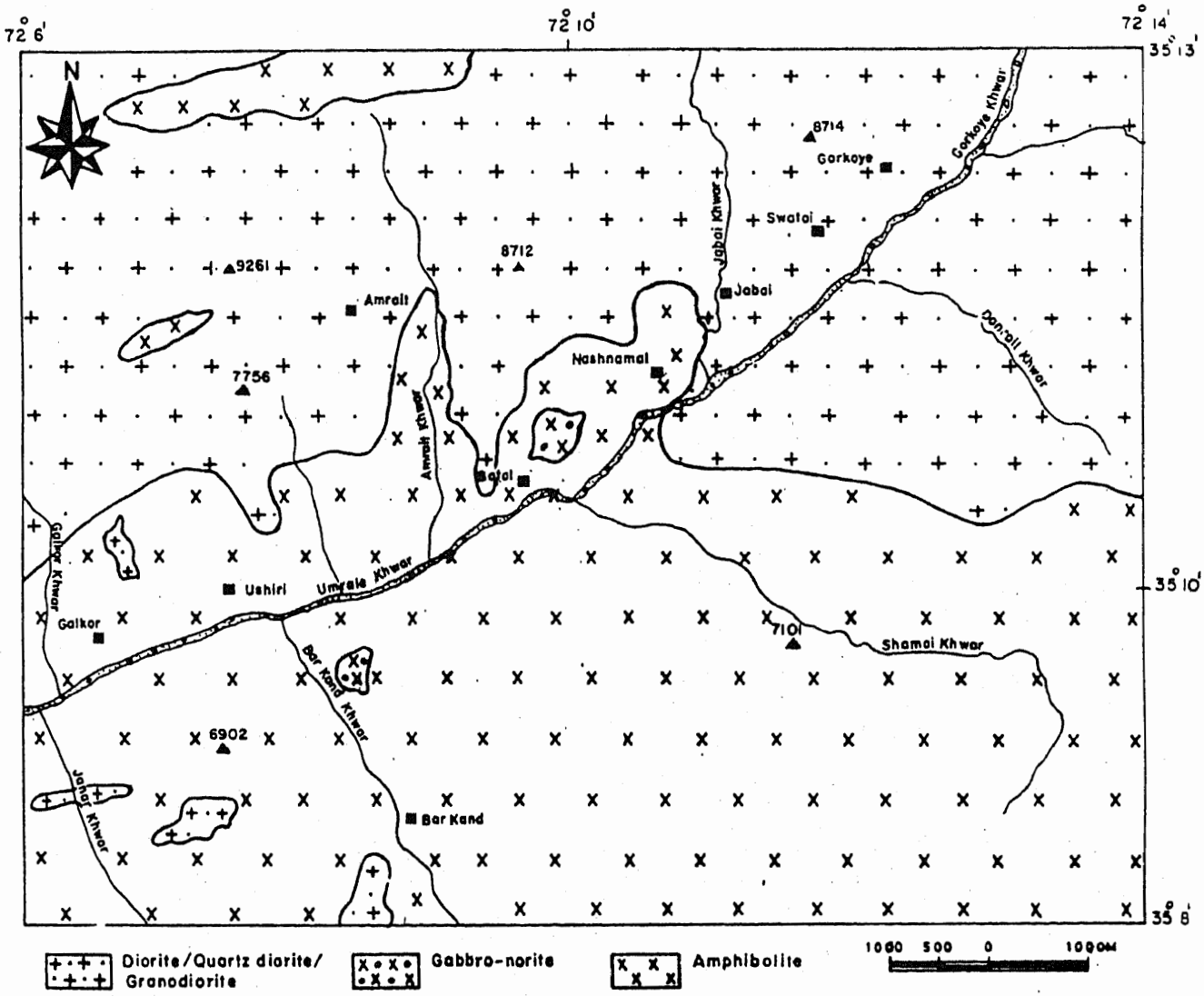

Fig. 3.1. GEOLOGICAL MAP OF USHIRI VALLEY, DISTRICT DIR N.W.F.P. PAKISTAN

prominant. Moderate to strong banding and microfolding is also common along these shear zones. Quartz and quartzo-feldspathic veining are the common features of these amphibolites (Plate 3.1). These viens at places form a net work. Quartz veins are generally barren but at few places the veins have copper mineralization in the form of tetrahedrite, chalcopyrite, malachite and azurite. The rock, whereever has mineralized quartz veins, is highly weathered and shows reddish brown weathered surface which appears as gossan.

Dark coloured patches, containing high concentration of hornblende (>95%), are present at many places within the amphibolites. These form coarse grained bodies of various shapes and sizes.

Amphibolites have variable proportion of plagioclase and hornblende. At places, where the plagioclase is in high concentration (>60%) there the amphibolites have greenish-grey colour and where the hornblende is in high concentration (>60%) there the amphibolites attained dark green colour. The banded amphibolites have alternate bands of light (having high amount of plagioclase) and green (having high hornblende) are observed. Bedded quartzite which is highly tectonized, having microfolds, is also exposed within this unit at various places. At places, small angular to subangular xenoliths of quartzite are also noticed within these amphibolites (Plate. 3.2).

These amphibolites and hosted gabbro-norites could be a part of either Southern (Kamila) amphibolite belt (Jan et al., 1979; 1988) or Chilas complex (Jan et al., 1984; Khan et al. 1989).

Plate. 3.1. Photograph showing the quartzo-feldspathic veining within the amphibolites which imparted banded appearance to the rock.

Plate. 3.2. Photograph showing angular to subangular xenoliths of quartzite within amphibolites.

METAGABBRO-NORITES

Metagabbro-norites occur as small size patches (some time unmapable) within the amphibolites at various places (Fig. 3.1). These are medium to coarse-grained, homogenous and less foliated rocks of dark grey to greenish grey colour on fresh surface and light brown to yellowish brown on weathered surface. Plagioclase, pyroxene and hornblende are easily distinguished in hand specimen. At some places, these rocks appear as homogeneous amphibolite as these have developed high concentration of amphibole due to regional metamorphism. It appears that these rocks were the protoliths of amphibolites which have suffered negligible or mild degree of metamorphism and have escaped the main phase of amphibolite facies regional metamorphism. These rocks retained primary texture and mineralogy and are, therefore, remnants of large bodies which have been completely transfered to amphibolite. At certain places, micro veins of quartz are common in these rocks.

METADIORITES, QUARTZ-DIORITES AND METAGRANDIORITES

These rocks have covered mainly the northern part of the study area (Fig. 3.1 Plate 3.3) and generally have intrusive contact with the amphibolites. These rocks also occur as small plugs within the amphibolites (Fig.3.1). These are medium to coarse grained massive rocks of greenish grey to dark-grey on fresh surface and brownish grey on weathered surface. These have angular joints,local faulting and fractuers(Plate 3.4) and exhibit moderate to weak foliation, generally trending north-east and south-west. These three rock types are not easily distinguished in the field. However, the metagranodiorites are more lighter in colour because of having higher contents of quartz and feldspar relative to that of metadiorite / quartz

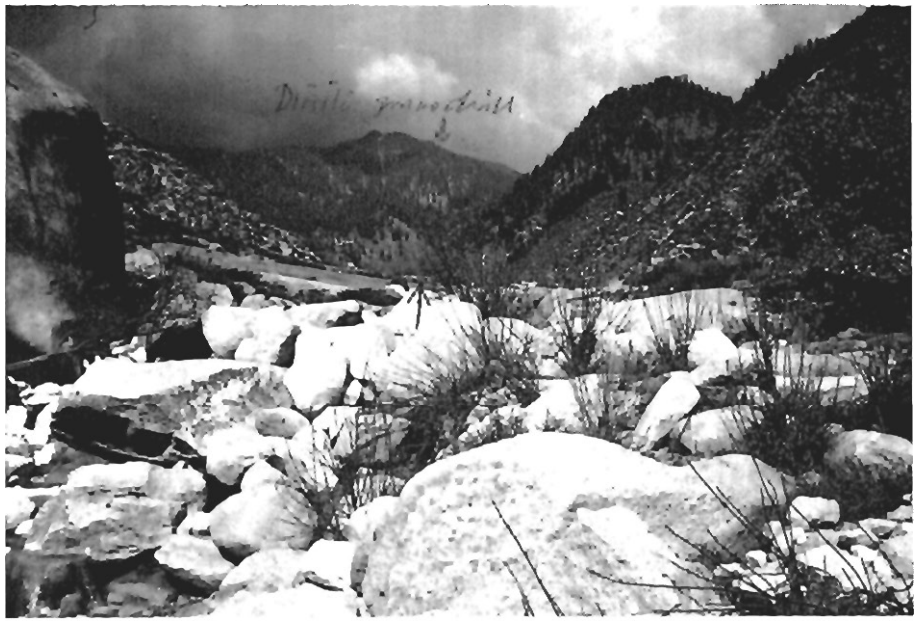

Plate. 3.3. Photograph showing the view of metadiorite/ granodiorite plutons exposed mainly in the northern part of the study area. The view is from the Gorkoye stream.

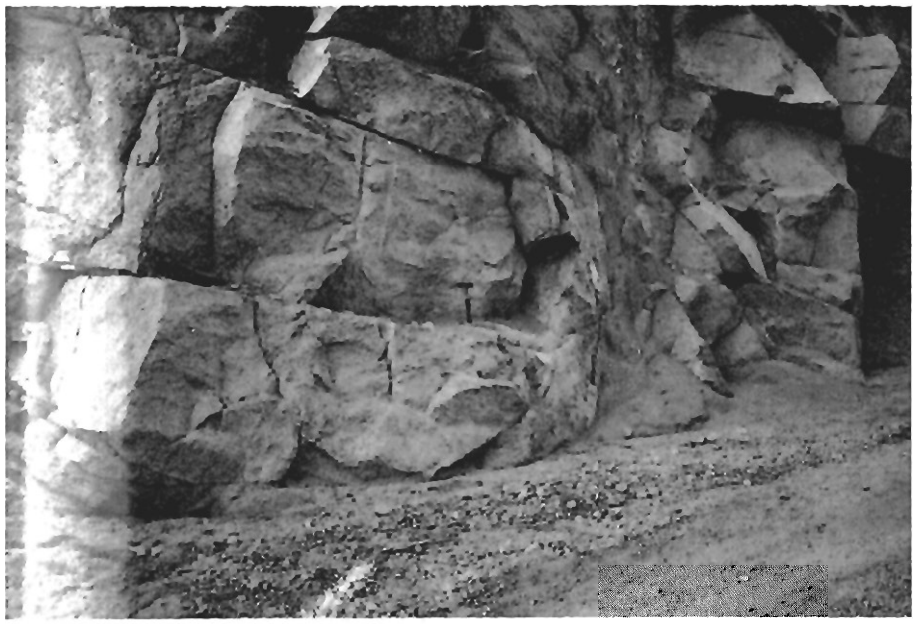

Plate. 3.4. Photograph showing massive metadiorite/ granodiorite having angular joints. The photograph also exhibits local fault along which the rock is sheared and weathered.

diorites. All these three types are, therefore, shown as one unit on the map (Fig. 3.1).

At certain places these rocks have developed shear zones, with profuse development of quartz and epidote veins along micro fractures. These rocks, at places, also have xenoliths (rounded to subrounded) of amphibolites (Plate 3.5). This feature along with the intrusive contact with associated amphibolites suggest that these have been formed after the amphibolites.

Quartz veins and aplite dikes are very common in these rocks. The aplite dikes have fine grained garnet in the form of microbands, especially along the contact. The quartz veins are generally barren but, at places, show copper mineralization in the form of tetrahedrite, chalcopyrite and supergene enrichment in the form of malachite and azurite. This has imparted green colour to the weathered surface (Plate 3.6). Copper-bearing zones (<2m thick and 75m long) within these rocks are commonly weathered and granulated at the surface (Plate 3.7). This type of surface weathering is a characteristic feature of these rocks.

Plagioclase, quartz, alkali feldspar, biotite are easily distinguished in hand specimens. The metagranodiorites, however, have pinkish colour xenocrysts of alkali feldspar (~1cm long) and relatively more biotite.

These metadiorite / metagranodiorite could be related to the second phase (stage II) of gabbro, diorite and granite plutonism of Kohistan batholiths (see Petterson & Windly, 1985).

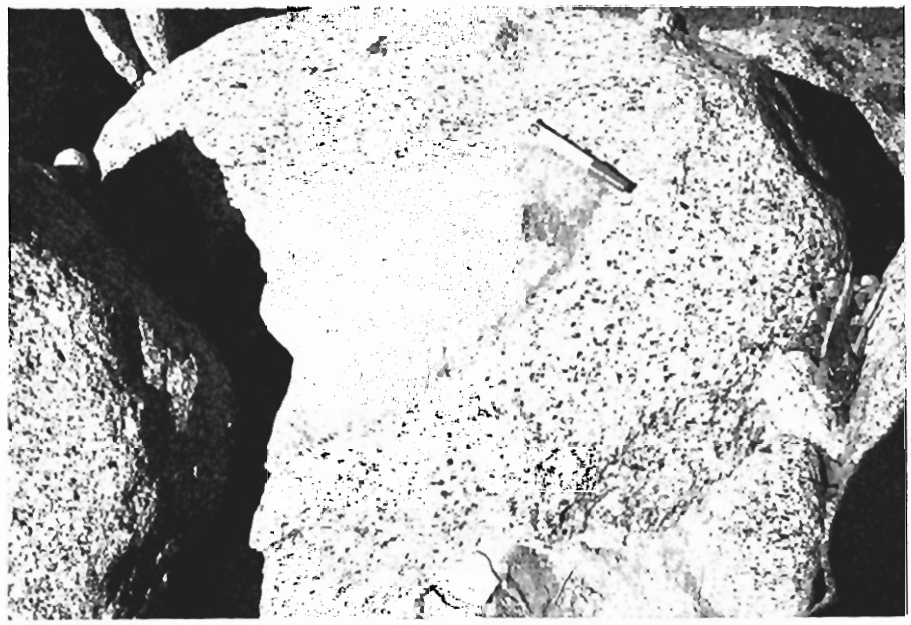

Plate. 3.5. Photograph showing rounded to subrounded xenolith of amphibolite within metadiorite/granodiorite boulder in the study area.

Plate. 3.6. Photograph showing the mineralized quartz vein within metadiorite/granodiorite.

COPPER MINERALIZATION

Copper mineralization in the area is generally found along quartz veins (Plate. 3.6) within both the amphibolite and metadiorite/ metagranodiorite units. The quartz veins are <1m thick and up to 30 m long. These veins, wherever intruded, are showing chilling effects and shearing on bothsides within the host rock. There are mineralized quartz microveins following the foliation planes and are probably the offshoots of the main quartz veins. The veins also contain clasts and pieces of the host rocks (diorites and amphibolites) which have been incorporated in these veins during precipitation.

Copper mineralization is generally present as disseminated grains of tetrahedrite and chalcopyrite within the quartz veins and associated meta diorites. The supergene enrichment of copper in the form of melachite and azurite is well noticed along leached zones adjacent to the mineralized quartz veins(Plate. 3.7). This mineralization is localized in few spots especially near Jabai (Fig. 3.1).

Plate. 3.7. Photograph showing the supergene enrichment of copper in the form of malachite. The rock is granulated on the surface due to weathering and erosion in the zones of copper mineralization.

CHAPTER-4

METHODOLOGY

A. FIELD METHODS

Collection of rock samples

Representative grab samples (@ 2-4 kg) were hammered through the rock exposures in the field. Both fresh and weathered rock samples were collected in different sample bags. The crushed material along various sheared zones were also collected for base and precious metals determination. These samples were properly numbered in the field and brought to the laboratory for further analyses.

Collection of stream sediments

The drainage sample sites and associated drainage cell (catchments) were outlined on topographic map and transfered onto the base map. The cells sizes were kept 2-50 square kilometers and check samples along main drainage were taken to cover an area which is not represented by single cell such as small drainages and the slopes along the main drainage samples. At each location a keen examination of stream floats (transported rock fragments) was made and local geology was noted. Heavy mineral pan-concentrates and fine sediment (-80 mesh) samples were collected for subsequent geochemical analyses for various target and indicator metals. All samples were assigned unique numbers. The details of relevant samples and geological observations were recorded on site and are given in the appendix.

Pan concentrate samples: A standard volume (about 20 Kg of < 7mm) of stream sediments were collected from at least three natural heavy mineral spots along the active streams. These sediments were than panned in plastic panning dishes and reduced the volume to about 50-100 g containing heavy mineral concentrates. These pan-concentrates were then transferred to self-sealed plastic bags for detailed mineralogical and geochemical studies. Before

transferring into plastic bags, these concentrates were examined closely with a pocket microscope for visible gold as well as other ore-indicators and necessary minerals. The visible gold was divided into different sizes such as piece (>0.5mm), speck (0.5-0.3mm) and colour (<0.3mm). The presence or absence of gold along with other recognizable heavy minerals are recorded at the site (see appendix). These have helped in comparing field observations with the analytical data obtained through laboratory.

Fine fraction (-80 mesh): Fine stream sediment sample at each site was collected from at least three locations in active drainage channel. Among these two were from heavy mineral traps and one from low energy/fine sediments area of drainage sample site. These fine sediments were collected about 100-200 g of (-80 mesh) material for subsequent chemical analyses. Each fine stream sediment sample was transferred to plastic bag and properly numbered.

Stream floats: At each sample site, stream float (transported rocks and mineral fragments) were closely examined in hand spacimen by the magnifying lens to identify rock types, alteration and mineralization that have come from within the particular drainage cell represented by that stream sediment sample site. The observations were recorded for further interpretation and mapping purposes. The detail is given in appendix.

Field data recording

The following observations were recorded for each sample site during the field (given in appendix):

1. Sample Number
2. Sampling interval
3. Prospect/location
4. Map sheet Number

5. Sample site latitude/longitude
6. Drainage Characteristics
7. Grid reference
8. Description of float
9. Pan mineralogy
10. Visible Gold content
11. Visible Gold Description

B. LABORATORY METHODS

Crushing and pulverizing of rock samples

Various types of rocks collected during field from the study area were thoroughly checked for their extensive alteration and weathering. Representative samples were then selected for further experimental work. The rock samples were crushed in a Jaw crusher and then the crushed chips were pulverized in a tungsten carbide ball mill to - 75 micron (200 mesh size) with a quartz flush between samples. A portion of individual sample was collected after proper quartering and coning. During this whole process greater care was practiced to avoid contamination. The powdered samples were stored in the air tight glass bottles. These bottles, after removing the lids, were kept in the oven at 110 °C for two hours in order to remove the moisture.

Preparation of stock solutions

1.Stock Solution A

HF and $HClO_4$ digestion method: 0.5g of powdered rock sample was accurately weighed in a platinum crucible and was moist with few drops of deionized water and 5 drops of $HClO_4$. Then 10 ml of concentrated (49%) HF was added and heated on a sand bath to break down clay minerals and to drive off all silica as SiF_4 . The solution is evaporated and dried. The

crucible was then removed from the sand bath and was cooled for few minutes. Five additional drops of $HClO_4$ were added and was again kept on sand bath until dry residue was obtained. The residue was then dissolved in 10 ml HCl and again heated for a while and is then diluted to about 20 ml with distilled water. The solution was kept hot and transfered to 100 ml flask for the final dilution. This procedure prevented the formation of colorless precipitates occasionally produced by Fe-rich samples when the solution came in contact with the cold flask. All the samples were treated by the same procedure for the preparation of solution A. This solution was kept for the determination of all the major oxides, minor and trace elements except SiO_2 and Al_2O_3 .

1. Stock Solution B

HF + HNO_3 digestion method: Accurately weighed 0.500 g of finely powdered sample, each of both rocks and stream sediments, was taken in a 100 ml teflon beaker. 5ml of hydrofluoric acid (HF) was added to it and was kept on hot plate at a temperature of approximately 75°C. After 10 minutes about 15 ml of concentrated HNO_3 was added and the heating was continued until complete dryness. 3N HCl was added to the residue and was heated until the maximum dissolution of residue. The volume was made to 50 ml with 3N HCl and was stored in polythene bottle. This solution was then used for trace elements determination by using atomic absorption spectrophotometer (AAS).

2. Stock Solution C

Sodium hydroxide fusion method: 30 g of NaOH pellets were dissolved in 100 ml deionized water and stored in a polythene bottle. 5 ml aliquots of NaOH solution was added to a series of already cleaned nickle crucibles. The

crucibles were kept on hot plate at approximately 100 C^{O} for complete dryness. These were then cooled in a desicator. Accurately weighed 0.05g of rock samples and certified rock Standards were added to separate crucibles. One crucible was used for the preparation of blank. The crucibles were covered with lids and each crucible was heated to dull redness over a gas burner for a period of 5 minutes. The crucibles were swirled while hot. Deionized water (5-10ml) was added to each crucible. The contents of each crucible were washed into different 600 ml polythene beakers which already contained 400 ml of deionized water and 10 ml of concentrated HCl. In most cases clear solution was obtained at this stage. However, in few cases the solution was not clear. This type of solution was then warmed until the clear solution was obtained. The resulting solution was transferred to one litre volumetric flask and was made to the volume with deionized water and stored in polythene bottles for the determination of silica and alumina. This solution was used for the determination of SiO2 and Al2O3 in both Mn-ores and metacherts.

3. Stock Solution D

Aqua Regia digestion method for gold: 10-20 g each of rock and stream sediment powder sample was weighed in the 200 ml Pyrex beakers. 50 ml of aqua regia was added to it and was heated for about half an hour at low heat. After half an hour about 35 ml of deionized water (D.I) was added. Heating and evaporation was continued until about 50 ml solution was left in the beaker. The whole beaker contents were then filtered in a test tube. The residue and beaker was washed several times with 6N HCl and the contents were collected in the test tube. This filtrate was of about 50 ml volume. The whole filtrate was then transferred to a 250 ml seperatory funnel. In order to keep the normality of filtrate to 6N, about 50 ml of D.I. water was added to it. Then 10 ml of Methyle Isobutyle Ketone (M.I.B.K.) was added to the

separatory funnel. The funnel was then shaked for 6-8 minutes on automatic flask shaker. The lower layer was removed and 20 ml of 0.2N HCl was then added to the M.I.B.K in the funnel and was shaked for about 5 minutes more. The most probable interference of Fe was removed by this process. The M.I.B.K was collected and stored in a glass test tube for further determination of gold on atomic absorption.

DETERMINATION OF MAJOR AND MINOR OXIDES

DETERMINATION OF SiO_2

Spectrophotometric method

The method by Shapiro and Brannock in the book "Chemical Methods of Rock Analysis" by Jeffery (1987) was adopted. In this method the silica in the solution B is determined by reducing the yellow colour of silico molybdate to blue colour.

Instrument: SP8-400 PYE UNICAM UV/VIS spectrophotometer.

Reagents

1. Ammonium molybdate solution: 7.5g of ammonium molybdate was dissolved in 70 ml deionized water by adding 20 ml of 9 N H_2SO_4. The solution was made to the volume of 100 ml and was stored in a polythene bottle.

2. Tartaric acid solution: 25g of the tartaric acid was dissolved in deionized water and was diluted to 250 ml with deionized water.

3. Reducing solution: 0.7g of sodium sulfite Na_2SO_3, 0.15g of 1-amino-2-naphthol-4-sulphonic acid and 9g of sodium metabisulfite ($Na_2S_2O_5$) was dissolved in 100 ml of deionized water. The solution was kept in a cool and dark place and was prepared freshly as this solution deteriorate after few days.

Procedure: 10 ml of stock solution C of each of the Mn-ores, metachert and each rock standards and a blank was taken in a series of 100 ml volumetric flasks. About 50 ml of deionized water was added to each flask. 2 ml of ammonium molybdate solution was added to each flask and was swirled to mix well. After exactly 10 minutes, 4 ml of tartaric acid solution was added to each flask and again swirled and mixed well. At the end 1 ml of reducing solution was added to these flasks and each flask was diluted to 100 ml with deionized water. All these solutions were set aside for at least 30 minutes. Blue color solution was obtained at the end. The silica determination was then made on the spectrophotometer at a wavelength of 650nm relative to the reference rock standards.

DETERMINATION OF Al_2O_3

Spectrophotometric Method

Instrument: SP8-400 PYE UNICAM UV/Visible spectrophotometer

Reagents

1. 8-hydroxyquinoline solution: 1.25g of the 8-hydroxyquinoline was dissolved in 250 ml of pure grade of chloroform and was stored in a refrigerator.

2. Complexing reagent: 1g of hydroxylamine hydrochloride ($HONH_2HCl$), 3.6g of sodium acetate trihydrate and 0.4g of berillium sulphate tetrahydrate were dissolved in 50 ml of deionized water. 0.04g of 2,2 dipyridyl was also dissolved in 20 ml of 0.2N HCl. Both the solutions were then mixed and diluted upto 100 ml with deionized water.

Procedure: 5 ml of each stock solution C of Mn-ores, metachert and 3 known standards and a reagent blank were taken into a series of 100 ml seperatory funnels. 5 ml of deionized water and 10 ml of complexing reagent solution were added to these funnels and mixed well. After few minutes 20 ml of 8-hydroxyquinoline solution was added to each funnel. These solutions were then shaked for about 8 minutes by an automated flask shaker. The organic layers obtained at the bottom of these solutions in the seperatory funnels were then separated into 25 ml volumetric flasks by washing the funnels with chloroform for several times. The final volume of 25 ml for each sample was made with chloroform. The yellow color extracts obtained through this process were suitable for spetrophotometric determination. The Al_2O_3 was determined at wavelength of 381 nm relative to the reference rock standards according to the method of Riley (1958).

DETERMINATION OF TOTAL IRON

The total iron as Fe_2O_3 in the studied rock samples was determined by atomic absorption spectrophotometer by using the stock solutions A.

Instrumental conditions

Mode	Absorption
Wavelength	248.3 nm
Slit width	0.2 nm

Air flow	5litre/minute
Fuel flow	1litre/minute
Burner hight	10 mm

1. Stock solution of 1000 ppm for Fe: I gram of pure iron metal was dissolved in minimum amount of HCl and was made to the volume with deionized water in one litre volumetric flask.

2. Stock solution of 100 ppm: 10 ml from 1000 ppm stock solution was taken in 100 ml volumetric flask and made to the mark with deionized water.

3: Working standard solutions: 1, 2, 4 and 8 ppm working standard solutions were prepared by taking 1, 2, 4 and 8 ml from the 100 ppm stock standard solution in a 100 ml volumetric flask and made to the volume with deionized water.

Procedure: The atomic absorption spectrophotometer was set according to the above conditions. The instrument was calibrated with the iron working standard solutions of 4 and 8 ppm. The working standards 1, 2, 4 & 8 ppm were then run as unknown. After verification of accuracy, the stock solutions A of both certified rock standards and samples were run on the machine. The results were compared with the certified values and were found within the confidence limit. After making sure that the instrument is properly calibrated the rest of the sample solutions were run on the atomic absorption and the results of iron as Fe_2O_3 were determined.

DETERMINATION OF CaO AND MgO

The CaO and MgO in both the certified rock standards and the studied ores and metacherts were determined by atomic absorption spectrophotometric method by using the stock solutions A.

Instrument: SP 191 PYE UNICAM Atomic Absorption Spectrophotometer

Instrument conditions:

Element	Ca	Mg
Mode	Absorption	Absorption
Wavelength	422 nm	285.2nm
slit width	0.4nm	0.4nm
Air flow	5l/min	5 l/min
Fuel flow	5 l/min	To best flame
Burner hight	10mm	10mm

1. Stock solution of 1000 ppm for Ca & Mg: 2.497g $CaCO_3$ and 3.057g $MgCO_3$ were dissolved in 1N HCl and was diluted to one litre with deionized water in a 1000 ml volumetric flask.

2: Stock solution of 100 ppm for Ca & Mg: 10 ml of 1000 ppm stock solution was taken in 100 ml volumetric flask and was made upto the mark with deionized water.

3: Lanthanum 5% Solution: 58.64g of La_2O_3 was dissolved in 200 ml deionized water to which 150 ml 60 % $HClO_4$ was added. It was heated until complete dissolution. The solution was then filtered through ordinary filter paper into 1000 ml volumetric flask and the volume was made upto the mark with deionized water.

4. Working Standards: 1, 2, 4 and 8 ppm of working standards for Ca and Mg were prepared by taking 0.5, 1, 2 and 4 ml of 100 ppm stock solution in a series of 50 ml volumetric flasks. To these flasks 10 ml lanthanum solution was added and the volume was made upto the mark with deionized water.

5. Dilution of Samples: 5 ml (depending upon the expected concentration of Ca & Mg) of the stock solution A of both certified rock standards and the studied rock samples were taken in a series of 50 ml volumetric flasks. 10 ml of lanthanum solution was added to each flask and the volume was made to the mark.

Procedure: Atomic absorption spectrophotometer was set according to the above mentioned conditions for Ca and Mg separately. The cathode lamp for both Ca and Mg were turn ON to warm up for at least 10 minutes. The instrument was then calibrated and standardized with the working standards of 2 and 4 ppm. All the working standards were run as unknown and their actual concentration was verified. For further accuracy the certified rock standards were run as unknown and the results were compared. After making sure that the results of the certified standards were within the confidence limit, the studied rock sample solutions (in diluted form) were run on the atomic absorption and the concentrations of Ca and Mg were noted for each sample. The wt% of CaO and MgO in each sample was then calculated.

DETERMINATION OF $Na_2O + K_2O$

Both Na_2O and K_2O were determined by atomic absorption spectrophotometer by using the stock solutions A.

Instrument: SP 191 PYE UNICAM atomic absorption spectrophotometer

Instrument Conditions:

Element	Na	K
Mode	Emission	Emission
Wavelength	589 nm	766 nm
Slit width	0.2 nm	0.4 nm
Air flow	5 l/min	5 l/min
Fuel flow	1 l/min	1 l/min
Burner hight	20 mm	20 mm

1. Stock solution of 1000 PPM for Na & K: 3.087 g moisture free Na_2SO_4 and 2.228g moisture free K_2SO_4 were dissolved in deionized water and the volume was made to 1000 ml in a volumetric flask. The solution was stored in a polythene bottle.

2. Stock solution of 100 PPM Na & K: 10 ml of 1000 PPM stock solution was taken in a 100 ml flask and diluted to mark with deionized water.

3. Working Standards: 1, 2, 4 and 8 ppm working standards were prepared by taking 1, 2, 4, and 8 ml from 100 PPm stock solution in 100 ml volumetric flasks and was diluted up to the mark with deionized water.

4. Diluted samples: All the samples as well as certified rock standards were diluted to 20 times.

Procedure: The atomic absorption spectrophotometer was set according to the above mentioned instrumental conditions in order to get the maximum absorbance. The instrument was set on emission mode and a conical burner head was used. In this case no cathode lamp was required. The instrument

was calibrated and standardized by working standards of 4 and 8 ppm and then the working standards were also run as unknown in order to verify the standardization of the instrument. The diluted certified rock standards were then run and the results were compared to know the accuracy of the method. The diluted solutions of rock sample were sprayed one by one through the flame and the concentration of Na and K was noted in each sample. The wt% of Na_2O and K_2O were then calculated.

DETERMINATION OF MnO

MnO in the studied rock samples was determined by atomic absorption by using the stock solutions A & B.

Instrument: SP 191 PYE UNICAM atomic absorption spectrophotometer

Instrument conditions:

Mode	Absorption
Wave length	279.5nm
Slit width	0.2nm
Fuel flow	1 l/min
Air flow	5 l/min
Burner hight	10mm

1:Stock solution of 1000 ppm for Mn: 4.058g of $MnSO_4.4H_2O$ was dissolved in 20 ml of 1N H_2SO_4. It was then transferred to 1000 ml volumetric flask and was made upto the mark with deionized water.

2: Stock solution of 100 ppm: 10 ml of 1000 ppm stock solution was taken in 100ml volumetric flask and was made upto the volume with deionized water.

3: Working standards: 1, 2, 4 and 8 ppm working standards of Mn were prepared by taking 1 2, 4 and 8 ml of 100 ppm stock solution in a 100ml volumetric flask and was made to volume with deionized water.

Procedure: The atomic absorption spectrophotometer was set according to the above mentioned conditions and the cathode lamp for Mn was warmed up for 10 minutes. After warming up of the cathode lamp the instrument was calibrated and standardized with the working standards. The stock solutions of certified rock standards were then run to check the accuracy of the method. After making sure that the atomic absorption is calibrated properly, solution A of the unknown samples were sprayed into the flame and the concentration of Mn was noted for every samples. The wt% of MnO was then calculated.

DETERMINATION OF TiO_2

TiO_2 in the studied samples was determined by spectrophotometric method by using the stock solution A.

Instrument: SP8-400 PYE UNICAM UV/VIS spectrophotometer

Procedure: 10 ml of stock solution A of the ores and metacherts respectively and at least two certified rock standards were taken in 50 ml volumetric flask. Few drops of H_3PO_4 and 2 ml of H_2O_2 were added to each flask. The solution in each flask was made to volume with 10 % H_2SO_4 solution. A blank sample was also prepared by the same method. These

solutions were then shaked and mixed well and were ready for analysis. The spectrophotometer was turn ON and set to warm up for 30 minutes. The wave length optimization was done on the certified rock standards. A maximum peak was noticed at 445 nm. The instrument was set on a wavelength of 445 nm and was zeroed with the blank. The certified rock standards were run on the instrument and the results were calculated and compared with the certified values. After making sure that the results of the certified standards were within the confidence limit, the rock sample solutions were then run as unknown. The optical density of each sample was noted and the wt% of TiO_2 for each sample was then calculated.

DETERMINATION OF P_2O_5:

P2O5 in the studied samples was determined by spectrophotometric method by using the stock solution A.

Instrument: SP8-400 PYE UNICAM UV/VIS spectrophotometer.

Reagents:

1: Ammonium meta vanadate solution: 0.25g ammonium meta vanadate (NH_4VO_3) was dissolved in 120 ml of 33% HNO_3.

2. Ammonium molybdate solution: 10 g of ammonium molybdate was dissolved in 80 ml of deionized water.

Both the solutions were mixed and stored in polythene bottle.This mixture is used as vanadate molybdate reagent.

Procedure: 10 ml of stock solution A of ores and metacherts and at least two certified standards were taken in series of 50 ml volumetric flasks. To each

flask 2 ml of vanadate molybdate reagent was added. The volume was made to the mark with deionized water. The solutions were shaked and were run on spectrophatometer as under: The spectrophotometer was turn ON and set to warm up for 30 minutes. The wave length optimization was done on the certified rock standards. A maximum peak was noticed at 372 nm. The instrument was set at 372 nm and was zeroed with the blank. The certified rock standards were run on the instrument and the results were calculated and compared with the certified values. After making sure that the results of the certified standards were within the confidence limit, the rock sample solutions were then run as unknown. The optical density of each sample was noted and the wt% of P_2O_5 for each sample was then calculated.

DETERMINATION OF IGNITION LOSS

Gravimetric method

Sample of known weight were taken in already weighed porcelene crucibls. These crucibles along with the samples were kept in a furnace at 1000 C^O for 3 hours. Then cooled in a desicator and weighed after 15 minutes. The difference in weight was noted and the amount of ignition loss (in percent) was calculted for each sample.

TRACE ELEMENTS DETERMINATIONS

Both the rocks and stream sediment samples were analyzed for Cu, Pb, Zn, Ni, Cr, Co, Ag, and Au, by using partly Perkin Elmer 3300 (equipped with graphite furnace) and partly SP-191 Pye Unicam atomic absorption spectrophotometer in the geochemistry laboratory of the Centre of Excellence in Geology, University of Peshawar. The detail procedure and instrumental setting is given as follows:

DETERMINATION OF NICKEL (Ni)

Instrument: SP 191 PYE UNICAM Atomic Absorption Spectrophotometer

Instrument conditions:

Mode	Absorption
Wavelength	232nm
Slit width	0.2nm
Fuel flow	1.0 l/min
Air flow	4.5 l/min

1: Standard stock solution of 1000 ppm: 1g of Ni metal was dissolved in a minimum volume of(1:1) HNO_3 and was diluted to 1 litre with deionized water.

2. Standard stock solution of 100 ppm: 10 ml from 1000 ppm stock standard solution was transferred into a 100 ml volumetric flask and was made to the mark with deionized water.

3: Working standards: 0.5, 1, 2, 4 ppm standard solution were prepare by taking 0.5, 1, 2 and 4 ml from 100 ppm standard solution into a series of 100 ml volumetric flask and was made to the mark with deionized water.

Procedure: The atomic absorption spectrophotometer was set according to the above mentioned conditions. Ni cathode lamp was turned ON and allowed to warm up for 10 minutes. After warming up of cathode lamp, the air acetylene flame was ignited. The instrument was calibrated and standardized with working standards of 2 and 4 ppm. All the working standards were then run as unknown to verify the standardization. Stock solution of certified standards was run and the results were compared with

the certified values. After making sure that the result of the certified standards were within the confidence limit, the sample's stock solutions B were then aspired into the flame and the Ni concentration of each sample was noted. The Ni contents in ppm were calculated according.

DETERMINATION OF CHROMIUM (Cr)

Instrument: SP-191 PYE UNICAM Atomic Absorption Spectrophotometer

Instrument conditions

Mode	Absorption
Wavelength	357.9nm
Slit width	0.2nm
Fuel flow	1.5 l/min
Air flow	4.5 l/min

1: Standard stock solution of 1000 ppm: 3.735g of K_2CrO_4 was dissolved in deionized water and diluted to one litre with deionized water.

2. Standard stock solution of 100 ppm: 10ml of 1000ppm standard stock solution was taken in 100 ml volumetric flask and was made to the mark with deionized water.

3. Working standards: 0.5, 1, 2, 4 and 8 ppm of working standards were prepared by taking 0.5, 1, 2, 4 and 8 ml from the standard stock solution of 100 ppm in a 100ml volumetric flask and was made to the mark with deionized water.

Procedure: The atomic absorption spectrophotometer was set according to the above mentioned conditions. Cr cathode lamp was turned ON and let it to warm up for 10 minutes. After warming up of cathode lamp the air acetylene

flame was ignited. The instrument was calibrated and standardized with working standards of 4 and 8 ppm. All the working standards were then run as unknown to verify the standardization. Stock solution B of certified standards were run through the instrument and the results were compared with the certified values. After making sure that the results of the certified standards were within the confidence limit, the sample's stock solutions B were then aspired into the flame and the Cr concentration of each sample was noted. The Cr contents in ppm were calculated.

DETERMINATION OF COBALT (Co):

Instrument: SP 191 PYE UNICAM Atomic Absorption Spectrophotometer.

Instrument conditions:

Mode	Absorption
Wave length	240.7 nm
Slit width	0.4 nm
Fuel flow	0.9 l/min
Air flow	4.5 l/min
Burner height	10 mm

1: Standard stock solution of 1000 ppm: 1.0 g of cobalt metal was dissolved in 30 ml of (1:1) HCl and was diluted to one litre with deionized water.

2. Standard stock solution of 100 ppm: 10ml of 1000 ppm stock solution was taken in 100 ml volumetric flask and was made to the mark with deionized water.

3. Working standards: 0.5, 1, 2, 4 and 8 ppm of working standards were prepared by taking 0.5, 1, 2, 4 and 8 ml from 100 ppm standard stock solution in a series of 100 ml volumetric flasks and made to the mark with deionized water.

Procedure: The atomic absorption spectrophotometer was set according to the above mentioned conditions. Co cathode lamp was turned ON and let it to warm for 10 minutes. After warming up of cathode lamp the air acetylene flame was ignited. The instrument was calibrated and standardized with working standards of 4 and 8 ppm. All the working standards were then run as unknown to verify the standardization. Stock solution of certified standards were run through the instrument and the results were compared with the certified values. After making sure that the results of the certified standards were within the confidence limit, the sample stock solutions B were then aspired into the flame and the Co concentration of each sample was noted. The Co contents in ppm were calculated.

DETERMINATION OF COPPER (Cu)

Instrument: SP 191 PYE UNICAM Atomic Absorption Spectrophotometer.

Instrument conditions

Mode	Absorption
Wave length	325.8nm
Slit width	0.4nm
Fuel flow	1.0 l/min
Air flow	4.5 l/min
Burner height	10 mm

1. Standard stock solution of 1000 ppm: 1 g of copper metal was dissolved in 30 ml of (1:1) HNO_3 and was made to the volume of one litre with deionized water.

2. Standard stock solution of 100 ppm: 10 ml of 1000 ppm standard stock solution was taken in 100 ml volumetric flask and was made to the mark with deionized water.

3. Working standards: 0.5, 1, 2, 4 and 8 ppm of working standards were prepared by taking 0.5, 1, 2, 4, and 8 ml from 100 ppm standard stock solution into a series of 100 ml volumetric flasks and made to the volume with deionized water.

Procedure: The atomic absorption spectrophotometer was set according to the above mentioned conditions. Cu cathode lamp was turned ON and let it to warm up for 10 minutes. After warming up of cathode lamp the air acetylene flame was ignited. The instrument was calibrated and standardized with working standards of 4 and 8 ppm. All the working standards were then run as unknown to verify the standardization. Stock solution A of certified standards were run through the instrument and the results were compared with the certified values. After making sure that the results of the certified standards were within the confidence limit, the sample stock solutions B were then aspired into the flame and the Cu concentration of each sample was noted. The Cu contents in ppm were calculated.

DETERMINATION OF LEAD (Pb):

Instrument: PERKIN ELMER 3300 Atomic Absorption Spectrophotometer.

Instrument conditions:

Mode Absorption

Wavelength	217 nm
Slit width	0.4 nm
Fuel flow	0.9 l/min
Air flow	4.5 l/min
Burner height	10 mm

1. Standard stock solution of 1000 ppm: 1.598 g of lead nitrate $Pb(NO_3)_2$ was dissolved in 1% HNO_3 and was diluted to 1 litre with deionized water.

2. Standard stock solution of 100 ppm: 10 ml of 1000 ppm standard stock solution was taken in 100 ml volumetric flask and was made to the volume with deionized water.

3. Working standard solutions: 0.5, 1, 2, 4 and 8 ppm of working standards were prepared by taking 0.5, 1, 2, 4 and 8 ml of 100 ppm stock solution in a series of 100 ml volumetric flasks and volume was made to the mark with deionized water.

Procedure: The atomic absorption spectrophotometer was set according to the above mentioned conditions. Pb cathode lamp was turned ON and allowed to warm up for 10 minutes. After warming up of cathode lamp the air acetylene flame was ignited. The instrument was calibrated and standardized with working standards of 4 and 8 ppm. All the working standards were then run as unknown to verify the standardization. Stock solution B of certified standards were run through the instrument and the results were compared with the certified values. After making sure that the results of the certified standards were within the confidence limit, the sample stock solutions B were then aspired into the flame and the Pb concentration of each sample was noted. The Pb contents in ppm were calculated.

DETERMINATION OF SILVER (Ag)

Instrument: PERKIN ELMER 300 Atomic Absorption Spectrophotometer.

Instrument conditions:

Mode	Absorption
Wavelength	28.1 nm
Slit width	0.4 nm
Fuel flow	1.l/min
Air flow	5 l/min
Burner height	10 mm

1. Standard stock solution of 1000 ppm: 1.575 g of silver nitrate ($AgNO_3$) was dissolved in 100 ml of deionized water and was transferred to 1 litre volumetric flask. The volume was made to the mark with deionized water.

2. Stock solution of 100 ppm: 10 ml of 1000 ppm standard stock solution was taken in 100 ml volumetric flask and was made to the volume with deionized water.

3. Working standard solutions: 0.5, 1, 2, 4 and 8 ppm solution were prepared by taking 0.5, 1, 2, 4 and 8 ml from 100 ppm standard stock solution in a series of 100ml volumetric flasks and the volume was made to the mark with deionized water.

Procedure: The atomic absorption spectrophotometer was set according to the above mentioned conditions. Ag cathode lamp was turned ON and let it to warm up for 10 minutes. After warming up of cathode lamp the air acetylene flame was ignited. The instrument was calibrated and standardized with working standards of 4 and 8 ppm. All the working standards were then run as unknown to verify the standardization. Stock solution B of certified

standards were run through the instrument and the results were compared with the certified values. After making sure that the results of the certified standards were within the confidence limit, the sample stock solutions B were then aspired into the flame and the Ag concentration of each sample was noted. The Ag contents in ppm were calculated.

DETERMINATION OF ZINC (Zn)

Instrument: SP 191 PYE UNICAM Atomic Absorption Spectrophotometer

Instrument conditions:

Mode	Absorption
Wavelength	213.9nm
Slit width	0.4nm
Fuel flow	1 l/min
Air flow	5 l/min
Burner height	10 mm

1. Standard stock solution of 1000 ppm: 1 g zinc metal was dissolved in about 20 ml of (1:1) HCl and was diluted to 1 litre with deionized water.

2. Standard stock solution of 100 ppm: 10 ml of 1000 ppm standard stock solution was taken in 100 ml volumetric flask and was made to the volume with deionized water.

3. Working standard solution: 1, 2, 4 and 8 ppm working standard solutions were prepared by taking 1, 2, 4 and 8 ml of 100 ppm standard stock solution in a series of 100 ml volumetric flasks. The volume in each flask was made up to the mark with deionized water.

Procedure: The atomic absorption spectrophotometer was set according to the above mentioned conditions. Zn cathode lamp was turned ON and allowed it to warm up for 10 minutes. After warming up of cathode lamp the air acetylene flame was ignited. The instrument was calibrated and standardized with working standards of 4 and 8 ppm. All the working standards were then run as unknown to verify the standardization. Stock solution B of certified standards were run through the instrument and the results were compared with the certified values. After making sure that the results of the certified standards were within the confidence limit, the sample stock solutions B were then aspired into the flame and the Zn concentration of each sample was noted. The Zn contents in ppm were calculated.

DETERMINATION OF GOLD (Au)

Instrument: PERKIN ELMER Atomic Absorption Spectrophotometer

Instrument conditions:

Mode	Absorption
Wave length	242.8 nm
Slit width	0.4 nm
Fuel flow	0.9 l/min
Air flow	4.5 l/min

1: **Hydrobromic acid**, concentrated (48%).

2: **Hydrobromic acid - 10 % bromine solution:** Diluted 10 ml of bromine to 100 ml with concentrated hydrobromic acid.

1. Gold stock solution of 1000 ppm: 1 gram of pure gold was dissolved in aqua regia and was diluted to one litre with 10% HCl in a volumetric flask.

2. Standard stock solution of 100 ppm: 10 ml of 1000 ppm standard stock solution was taken in 100 ml volumetric flask and the volume was made to the mark with deionized water.

3. Standard stock solution of 10 ppm: 10 ml of 100 ppm standard stock solution was taken in 100 ml volumetric flask and the volume was made to the mark with deionized water.

4. Working standards: 0.5, 1, 2, 4 and 8 ppm working standards of gold were prepared by taking 0.5, 1, 2, 4,8 and 16 ml of 10 ppm standard stock solution in test tubes and diluted to 20 ml with deionized water. O.22 ml of HBr 10% bromine solution was added to each test tube. It was followed by the addition of 10 ml MIBK. The solution was then shaked for 5 minutes and was centrifuged. The MIBK layer was separated and kept for further determination.

Procedure: The atomic absorption spectrophotometer was set according to the above mentioned conditions. Au cathode lamp was turned ON and allowed to warm up for 10 minutes. After warming up of cathode lamp the air acetylene flame was ignited. The instrument was calibrated and standardized with working standards of 4 and 8 ppm. All the working standards were then run as unknown to verify the standardization. Stock solution D (MIBK solution) of certified standards were run through the instrument and the results were compared with the certified values. After making sure that the results of the certified standards were within the confidence limit, the sample stock solutions D were then aspired into the flame and the Au concentration of each sample was noted. The Au contents in ppm were then calculated.

CHAPTER-5

PETROGRAPHY

AMPHIBOLITES

In hand specimens, the amphibolites are light-green to grayish-green in colour and are medium to coarse-grained. Hornblende, plagioclase, biotite and quartz can easily be recognized in handspecimen. Some samples have micro viens of light coloured material (quartz, feldspar etc.). All the minerals have preferred orientation along the fabric direction.

In thin section the amphibolites are medium to coarse-grained, inequigranular, hypidioblastic to subideoblastic texture. Hornblende and plagioclase are the dominant while orthoclase and quartz are the minor constituents (Table. 5.1) Biotite, muscovite, chlorite, epidote, apatite, sphene, rutile, calcite and opaque occur as accessories (Table 5.1).

Hornblende (32 to 60%) is generally light-green to dark-green in colour, however, grains of bluish-green and light-brown pleochroism are also noticed. It is prismatic subhedral in shape and has well developed cleavages. Most of the hornblende grains enclose fine-grained rounded to subrounded quartz (Plate. 5.1) which imparted sieve or pepper-mesh texture to the amphibole grains. This quartz probably represent the silica released during the transformation of some mafic phases (i.e., Pyroxene) to hornblende. At places, chlorite and trimolite/actinolite occur as core material to hornblend (Plate. 5.2a & 5.2b) which indicates that the former is replaced by the later. Some time biotite is also enclosed within hornblende (Pate 5.3). In some

Table. 5.1 Modal analyses (Visual estimates) of amphibolites from Ushiri valley. District Dir.

	US70	US54	US84	US49	US61	US89	US45	US58	US46	US33	US31	US72
Hornblende	35	50	60	45	42	50	32	42	45	48	40	50
Plagioclase	50	40	30	32	35	37	40	45	40	40	42	40
Orthoclase	5	-	4	4	3	2	3	4	2	2	4	5
Quartz	3	5	Tr	3	3	3	2	3	2	2	3	3
Chlorite	2	2	Tr	10	15	5	20	-	-	-	-	-
Biotite	Tr	1	3	-	-	1	1	5	10	8	10	Tr
Trimolite/ Actinolite	3	-	1	2	-	Tr	-	-	-	-	-	Tr
Epidote	Tr	Tr	Tr	2	Tr	Tr	Tr	Tr	Tr	Tr	Tr	Tr
Muscovite	Tr	Tr	Tr	-	-	-	-	Tr	-	Tr	-	-
Sericite	Tr	Tr	Tr	-	-	Tr	Tr	Tr	Tr	Tr	Tr	Tr
Apatite	Tr	Tr	-	Tr	-	Tr	-	-	Tr	Tr	Tr	Tr
Sphene	-	-	-	Tr	-	-	-	Tr	Tr	-	-	-
Rutile	-	-	-	Tr	Tr	-	-	Tr	-	Tr	-	-
Opaque	1	Tr	1	Tr	Tr	Tr	Tr	Tr	Tr	Tr	Tr	1

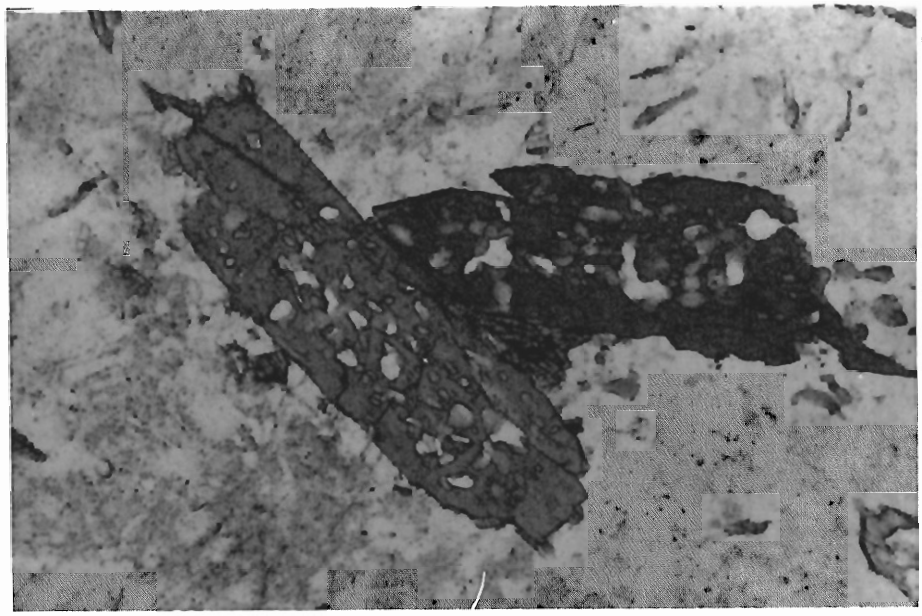

Plate. 5.1. Photomicrograph showing prismatic grains of green-to light-green hornblende having inclusions of rounded to subrounded quartz in amphibolites. This has imparted pepper mesh or sieve texture to the hornblende (Plane light; X4).

cases the hornblende grains are relatively small which are interlocked and oriented along the fabric direction in such a way that it has developed schistosity in the rock. These types of rocks are common along the shear zones.

Plagioclase (30 to 50%) is in the range of oligoclase to andesine, however, some grains of albitic in composition are also observed. Plagioclase is partially altered to sericite, epidote and carbonates (Plate 5.4). However, pseudomorphs and relics of plagioclase are also common due to more or less complete alteration. Sericitization and epidotization are the common features of these rocks. Plagioclase grains are also fractured and strained at places which is clearly evident by the bending and fracturing of elongated grains, of plagioclase.

Biotite (1 to10%) is generally brown to light-brown pleochroic, however, biotite with greenish tint of chlorite are also noticed. In few cases, the flakes of biotite are having light-green to dark-green pleochroism too. Both these varities have shreds or exolusions of magnetite. Biotite is usually present as flakes and bundles in association with hornblende and opaque phases. At places biotite and hornblende are intergrown, indicating simultaneous crystallization of both the phases. In some cases, the biotite encloses small flakes of muscovite while in others, it is by itself enclosed within hornblende. Both biotite and muscovite flakes exhibit bending due to strain and stress conditions.

Alkali feldspar (2 to 5%) occurs as subhedral, medium-grained phase which is partially or completely altered to kaolinite, sericite, muscovite etc. Quartz is present as inclusions within hornblende and also as anhedral individual grains within the interstices of plagioclase. The later phase, occasionally , exhibits pressure shadows.

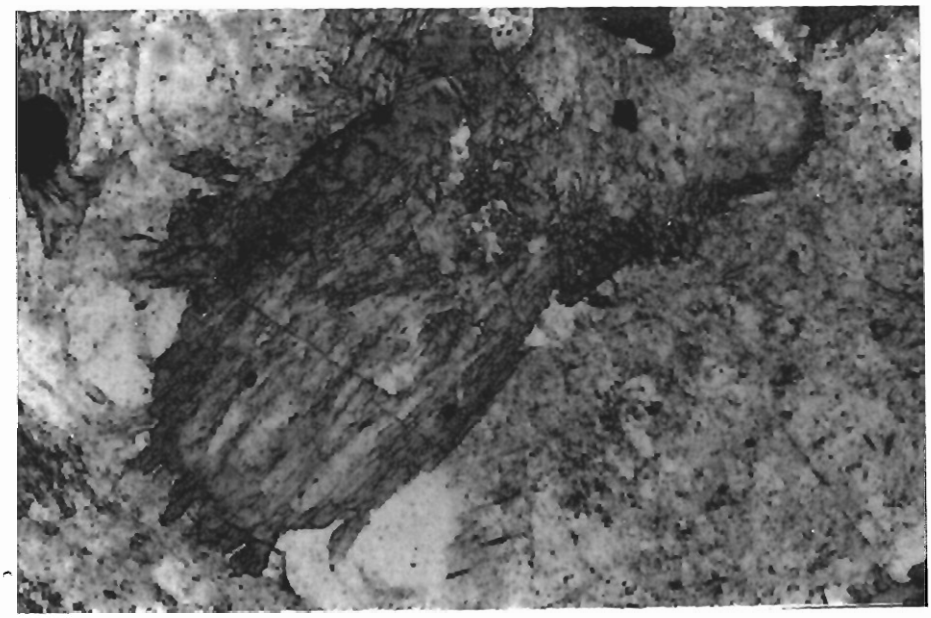

Pate. 5.2a. Photomicrograph showing the development of hornblende along the margins within amphibolite while the central part has trimolite/actinolite and chlorite. It appears that the original mineral was pyroxene which has been replaced by chlorite and trimolite/actinolite and then by hornblende during prograde metamorphism (Plane light; X4).

Plate 5.2b. Same view of the Plate-5.2a in cross light.

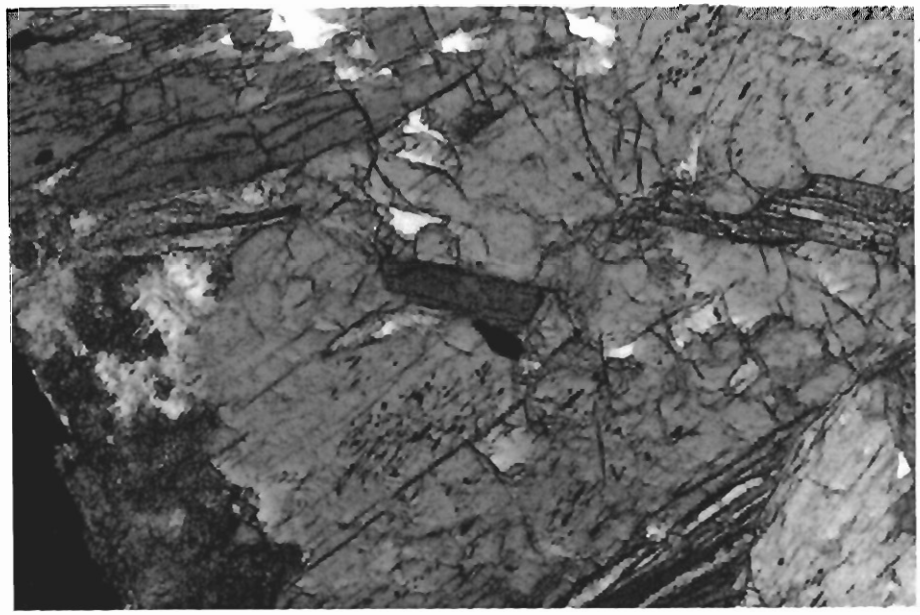

Plate. 5.3. Photomicrograph showing light-green to green hornblende enclosing brown colour biotite flake within amphibolite (Plane light; X2.5).

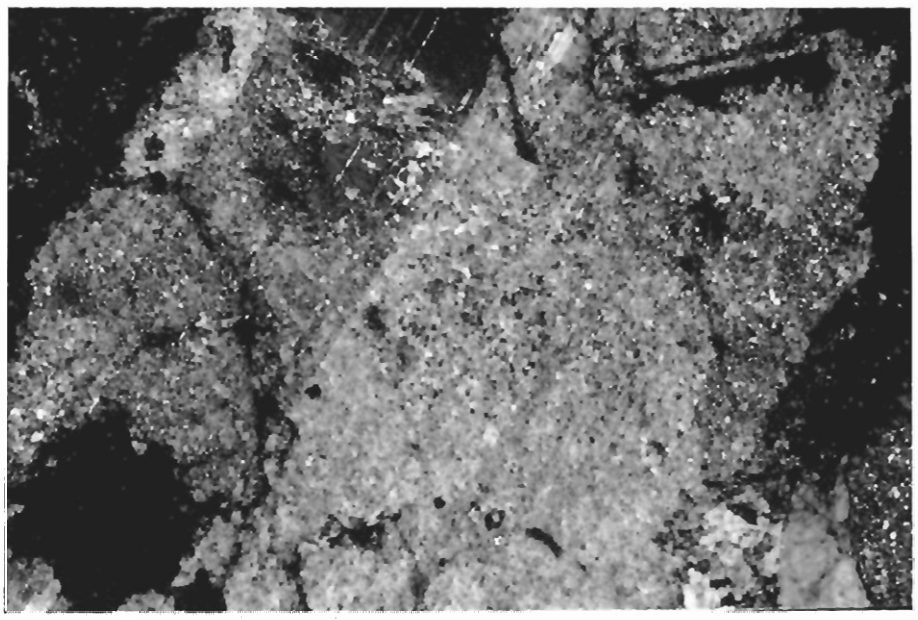

Plate. 5.4. Photomicrograph showing pseudomorph of plagioclase where plagioclase has been completely altered to sericite, epidote and carbonates (Cross light, X 2.5).

Fibrous amphibole, mainly trimolite/actinolite, (trace to 3%) occurs as light-green to colourless elongated grains in the form of bundles (Plate 5.5). It is usually present in association with hornblende or also as core material to hornblende.

Chlorite (trace to 20%) is generally present in association with opaque phase along fractures. It is usually replaced along margins by fibrous amphibole and hornblende. In few cases the replacement of chlorite by biotite along margins is also noticed. Sphene, apatite and rutile (in traces) is present in most of the samples as accessory minerals. Opaque phase (trace to 1%) is probably magnetite or titanomagnetite. It generally occurs as irregular mass, however, the disseminated grains are also not uncommon. In few cases leucoxene has also developed around the opaque phase. Epidote (trace to 2%) usually occurs as alteration product of plagioclase, mainly in the form of granular aggregates (Plate 5.6a &b). However, in few cases prismatic grains of bluish-grey colour (probably zoisite) have also been noticed.

There are fracture filled microveins of quartz, quartzo-feldspathic material and carbonates (Plate 5.7) which generally cross cut the hornblende and plagioclase grains. However, these veins also follow the foliation planes. These types of veins are very common within the shear zones. The amphibolites from these shear zones also have hornblende and plagioclase which are generally fractured, mortered and also reduced in size due to granulation.

It is evident from the mineralogical and textural faectures of these amphibolits that these are formed from an igneous rock of gabbro or gabbro-norite composition during prograde regional metamorphism. This rock has been subjected to greenschist facies metamorphism for considerable time

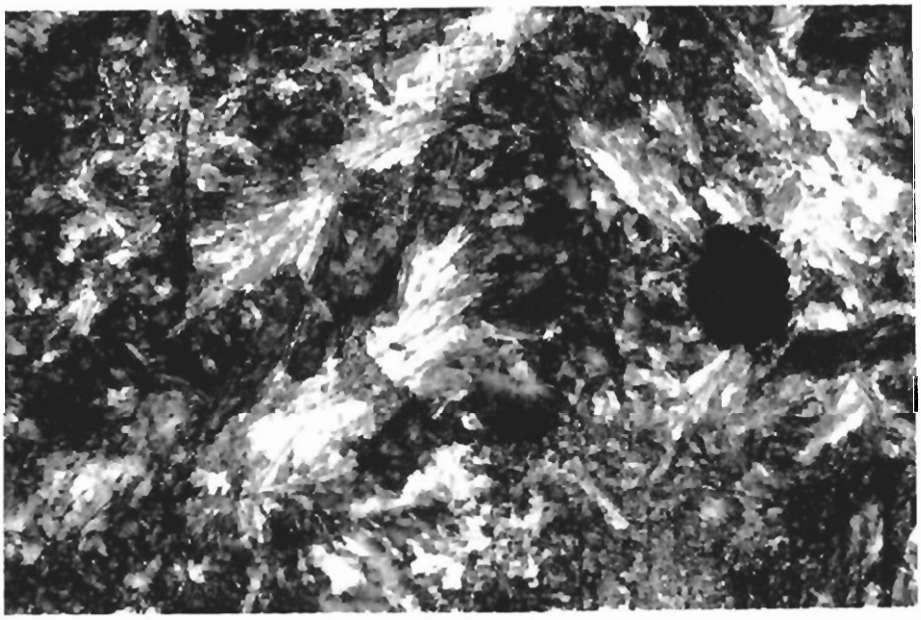

Plate. 5.5. Photomicrograph showing bundles of trimolite/ actinolite within amphibolite. (Cross light; X2.5).

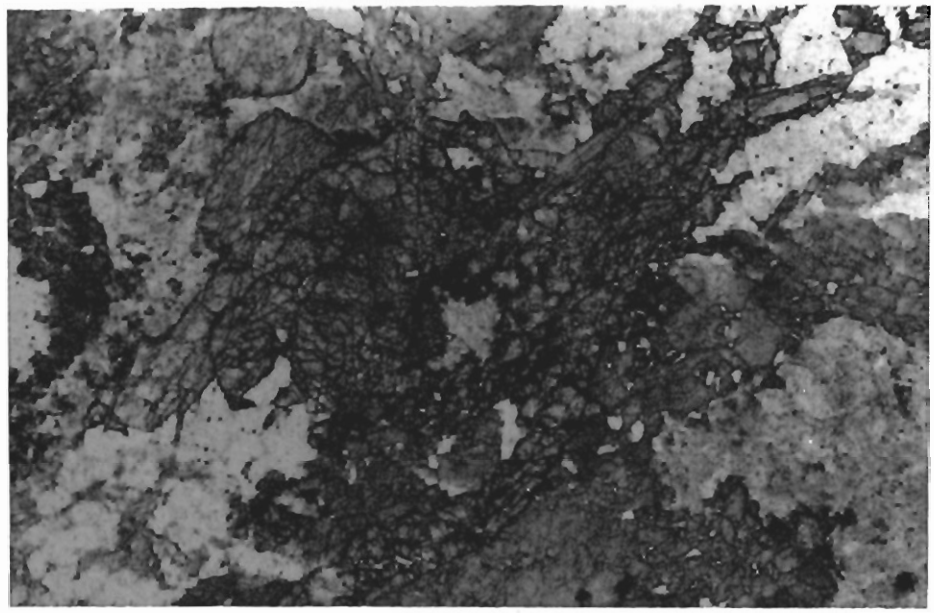

Plate. 5.6a. Photomicrograph showing the granular aggregates of epidote within amphibolite. The hornblende grains are also visible (Plane light; X2.5).

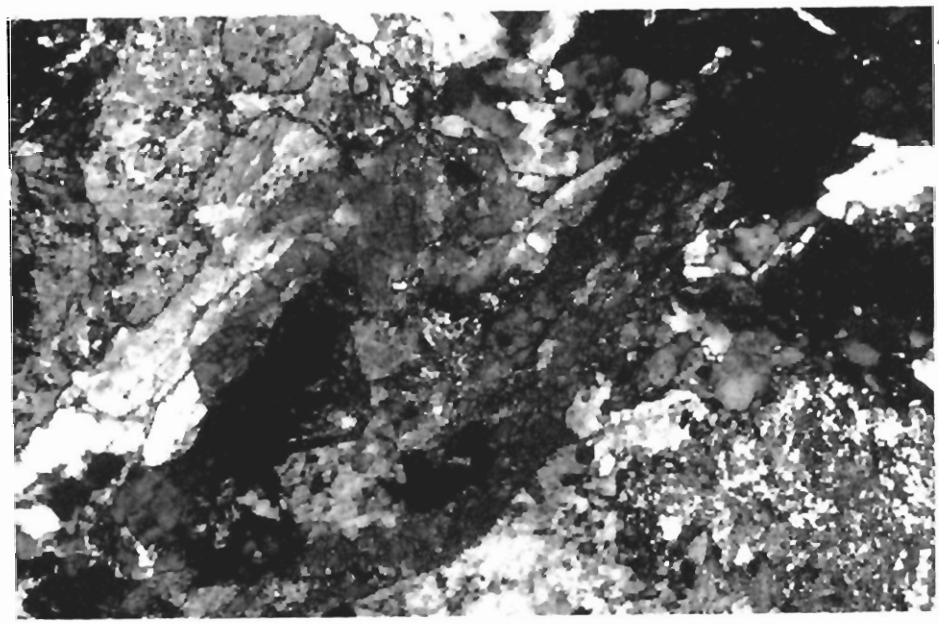

Plate. 5.6b. Same view of the Plate 5.6a in cross light.

which is indicated by the presence of chlorite, trimolite/actinolite, epidote and plagioclase of oligoclase to andesine composition. This is then followed by the amphibolite facies condition during regional metamorphism which is evident from the development of high proportion of hornblende and also progressive replacement of chlorite and trimolite/actinolite along the margins by hornblende. This whole paragenetic sequence suggests that the pyroxene, plagioclase and opaque phases within the protolith has played an important role in the development of existing mineralogy and texture of these amphibolite.

It has already been mentioned that the amphibolites have small bodies of gabbro-norites (Chapter-3). These rocks are probably the relics of protolith within these amphibolites. These rocks may have escaped the regional metamorphism by any reason and, therefore, have retained the original texture and mineralogy. This evidence also favour the petrographic observations whereby there is a systematic transformation of gabbro-norite to amphibolites with an intervening stage of greenschist facies metamorphism.

METAGABBRO-NORITE

It is medium-to coarse-grained rock having dark-grey to green colour on fresh surface and light-brown to yellowish-brown on weathered surface. Plagioclase, clinoproxene, orthopyroxene, biotite and hornblende can very easily be recognized in handspecimens.

In thin section, the rock is dominantly composed of plagioclase, clinopyroxene and orthopyroxene. However, in some cases the hornblende and biotite are also found in same proportion as of clinopyroxene and orthopyroxene (Table 5.2). Quartz, sphene, apatite, chlorite, epidote and opaque occur as minor constituents. It has hypidiomorphic to ideomorphic

Table. 5.2 Modal analyses (Visual estimates) of metagabbro-norites from Ushiri valley, District Dir.

	US31	US32	US35
Plagioclase	60	62	58
Orthopyroxene	18	15	16
Clinopyroxene	14	12	16
Hornblende	5	6	4
Biotite	2	1	3
Quartz	1	2	2
Sphene	Tr	Tr	Tr
Apatite	Tr	Tr	Tr
Chlorite	Tr	Tr	Tr
Epidote	Tr	Tr	Tr
Opaque	Tr	Tr	Tr

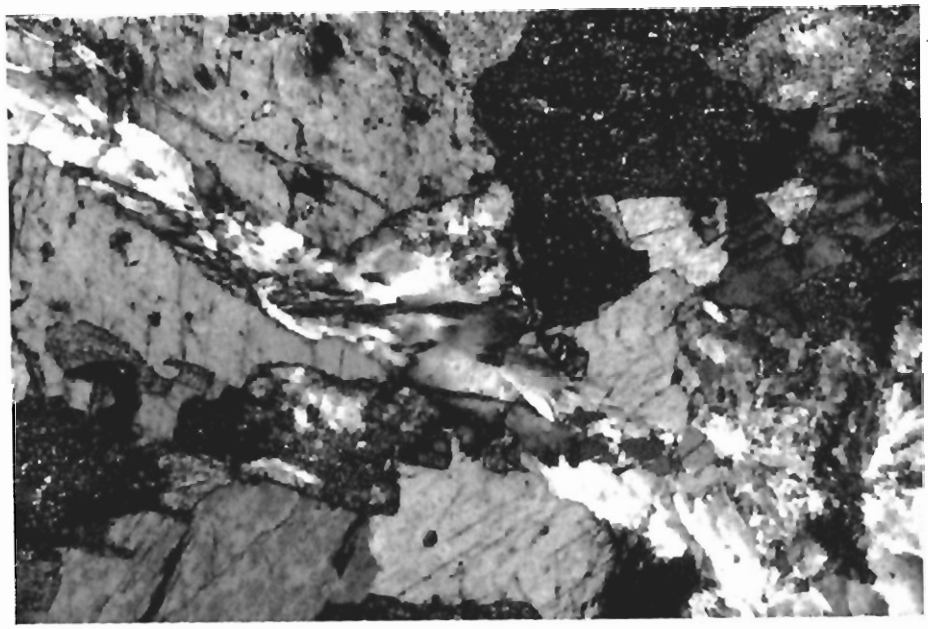

Plate. 5.7. Photomicrograph showing microvein of quartzo-feldspathic material cross cutting the hornblende grains within amphibolite (Cross light; X2.5).

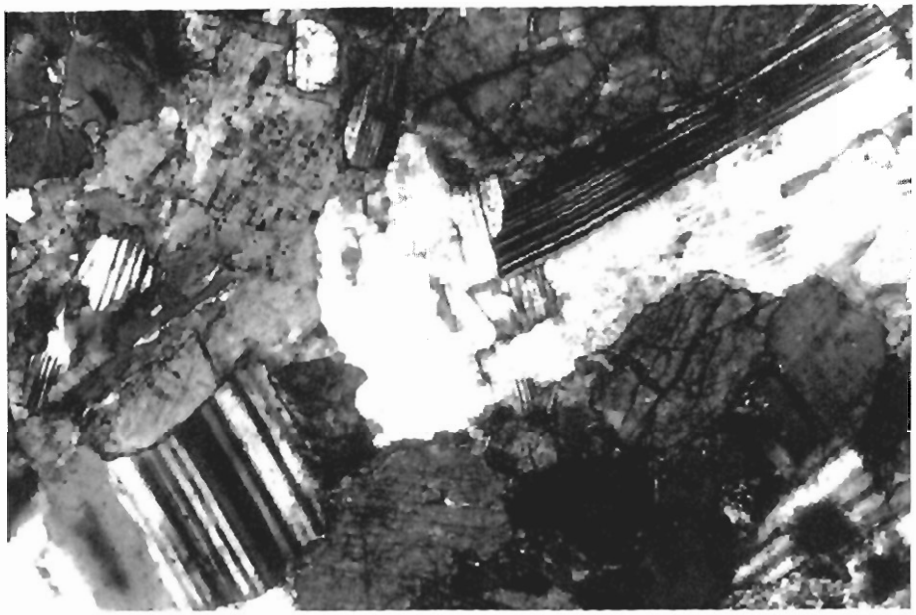

Plate. 5.8a. Photomicrograph showing the anhedral grains of ortho and clinophyroxene as an interstitial phase to plagioclase forming the ophetic texture within gabbro-norites (Cross light; X2.5).

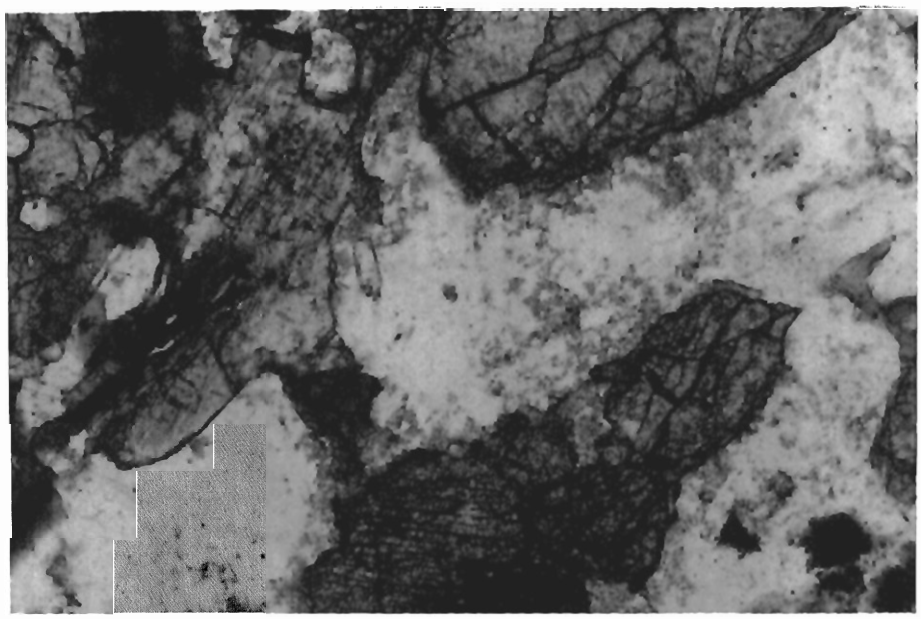

Plate. 5.8b. Same view of the Plate 5.8a in plane light.

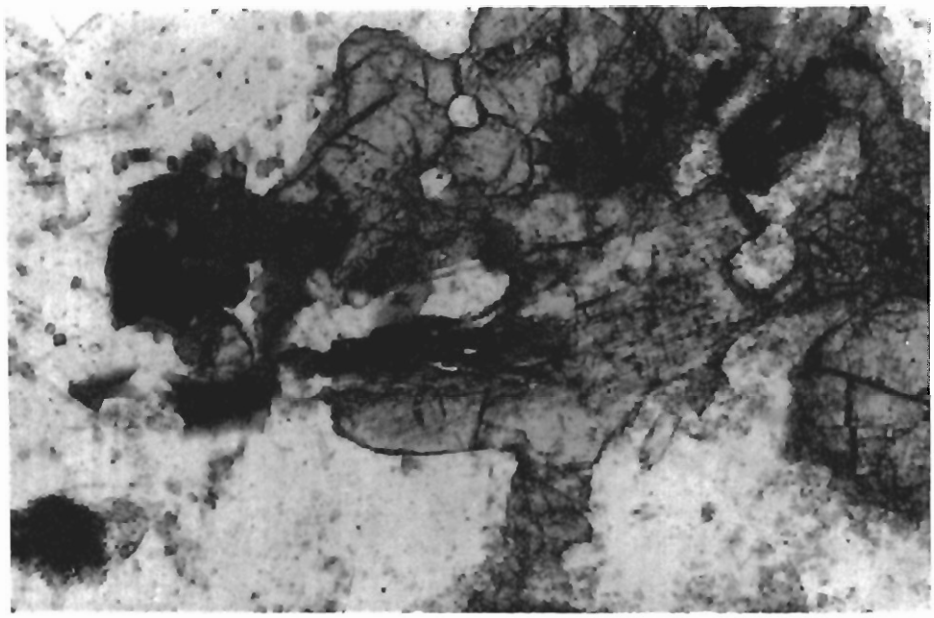

Plate. 5.9. Photomicrograph showing the prismatic grains of orthopyroxene. These are partially replaced along the margins by hornblende. Brown colour biotite has also developed in association with the opaque phase. (Plane light; X 2.5).

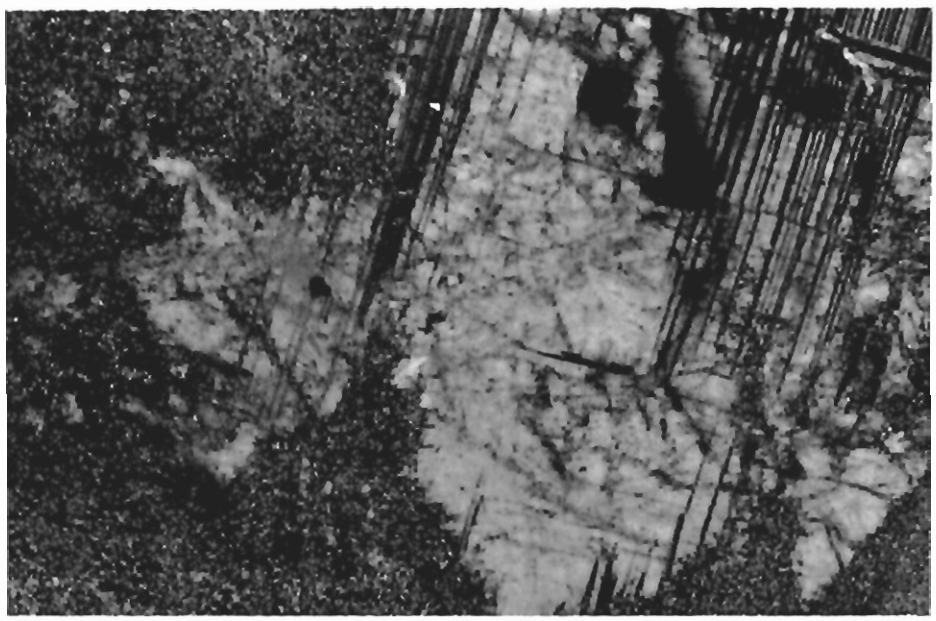

Plate. 5.10. Photomicrograph showing plagioclase grain having partial alteration to sericite and epidote along margins and fractures within the metadiorites (cross light; X2.5).

texture. At places, ophitic texture is also noticed (Plate 5.8a & b). Plagioclase (58 to 62%) is the dominant mineral phase and is ranging in composition from andesine to labradorite (An_{45-65}). It is medium-to coarse-grained subhedral to euhedral and is generally fresh. However, partially altered grains are also noticed. In some cases the plagioclase also has inclusions of pyroxene.

Orthopyroxene (15 to 18%) is medium to coarse-grained (Plate 5.9). It has pink to green or colourless pleochroism and is probably hypersthene or bronzite in compostion.

Clinopyroxene (12 to 16%) is medium to coarse-grained, colourless, non-pleochroic, and probably of augite composition (Plate 5.8a &b). Both clinopyroxene and orthopyroxene are present together and are generally of same proportion.

Occassionally, the clino and orthopyroxene are replaced by chlorite and hornblende along margins. In some cases, the corona structures with core of orthoproxene, middle rim of chlorite and the outermost rim of hornblende are noticed. In few cases, the pyroxene relics are noticed within the hornblende. Both clino and orthopyroxene are having exsolution of magnetite and or tintanomagnetit. These exsolved minerals occur in dissimination as well as in the form of striation, oriented paralld to cleavages, within these pyroxene.

Hornblende (4 to 6%) is light-green to green in colour. It is present as prismatic grains and has rounded to subrounded inclusions of quartz which impart peper mesh/seive texture to hornblende. These quartz grains may have been formed due to the release of excess silica during the transformation of pyroxene to hornblende. This suggest the metamorphic nature of these hornblendes.

Biotite (1 to 3%) has light-brown to dark-brown pleochroism. It is presant as elongated flakes in association with opaque phase. Fine grained opaque phase (magnetite/titanomagnetite) is usually found in dissimination, however, irragular grains are also noticed.

It is evident from the petrographic as well as field studies that these rocks could be the protoliths of amphibolites of the area. The replacement of pyroxene by chlorite and then by hornblende along the margins and the prismatic grains of metamorphic hornblende, having inclusions of quartz, are the evidence of systematic transformation of greenschist to amphibolite facies conditions. This rock, however, by any reason did not attain prolonged regional metamorphism due to which it retained the original mineralogy.

METADIORITE / QUARTZ-DIORITE

In handspacemen this rock is medium-to coarse-grained, compact, hard and massive in character. It has light-grey to dark-grey colour on fresh surface and brownish-grey on weathered surface. Plagioclase quartz, biotite and hornblende are easily recognized in hand spacimen.

In thin section, it is mainly composed of plagioclase with minor amount of alkali feldspar, quartz, biotite, muscovite and hornblende. Sphene, apatite, zircon, garnet and opaque occur as accessories. Kaolinite, sericite, muscovite, epidote carbonates and chlorite occur as alteration product (Table 5.3). It is having subhedral-to anhedral-minerals with hypidiomorphic to allutriomorphic texture. The rock has developed fabric due to the preferred orientation of minerals.

Table. 5.3. Modal analyses (Visual estimates) of metadiorite/Quartz-diorite from Ushiri valley, District Dir.

	US42	US62	US22	US21	US17	US11	US13	US15
Plagioclase	50	50	50	60	50	73	65	62
Orthoclase	25	30	30	25	30	15	25	17
Quartz	8	10	6	5	6	5	3	4
Epidote	5	3	2	1	Tr	Tr	1	Tr
Biotite	5	6	10	8	10	5	3	5
Muscovite	Tr	Tr	1	Tr	-	Tr	Tr	Tr
Hornblende	-	Tr	-	-	3	1	2	10
Garnet	-	-	Tr	-	-	-	Tr	-
Apatite	Tr	Tr	Tr	-	Tr	Tr	-	Tr
Sphene	Tr	Tr	Tr	-	-	-	Tr	-
Zircon	Tr	Tr	-	-	Tr	-	-	-
Opaque	Tr	Tr	Tr	Tr	Tr	Tr	Tr	Tr
An % Plagioclase	42	34	38	45	40	36	45	38

Plagioclase (50 to 73%) is in the range of oligoclase to andesine having An_{34-45}. It is subhedral to anhedral and is variably altered. In some samples the plagioclase grains are generally fresh and have partial alteration along margins to sericite and epidote (Plate 5.10) while in others it is severely altered. In the specimens of intense alteration the majority of plagioclase grains are completely saussuritized / epidotized, leaving behind pseudomorphs of plagioclase. Relics of plagioclase are also observed within the matrix of sericite, epidote and carbonate. Plagioclase is occasionally fractured and these fractures are filled in by epidote and carbonates (Plate 5.11). The samples from sheared zones are highly tectonized. Here the plagioclase porphyroblsts are mortared and rotated. Biotite and muscovite swirl and wind around the porphyroblasts and imparted gneissosity in the rock. In some cases the plagioclase grains exhibit alteration from core towards margin where the plagioclase rim is left unaltered (Plate 5.12).

Alkali feldspar (15 to 30%) occurs as irregular-to subhedral-grains, mainly within the interstices of plagioclase. It is generally partially altered to kaolinite and muscovite, however, the fresh grains are not uncommon. It usually shows undulose extinction. Quartz (3 to 10%) is an interstitial phase and is generally irregular and strained.

Biotite (3 to 10%) is generally brown-to light-brown in colour but co-existing green to light-green pleochroic flakes of biotite are also noticed (Plate 5.13). Muscovite is generally present in association with biotite. These micaceous phases occasionally swirl/and wind around the plagioclase and orthoclare grains. In some samples (S.No.17) the amount of biotite reaches to >10%. These rocks could be named as biotite-diorite.

Epidote (trace to 5%) generally occurs as small granular aggregates, however, prismatic grains with high birefregent colours are also noticed. It is

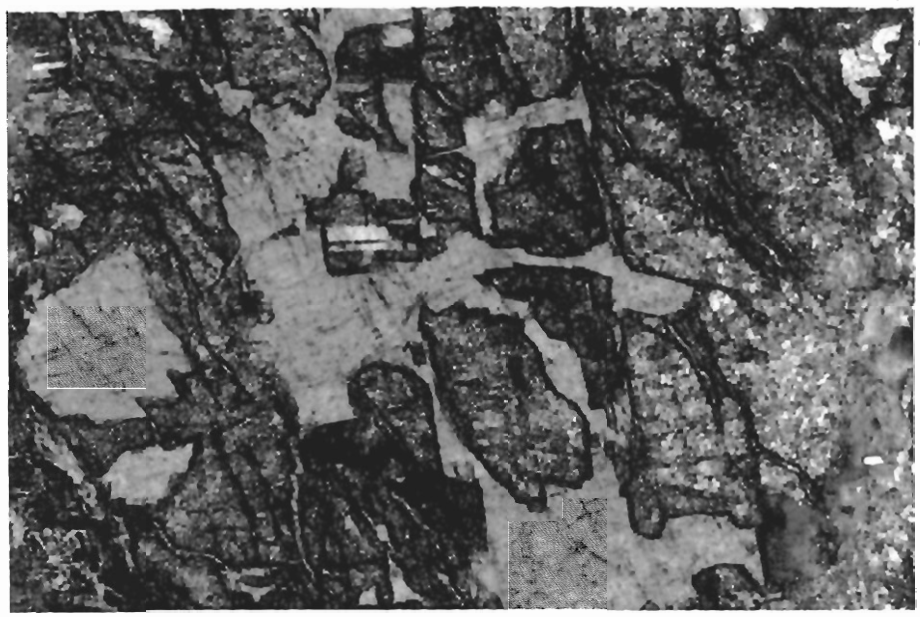

Plate. 5.11. Photomicrograph showing the plagioclase grain which has been altered to epidote and carbonate along fractures within the metadiorite/quartz-diorite (cross light; X2.5).

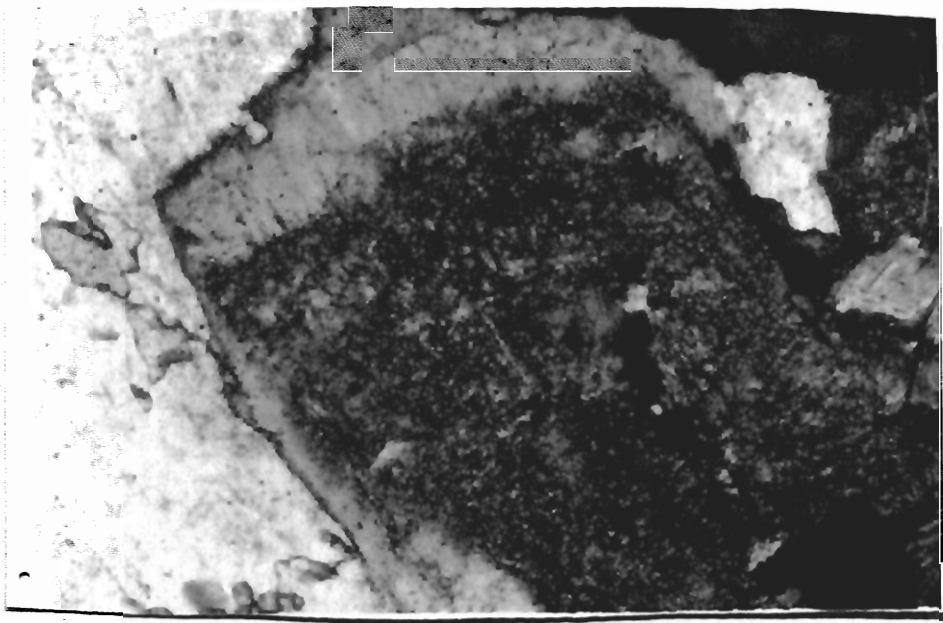

Plate. 5.12. Photomicrograph showing sauseritization and epidotization of plagioclase grain from core towards margin. The margins are, however, not altered and form a rim around the altered plagioclase within metadiorite/quartz-diorite (cross light; X4).

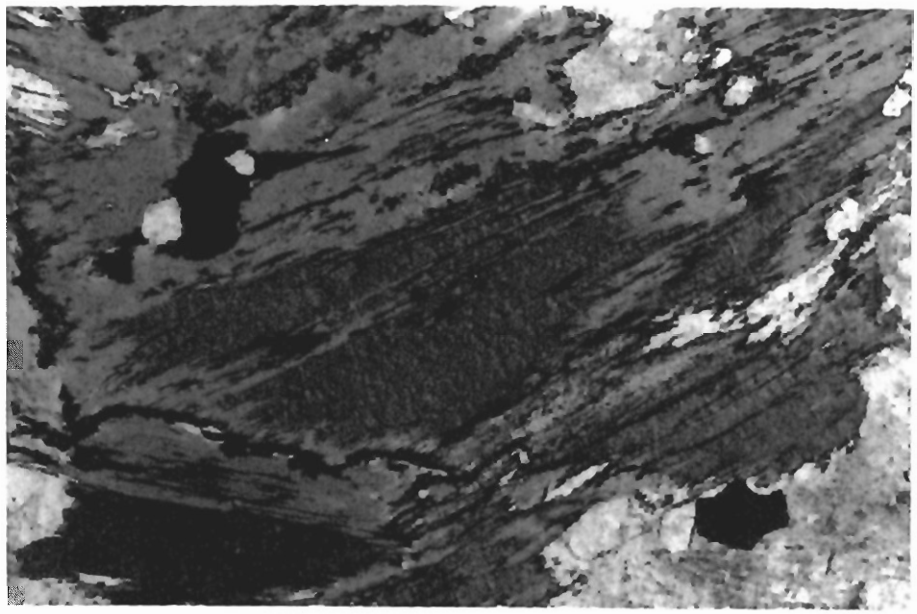

Plate. 5.13. Photomicrograph showing coexisting green and brown colour biotite within metadiorite/quartz-diorite (Plane light; X2.5).

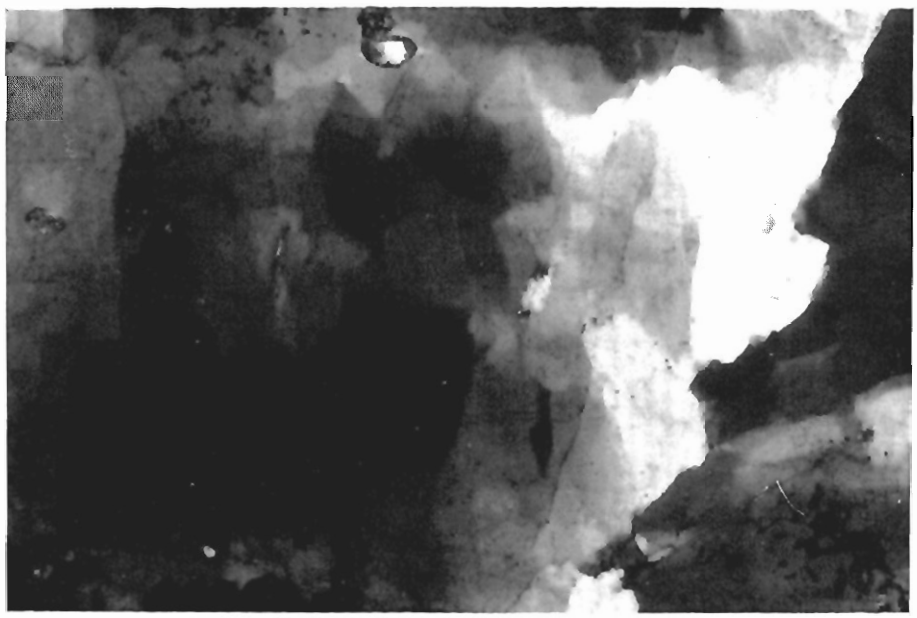

Plate. 5.14. Photomicrograph showing the undulose extinction/ pressure shadows in the grains of orthoclase within the metagranodiorite (cross light; X2.5).

usually associated with opaque phase and is the alteration product of plagoiclase.

Few small rounded to subrounded and fractured grains of garnet are also noticed in some slides . It is present in proximity to opaque phase. Chlorite, if present, is usually developed around the opaque phase.

Hornblende (trace to 10%) is present in some samples. It occurs as prismatic grains of light-green to green colour. In one sample (No.15) the amount of hornblende reaches up to >10% and can be named as hornblende-diorite.

In some cases, microfractures in these rocks are filled in by the quartz, quartzo-feldspathic and carbonate material.

Sphene, apatite, zircon and opaque (magnetite/ titanomagnetit) are present in traces.

METAGRANODIORITE

The rock is generally medium-to coarse-grained, light-grey to grey in colour. Plagioclase, orthoclase, quartz, biotite and muscovite are easily recognizable in hand specimens. These minerals have preferred orientation along the fabric direction.

Petrographically the rock is dominantly composed of alkali feldspar, plagioclase and quartz with minor amount of biotite, muscovite, and epidote. Garnet, zircon and opaque occur as accessories. This rock generally has subhedral grains and hypidiomorphic texture. The modal composition is shown in Table 5.4.

Table. 5.4. Modal analyses (Visual estimates) of metagranodiorite from Ushiri valley, District Dir.

	US77	US78	US45	US57
Plagioclase	30	32	28	30
Orthoclase	43	42	40	41
Quartz	20	22	25	24
Biotite	3	2	3	2
Muscovite	2	1	2	2
Epidote	Tr	Tr	1	Tr
Garnet	Tr	Tr	-	-
Apatite	-	Tr	Tr	Tr
Sphene	-	-	-	Tr
Zircon	Tr	-	-	-
Opaque	Tr	Tr	Tr	Tr

Alkali feldspar (~ 40%) occurs as subhedral grains. It is usually altered to kaolinite, sericite and muscovite. However, fresh grains with undulose extinction are not uncommon (Plate 5.14). Some grains also show vermicular intergrowth.

Plagioclase (28 to 32%) is oligoclase (An_{12-22}) in composition and is usually zoned (Plate 5.15). However, unzoned grains are also not uncommon. Occasionally, the outermost zone of plagioclase is unaltered while rest of the plagioclase is altered. It is generally partially altered to epidote, sericite and carbonates (Plate 5.16). In some cases the alteration is so intense that the whole grain is saussuritized. Plagioclase is generally fractured whereby the epidote is developed (Plate 5.17). Quartz (20 to 25%) is present as irregular grains within the interstices of feldspar. It generally shows pressure shadows due to high strain.

Biotite (up to 3%) and muscovite (up to 2%) occur together in the form of bundles within the interstices of feldspar (Plate 5.18). Biotite usually exhibits light-green to green pleochroism, however, light-brown to brown pleochroic grains are also noticed.

Epidote (up to 1%) occurs as granular aggregates and is usually the alteration product of feldspar. It is also found in association with biotite and muscovite lying adjacent to the opaque phase. In one thin section small rounded colourless and fractured grains of garnet are also noticed. Opaque phase (magnetite) is found in dissimination.

The rock, at places, is highly tectonized. In these rocks the large grains (porphyroblast) of feldspar and quartz are rotated and mortered and are usually present within the fine grained felsic mass. Large flakes of biotite and

Plate. 5.15. Photomicrograph showing zoned plagioclase within the granodiorites. This plagioclase grain has been altered along the core to epidote and sericite etc. (Cross light; X2.5).

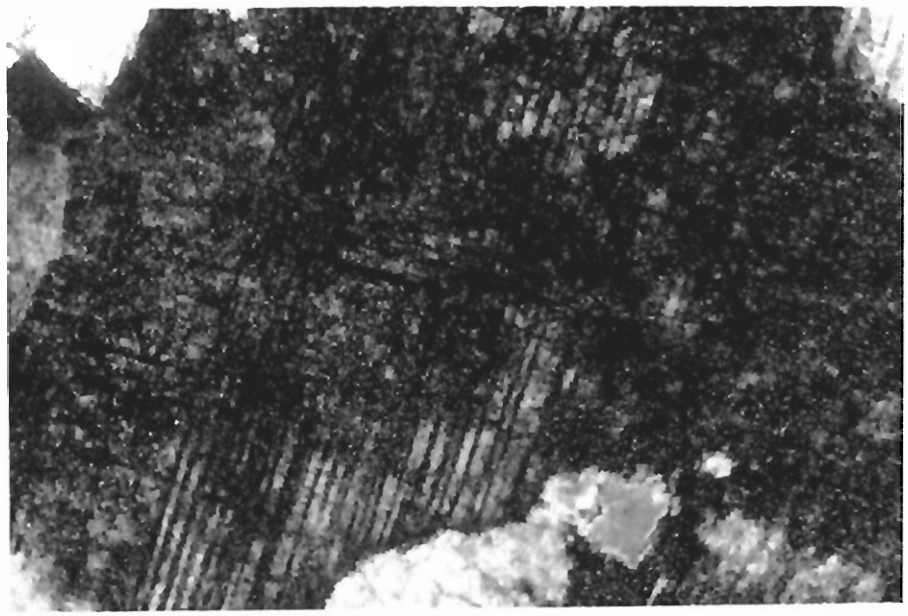

Plate. 5.16. Photomicrograph showing partially altered plagioclase grain within the metagranodiorite. The alteration product is mainly epidote and sericite (cross light; X2.5).

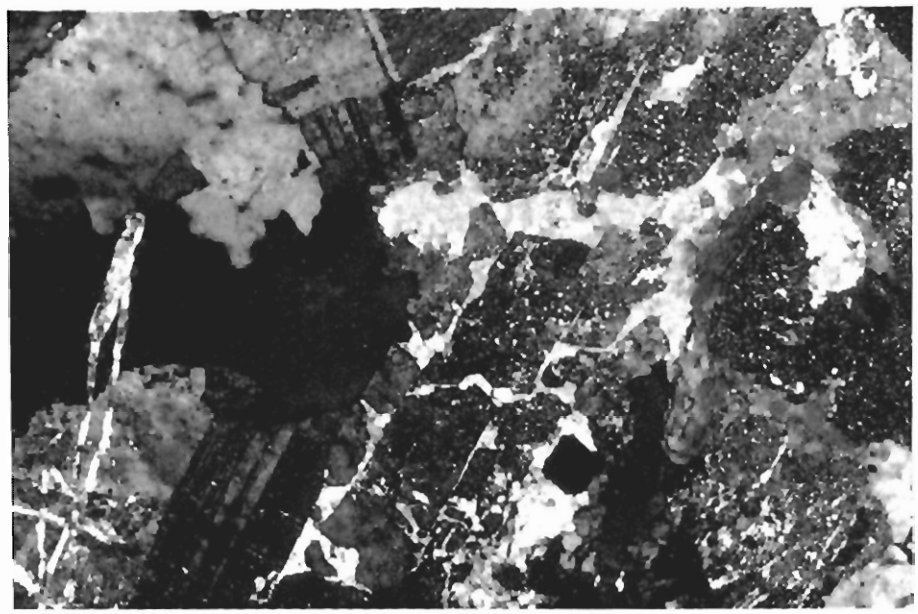

Plate. 5.17. Photomicrograph of fractured plagioclase within metagranodiorite. The fractures are filled in by the epidote (cross light; X2.5).

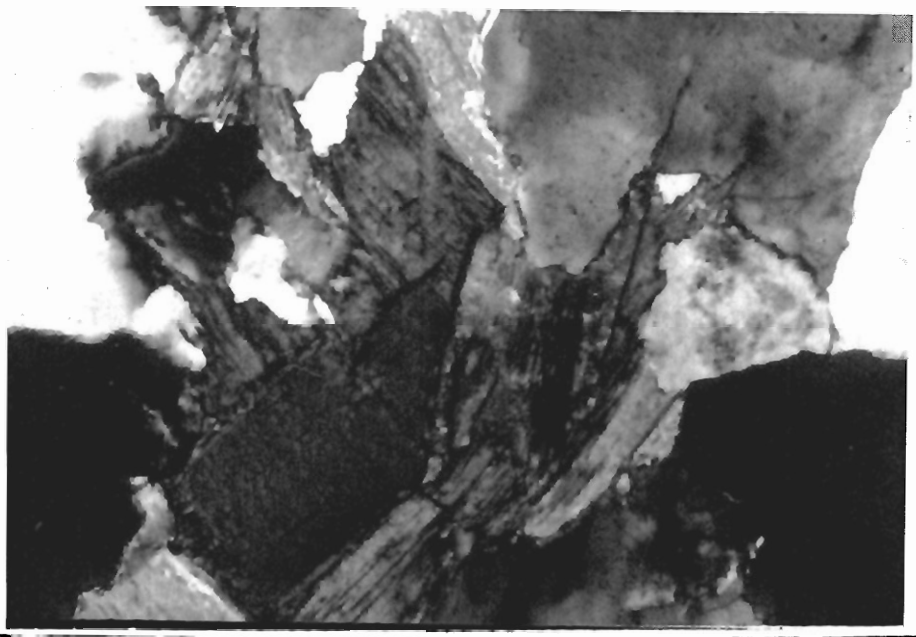

Plate. 5.18. Photomicrograph showing the biotite and muscovite flakes within the interstices of feldspar in metagranodiorite (cross light; X2.5).

muscovite swirl and wind around the porphyroblasts of feldspar and quartz. This has imparted gneissose texture to these rocks. At places where the rock is intensely tectonized and altered, there only relics of plagioclase and alkali feldspar are present within the fine grained matrix of epidote, sericite , muscovite, kaolinite and carbonates which are the alteration products of the former phases (i.e., plagioclase and alkali feldspar).

CHAPTER-6

WHOLE ROCK GEOCHEMISTRY

Representative samples of amphibolites, gabbro-norites, diorites/quartz-diorite and granodiorite from the studied area have been selected on the basis of petrographic studies.

In order to establish the original geochemical constraints including nomenclature classification, chemical verification and tectonic affinity of these rocks, fresh samples have been selected for analyses. Keeping in view the field relationships and the petrographic features of various types of rocks of the area (see chapter 3 & 5), two main groups a) amphibolites and gabbro-norites and b) diorite/quartz-diorite and granodiorite have been treated separately in this chapter.

The major and trace elements have been determined by using Atomic absorption spectrophotometer and UV/visible spectrophotometer at the geochemistry laboratory of the National Centre of Excellence in Geology, University of Peshawar. The detail methodology has been given in the Chapter 4.

A) AMPHIBOLITES AND GABBRO-NORITES

Major and trace element data along with CIPW norms and Niggli values have been presented in Table 6.1. As the iron has been determined as Fe_2O_3 and then calculated as FeO and Fe_2O_3 only for norms calculation, therefore, the calculated CIPW norms may be slightly different from what they would be if the FeO and Fe_2O_3 would have been chemically determined separately. However, this effect should not be too high.

Table 6.1. Major and trace element data along withC.I.P.W. norms and Niggli values for the amphibolite and gabbro-norite from Ushiri valley, central Dir.

Amphibolites

S.No	US25	US27	US30	US33	US36	US47	US49	US50	US52
SiO_2	50.88	53.19	52.13	50.16	52.89	47.56	51.36	51.56	53.10
TiO_2	0.82	0.69	0.60	0.86	0.69	0.95	0.66	0.64	0.63
Al_2O_3	19.76	18.12	19.45	19.88	18.78	20.12	19.56	20.45	18.75
Fe_2O_3	7.34	6.18	7.12	7.06	6.45	8.45	6.77	6.67	6.41
MnO	0.14	0.12	0.15	0.13	0.12	0.14	0.14	0.16	0.11
MgO	5.12	4.73	4.98	5.45	4.45	5.34	4.85	4.78	4.23
CaO	9.08	8.12	8.56	9.23	8.34	11.67	8.69	8.58	8.02
Na_2O	2.89	3.25	2.94	2.84	3.20	2.09	2.40	2.50	3.08
K_2O	1.10	1.23	1.09	1.03	1.18	0.78	0.89	0.88	1.34
P_2O_5	0.25	0.20	0.26	0.21	0.21	0.28	0.18	0.20	0.21
L.O.I	2.15	3.13	1.98	1.14	1.45	3.13	2.17	1.58	3.05
Total	99.83	99.11	99.34	98.36	97.96	100.90	97.87	98.16	99.08
Trace elements in ppm (Au in ppb)									
Cu	70	51	53	51	14	58	52	14	39
Pb	31	39	48	57	43	38	28	30	24
Zn	134	142	124	145	114	109	74	121	61
Ni	87	72	76	98	70	94	78	76	67
Cr	134	129	129	156	120	145	132	98	89
Co	56	45	57	58	34	63	38	30	29
Ag	<0.5	<0.5	<0.5	<0.5	<0.5	<0.5	<0.5	<0.5	<0.5
Au	3	4	2	0	0	4	7	8	3

(continued table 6.1)

C.I.P.W. norms

S.No	US25	US27	US30	US33	US36	US47	US49	US50	US52
Q	1.07	4.40	2.93	0.27	4.16	0.00	5.83	5.37	5.14
Or	6.71	7.62	6.67	6.31	7.28	4.76	5.54	5.42	8.30
Ab	25.18	28.79	25.69	24.85	28.19	18.21	21.33	22.01	27.27
An	38.80	32.67	37.85	39.76	34.76	44.49	41.98	43.02	34.92
Di	4.87	6.67	3.54	5.08	5.68	10.90	1.76	0.00	4.32
Hy	19.14	16.45	19.96	19.41	16.37	13.45	20.04	20.53	16.64
Ol	0.00	0.00	0.00	0.00	0.00	3.24	0.00	0.00	0.00
Mt	1.48	1.27	1.44	1.43	1.32	1.70	1.39	1.36	1.31
Il	2.19	1.67	1.34	2.42	1.76	2.62	1.72	1.58	1.55
Ap	0.56	0.46	0.59	0.47	0.48	0.63	0.41	0.45	0.48
Niggli values									
si	133	151	141	130	149	115	142	141	153
al	30	30	31	30	31	29	32	33	32
fm	35	34	35	35	33	35	34	34	32
c	26	25	25	26	25	30	26	25	25
alk	9	11	10	9	11	6	8	8	11
k	0.20	0.20	0.20	0.19	0.20	0.20	0.20	0.19	0.22
mg	0.58	0.60	0.58	0.60	0.57	0.55	0.58	0.58	0.56
Mg#	58.02	60.26	58.08	60.46	57.75	55.59	58.66	58.67	56.66

(continued table 6.1)

Amphibolite

S.No	US58	US60	US64	US65	US70	US72	US84	US89
SiO_2	53.74	49.59	52.78	48.98	51.53	48.78	49.45	50.20
TiO_2	0.65	0.83	0.70	0.92	0.81	1.02	0.86	0.84
Al_2O_3	18.67	20.14	19.67	20.45	19.68	20.34	20.12	20.43
Fe_2O_3	6.58	8.36	6.30	8.49	7.16	8.33	8.44	7.24
MnO	0.14	0.13	0.12	0.18	0.14	0.15	0.16	0.15
MgO	4.12	5.23	4.47	5.39	4.68	5.34	5.12	4.97
CaO	8.12	9.64	8.57	9.12	8.38	9.28	9.39	8.38
Na_2O	3.06	2.76	2.90	2.68	2.87	2.81	3.11	2.95
K_2O	1.04	0.78	0.83	0.68	0.75	0.81	1.14	0.88
P_2O_5	0.19	0.21	0.18	0.28	0.20	0.27	0.28	0.19
L.O.I	1.90	2.09	2.63	3.93	1.72	1.89	1.65	3.21
Total	98.25	100.05	99.34	101.42	98.19	99.34	99.95	99.73
Trace elements in ppm (Au in ppb)								
Cu	40	87	84	95	78	64	39	45
Pb	34	30	27	32	37	29	30	27
Zn	64	113	118	81	98	110	106	99
Ni	60	89	73	96	72	87	82	79
Cr	95	112	121	145	105	122	118	108
Co	34	54	32	61	55	62	59	42
Ag	<0.5	<0.5	<0.5	<0.5	<0.5	<0.5	<0.5	<0.5
Au	0	2	5	0	7	4	1	3

(continued table 6.1)

C.I.P.W. norms

S.No	US58	US60	US64	US65	US70	US72	US84	US89
Q	6.77	0.00	5.92	0.05	4.56	0.00	0.00	1.38
Or	6.42	4.75	5.11	4.16	4.63	4.95	6.91	5.43
Ab	27.01	24.00	25.49	23.42	25.31	24.56	26.95	26.01
An	35.60	41.36	39.68	43.12	40.23	41.82	38.47	41.57
Di	4.26	5.23	2.73	1.47	1.49	3.26	6.10	0.43
Hy	16.79	19.58	17.62	22.99	19.73	17.56	9.36	21.03
Ol	0.00	0.69	0.00	0.00	0.00	2.91	7.76	0.00
Mt	1.34	1.68	1.28	1.72	1.46	1.69	1.69	1.48
Il	1.37	2.19	1.76	2.44	2.14	2.63	2.12	2.24
Ap	0.43	0.47	0.41	0.63	0.46	0.61	0.63	0.43
Niggli values								
si	155	125	148	124	142	123	124	134
al	32	30	32	30	32	30	30	32
fm	33	36	32	37	34	36	36	35
c	25	26	26	25	25	25	25	24
alk	10	8	9	8	9	8	9	9
k	0.18	0.16	0.16	0.14	0.15	0.16	0.19	0.16
mg	0.55	0.55	0.58	0.55	0.56	0.56	0.54	0.57
Mg#	55.37	55.34	58.43	55.71	56.42	55.95	54.58	57.63

(continued table 6.1)

Gabbro-norites

S.No	US31	US32	US35
SiO_2	53.45	49.78	52.98
TiO_2	0.70	0.77	0.73
Al_2O_3	18.65	19.67	18.78
Fe_2O_3	7.03	8.34	7.28
MnO	0.15	0.13	0.12
MgO	5.45	5.68	5.59
CaO	9.34	9.42	9.38
Na_2O	2.94	2.74	2.99
K_2O	0.78	0.72	0.75
P_2O_5	0.26	0.21	0.21
L.O.I	1.42	1.36	1.45
Total	100.25	99.17	100.33
Trace elements in ppm (Au in ppb)			
Cu	48	67	54
Pb	39	54	43
Zn	108	134	98
Ni	87	92	89
Cr	110	142	138
Co	54	43	39
Ag	<0.5	<0.5	<0.5
Au	2	4	6
C.I.P.W norms			
Q	4.28	0.03	3.13
Or	4.70	4.39	4.52
Ab	25.31	23.98	25.73
An	35.99	40.45	36.20
Di	7.73	5.19	7.98
Hy	18.51	21.87	18.90
Mt	1.40	1.51	1.45
Il	1.51	2.19	1.55
Ap	0.58	0.47	0.47
Mg#	60.56	57.43	60.34

The amphibolites have wide range of SiO_2 (47.56 - 53.74%), low TiO_2 (0.60- 1.02%), high Al_2O_3 (18.12-20.45%). Fe2O3 is ranging from 6.18 to 8.49%, MnO from 0.11 to 0.18%, MgO from 4.12 to 5.45%, CaO from 8.02 to 11.67%, Na_2O from 2.09 to 3.25%, K_2O from 0.68 to 1.34% and P_2O_5 from 0.18 to 0.28% (Table-6.1). Among the trace elements Cu is ranging from 14 to 95 ppm, Pb from 24 to 57 ppm, Zn from 61 to 145 ppm, Ni from 60 to 98 ppm, Cr from 89 to 156 ppm, Co from 29 to 62 ppm, Ag is <0.5 ppm. Among the normative minerals Q = 0.05-6.77%; Or = 4.16 - 8.30%; Ab = 18.21-28.79%; An = 32.67-44.49%; C= 0- 0.24%; Di = 0.43- 10.90%; Hy = 9.36-22.99%; Ol = 0.69-7.76%; Mt = 1.27-1.72%; Il = 1.34-2.63% and Ap = 0.41 - 0.63% (Table 6.1). The Mg# is ranging from 54.58-60.46 (Table 6.1).

The gabbro-norites have SiO_2= 49.78-53.45%; TiO_2 = 0.70-0.77%; Al_2O_3 = 18.65-19.67%; Fe_2O_3 = 7.03-8.34%; MnO = 0.12-0.15%; MgO = 5.45-5.68%; CaO = 9.34-9.42%; Na_2O = 2.74-2.99%; K_2O = 0.72-0.78% and P_2O_5 = 0 21-0.26% (Table 6.1). Among the trace elements these rocks have Cu in the range of 48 to 54 ppm; Pb 39 to 54 ppm; Zn 98 to 134 ppm; Ni 87 to 92 ppm; Cr 110 to 142 ppm; Co 39 to 54 ppm, Ag is less than 0.5 ppm and Au is 2 to 6 ppb (Table 6.1).

Normative minerals include Q (0.03-4.28%), Or (4.39-4.70%), Ab (23.98-25.73%), An (35.99-40.45%), Di (5.19-7.98%), Hy (18.51-21.87%), Mt (1.40-1.51%), Il (1.51-2.19%) and Ap (0.47-0.58%) (Table 6.1). Mg# (57.43-60.56) of the gabbro-norites is within the range of host-amphibolite (Table 6.1). It is evident from the Table 6.1 that both amphibolites and gabbro-norites are having more or less same major and trace element and CIPW norms and are, therefore, treated together in all the geochemical diagrams.

ORTHO OR PARA AMPHIBOLITES

The studies show that the amphibolites can be formed by metamorphism of a) basic igneous rocks, b) mixture of sediments and tuffs. c) mixture of limestone, dolomite and pelite in an appropriate proportion and d) metasomatism of igneous and sedimentary rocks. In the past, the homogeneous amphibolites were termed as igneous and those having banded structures and association with sedimentary rocks were termed as sedimentary in origin (Wilcox and Poldervaart, 1958; Walker et al., 1960; Heier, 1962). Later studies, however, suggest that the banded nature or association of sedimentary rocks are not proof of formation of amphibolites from sedimentary rocks. The banding can be produced by the metamorphic segregation processes (Evans and Leake, 1960; Orville, 1969).

Inspite of field features, e.g., having homogeneous nature, various geochemical characteristics are employed to determine the type of protolith, whether igneous (ortho) or sedimentary (para), for the studied amphibolites.

In this regard the work of Leak 1964, is of greater importance. He has employed Niggli values (Niggli, 1954) as genetic indicators whereby they have distinguished the parent rocks of amphibolites by comparing their variation trend to those of igneous and sedimentary rocks.

The data when plotted in the c-mg-(al-alk) (Fig.6.1) and C vs mg (Fig. 6.2) diagrams of Leake (1964), all the data follow the magmatic trend represented by the middle stage differentiation of Karro-dolorite of S. Africa. It suggests that the clinopyroxene and calcic-plagioclase were probably the dominant phases during fractionation (see Leake, 1964). The data, however,

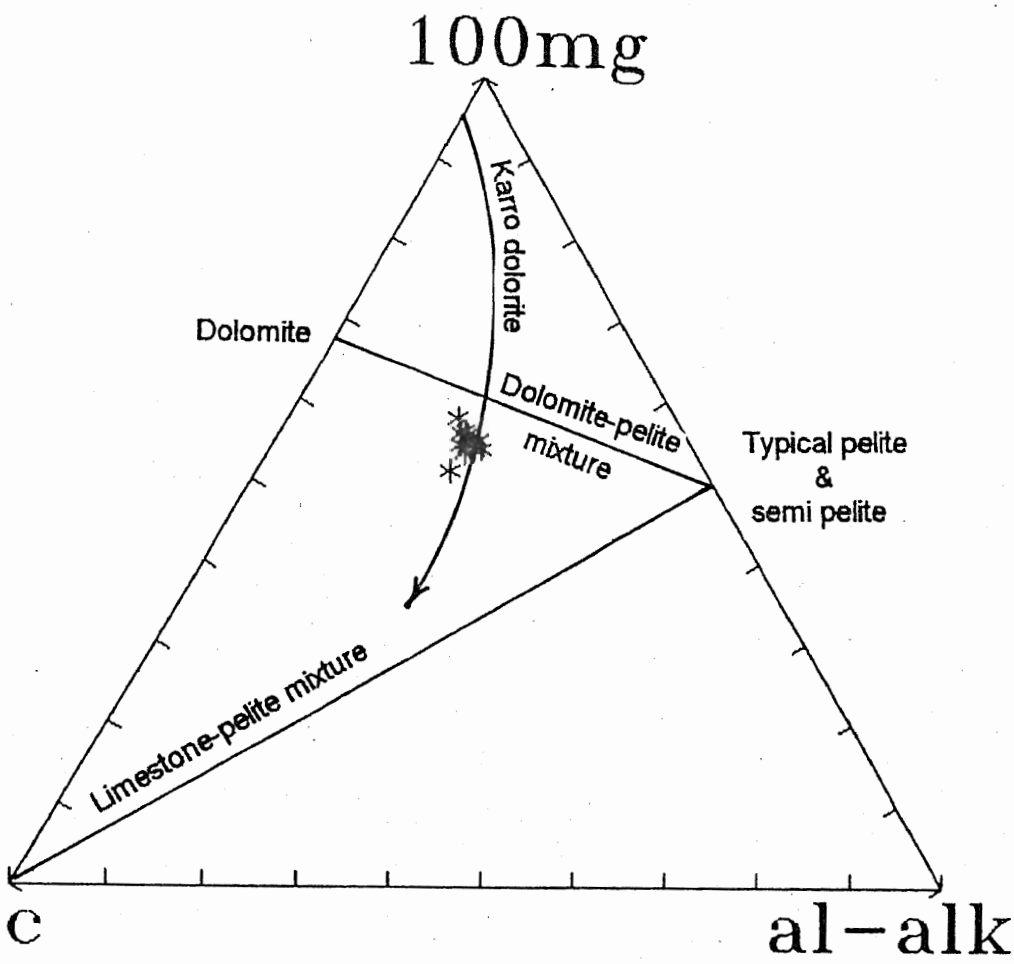

Fig.6.1. Plot of mg+(al-alk)+C=100 for the amphibolites and gabbor-norites of the Ushiri valley, central Dir, Trend of Karroo dolorites is after Leak, 1964.

Symbols: * = Amphibolite
* = Gabbro-norite

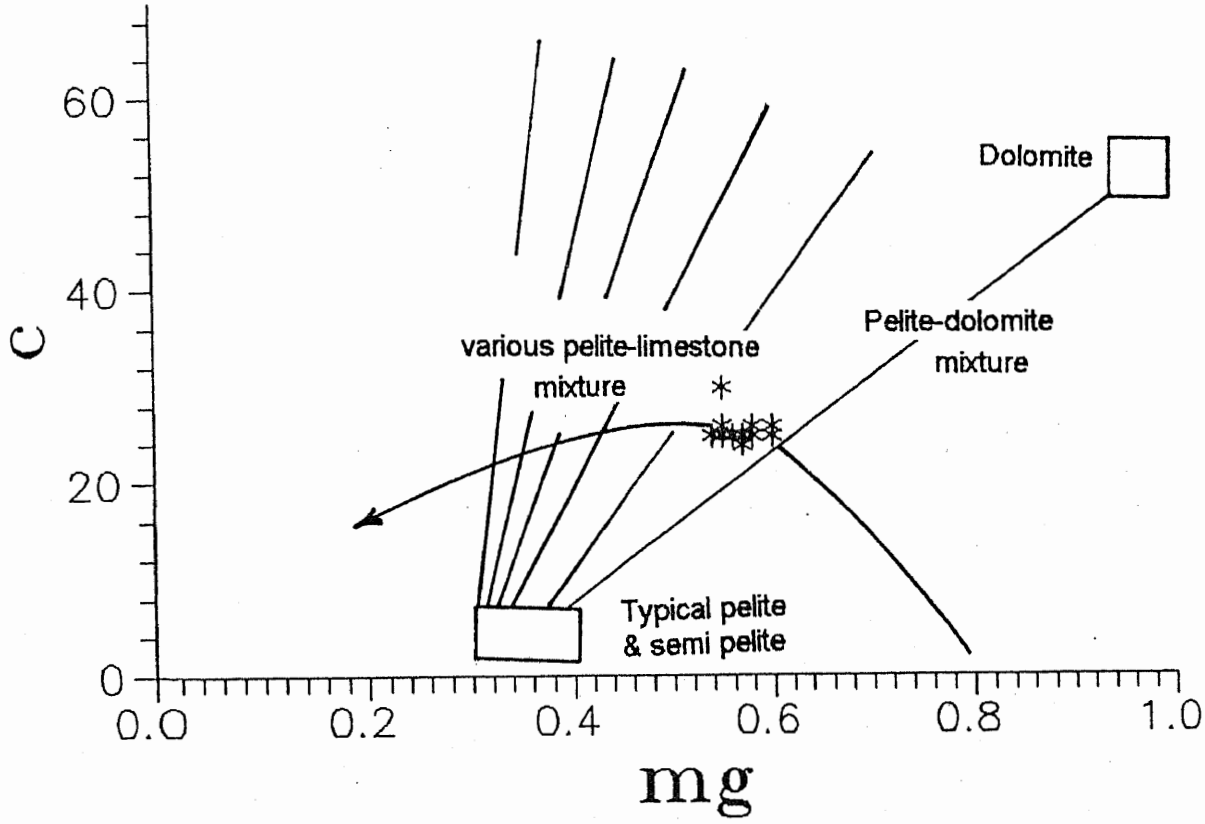

Fig.6.2. Plot of Niggli mg against C for the amphibolites and gabbro-norites of Ushiri valley, central Dir. The igneous trend is shown by arrow after Leake, 1964. Key as in Fig.6.1.

fall out side but very close to the field defined by Karro-dolorite in Figure 6.3.

During differentiation of basic magma, the Cr and Ni have positive correlation, where as the pelites show no or little systematic change with mg or if there is a mixture of pilites with limestone and dolomite then the correlation would be negative (Leake, 1964). The studied amphibolite show no distinct positive correlation of Ni and Cr with mg (Fig. 6.4 a & b) but the trend is certainly not indicative of sediments. On the TiO_2 vs SiO_2 diagram (Fig. 6.5) of Tarney (1977) all the studied amphibolites plot in the igneous field.

These diagrams suggest that the studied amphibolites could be the product of magmatic differentiation. These amphibolites, therefore, have the igneous parentage rather than sedimentary.

The magmatic origin of the studied amphibolites is also confirmed by the petrographic and chemical studies. This interpretation is supported by the preservation in some instances of relict igneous texture within the gabbro-norites hosted by these amphibolites. These gabbro-norites could be considered as the protolith for the amphibolites which has been confirmed by the petrographic studies where there is the progressive transformation of clino and orthopyroxene to hornblend of amphibolite facies with the development of intervening phases of chlorite, epidote and trimolite/actinolite of greenschist facies. The greenschist facies conditions, however, prevailed for a short time. This can be evident by the riming of clino and orthopyroxene by chlorite and epidote and then by hornblende in the gabbro-norites. The relics of clinopyroxene / orthopyroxene and plagioclase within the amphibolites were probably the two dominant liquidus phases and are considered to be the original gabbro-norite assemblage.

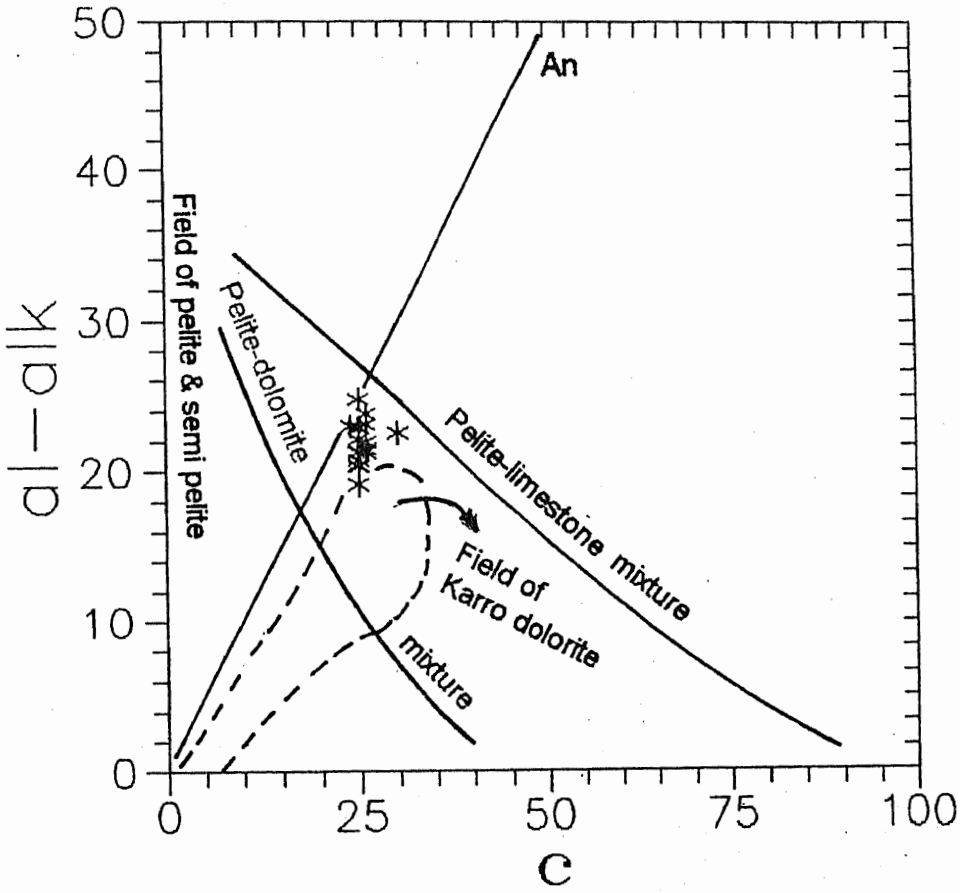

Fig.6.3. Plot of Niggli al-alk against C for the amphibolites and gabbro-norites of Ushiri valley, central Dir, various boundaries are after Evans and Leake, 1960. Key as in Fig.6.1.

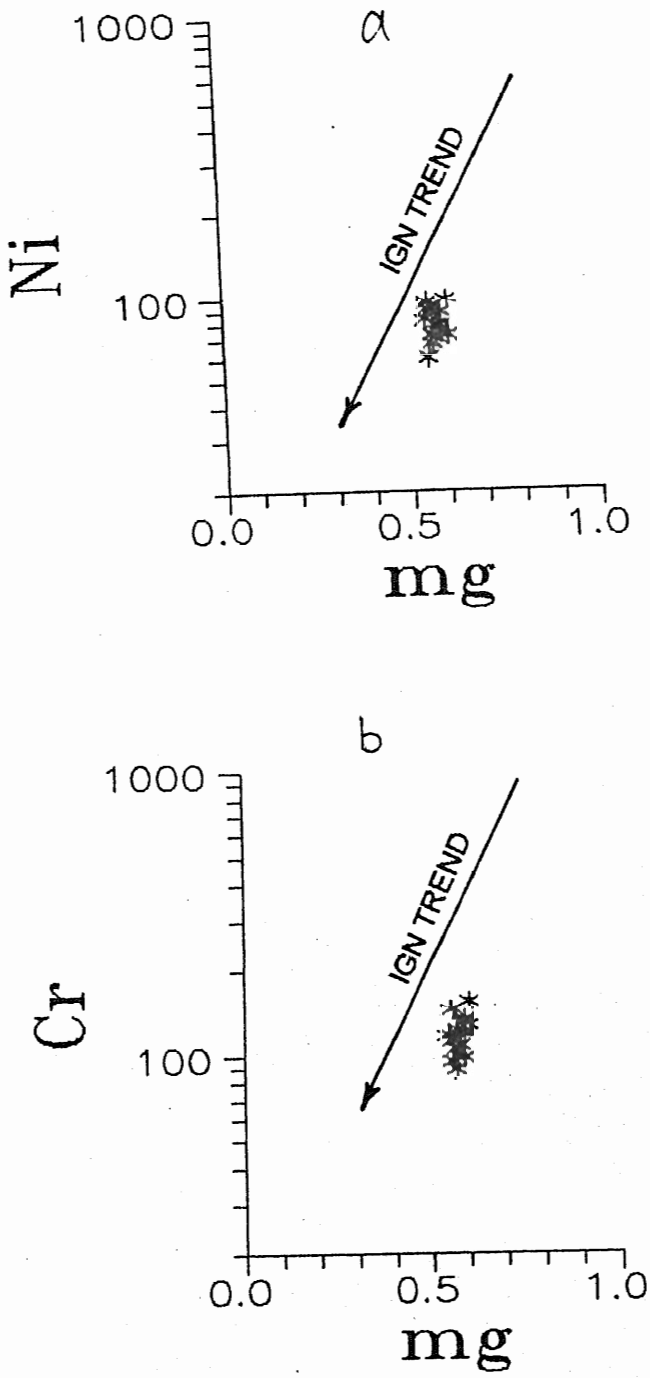

Fig.6.4. Trace element variation against mg for the amphibolites and gabbro-norites of the Ushiri valley, central Dir. Pelites are enclosed by ringed area (after Leake, 1964). Key as in Fig.6.1.

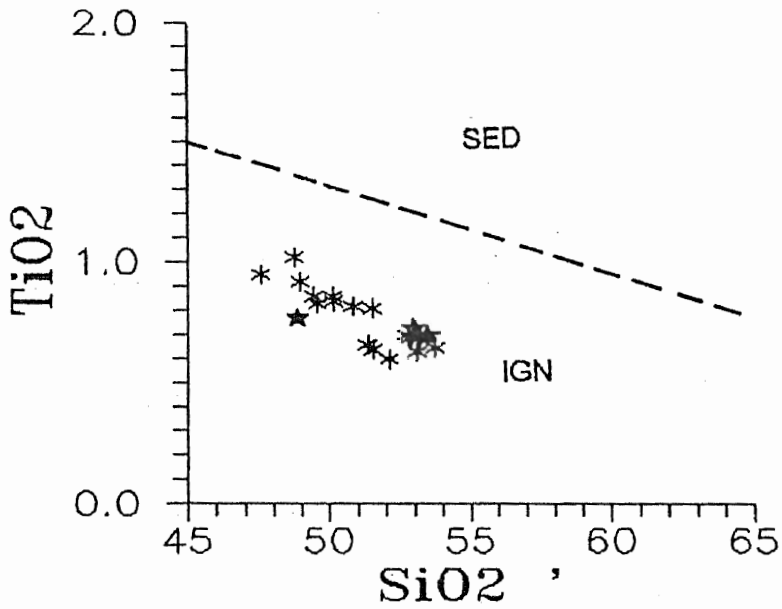

Fig.6.5. Plot of SiO_2 against TiO_2 for the amphibolites and gabbro-norites of Ushiri valley, central Dir (after Tarney, 1977). Key as in Fig.6.1.

VARIATION DIAGRAMS

Variation diagram is a variable graph or scattergram on which two selected variables are plotted. Variation diagrams are constructed by the geoscientists in order to devise a way in which the variation between individual rocks may be simplified and condensed so that relationship between the individual rocks may be identified. It is now proved that the variation diagrams have condensed and rationalized a large volume of numerical information and show qualitatively that there is an excellent correlation (either positive or negative) between each of the major element plotted against the index phase. Traditionally this strong geochemical coherence between the major elements (some time trace elements) has been used to suggest that there is an underlying process (i.e. fractional crystallization, magma mixing partitioning etc) which will explain the relationship between the major elements.

There are many variation diagrams which are most frequently used for establishing the correlation and coherence between the elements. Some of these are discussed here. The oldest method, still widely used, is a variation diagram in which oxides are plotted against SiO_2 (Harker; 1909), often refered to as a Harker diagram.

Indices based on the magnesium-iron ratio (e.g.,100 MgO/MgO+FeO) have been widely and usefully employed (e.g. Wager & Qcer, 1939). The Felsic Index of Simpson (1954) is the index which is calculated as the ratio of normative Ab/Ab + An and is used as abscissa in many variation digrams. Authors particularly those concerned with basaltic rocks, have prefered to use MgO as the abscissa for variation diagrams. These diagrams already discussed have certain limitations and can only be usefully applied to certain

ranges of rock types. To over come this problem several attempts have been made to devise more complex indices intended to have more comprehensive use. Two of these in particular are widely used, the solidification index (S.I.) of Kuno (1968) and the Differentiation index (D.I.) of Thornton and Tuttle (1960). Solidification index is expresed as: S.I = 100 MgO/MgO + FeO+ Fe_2O_3+ Na_2O+ K_2O and the Thornton and Tuttle index is expressed as: D.I.= Q+ Or+ Ab+ Ab+Ne+Ks+Lc.

Keeping in view various geochemical aspects of the rocks of the study area, the variation diagrams in which the SiO_2 is used as abscissa (Fig 6.6) are employed for both major and trace elements during this study inorder to see the crystallization behaviour of the rocks and their correlation among themselves.

Both major and trace elements of the studied amphibolites and the gabbro-norites are plotted against SiO_2 in figure 6.6 and 6.7 respectively. It is evident from these diagrams that many of the major and trace elements display well defined smooth variation trends against SiO_2 which further confirm the magmatic character of the protolith of these amphibolites. The gabbro norites-have more or less similar behaviour as that of amphibolites in these diagrams (Fig.6.6 & 6.7) and are considered as co-genetic.

TiO_2, Fe_2O_3, Al_2O_3, CaO and MgO exhibit well defined negative correlation while the Na_2O, K_2O and Na_2O + K_2O show positive correlation with SiO_2 (Fig.6.6) during fractionation. MnO and P_2O_5 are more or less constant behaviour with change in SiO_2 (Fig.6.6). Among the trace elements Ni, Cr and Co show well defined negative correlation while Pb, Zn and Cu have greater scatter with increasing SiO_2 during fractionation (Fig.6.7). The trace elements have also been plotted against these major oxides for which they have greater affinity (Fig. 6.8).This diagram clearly indicates that the Cr

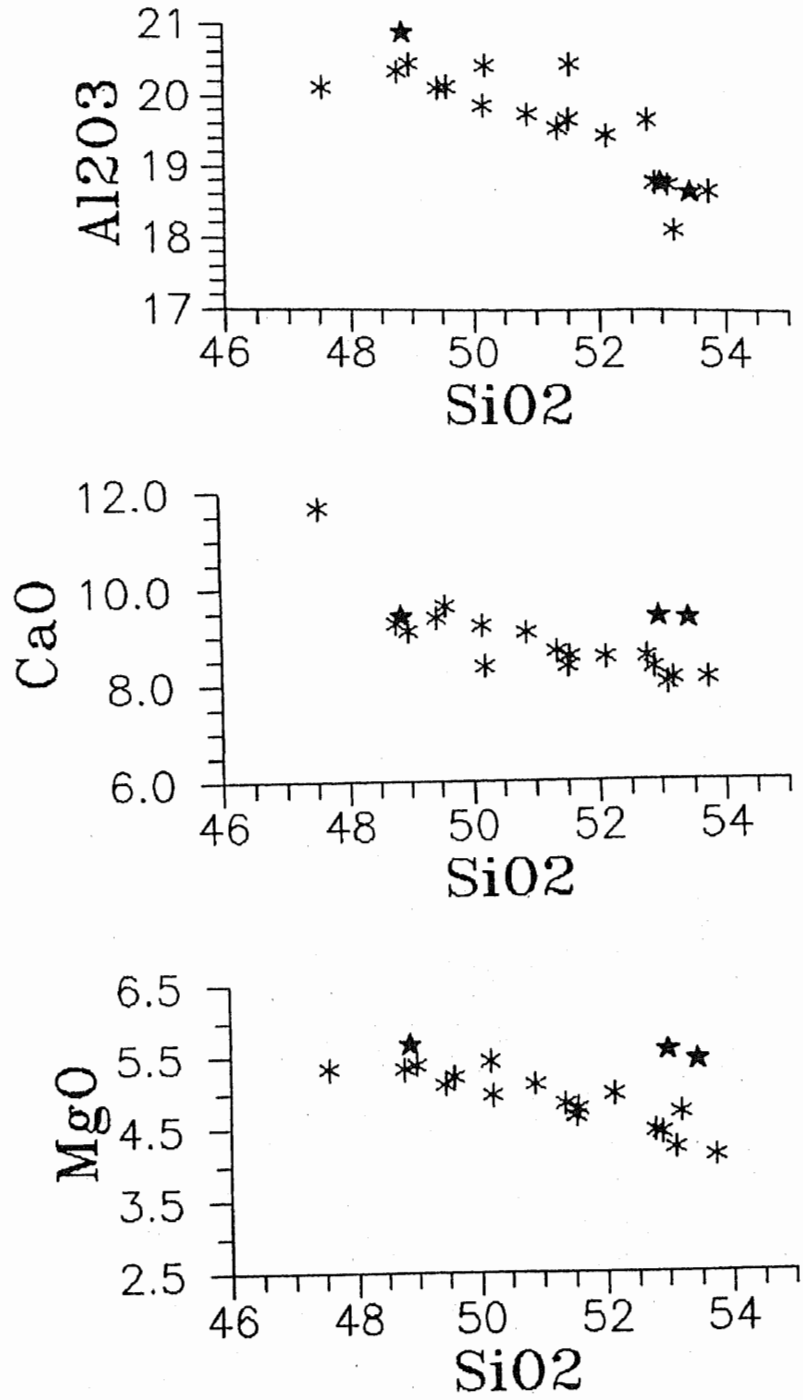

Fig.6.6. Plot of various oxides against SiO_2 for the amphibolites and gabbro-norites of the Ushiri valley, central Dir. Key as in Fig.6.1.

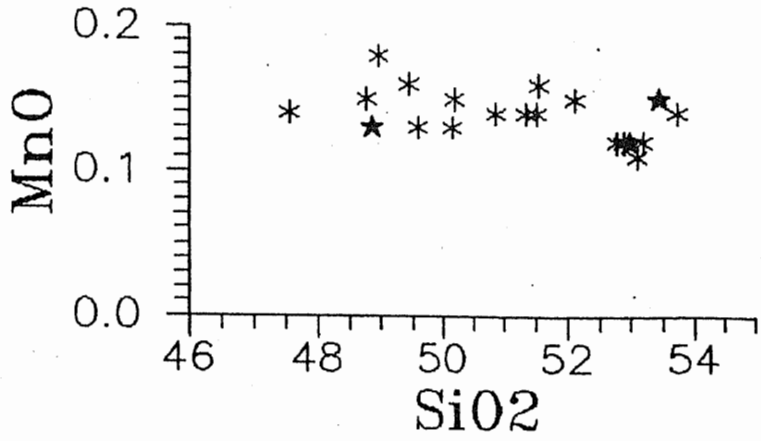
MnO
0.2
0.1
0.0
46
48
50
52
54
Si02

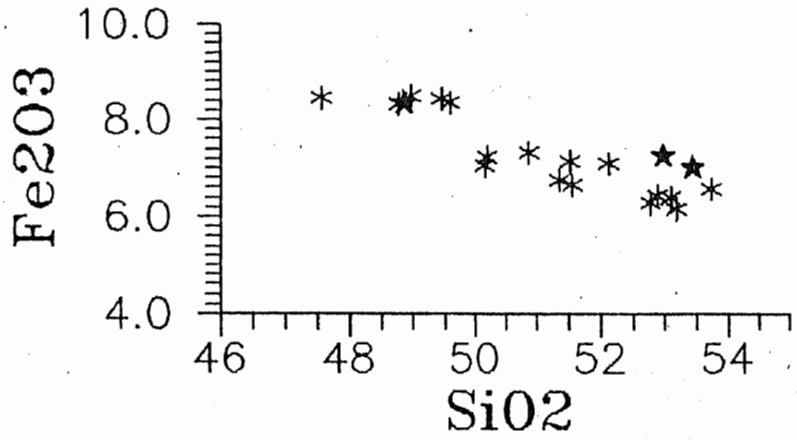
Fe203
10.0
8.0
6.0
4.0
46
48
50
52
54
Si02

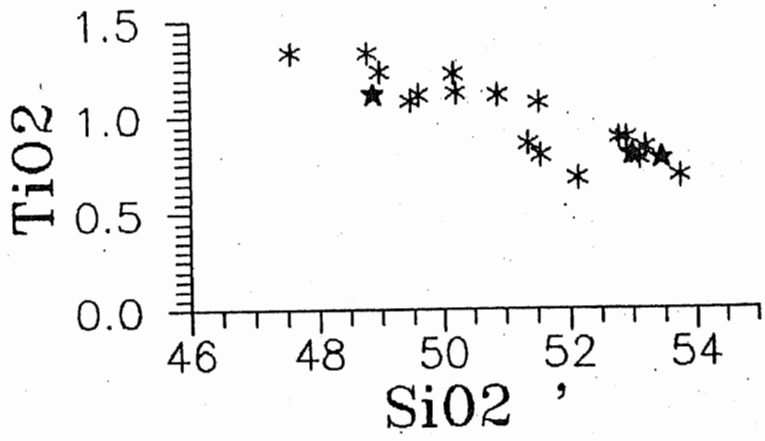
Ti02
1.5
1.0
0.5
0.0
46
48
50
52
54
Si02

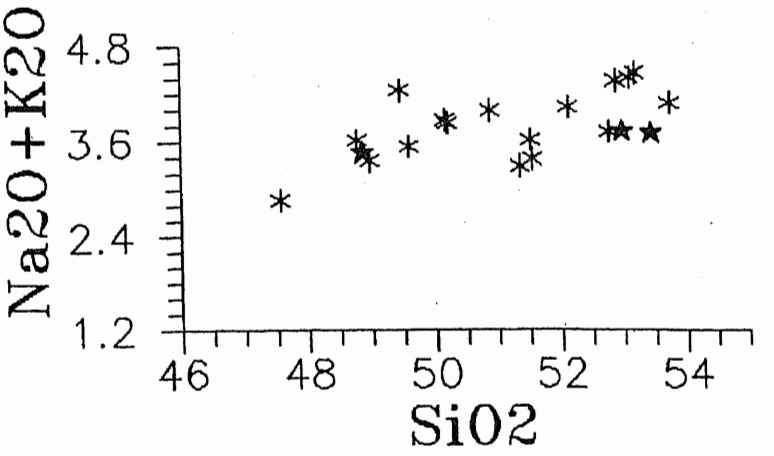
Na20+K20
4.8
3.6
2.4
1.2
46
48
50
52
54
Si02

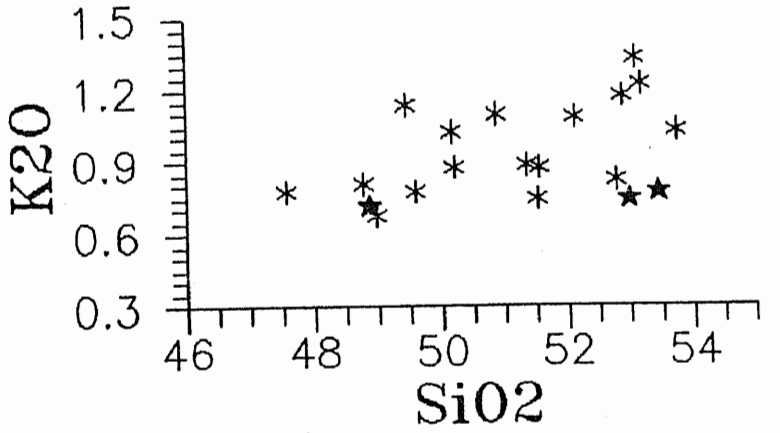
K20
1.5
1.2
0.9
0.6
0.3
46
48
50
52
54
Si02

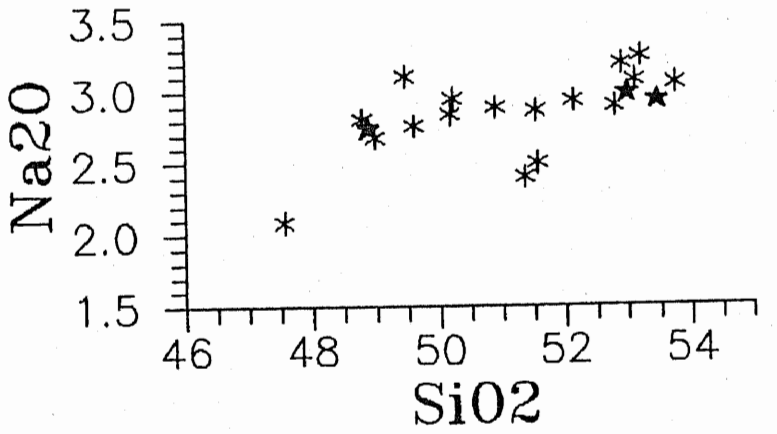
Na20
3.5
3.0
2.5
2.0
1.5
46
48
50
52
54
Si02

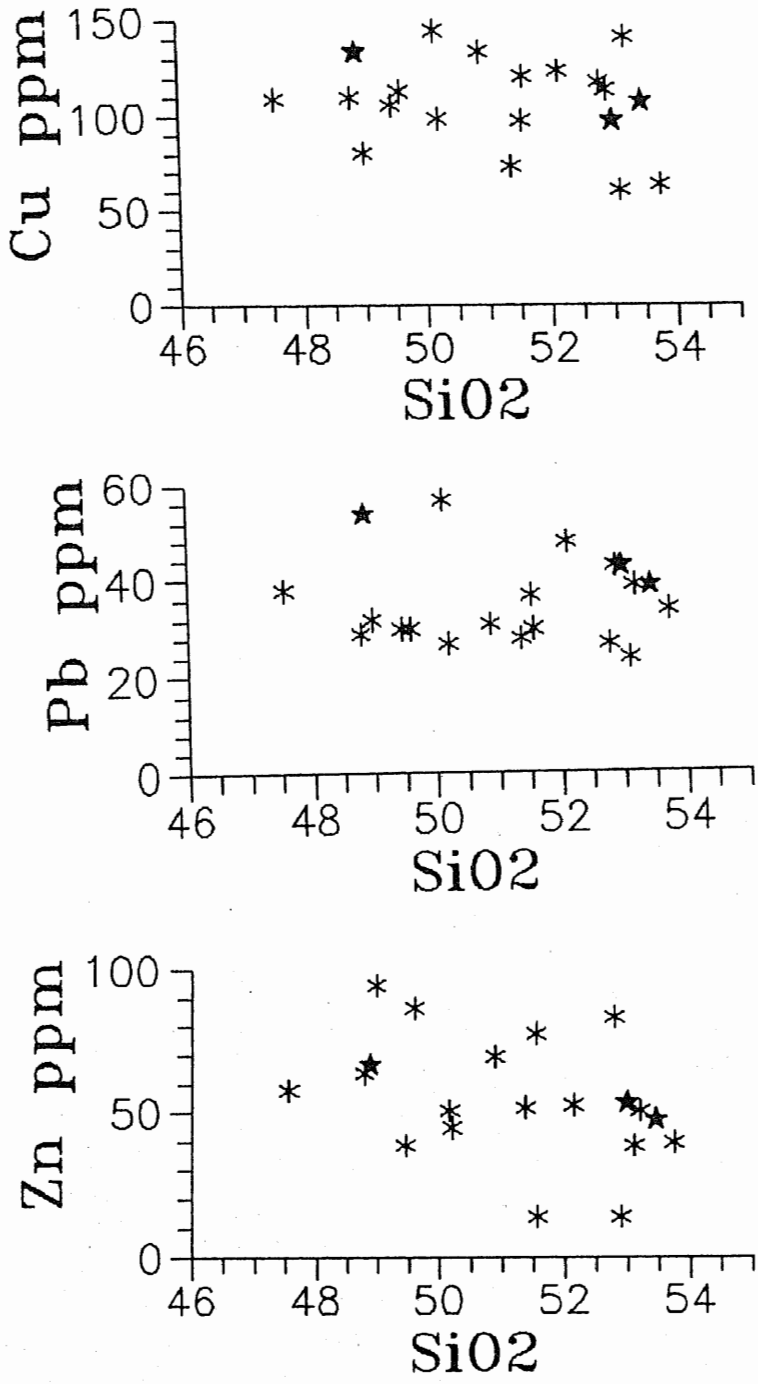

Fig.6.7. Plot of various trace elements against SiO_2 for the amphibolites and gabbro-norites of the Ushiri valley, central Dir. Key as in Fig.6.1.

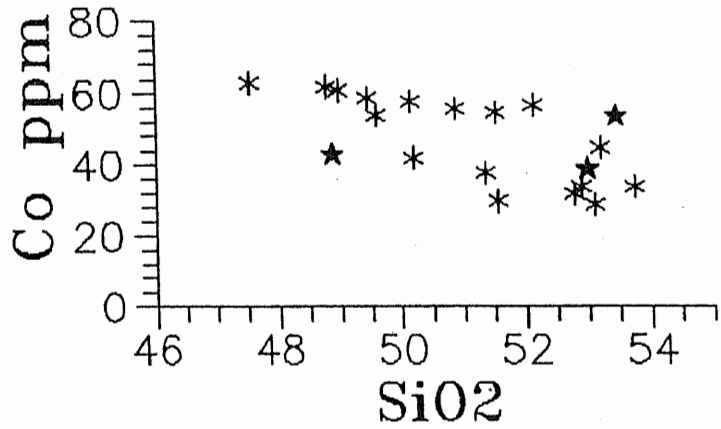
Co ppm
80
60
40
20
0
46
48
50
52
54
Si02

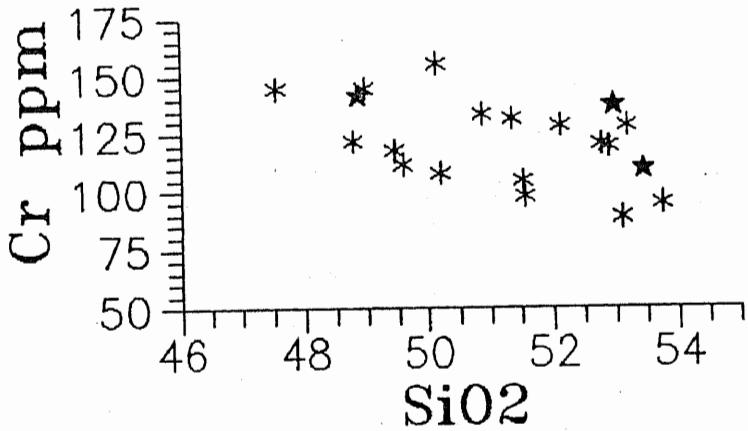
Cr ppm
175
150
125
100
75
50
46
48
50
52
54
Si02

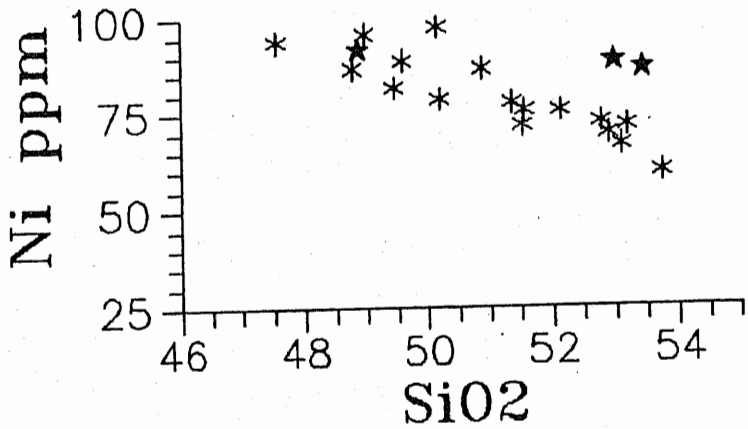
Ni ppm
100
75
50
25
46
48
50
52
54
Si02

and Ni have positive correlation with MgO and Co has positive correlation with Fe_2O_3. All these major and trace element behaviour during fractionation is the characteristic feature of magmatic differentiation. The negative differentiation trend for TiO_2 and Fe_2O_3(t) (Fig 6.6) signify crystallization. By looking at the variation trends (especially of CaO, MgO, CaO, Cr and Ni vs SiO_2) very carefully, it can be concluded that the clinopyroxene and plagioclase have played an important role in the formation of these rocks. The negative differentiation trends for TiO_2 and Fe_2O_3(t) further signify crystallization of magnetite/titanomagnetite/or hornblende and is the characteristic feature of calc-alkaline magma (see e.g., Miyashiro, 1977; Green, 1980).

Triangular variation diagrams are used when it is necessary to show simultaneous change between three variables. These types of diagrams have the disadvantage that they do not show absolute values of the parameters. They are, however, very useful in demonstrating various textures such as the change of inter-element ratios, which do not necessary show up clearly on bivariate oxide (two-oxide) diagrams. The triangular diagram known as the AFM diagram is the most popular of triangular variation diagrams and takes it name from the oxide plotted at its apices,alkalis (Na_2O+K_2O), Iron oixide ($FeO+ Fe_2O_3$) and MgO.

The AFM diagram is most commonly used to distinguish between tholeiiIic and calc-alkaline diffrentiation trends in the sub alkaline magma series. Kuno (1968) and Irvine and Baragar (1971) present dividing lines separating the rocks of the calc-alkaline series and that of the tholleitic series. However, the dividing line of Irvine and Baragar (1971), is most frequently and widely used. The AFM diagrams are not useful in petrogenetic studies to extract quantitative information about processes. The main usefulness of AFM diagrams, therefore, is to show trends which can be used to identify

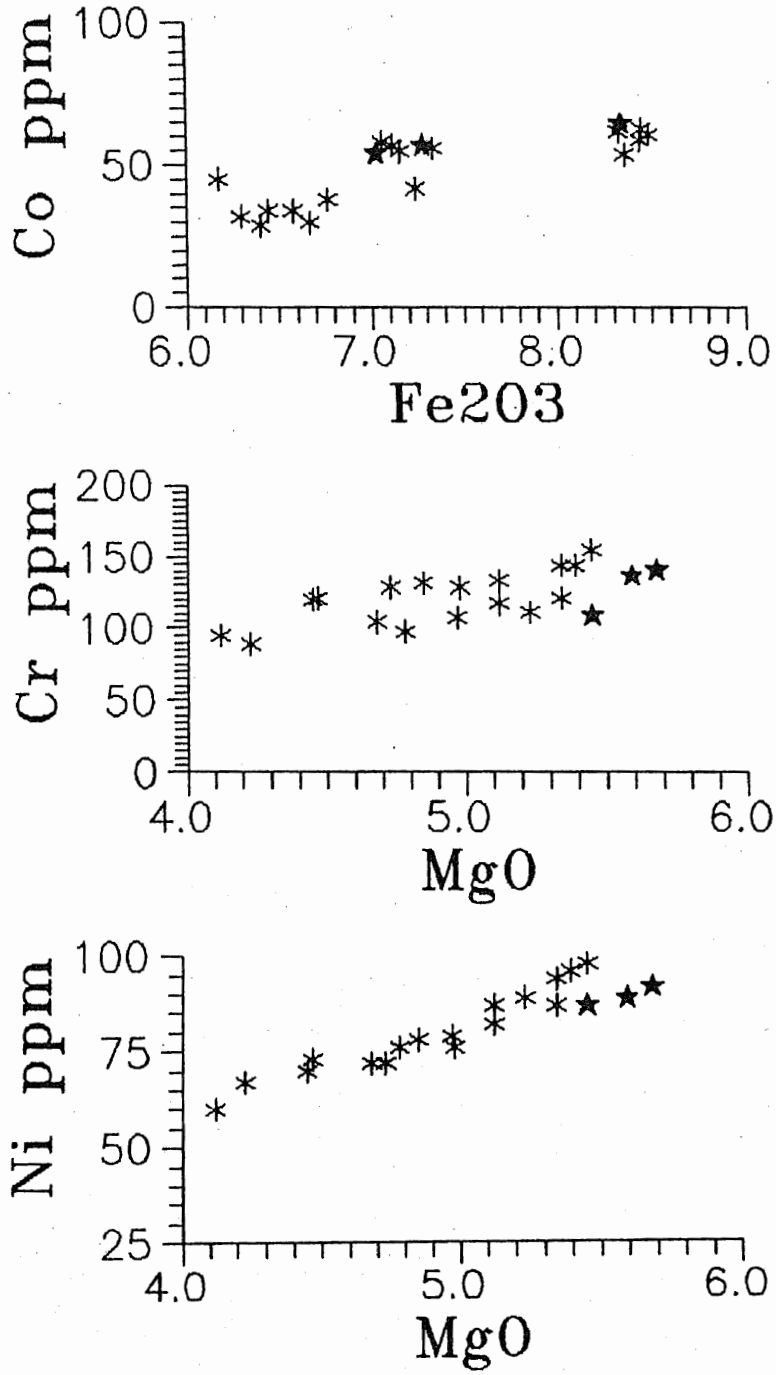

Fig.6.8. Plot of some trace elements against the selected major oxides for the amphibolites and gabbro-norites of the Ushiri Valley, central Dir. Key as in Fig. 6.1.

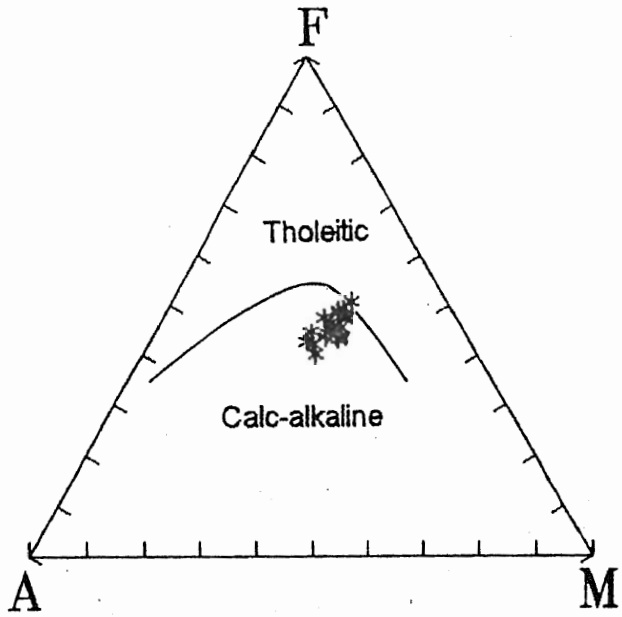

Fig.6.9. AFM, plot for the amphibolites and gabbro-norites of the Ushiri valley, central Dir. The Separation line is of Irvin and Baragar (1971), between calc-alkaline (at the bottom) and tholeiitic rocks (at the top). Key as in Fig.6.1.

rock series. The analyses of amphibolites and gabbro-norites when plotted in the AFM diagram (Fig. 6.9) fall within the calc-alkaline field.

b. Metadiorite / quartz-diorite and metagranodiorite

Eight samples of metadiorite/quartz-diorite and twelve samples of metagranodiorite of the study area have been selected for chemical analyses. The selection of samples for chemical analyses was performed after petrographic study in order to avoid alteration and weathering effect. Both major and trace elements along with CIPW norms are presented in table 6.2.

To classify these rocks, the classification scheme (Fig. 6.10) of Cox et al. (1979) has been used. In this diagram the samples named as metadiorite/quartz diorite and metagranodiorite plot within their respective fields. This cofirms the nomenclature based on petrographic studies for these rocks.

Metadiorite/quartz-diorite have SiO_2 in the range of 53.10-61.78%, Al_2O_3: 18.34- 20.36%, Fe_2O_3: 3.21-5.56%, MgO: 2.23-4.18%, CaO: 6.08-8.34%, Na_2O: 2.66-3.56%, K_2O: 0.70-0.92%, TiO_2: 0.40-0.86%, MnO: 0.05-0.14% and P_2O_5: 0.32-0.84%. Among the trace elements Cu is ranging from 48 to 104 ppm, Pb from 29 to 51 ppm, Zn from 68 to 115 ppm, Ni from 34-59 ppm, Cr from 26 to 54 ppm, Co from 36 to 68 ppm, Ag is <0.5 ppm and Au is present up to 11 ppb (Table 6.2). These rocks have normative quartz (Q) in the range of 10.24 -20.90, OR: 4.32 - 5.59, Ab: 23.47- 30.72, An: 28.88-39% C: 1.39-2.74, Hy: 10.71-17.26, Mt: 0.65-1.14, Il: 0.79-1.30 and Ap:0.72-1.90 (Table 6.2).

Granodiorites are having SiO_2 from 63.21 to 66.78%, Al_2O_3 from 16.12 to 17.89%, Fe_2O_3 from 2.67 to 3.88%, MgO from 0.78 to 1.75, CaO from

Table 6.2. Major and trace element data along with C.I.P.W. norms of diorites/ quartz diorites and granodiorites from Ushiri valley, central Dir.

Diorites/quartz diorites S.No.	US15	US17	US69	US44	US42	US11	US13	US73
SiO_2	55.51	56.78	53.10	54.34	57.56	60.10	60.23	61.78
TiO_2	0.54	0.52	0.86	0.65	0.40	0.57	0.41	0.61
Al_2O_3	20.36	20.12	20.23	20.34	19.89	18.98	18.78	18.34
Fe_2O_3	5.11	4.89	5.56	5.00	5.12	4.47	4.86	3.21
MnO	0.14	0.12	0.10	0.09	0.08	0.08	0.05	0.08
MgO	3.23	3.32	4.18	3.32	2.56	2.79	2.23	2.82
CaO	7.56	6.98	8.34	7.98	7.17	6.45	6.45	6.08
Na_2O	3.14	3.24	2.66	2.88	3.25	3.56	3.42	3.45
K_2O	0.74	0.75	0.70	0.72	0.78	0.86	0.83	0.92
P_2O_5	0.84	0.58	0.62	0.52	0.42	0.54	0.36	0.32
L.O.I	1.94	1.78	3.45	1.34	1.45	1.23	1.43	1.75
Total	99.11	99.08	99.80	97.18	98.68	99.63	99.05	99.36
Trace elements in ppm (Au in ppb)								
Cu	48	56	78	53	67	104	87	84
Pb	32	31	37	34	42	51	41	29
Zn	76	68	95	115	89	91	71	81
Ni	34	54	59	48	37	39	41	46
Cr	26	43	54	39	28	33	32	38
Co	63	59	68	61	59	47	43	36
Ag	<0.5	<0.5	<0.5	<0.5	<0.5	<0.5	<0.5	<0.5
Au	4	0	6	8	3	2	0	11
C.I.P.W. norms								
Q	13.45	14.62	10.24	12.22	15.35	17.70	18.94	20.90
Or	4.53	4.58	4.32	4.47	4.77	5.19	5.05	5.59
Ab	27.47	28.29	23.47	25.55	28.40	30.72	29.75	29.97
An	33.18	31.89	39.00	37.99	33.97	29.10	30.54	28.88
C	2.70	2.74	1.45	1.60	1.70	1.77	1.41	1.39
Hy	14.66	14.56	17.26	14.66	13.05	12.32	11.72	10.71
Mt	1.04	0.99	1.14	1.03	1.04	0.89	0.98	0.65
Il	1.06	1.02	1.71	1.30	0.79	1.11	0.80	1.19
Ap	1.90	1.31	1.41	1.19	0.95	1.20	0.81	0.72

(continued table 6.2)

Granodiorites

S.No.	US10	US19	US20	US24	US38	US39	US40	US41	US45
SiO_2	65.89	66.78	64.10	64.23	64.29	63.21	64.34	64.67	66.67
TiO_2	0.36	0.37	0.45	0.40	0.47	0.37	0.56	0.40	0.30
Al_2O_3	16.98	16.12	17.89	17.64	17.68	17.78	17.76	17.89	16.87
Fe_2O_3	3.10	3.13	3.14	3.32	3.88	3.45	3.05	3.38	2.67
MnO	0.08	0.07	0.07	0.08	0.08	0.08	0.07	0.08	0.07
MgO	1.75	1.23	1.21	1.12	1.22	1.26	1.25	1.08	0.78
CaO	4.71	4.60	4.99	4.16	4.13	4.74	4.57	4.74	4.61
Na_2O	4.45	4.52	4.70	4.65	4.50	3.98	4.21	4.12	4.50
K_2O	1.32	1.34	1.21	1.22	1.26	1.19	1.21	1.32	1.54
P_2O_5	0.67	0.63	0.40	0.71	0.63	0.62	0.32	0.48	0.62
L.O.I	1.05	1.05	1.23	1.34	1.21	1.12	1.21	1.17	1.10
Total	100.36	99.84	99.39	98.87	99.35	97.80	98.55	99.33	99.11
Trace elements in ppm (Au in ppb)									
Cu	45	34	65	32	48	52	73	39	45
Pb	34	33	40	29	44	35	39	28	36
Zn	28	46	34	37	28	42	36	32	41
Ni	22	18	16	16	17	19	16	15	14
Cr	27	21	19	18	18	20	17	17	16
Co	47	49	56	61	66	48	34	48	29
Ag	<0.5	<0.5	<0.5	<0.5	<0.5	<0.5	<0.5	<0.5	<0.5
Au	4	8	2	6	0	7	10	8	4
C.I.P.W. norms									
Q	22.75	24.20	19.62	22.86	22.91	24.29	23.73	24.00	24.32
Or	7.89	8.05	7.32	7.43	7.63	7.31	7.38	7.98	9.26
Ab	38.01	8.81	40.60	40.45	38.92	34.93	36.67	35.60	38.68
An	19.21	9.03	22.65	16.49	16.78	20.24	21.23	20.86	19.17
C	1.26	0.36	0.73	2.87	2.96	2.90	2.02	2.24	0.90
Hy	8.09	6.82	6.69	6.85	7.70	7.50	6.54	6.78	5.19
Mt	0.61	0.62	0.63	0.67	0.78	0.70	0.62	0.68	0.53
Il	0.69	0.71	0.87	0.78	0.91	0.73	1.10	0.78	0.58
Ap	1.48	1.40	0.89	1.60	1.41	1.41	0.72	1.07	1.38

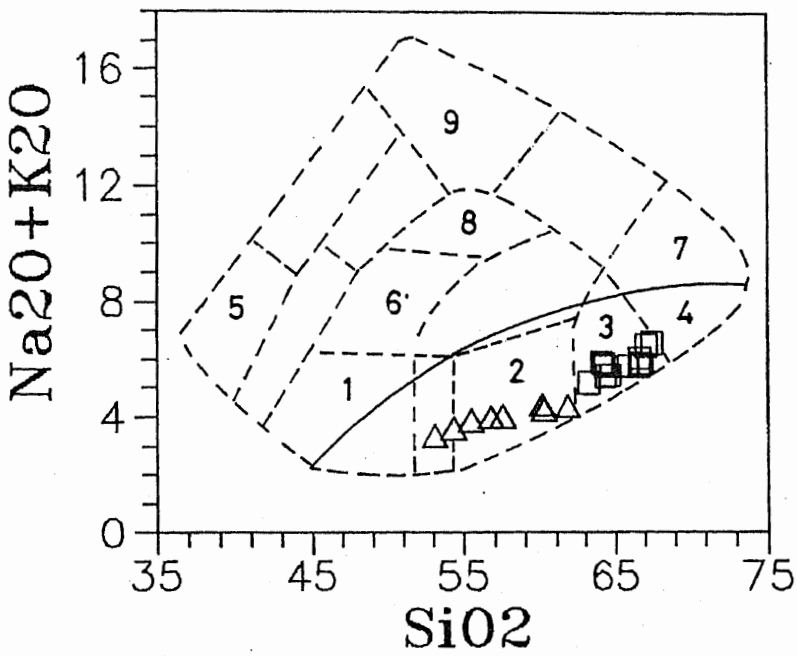

Fig. 6.10. Plotting of diorites/quartz diorites and granodiorites from Ushiri valley, central Dir in the classification diagram of Cox et al. (1979) adopted by Wilson (1989).

Symboles:

△ = Diorite/quartz diorite

□ = Granodiorite

3.08 to 4.8%, Na_2O from 3.98 to 4.87%, K_2O from 1.19 to 1.89%, TiO_2 from 0.28 to 0.56%, MnO from 0.07 to 0.08% and P_2O_5 from o.20 to 0.71% (Table 6.2). The trace elements vary as follows: Cu:32-73 ppm, Pb:28-44 ppm, Zn:28-46 ppm, Ni: 8-22 ppm, Cr: 12-27 ppm, Co:27-66 ppm, Ag is <0.5 ppm and Au is <10 ppb (Table 6.2). According to the CIPW norms, these rock have normative Q:19.62- 28.25, Or: 7.31-10.42, Ab: 8.81-41.98, An: 9.03-22.65, C:0.73-3.48, Hy:4.53-8.09, Mt: 0.45-0.87, Il:0.54-1.10, and Ap:0.45-1.60.

In order to see the crystallization behaviour of these rocks the Harker diagram (Fig 6.11) is used where the major oxides and trace elements are plotted against SiO_2. There are consistent well defined decreasing trends of MnO, Fe_2O_3, Al_2O_3, CaO, and MgO (Fig. 6.11). However, P_2O_5 and TiO_2 exhibit vaguely defined negative correlation with SiO_2 (Fig. 6.11). The alkalies show positive correlation against SiO_2 (Fig 6.11). Among the trace elements Ni, Cu, Cr and Co show negative correlation with SiO_2 while the Zn exhibits scatter against SiO_2 (Fig 6.11). Various trace elements are also plotted against major oxides for which they have greater affinity (Fig. 6.12). Ni and Cr have well defined positive correlation with MgO (Fig. 6.12) while Co has positive correlation with Fe_2O_3 (Fig 6.12). By considering the behaviour of major and trace elements in the Harker diagram it can be concluded that these rocks are comagmatic and that the fractionation of plagioclase and clinopyroxene had played a major role in the early stages which was soon joined by the fractionation of alkali-feldspar, quartz and titanomagnetite.

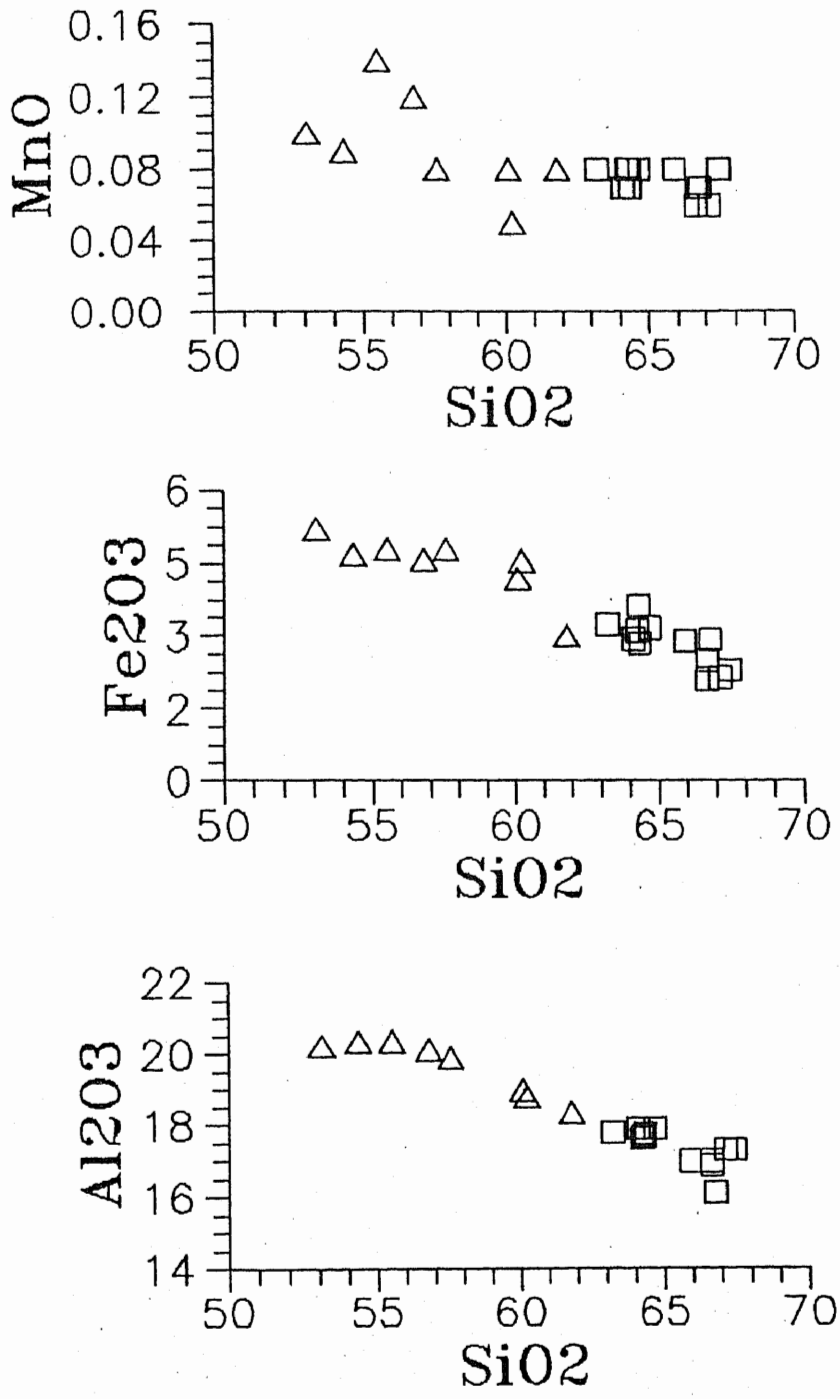

Fig.6.11. Plot of various oxides against SiO_2 for the diorites/quartz diorites and granodiorites of the Ushiri valley, central Dir. Key as in Fig.6.10.

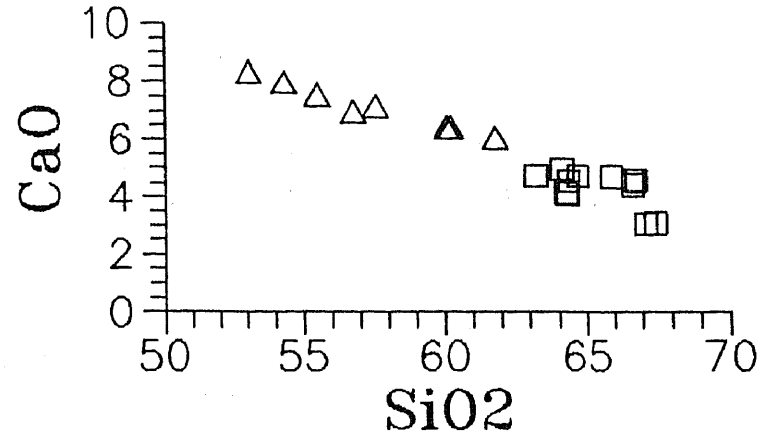
CaO
10
8
6
4
2
0
50
55
60
65
70
SiO2

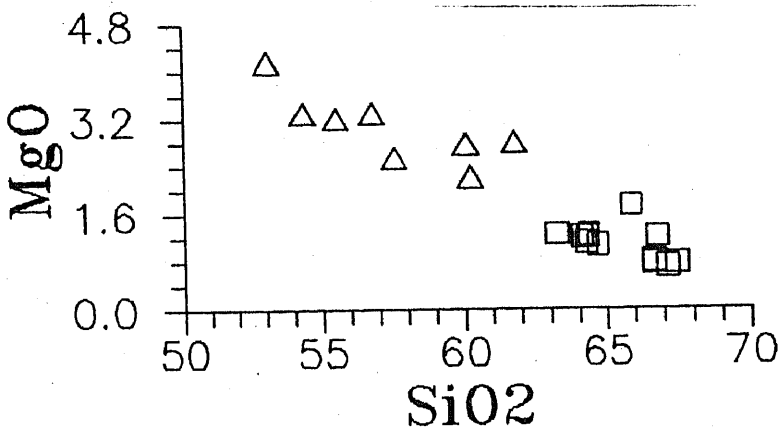
MgO
4.8
3.2
1.6
0.0
50
55
60
65
70
SiO2

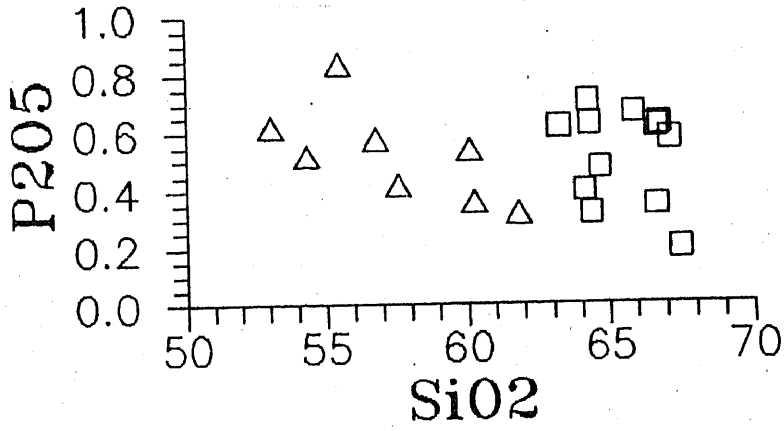
P2O5
1.0
0.8
0.6
0.4
0.2
0.0
50
55
60
65
70
SiO2

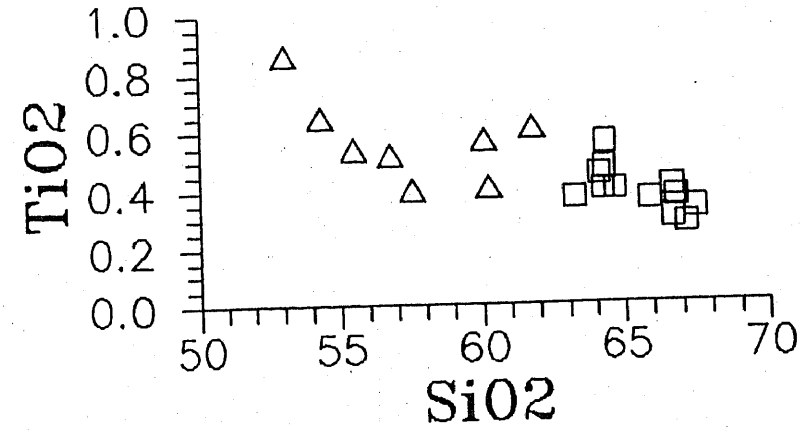
TiO2
1.0
0.8
0.6
0.4
0.2
0.0
50
55
60
65
70
SiO2

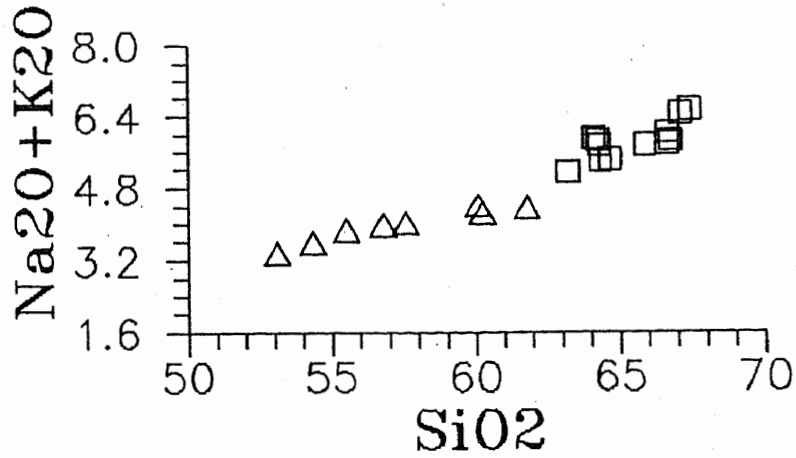
Na20+K20
8.0
6.4
4.8
3.2
1.6
50
55
60
65
70
Si02

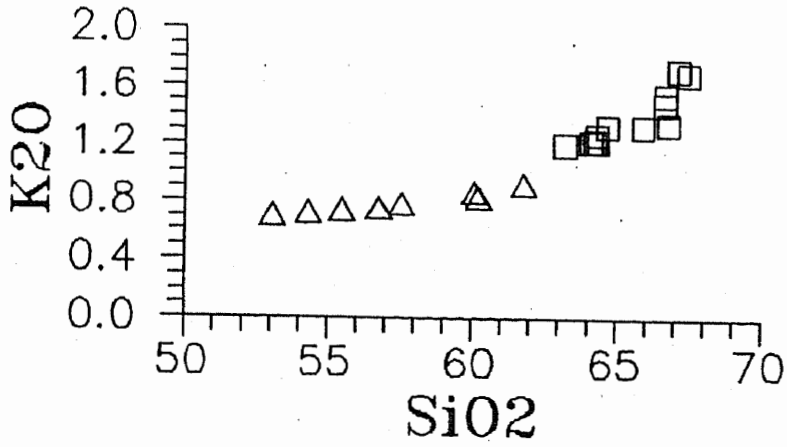
K20
2.0
1.6
1.2
0.8
0.4
0.0
50
55
60
65
70
Si02

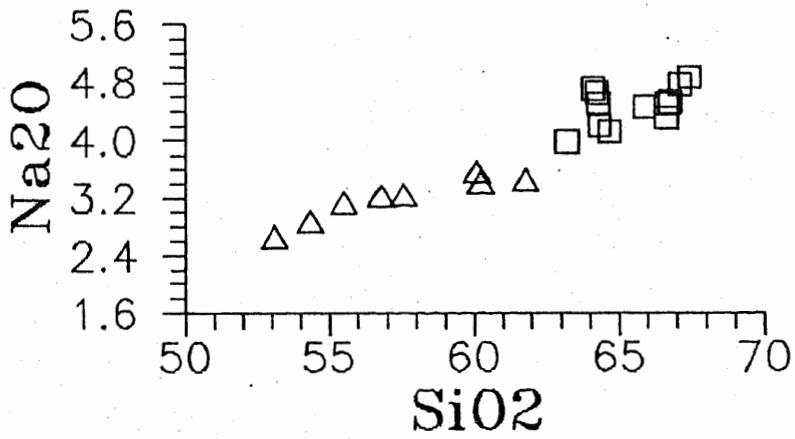
Na20
5.6
4.8
4.0
3.2
2.4
1.6
50
55
60
65
70
Si02

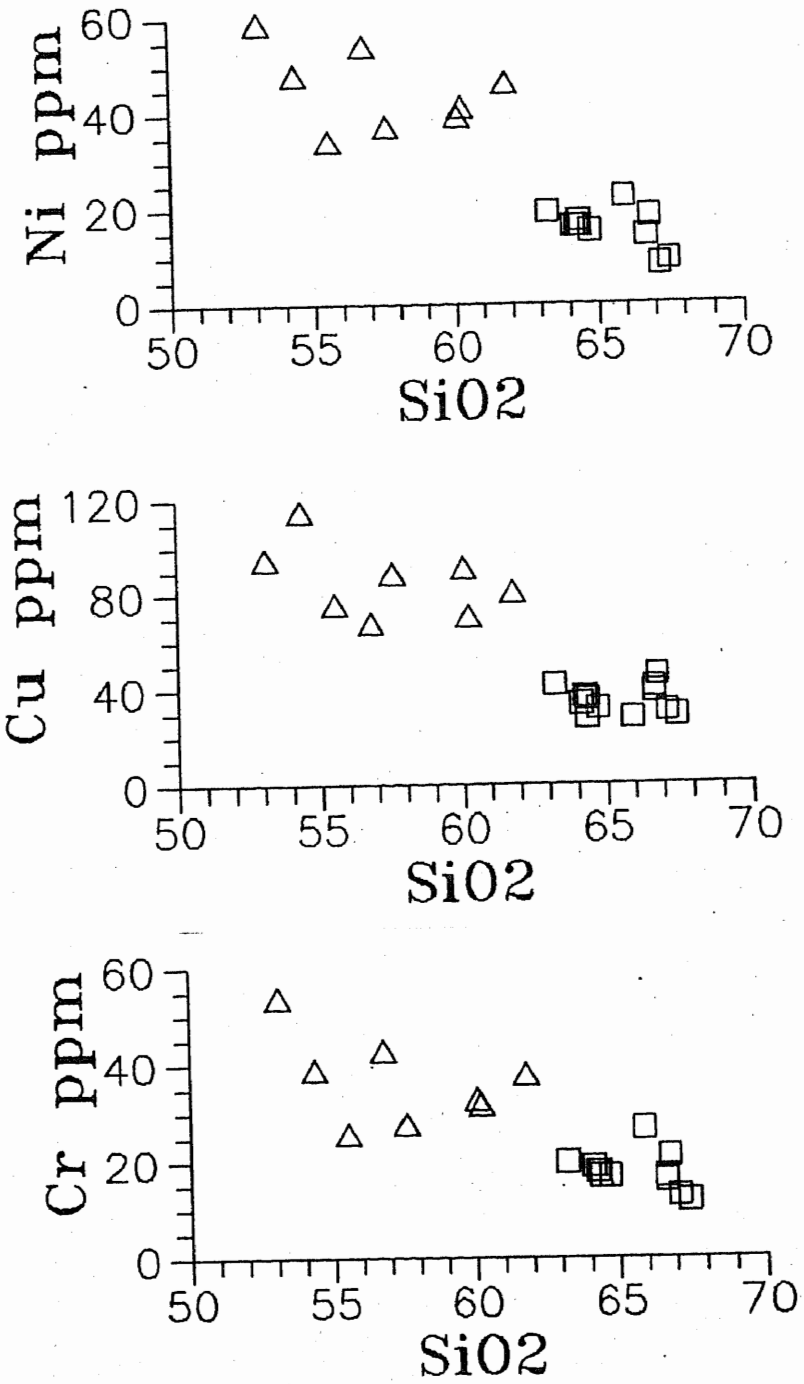

Fig.6.12. Plot of various trace elements against SiO2 for the diorites/quartz diorites and granodiorites of the Ushiri valley, central Dir. Key as in Fig.6.10.

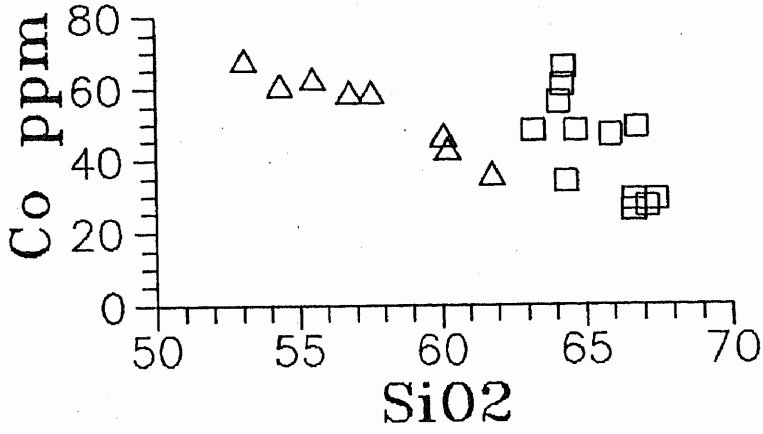
Co ppm
80
60
40
20
0
50
55
60
65
70
Si02

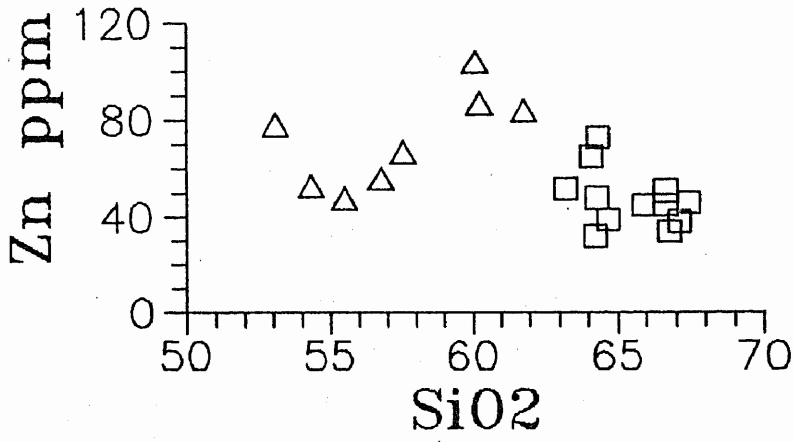
Zn ppm
120
80
40
0
50
55
60
65
70
Si02

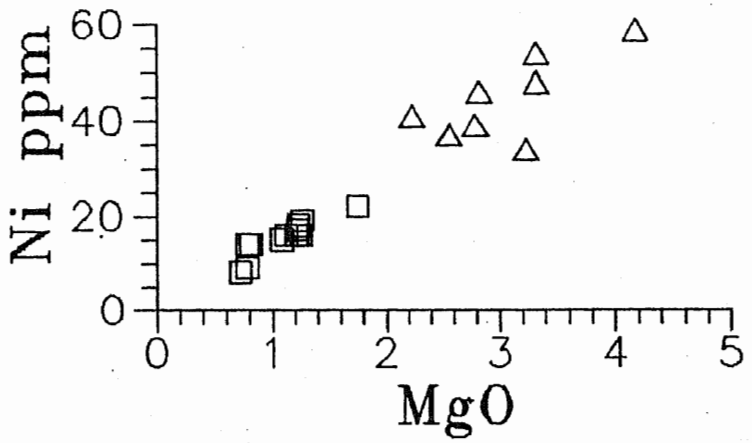
Ni ppm
60
40
20
0
0
1
2
3
4
5
MgO

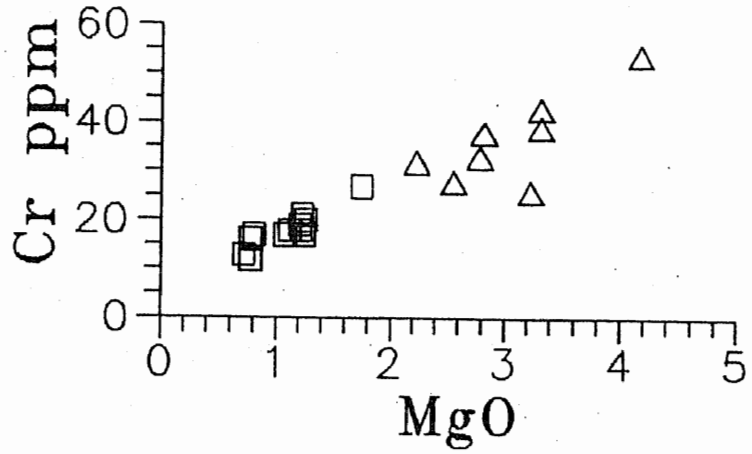
Cr ppm
60
40
20
0
0
1
2
3
4
5
MgO

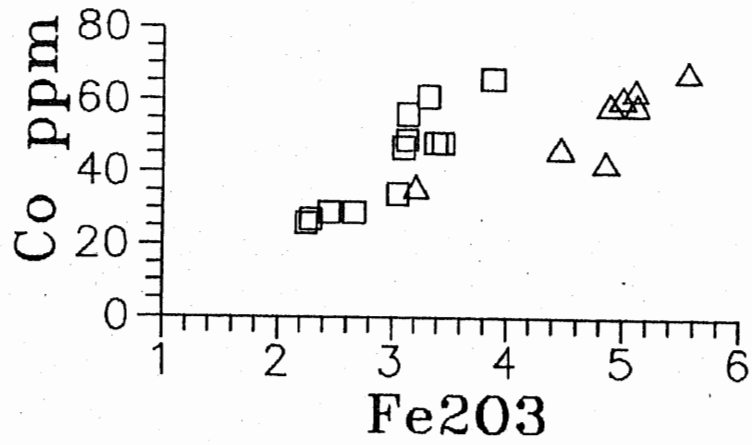
Co ppm
80
60
40
20
0
1
2
3
4
5
6
Fe203

CHAPTER-7

PALEOTECTONIC SETTINGS

The petrogenetic and paleotectonic studies play an important role in the identification of source regions of magma in the context of global tectonic setting of igneous rocks. Based on the major and trace elements, REE and isotopic studies of the present day volcanic rocks, especially basalt, various tectonomagmatic discrimination diagrams have been established to understand the tectonic setting of ancient volcanic rocks (see for example Pearce, et al., 1973; Pearce et al., 1975; Floyed and Winchester, 1975; Pearce and Norry, 1977; Shervais, 1982; Weedon, 1970; Mullen, 1983; for more references see Shah and Jan, 1996). The present day magmas originated in different tectonic settings have specific geochemical characteristics. By knowing these characteristics of igneous rocks the source region of their ancient counterparts in specific tectonic environment can be elucidated.

It this section the chemical characteristics of the rocks of the studied area are discussed in a genetic context and presented diagrammatically in a series of plots to identify in a qualitative sense the nature of the parent material(s), type(s) of tectonic settings of their formation and to demonstrate the degree of coincidence elements of the studied rocks with identical rock populations, developed in similar tectonic regions elsewhere in the world.

TECTONIC AFFINITY OF AMPHIBOLITES AND GABBRO-NORITES

Pearce and Cann (1971) are the poineer to establish tectonomagmatic discrimination diagrams, geochemical variation diagrams

on the basis of which magmas produced in different tectonic settings may be distinguished from one another on the basis of their chemistry (Pearce and Cann, 1971;1973). Subsequent to Pearce and Cann (1971 and 1973) large number of discrimination diagrams have been established (Miyashiro 1975; Pearce, 1976; Pearce, 1982; Pearce & Norry, 1979; Pearce & Gale, 1977; Wood, 1989; Shervais 1982; Floyed & Winchester, 1975; Pearce et al., 1977; Pearce et al, 1975; Mullen, 1983; Muenow et al., 1990;). Most of these discrimination diagrams use individual elements as the discriminant functions rather than a composite of several elements, making the diagrams easy both to use and to understand.

However, there are certain diagrams which use mostly the major and minor oxides for the discrimination of various types of rocks formed in specific tectonic environments. The distinction of rocks of various type of tectonic environments (e.g. Oceanic ridges, back-arc basin, volcanic arc, collisional setting, intraplate setting and passive continental margins) can very easily be determined by using the geochemical criteria.

This study is mainly based on the major and minor element chemistry. Therefore, only those discrimination diagrams are used here which use the major and minor element chemistry. These diagrams are discussed here in detail.

Mullen (1983) presented a discrimination diagram for the basic rocks (45-54-wt% SiO_2) on the basis of their MnO, TiO_2 and P_2O_5 concentration (Fig.7.1). This diagram has been subdivided into various fields such as mid oceanic ridge basalt, ocean-Island tholeiites; Ocean-Island alkali basalts; island arc tholeiites; calc-alkaline basalts as shown in figure 7.1. The amphibolites and gabbro-norites of the study area when plotted in this

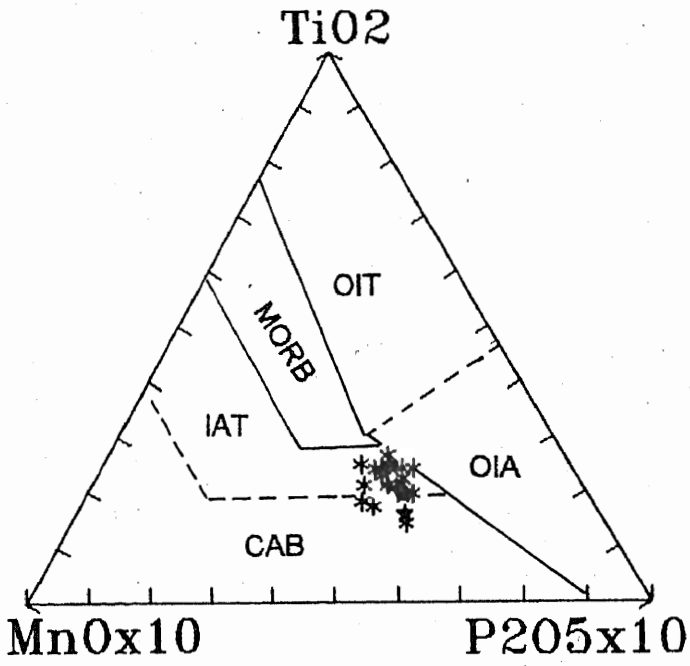

Fig.7.1.The MnOXIO/TiO_2/P_2O_5x10 discriminations diagram for the amphibolites and gabbro-notirtes of the Ushiri valley, central Dir (after Mullan 1983).

CAB = Calc-alkaline basalt.
IAT = Island arc tholeiites.
MORB = Mid oceanic ridge basalt.
OIT = Oceanic island tholeiites.
OIA = Oceanic island alkali basalt

diagram majority of these fall within the field of calc-alkaline basalt with few of them in the field of island arc tholeiites (Fig. 7.1).

Pearce et al. (1977) found that the MgO, Al_2O_3 and FeO (total iron recalculated as FeO) were able to discriminate between the following tectonic environments: Ocean ridge and floor basalts (MORB); Ocean island basalt; continental basalts; volcanic arc and active continental basalts (orogenic basalt in the terminology of Pearce et al., 1977); spreading centre island basalts. The boundaries between the different fields are shown in figure 7.2. The analyses of studied amphibolites and gabbro-norites when plotted in this diagram fall within the field of orogenic basalts of Pearce et al. (1977). This clearly indicates that the studied rocks have been originated in an island arc type of setting.

Weedon, (1970) has differentiated the "alpine" type mafic and ultramafic rocks from that of Bushveld Complex on the basis of Mg-Ca-Fe plot (Fig.7.3) and alk-Fe-Mg plot (Fig. 7.4). These diagrams show both alpine and Bushveld trends very clearly and there is a small overlap of the data in these diagrams. The studied metagabbros / metagabbro-norite when plotted in these diagrams exhibit close affinity to the Bushveld field. In the Alks-Fe-Mg diagram (Fig. 7.4) most of data points fall within the Bushveld field, however, in Mg-Ca-Fe diagram (Fig. 7.3) the data points fall out side the fields defined for alpine type and Bushveld type but closer to the field of Bushveld. This suggest that these rocks are non-ophiolitic and are cumulate rocks from island arc.

Yoder (1969) proposed a discrimination diagram of MgO vs FeO + Fe_2O_3 (Fig. 7.5) where he defined the fields for the rocks of calc-alkaline series (both from island arc & continental margin), tholeiitic series and alkalic series. Majority of the data points of the amphibolites and gabbro-norites,

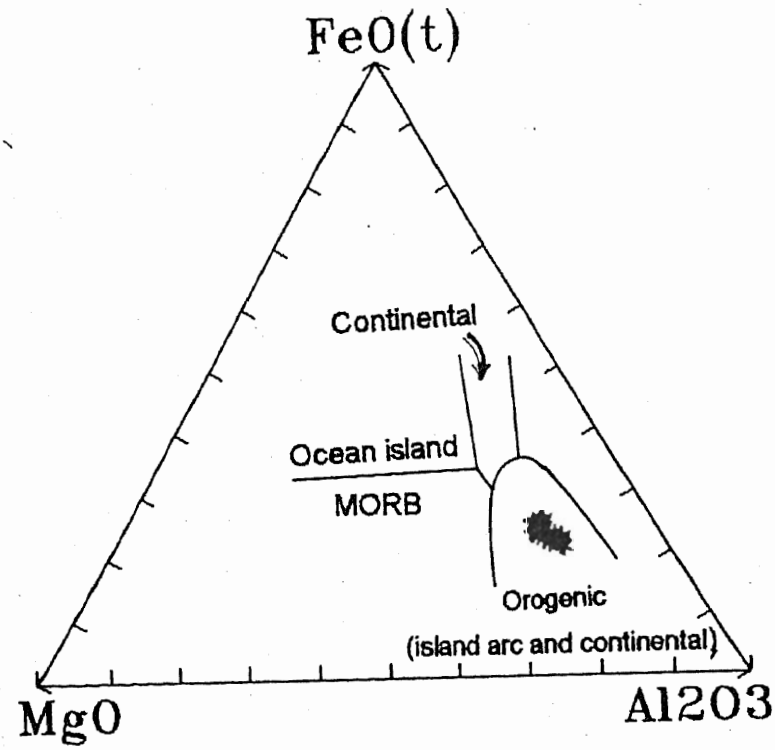

Fig.7.2.Tectonomagmatic discrimination diagram for the amphibolites and gabbro-norites of the Ushiri valley, central Dir (after Pearce et al, 1977). Key as in Fig.6.1.

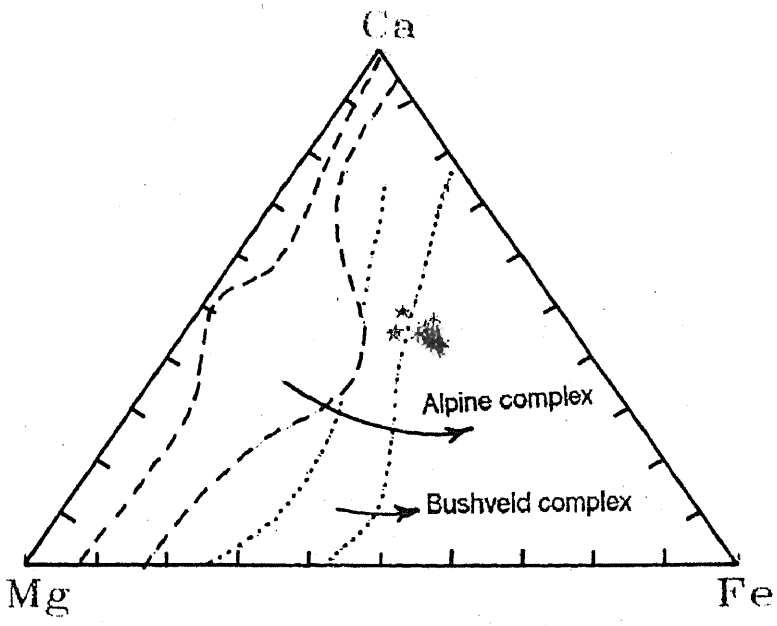

Fig.7.3.Mg-Ca-Fe plot for the amphibolites and gabbro-norites of the Ushiri valley, central Dir (after Weedon, 1970).

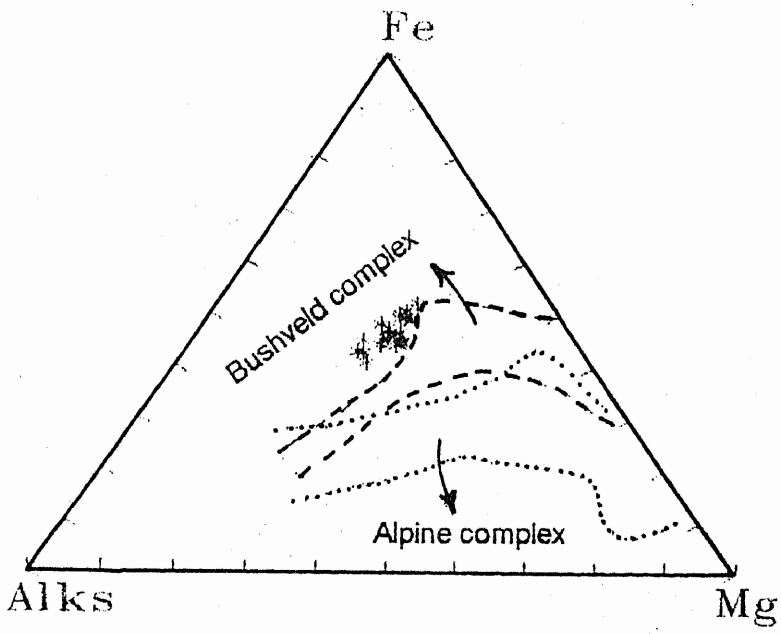

Fig.7.4.Alk-Fe-Mg plot for the amphibolites and gabbro-norites of the Ushiri valley, central Dir (After Weedan, 1970).

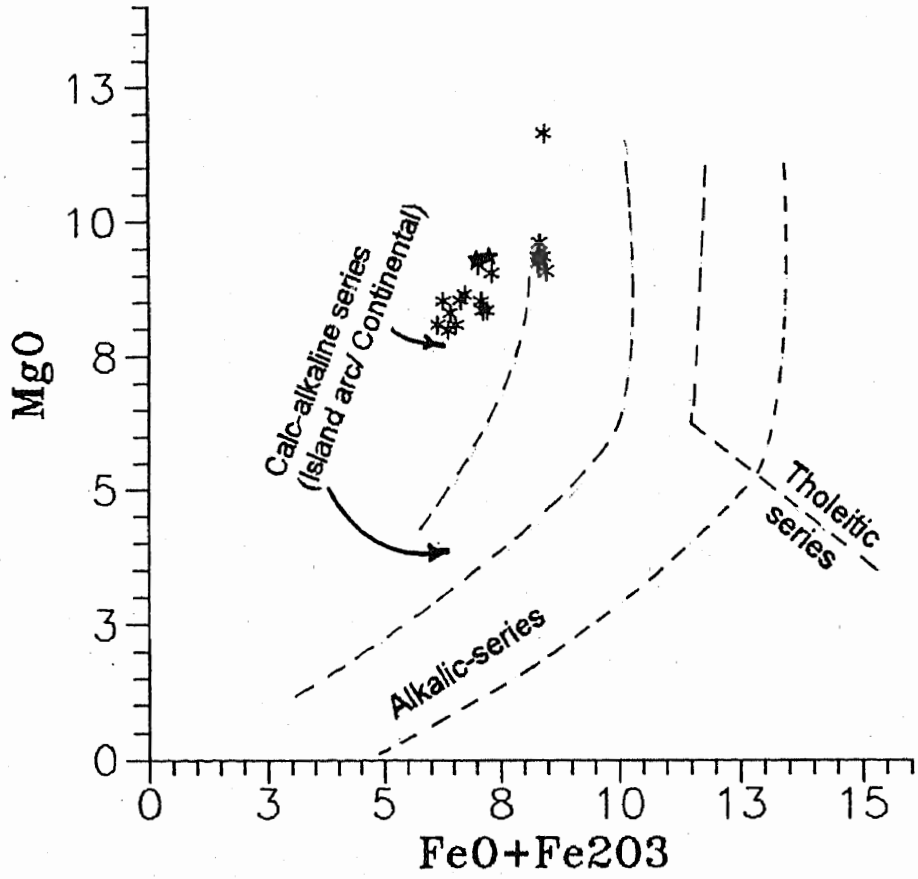

Fig.7.5.MgO against $FeO+Fe_2O_3$ plot for the amphibolites and gabbro-norites of the Ushiri valley. Various fields are after Yoder (1969).

however, fall within the field of calc-alkaline series from continental margin with few of them plot within that of island arc (Fig. 7.5).

Miyashiro (1977) has differentiated the abysal tholeiites (mid ocean ridge volcanics) from those of the island arc on the basis of TiO_2 vs FeO(t)/MgO (Fig. 7.6). The studied amphibolites and gabbro-norites are poor in TiO_2 and are, therefore, located in the field of island arc volcanics. However, two of the analyses fall within the overlapping field of abysal tholeiites and island arc volcanics (Fig.7.6)

Pearce (1975) has constructed a Ti vs Cr diagram (Fig.7.7) for the rocks of basaltic composition. This diagram separate the field of volcanic arc basalt (VAB), including island arc tholeiites and calc-alkaline basalt from the field of Ocean floor (OFB) or mid-Oceanic ridge basalts (MORB). The rocks under discussion when plotted in this diagram (Fig.7.7), all of the analyses fall within the field of volcanic arc basalts.

MAGMA TYPE AND TECTONIC AFFINITY OF THE METADIORITE / QUARZ-DIORITE AND METAGRANODIORITE

As this study is mainly based on the major and minor oxides of the metadiorite / quartz-diorite and metagranodiorite, therefore, only those discrimination diagrams which are appropriate for the determination of magma type and paleotectonic environment of these rocks are used here.

Both metadiorite/quartz-diorite and metagranodiorite are plotted in AFM diagram (Fig.7.8) of Irvine and Baragar (1971); in Ti vs Cr diagram (Fig.7.9) of Pearce (1975) and in FeO(t)/MgO vs SiO2 diagram (Fig.7.10) of Miyashiro (1974). The plotting of the data in these diagrams suggest that the studied rocks are derived from the differentiation of calc-alkaline magma.

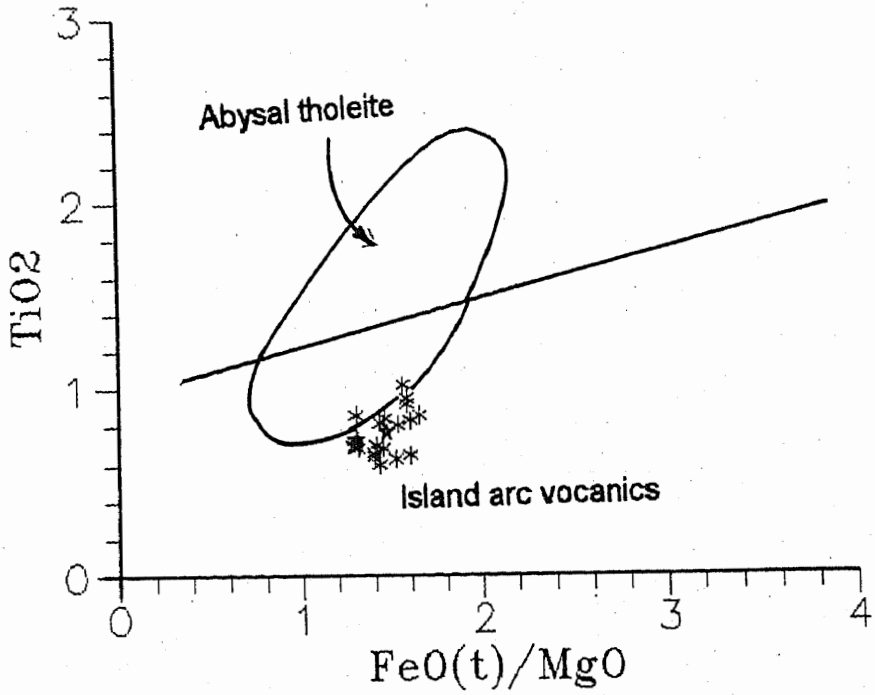

Fig.7.6.TiO_2 vs FeO(+)/MgO plot for the amphibolites and gabbro-norites of the Ushiri valley, central Dir. Field of abyysal tholeiites with an ellipitical out line is shown after Miyashiro (1977). Straight line is the upper limit of TiO_2 in ordinary volcanic rocks of island arc. Key as in Fig.6.1.

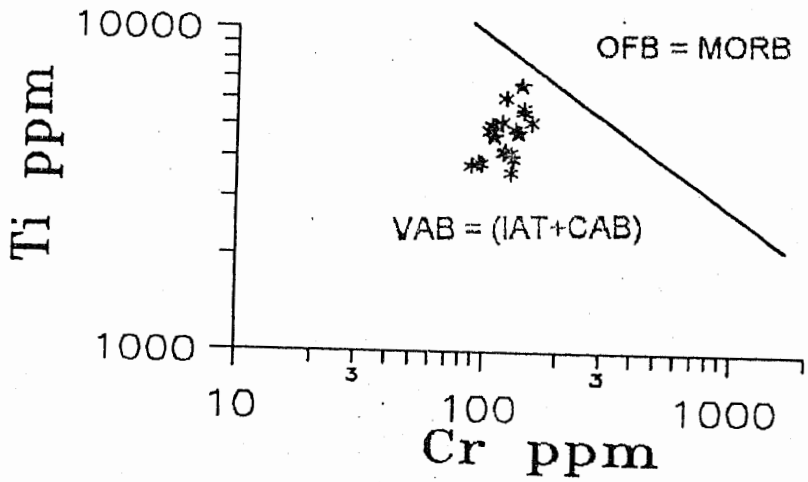

Fig.7.7.Ti vs Cr plot for the amphibolites and gabbro-norites of the Ushiri valley, central Dir. The straight line discrimination between island arc tholeiite and ocean floor basalt (after Pearce, 1975). Key as in Fig.6.1.

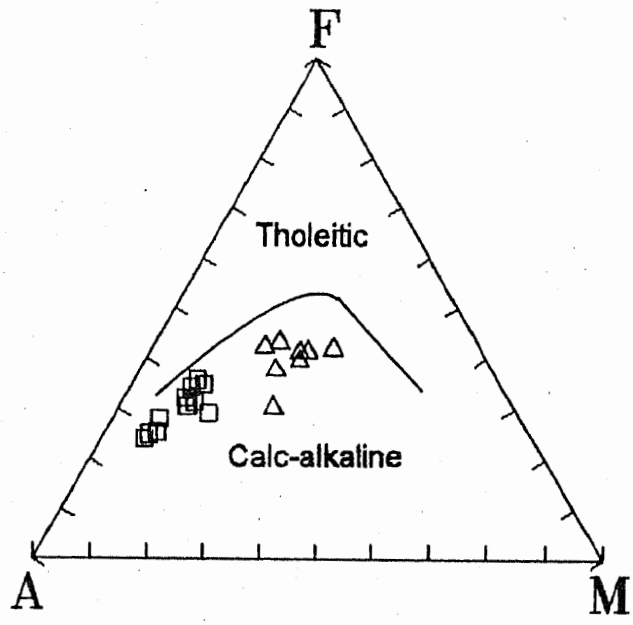

Fig.7.8. AFM plot for the diorites/quartz diorites and grenodiorites of the Ushiri valley, central Dir. The separation line is of Irvin and Baragar (1971), between calc-alkaline at the bottom) and tholeiitic rocks (at the top)

Symbols: △ = Diorites/quartz diorites
□ = Granodiorites

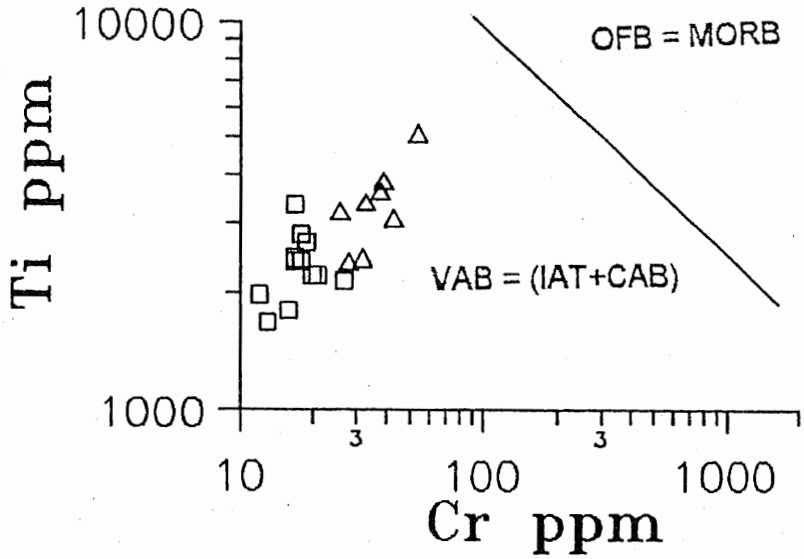

Fig.7.9. Ti vs Cr plot for the diorites/quartz diorites and grenodiorites of the Ushiri valley, central Dir. The straight line discriminate between island arc tholeiite and ocean floor basalt (after Pearce, 1975). Key as in Fig. 7.8

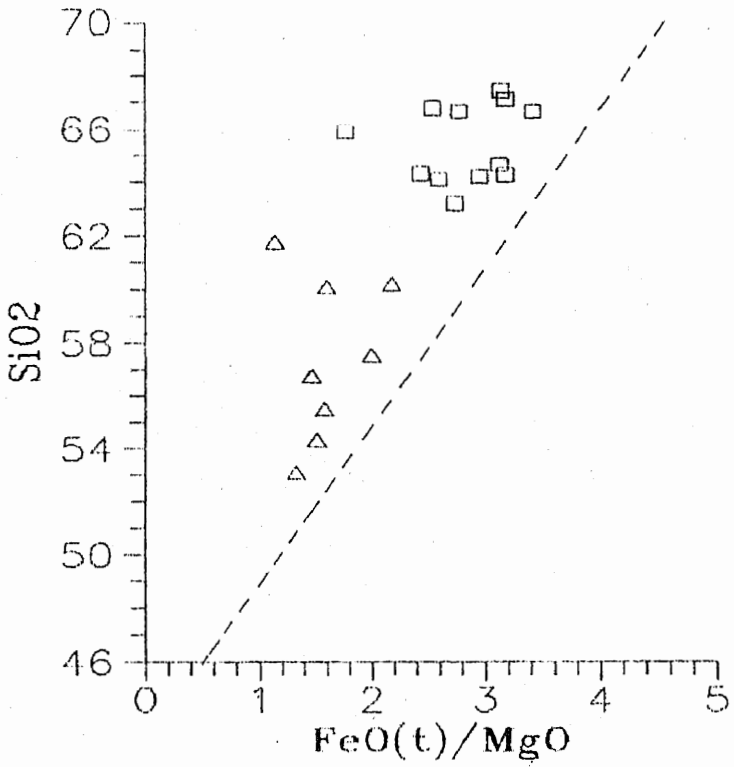

Fig.7.10. SiO2 vs FeO(+)/MgO plot for the diorites/quartz diorites and granodiorites of the Ushiri valley, central Dir. The straight line separate the tholeiitic rocks from the calc-alkaline rocks (After Miyashiro 1974). Key as in Fig.7.8.

The tectonic affinity of the studied rocks could well be understood by plotting them in the TiO_2-MnO-P_2O_5 diagram (Fig.7.11) of Mullen (1983); in MgO-$FeO_{(t)}$-Al_2O_3 diagram (Fig.7.12) of Pearce et al. (1977) and in MgO vs FeO & Fe_2O_3 diagram (Fig.7.13) of Yoder (1969). Majority of the data plot in the field of calc-alkaline basalt in the diagram (Fig.7.11) of Mullen (1983). The plotting of data in Figure 7.12 of Pearce et al. (1977) suggest that the studied rocks have affinity towards orogenic basalt and are originated in island arc type set up. The origination of these rocks in the island arc type set up can also be evident from the diagram (Fig.7.13) of Yoder (1969).

The metaluminous, peraluminous and peralkaline granitoids have been distinguished on the basis of molar Al_2O_3 / Na_2O+K_2O vs molar Al_2O_3 / Ca $+Na_2O+K_2O$ by Shand (1922). The majority of metagranodiorites in this diagram (Fig.7.14) plot within the field of peraluminous while few in the field of metaluminous. Maniar and Piccoli (1989) have distinguished granitoids of various tectonic environments by using binary and ternary diagrams. They differentiated the granitoid as orogenic granitoid rocks: for example 1. island arc granitoid (IAG), 2. continental arc granitoids (CAG), 3. continental collision granitoids (CCG), 4. post orogenic granitoids (POG)] and as an-orogenic granitoids: for example1. rift related granitoids (RRG), 2. continental epirogenic uplift granitoids (CEUG), and 3. oceanic plagio granitoids (OP). The studied metagranodiorites are plotted in these diagrams of Manior and Piccoli (1989) in order to establish the tectonic affinity of these rocks. These metagranodiorites are distinguished as either island arc granitoids (IAG), continental arc granitoids (CCG) or post-orogenic granitoids (POG) of group 1 of Maniar and Piccoli (1989). This clearly indicates that the studied metagranodiorites at least display orogenic characteristics (Fig.7.14)

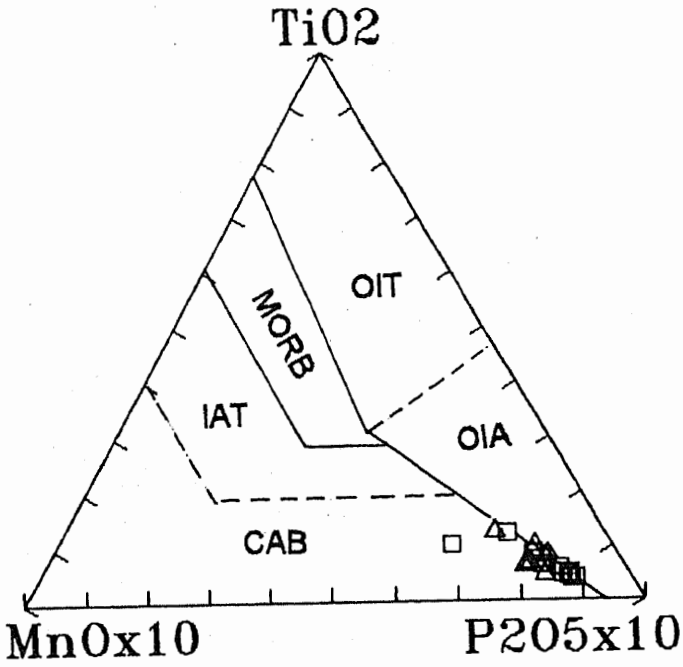

Fig.7.11. The MnOx10/TiO2/P2O5 x10 discrimination diagram for the diorites/quartz diorites and granodiorites of the Ushiri valley, central Dir (after Mullen, 1983). Key as in Fig.7.8

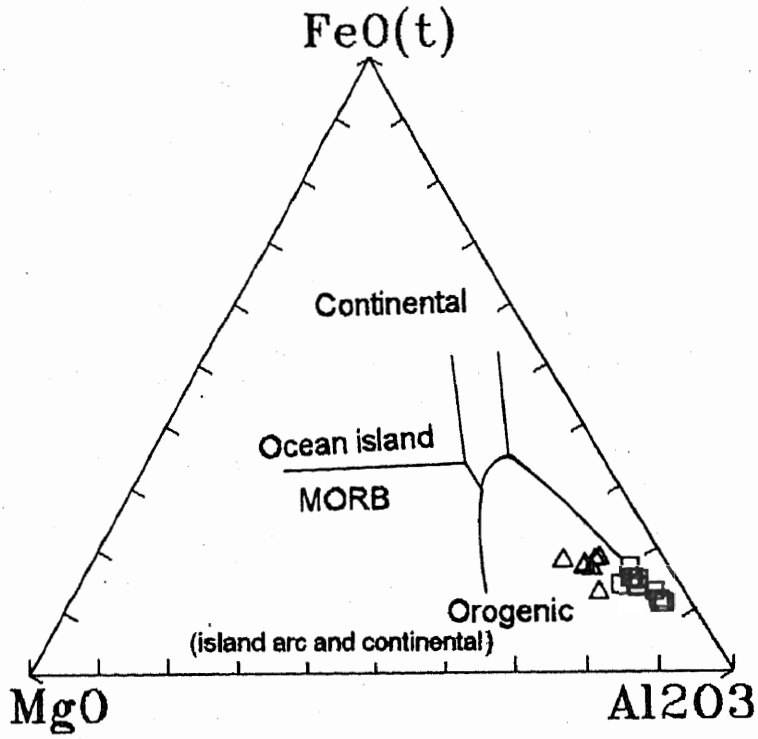

Fig.7.12. Discrimination diagram for the diorites/quartz diorites and granodiorites of the Ushiri valley, central Dir (after Pearce et al, 1977). Key as in Fig.7.8

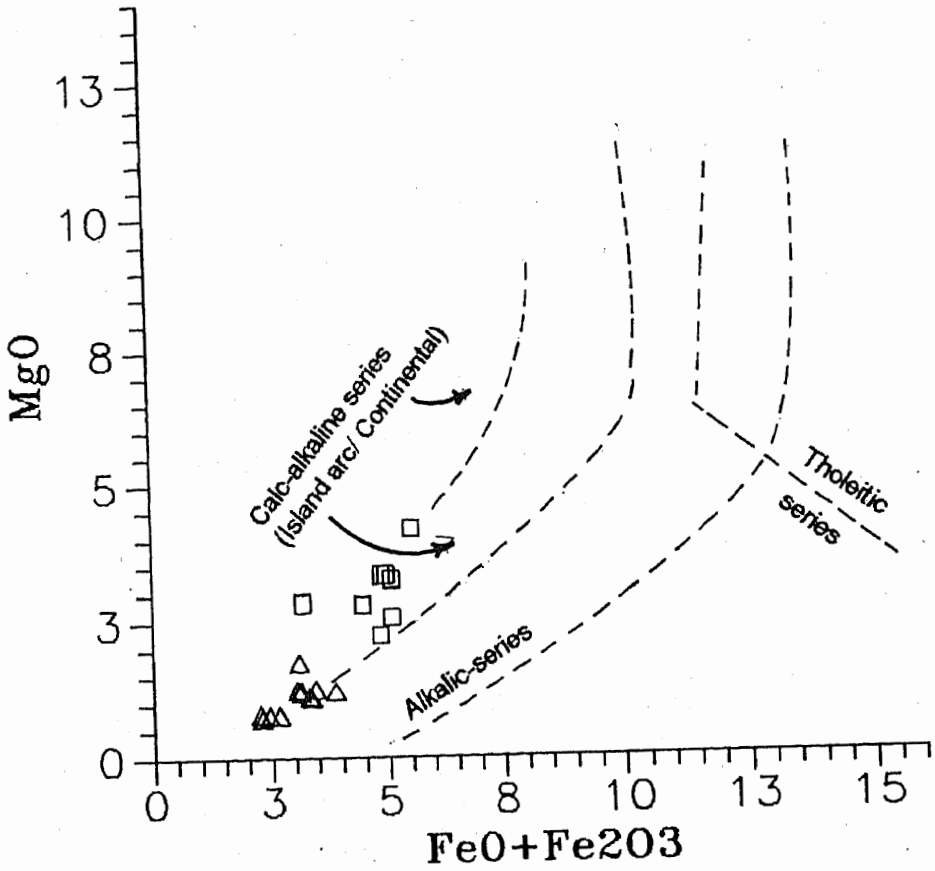

Fig.7.13. MgO against FeO+Fe2O3 plot for the diorites/quartz diorites and granodiorites of the Ushiri valley, central Dir. Various fields are after Yoder (1969). Key as in Fig.7.3.

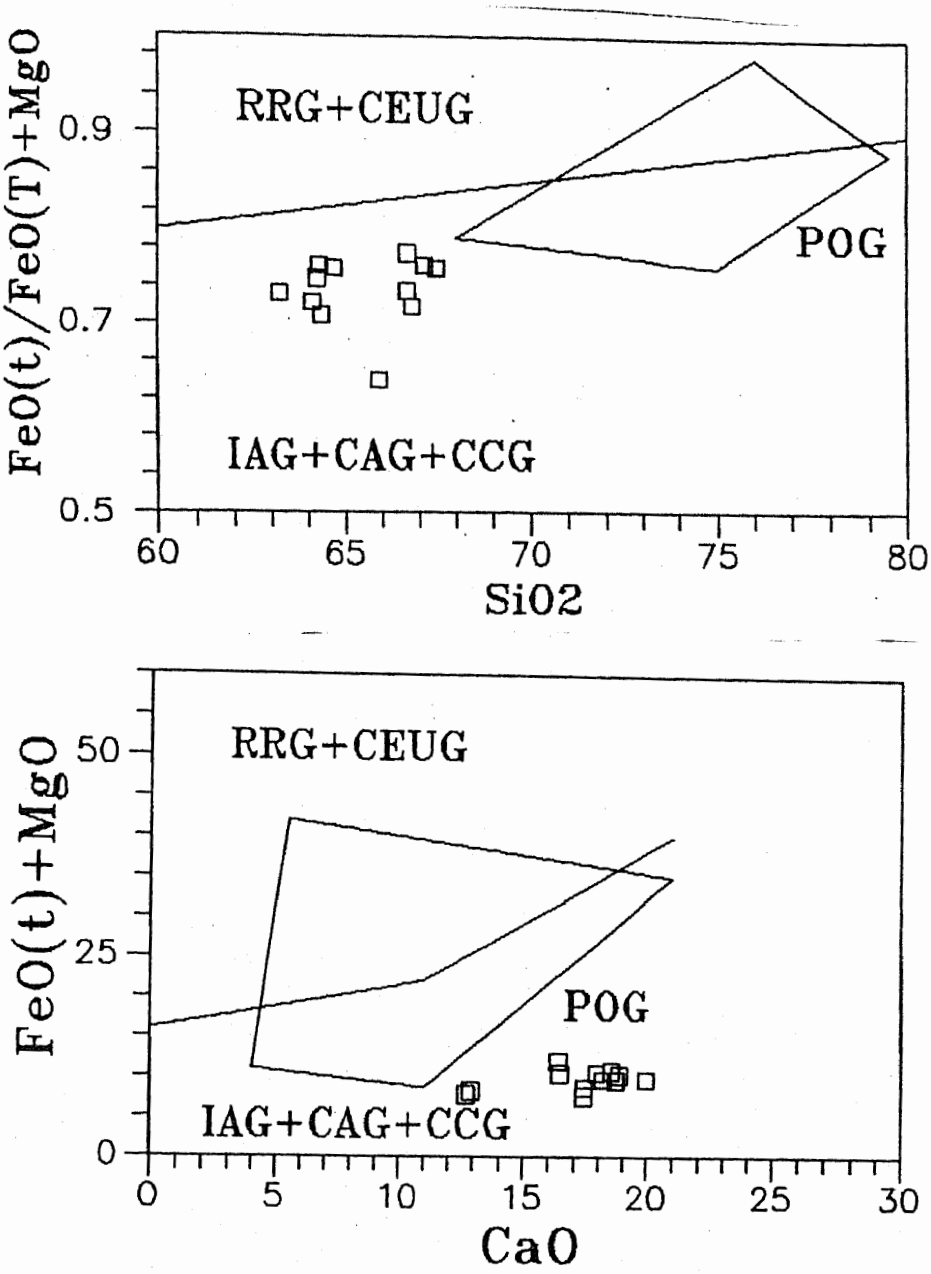

Fig.7.14. Discrimination diagram for the diorites/quartz diorites and granodiorites of the Ushiri valley, central Dir (after Maniar and Piceoli, 1989).

Orogenic Grenitoid Rocks

1AG = Island Arc granitoids
CAG = Continental arc granitoids
CCG = Continental collision grenitoids
POG = Post Orogenic granitoids

An-orogenic granitoids

RRG = Rift related granitoids
CEUG = Continental epirogenic granitoids
OP = Oceanic plagio grenitoids

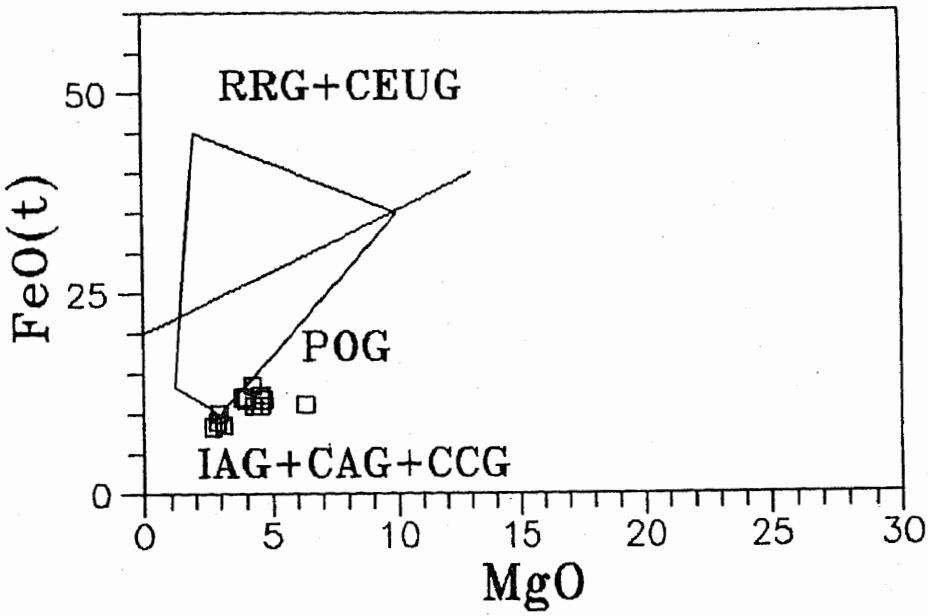
RRG+CEUG
POG
IAG+CAG+CCG
FeO(t)
MgO
0
25
50
0
5
10
15
20
25
30

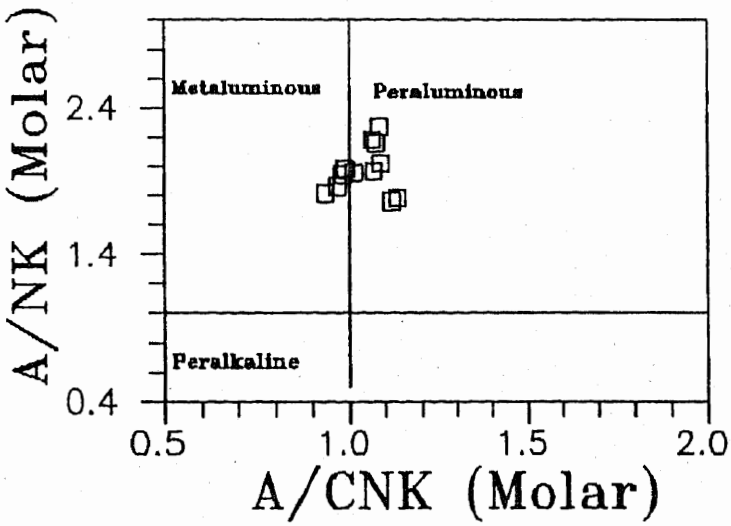
Metaluminous
Peraluminous
Peralkaline
A/NK (Molar)
A/CNK (Molar)
0.4
1.4
2.4
0.5
1.0
1.5
2.0

These tectono-discrimination diagrams clearly suggest that the studies metadiorite/quartz-diorite and metagranodiorite have close affinity to the calc-alkaline rocks developed in the subduction related compressional environments. Such rocks occur in both island arc and continental margin and the distinction between the two is not always clear. However, the diagram (Fig.7.13) of Yoder (1969) has provided a clear distinction of these rocks to have been formed in the island arc type of setting instead of continental margin.

CHAPTER 8

STREAM SEDIMENTS SURVEY

Stream sediment survey is generally carried out during the reconnaissance mineral exploration. During this survey various detrital material (both pan-concentrate and fine-fraction) are collected from widely spread sediment catchment areas. These detritus materials are having specific indicator metals from any mineralization in the catchment areas. This produce anomaly of indicator element in the drainage material. The intensity of drainage anomaly is the amount of material eroded or leached from the catchment area, minus what has been precipitated from ground water below the surface, accumulated in overburden, or carried past the same site. The presence of a strong anomaly in the drainage material is, therefore, the indication of existence of ore body in the adjacent catchment cell. However, the absence of strong anomaly in the drainage sediments does not necessarily mean the absence of an ore body. This absence of such anomaly could be attributed to the dilution of precipitation of metals some where along the drainage system between the source and the sample site.

The anomalies can either be determined by mineralogical studies or geochemical studies of the stream sediments. These studies are useful guide in pin pointing the sources of these anomalies. The characterization of these sources can be evaluated by the type of material collected from streams.

Considering these facts, the present study was partly focused on the mineralogical and geochemical investigation of heavy mineral concentrate (Pan-concentrate) and fine-fractions (-80 mesh size) of the stream sediments. The data obtained through this study has also been compared with that of the rocks of the catchment area in order to find out areas of concentration (if any) of base metal, Gold and Silver.

COLLECTION AND ANALYSES OF SAMPLES

About fifteen sites have been selected for the collection of stream sediment samples along Umrali khwar (stream) and its tributaries in Ushiri valley (Fig.8.1). From each sample site two samples 1) pan-concentrate and 2) fine-fraction (-80 mesh size) have been collected. Pan-concentrates were obtained by sieving <850 mm (-20 mesh) and the heavy mineral concentrate were prepared by panning. The fine-fractions were obtained by sieving the clay size material to <177 mm (-80 mesh) size.

The mineralogy of pan-concentrates was studied by the binocular microscope and the elemental determinations for Au, Ag, Cu, Pb, Zn, Ni, Co and Cr in both pan-concentrates and -80 mesh fraction have been carried out by both flame and flameless atomic absorption techniques at the geochemistry laboratory of the NCE in Geology, University of Peshawar.

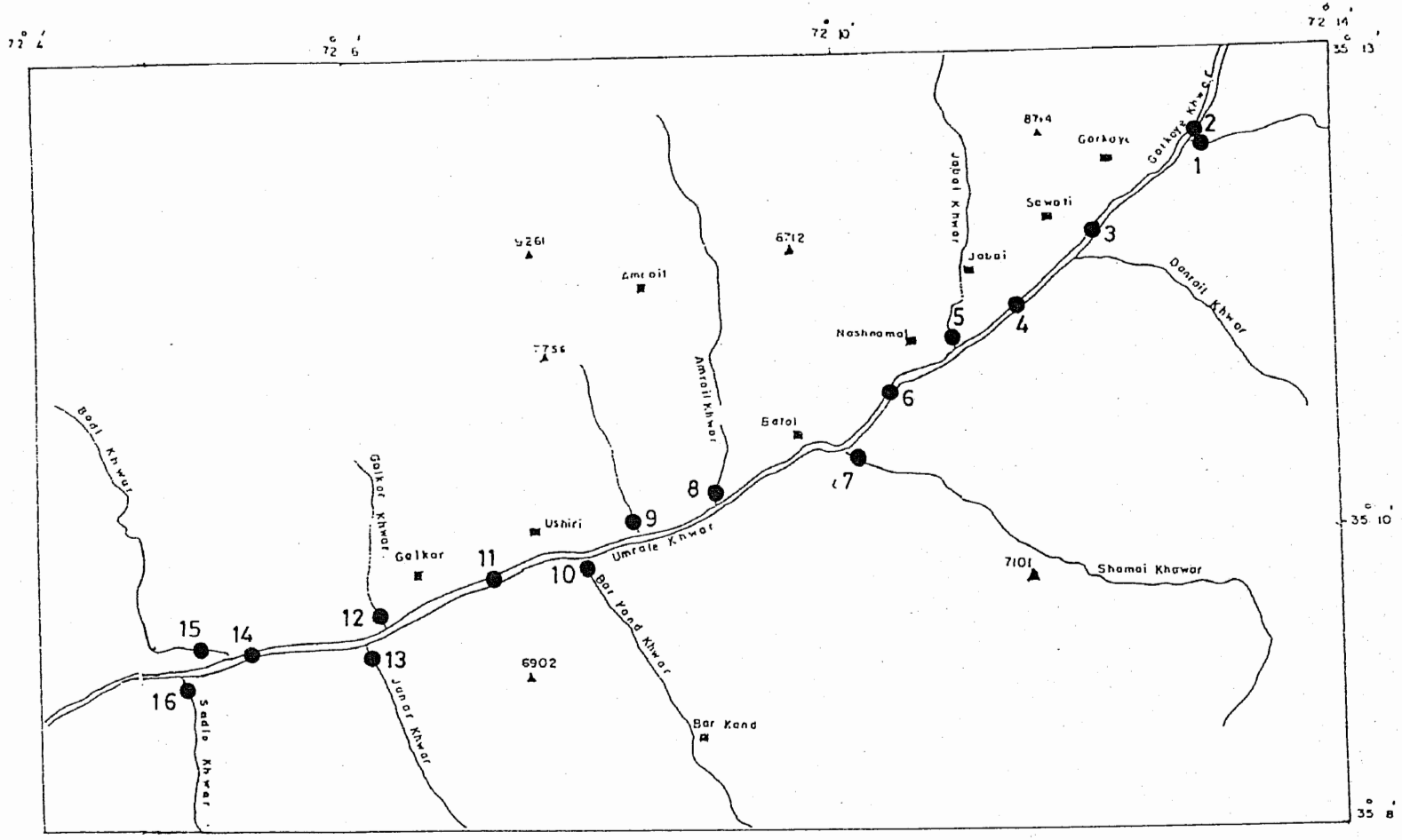

Fig.8.1. Map showing sample numbers along with sample sites of the Ushiri valley, central Dir.

Because of varying concentration factors, reflected in the wide range of weight (amount) of heavy mineral concentrate produced from standard sample volumes (20 litres), it is necessary to normalized or standardized the data to a nominal 100 grams concentrate weight for comparative purposes. It is very necessary in the case when the elements (e.g., gold) having nuggets effects are needed to be evaluated. However, there is no need to normalize the fine-fraction data. The pan-concentrate data of the studied samples are, therefore, normalized to 100g and the results are presented in Table 8.1. This standardized data is then used during interpretation. However, for fine-fraction, no standardization is made and the data is presented in Table 8.2. Summary statistics of the geochemical data of both pan-concentrate and fine-fraction are given in Tables 8.3 & 8.4.

FLOAT AND PAN CONCENTRATE STUDY

Float Study: Float study is usually carried out in the regions of thick vegetation where the study of rock exposure is not possible. In that case the float study is very useful for determining the general geology of an area. The study area is not having thick vegetation and the rocks are very well exposed. Therefore, the study area can very easily be mapped geologically. However, the float study at each sample site has been made. These floats are mainly of amphibolite, granodiorite, diorite and quartz- diorite. However, in some streams floats of quartz veins (both mineralized and unmineralized), gabbro-norite, quartzites, and metasediments etc. are also found along with the above mentioned main float types.

Pan Concentrate: Mineralogical studies of pan concentrates were carried out under the binocular microscope. The pan concentrates, on average, have magnetite as the dominant (>70%) phase while rock fragments, hornblende, zircon, quartz, pyroxene, feldspar, garnet and pyrite are present in lesser

Table. 8.1. Geochemical data of the stream sediments pan-concentrates of Ushiri valle

S.No.	Cu ppm	Pb ppm	Zn ppm	Co ppm	Ni ppm	Cr ppm	Au ppm	Ag ppm
PC1	265	2	48	12	13	45	0.045	0.023
PC2	286	3	38	16	21	59	0.054	0.027
PC3	112	3	25	9	11	23	0.021	0.016
PC4	296	3	43	15	16	63	0.058	0.034
PC5	195	4	52	12	10	59	0.034	0.012
PC6	67	2	34	11	6	42	0.028	0.016
PC7	35	8	45	25	63	623	0.027	0.014
PC8	93	6	47	12	16	99	0.016	0.007
PC9	34	4	37	8	18	95	0.015	0.005
PC10	65	45	56	19	42	345	0.012	0.002
PC11	24	14	34	12	16	45	0.004	0.003
PC12	49	10	54	6	8	65	0.021	0.006
PC13	56	28	57	14	41	168	0.026	0.008
PC14	23	17	32	5	12	58	0.005	0.004
PC15	46	7	53	5	12	75	0.024	0.007
PC16	187	4	37	7	14	54	0.021	0.005

Table. 8.2. Geochemical data of the stream sediments fine-fraction of Ushiri valley.

S.No.	Cu ppm	Pb ppm	Zn ppm	Co ppm	Ni ppm	Cr ppm	Au ppm	Ag ppm
SS1	52	4	65	9	31	56	0.027	0.012
SS2	49	5	57	8	34	64	0.025	0.014
SS3	23	3	37	4	23	45	0.013	0.008
SS4	46	4	48	7	27	49	0.021	0.009
SS5	47	14	43	9	25	43	0.018	0.010
SS6	29	2	32	5	19	29	0.009	0.004
SS7	54	4	48	11	43	110	0.023	0.013
SS8	39	7	41	7	27	64	0.018	0.009
SS9	24	4	43	5	21	58	0.014	0.008
SS10	46	4	42	12	42	120	0.018	0.009
SS11	26	2	31	7	26	65	0.004	0.002
SS12	39	7	38	6	29	63	0.016	0.007
SS13	50	9	54	12	37	59	0.025	0.014
SS14	31	5	34	7	21	39	0.012	0.008
SS15	21	4	43	4	25	64	0.003	0.002
SS16	47	3	68	12	28	59	0.021	0.012

Table 8.3. Summery statistics for the stream sediment pan-concentrates from the Ushiri valley.

Item	Cu ppm	Pb ppm	Zn ppm	Co ppm	Ni ppm	Cr ppm	Au ppm	Ag ppm
N	16	16	16	16	16	16	16	16
AVG	114.56	10.00	43.25	11.75	19.94	119.88	0.03	0.01
VAR	9578.93	135.07	94.33	28.73	237.40	23845.85	0.00	0.00
STD	97.87	11.62	9.71	5.36	15.41	154.42	0.02	0.01
CV	0.85	1.16	0.22	0.46	0.77	1.29	0.61	0.79
T(5%)	1.75	1.75	1.75	1.75	1.75	1.75	1.75	1.75
D	42.89	5.09	4.26	2.35	6.75	67.68	0.01	0.00
UCL	157.45	15.09	47.51	14.10	26.69	187.55	0.03	0.02
LCL	71.67	4.91	38.99	9.40	13.19	52.20	0.02	0.01
MAX	296	45	57	25	63	623	0.058	0.034
MIN	23	2	25	5	6	23	0.004	0.002
CA	55	13	70	25	75	100	0.004	0.07

N, number of samples; AVG, average (mean); VAR, variance; STD, standard deviation;
CV, coefficient of variance;T, t-test; D, half width of confidence interval;
UCL, upper cofidence limit; LCL, lower confidence; MAX, minimum; MIN, minimum;
CA, crustal abundence.

Table 8.4. Summery statistics for the stream sediment fine fractions from the Ushiri valley.

Item	Cu ppm	Pb ppm	Zn ppm	Co ppm	Ni ppm	Cr ppm	Au ppm	Ag ppm
N	16	16	16	16	16	16	16	16
AVG	38.94	5.06	45.25	7.81	28.63	61.69	0.02	0.01
VAR	131.93	9.13	120.47	7.76	51.32	546.36	0.00	0.00
STD	11.49	3.02	10.98	2.79	7.16	23.37	0.01	0.00
CV	0.29	0.60	0.24	0.36	0.25	0.38	0.43	0.43
T(5%)	1.75	1.75	1.75	1.75	1.75	1.75	1.75	1.75
D	5.03	1.32	4.81	1.22	3.14	10.24	0.00	0.00
UCL	43.97	6.39	50.06	9.03	31.76	71.93	0.02	0.01
LCL	33.90	3.74	40.44	6.59	25.49	51.44	0.01	0.01
MAX	54	14	68	12	43	120	0.027	0.014
MIN	21	2	31	4	19	29	0.003	0.002
CA	55	13	70	25	75	100	0.004	0.07

N, number of samples; AVG, average (mean); VAR, variance; STD, standard deviation;
CV, coefficient of variance;T, t-test; D, half width of confidence interval;
UCL, upper cofidence limit; LCL, lower confidence; MAX, minimum; MIN, minimum;
CA, crustal abundence.

(<30%) amount (see appendix). No gold in the form of colour, speck and piece has been identified in any of the stream sediment sample (see appendix).

DATA INTERPRETATION

The interpretation of stream sediments geochemical data generally involves consideration of statistical methods, whereby multiple population of data is treated simultaneously. These populations may represent background samples, or the samples having significant or non-significant anomalies. Various methods have been designated to distinguish the anomalous populations from those of background during the data interpretation in geochemical exploration (Lepeltier, 1969; Sinclair, 1974; 1976; Otsu et al., 1948; Tennant and White, 1959). During this study the methods of Tennant and White (1959) and Sinclair (1974 & 1976), have been adopted for the data interpretation. The data was, therefore, ranked in increasing order for each element and then was divided in to specific intervals (Tables 8.5 & 8.6). The class frequency, relative frequency percent, cumulative frequency and cumulative relative frequency percent were than calculated (Tables 8.5 & 8.6). On the basis of this statistical data, the cumulative frequency curves for each element in both pan concentrates and fine fractions have been constructed (Figs. 8.2 & 8.3). Besides this the histograms of each elements for both pan concentrates and fine fractions have also been constructed (Figs. 8.4 & 8.5).

Based on the inspection of frequency diagrams the interpreted threshold values for each element in both pan concentrate and fine fraction have been determined. The data below threshold are considered as background populations and those above the threshold have been divided into low-order and high-order populations (Figs. 8.2 & 8.3). Both background along with low-order and high-order anomalous values, for each element are

Table 8.5. Statistical data calculated for the construction of cumulative frequency curve for various elements determined in pan-concentrates of the Ushiri valley

Copper (Cu)

1	2	3	4	5
0	0	0	0	
20	0	0	0	0
40	4	25	4	25
60	3	19	7	44
80	2	13	9	56
100	1	6	10	63
120	1	6	11	69
140	0	0	11	69
160	0	0	11	69
180	0	0	11	69
200	2	13	13	81
220	0	0	13	81
240	0	0	13	81
260	0	0	13	81
280	1	6	14	88
300	2	13	16	100

1 = class interval
2 = frequency
3 = relative frequency (%)
4 = cumulative frequency
5 = relative cumulative frequency (%)

Lead (Pb)

1	2	3	4	5
0	0	0	0	0
5	8	50	8	50
10	4	25	12	75
15	1	6	13	81
20	1	6	14	88
25	0	0	14	88
30	1	6	15	94
35	0	0	15	94
40	0	0	15	94
45	1	6	16	100
50	0	0	16	100

1 = class interval
2 = frequency
3 = relative frequency (%)
4 = cumulative frequency
5 = relative cumulative frequency (%)

Zinc (Zn)

1	2	3	4	5
20	0	0	0	0
25	1	6	1	6
30	0	0	1	6
35	3	19	4	25
40	3	19	7	44
45	2	13	9	56
50.	2	13	11	69
55	3	19	14	88
60	2	13	16	100

1 = class interval
2 = frequency
3 = relative frequency (%)
4 = cumulative frequency
5 = relative cumulative frequency (%)

Nickle (Ni)

1	2	3	4	5
0	0	0	0	0
5	0	0	0	0
10	3	19	3	19
15	5	31	8	50
20	4	25	12	75
25	1	6	13	81
30	0	0	13	81
35	0	0	13	81
40	0	0	13	81
45	2	13	15	94
50	0	0	15	94
55	0	0	15	94
60	0	0	15	94
65	1	6	16	100

1 = class interval
2 = frequency
3 = relative frequency (%)
4 = cumulative frequency
5 = relative cumulative frequency (%)

Chromium (Cr)

1	2	3	4	5
0	0	0	0	0
50	4	25	4	25
100	9	56	13	81
150	0	0	13	81
200	1	6	14	88
250	0	0	14	88
300	0	0	14	88
350	1	6	15	94
400	0	0	15	94
450	0	0	15	94
500	0	0	15	94
550	0	0	15	94
600	0	0	15	94
650	1	6	16	100
700	0	0	16	100

1 = class interval
2 = frequency
3 = relative frequency (%)
4 = cumulative frequency
5 = relative cumulative frequency (%)

Cobalt (Co)

1	2	3	4	5
0	0	0	0	0
3	0	0	0	0
6	3	19	3	19
9	3	19	6	38
12	5	31	11	69
15	2	13	13	81
18	1	6	14	88
21	1	6	15	94
24	0	0	15	94
27	1	6	16	100

1 = class interval
2 = frequency
3 = relative frequency (%)
4 = cumulative frequency
5 = relative cumulative frequency (%)

Silver (Ag)

1	2	3	4	5
0.000	0	0	0	0
0.005	5	31	5	31
0.010	4	25	9	56
0.015	2	13	11	69
0.020	2	13	13	81
0.025	1	6	14	88
0.030	1	6	15	94
0.035	1	6	16	100
0.040	0	0	16	100
0.045	0	0	16	100

1 = class interval
2 = frequency
3 = relative frequency (%)
4 = cumulative frequency
5 = relative cumulative frequency (%)

Gold (Au)

1	2	3	4	5
0.000	0	0	0	0
0.005	2	13	2	13
0.010	0	0	2	13
0.015	2	13	4	25
0.020	1	6	5	31
0.025	4	25	9	56
0.030	3	19	12	75
0.035	1	6	13	81
0.040	0	0	13	81
0.045	1	6	14	88
0.050	0	0	14	88
0.055	1	6	15	94
0.060	1	6	16	100
0.065	0	0	16	100

1 = class interval
2 = frequency
3 = relative frequency (%)
4 = cumulative frequency
5 = relative cumulative frequency (%)

Table 8.6. Statistical data calculated for the construction of cumulative frequency curve for various elements determined in fine fractions of the Usheri valley

Copper (Cu)

1	2	3	4	5
20	0	0	0	0
25	3	19	3	19
30	2	13	5	31
35	1	6	6	38
40	2	13	8	50
45	0	0	8	50
50	6	38	14	88
55	2	13	16	100

1 = class interval
2 = frequency
3 = relative frequency (%)
4 = cumulative frequency
5 = relative cumulative frequency (%)

Lead (Pb)

1	2	3	4	5
0	0	0	0	0
2	2	13	2	13
4	8	50	10	63
6	2	13	12	75
8	2	13	14	88
10	1	6	15	94
12	0	0	15	94
14	1	6	16	100
16	0	0	16	100

1 = class interval
2 = frequency
3 = relative frequency (%)
4 = cumulative frequency
5 = relative cumulative frequency (%)

Zinc (Zn)

1	2	3	4	5
30	0	0	0	0
35	3	19	3	19
40	2	13	5	31
45	5	31	10	63
50	2	13	12	75
55	1	6	13	81
60	1	6	14	88
65	1	6	15	94
70	1	6	16	100
75	0	0	16	100
80	0	0	16	100
85	0	0	16	100

1 = class interval
2 = frequency
3 = relative frequency (%)
4 = cumulative frequency
5 = relative cumulative frequency (%)

Nickle (Ni)

1	2	3	4	5
15	0	0	0	0
20	1	6	1	6
25	5	31	6	38
30	5	31	11	69
35	2	13	13	81
40	1	6	14	88
45	2	13	16	100

1 = class interval
2 = frequency
3 = relative frequency (%)
4 = cumulative frequency
5 = relative cumulative frequency (%)

Chromium (Cr)

1	2	3	4	5
20	0	0	0	0
30	1	6	1	6
40	1	6	2	13
50	3	19	5	31
60	4	25	9	56
70	5	31	14	88
80	0	0	14	88
90	0	0	14	88
100	0	0	14	88
110	1	6	15	94
120	1	6	16	100

1 = class interval
2 = frequency
3 = relative frequency (%)
4 = cumulative frequency
5 = relative cumulative frequency (%)

Cobalt (Co)

1	2	3	4	5
4	2	13	2	13
6	3	19	5	31
8	5	31	10	63
10	2	13	12	75
12	4	25	16	100

1 = class interval
2 = frequency
3 = relative frequency (%)
4 = cumulative frequency
5 = relative cumulative frequency (%)

Silver (Ag)

1	2	3	4	5
0	0	0	0	0
0.002	2	13	2	13
0.004	1	6	3	19
0.006	0	0	3	19
0.008	4	25	7	44
0.010	4	25	11	69
0.012	2	13	13	81
0.014	3	19	16	100

1 = class interval
2 = frequency
3 = relative frequency (%)
4 = cumulative frequency
5 = relative cumulative frequency (%)

Gold (Au)

1	2	3	4	5
0.002	0	0	0	0
0.004	2	13	2	13
0.006	0	0	2	13
0.008	0	0	2	13
0.010	1	6	3	19
0.012	1	6	4	25
0.014	2	13	6	38
0.016	1	6	7	44
0.018	3	19	10	63
0.020	0	0	10	63
0.022	2	13	12	75
0.024	1	6	13	81
0.026	2	13	15	94
0.028	1	6	16	100

1 = class interval
2 = frequency
3 = relative frequency (%)
4 = cumulative frequency
5 = relative cumulative frequency (%)

plotted on each stream site for both pan-concentrates (Fig.8.6) and fine-fractions (Fig. 8.7), on topographic maps. The anomalies and their possible source for each element is discussed as follows:

Gold (Au): There is a population break at about 30 percentile in the pan concentrate and at about 15 percentile in the fine fraction for gold (Figs.8.2 & 8.3). The pan concentrates have background, low order and higher order anomalous values of <0.017ppm, 0.017-0.040ppm and >0.040ppm respectively. The fine fractions, however, have background, low order and high order anomalous values of <0.008ppm, 0.008-018ppm and >0.018ppm respectively. The distribution maps of pan (Fig. 8.6) and fine fraction (Fig.8.7) show that high order anomalous values are wide spread in almost all the streams as compare to the pan concentrate in the area. The pan concentrates, however, have high anomaly in the Gorkoye Khawar in the north-eastern portion of the study area. No any piece, colour or speck has been found in the pan concentrate (see appendix).

By considering the gold concentration (up to maximum of 0.011ppm) in the rocks of the area (Tables 6.1 & 6.2) it can be concluded that the anomalous values, though not very high, in both pan concentrates and fine fractions could be contributed by the rocks of the area in the stream sediments.

Silver (Ag): The frequency distribution curves and histograms suggest background 0.010ppm, low order=0.010-0.020ppm and high order >0.020ppm in pan-concentrates and background =<0.006, low order =0.060-0.010ppm and high order = .0.010ppm in the fine fraction (Figs. 8.2 & 8.3). The distribution maps (Figs. 8.6 & 8.7) show the wide spread distribution of background and low-order values in most of the streams. However, the Gorkoye Khawar show high-order anomaly in the pan-concentrate samples.

The low and high order anomalous values for silver are also not very high which could not be related to the specific mineralization in the area. The rocks of the area generally have <0.5ppm silver (Tables 6.1 & 6.2). These anomalies could, therefore, be contributed by the rocks in the stream sediments.

Copper (Cu): Copper has background (<40ppm) and low-order anomaly (>40ppm) in fine fraction while background (<140ppm), low-order (140-240ppm) and high-order (>240ppm) anomaly in the pan concentrates (Figs. 8.2 & 8.3). The distribution map of copper show the wide spread of low-order anomaly in the streams of the area (Fig. 8.6 & 8.7). However, the Gorkoye Khawar has the high-anomalies for copper in the pan-concentrate samples (Fig. 8.6).

The anomalous values (maximum 240 ppm) of copper in the sediments are not very high and could not be related to specific mineralization. These anomalies can be contributed by the rocks of the area as these have up to 104 ppm copper (Tables 6.1 & 6.2).

Zinc (Zn): The frequency distribution diagrams (Figs.8.2 & 8.3) suggest that zinc has <25 ppm, 25-50 ppm and >50 ppm values for back ground, low-order and high-order anomalies respectively in pan-concentrates. The fine fraction has <50 ppm and 50-70 ppm as background and low-order values respectively. The distribution maps (Figs.8.6 & 8.7) suggest the wide spread of high-order anomalies in the pan concentrates and low-order anomalies in the fine fraction of stream sediments.

The rocks of the area have up to 145 ppm Zn (Tables 6.1 & 6.2). The zinc anomalies, though not very high, could be contributed by the rocks of the area and are not related to any kind of specific mineralization.

Lead (Pb): Lead exhibits <22 ppm, 22-35ppm and >35ppm as background, low-order and high-order anomalies respectively in the pan concentrate. The fine fractions have <5ppm, 5-10ppm and >10ppm of background, low-order and high-order anomalies respectively. The distribution maps (Figs. 8.6 & 8.7) have sporadic low and high order anomalies in the stream sediments and could be contributed by the rocks of the area.

Nickel (Ni): Nickel has the normal threshold at <25ppm in pan concentrates and <32ppm in fine fraction (Figs.8.2 & 8.3). The low and high order anomalies are 25-50 ppm and >50 ppm respectively in pan concentrate and only low order anomaly of >32ppm in the fine fraction (Figs.8.2 & 8.3). The distribution maps (Figs. 8.6 & 8.7) show high order anomaly in Shamai and Barkand Khawars but these still could also be contributed by the rocks of the area.

Chromium (Cr): The frequency distribution diagrams (Figs.8.2 & 8.3) of chromium suggest threshold of <200ppm and <70ppm in pan concentrate and fine fraction respectively. The low-order and high order anomalies in pan-concentrate are 200-400 ppm and >400 ppm respectively while the fine fractions have >70ppm of low-order anomalies. The distribution maps of chromium show similar distribution pattern as noticed for nickel and this could also be related to the rocks of the area.

Cobalt (Co): Cobalt has threshold value of <9ppm and <6 ppm for pan concentrate and fine fraction respectively (Figs.8.2 & 8.3). The low-order and high-order anomalies are 9-20ppm and >20ppm respectively in pan concentrate and 6-9ppm and >9ppm respectively in the fine fraction (Figs.8.2 & 8.3). The distribution maps for cobalt (Figs.8.6 & 8.7) show high-order anomalies in various streams but these could also be related to the rocks of the area and not to specific mineralization.

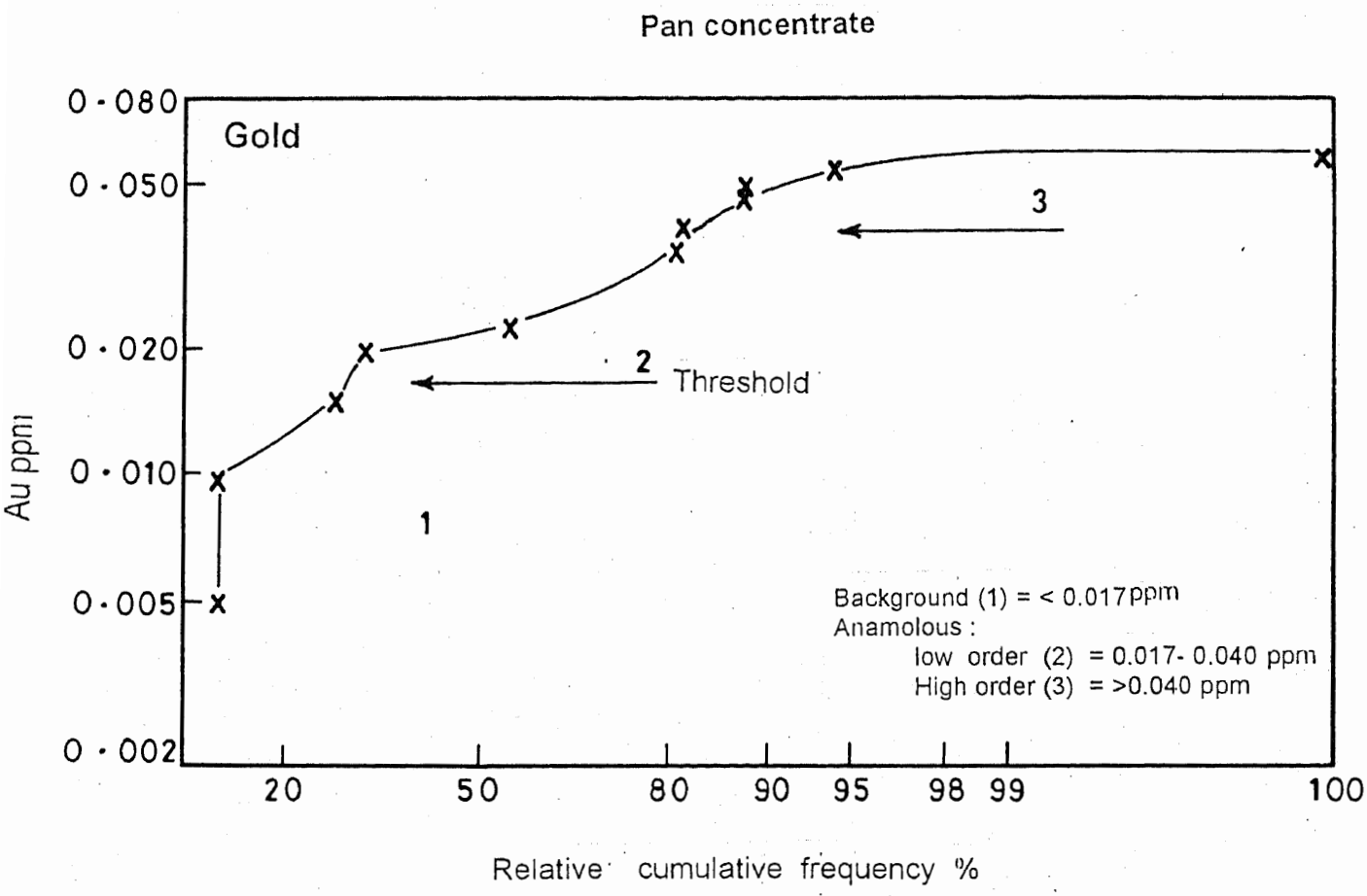

Fig. 8.2. Cumulative frequency curves for Au, Ag, Cu, Zn, Pb, Ni, Cr and Co for the pan concentrates of the study area.

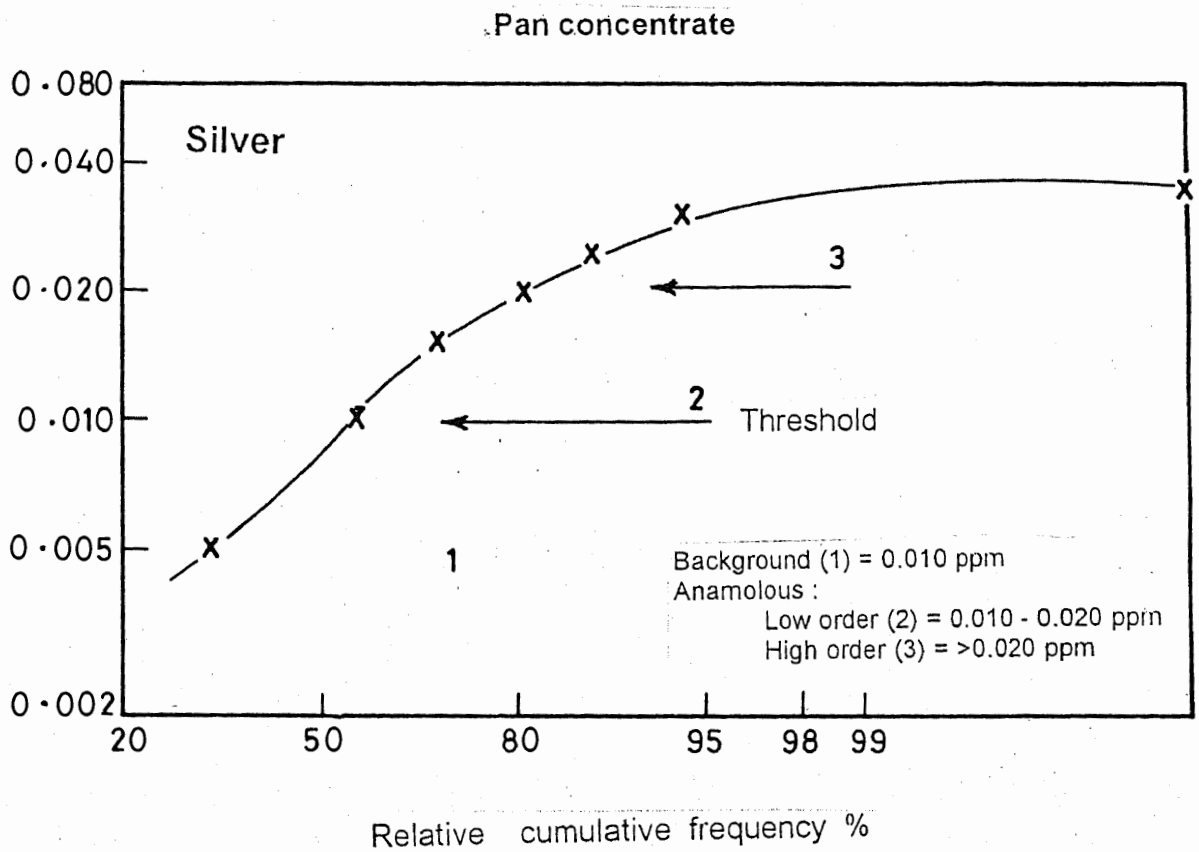
Pan concentrate
Silver
0·080
0·040
0·020
0·010
0·005
0·002
20
50
80
95
98
99
1
2
3
Threshold
Background (1) = 0.010 ppm
Anamolous :
Low order (2) = 0.010 - 0.020 ppm
High order (3) = >0.020 ppm
Relative cumulative frequency %

Pan concentrate

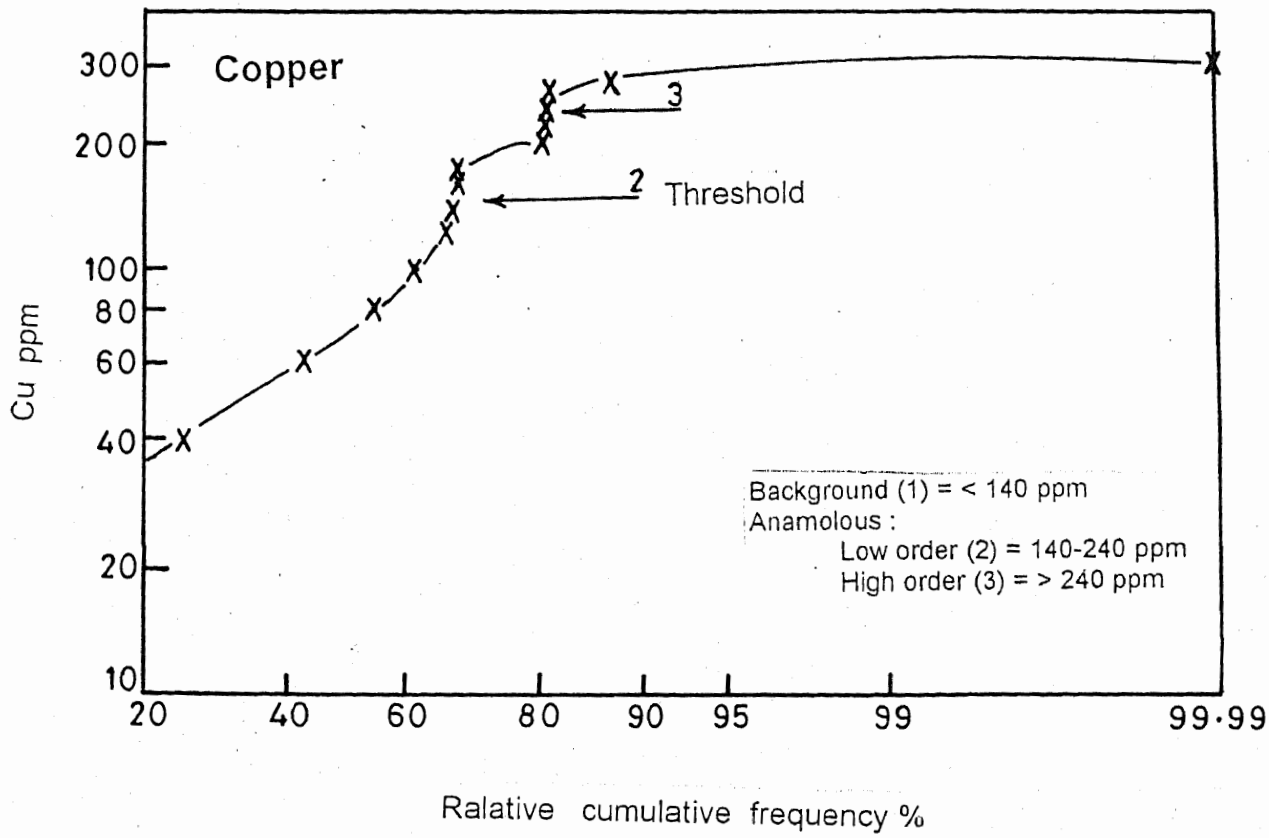

Pan concentrate

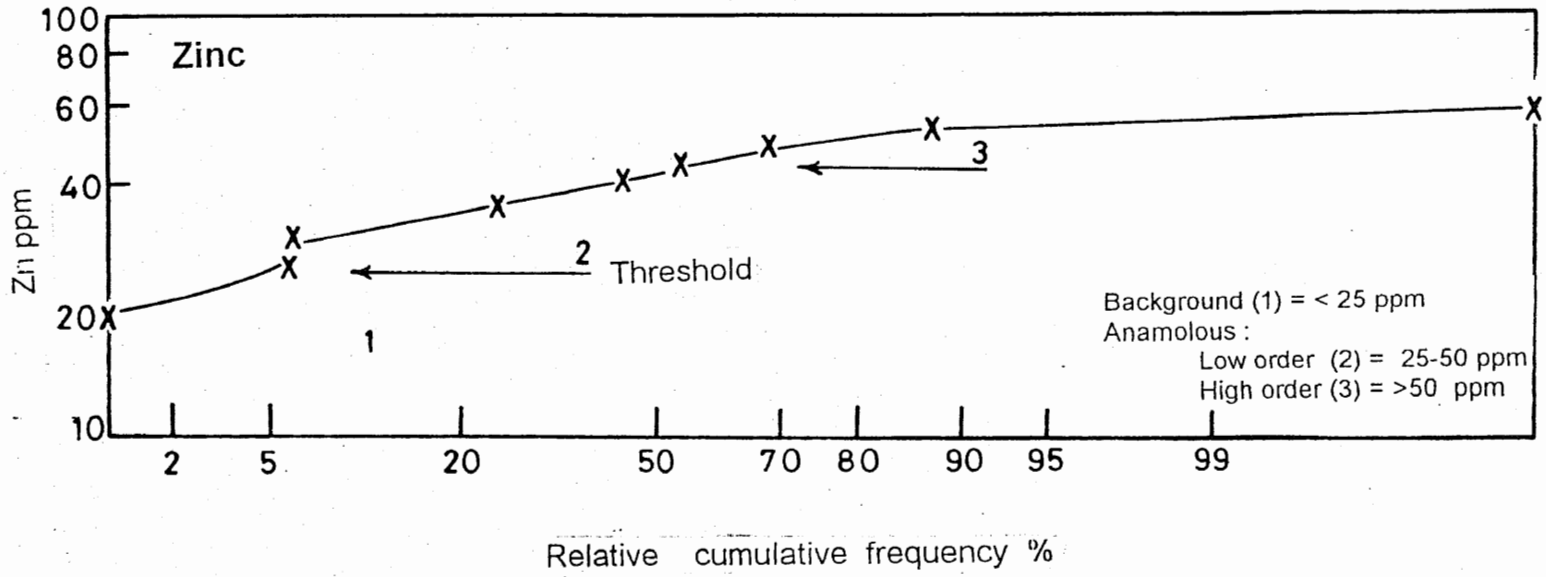

Pan concentrate

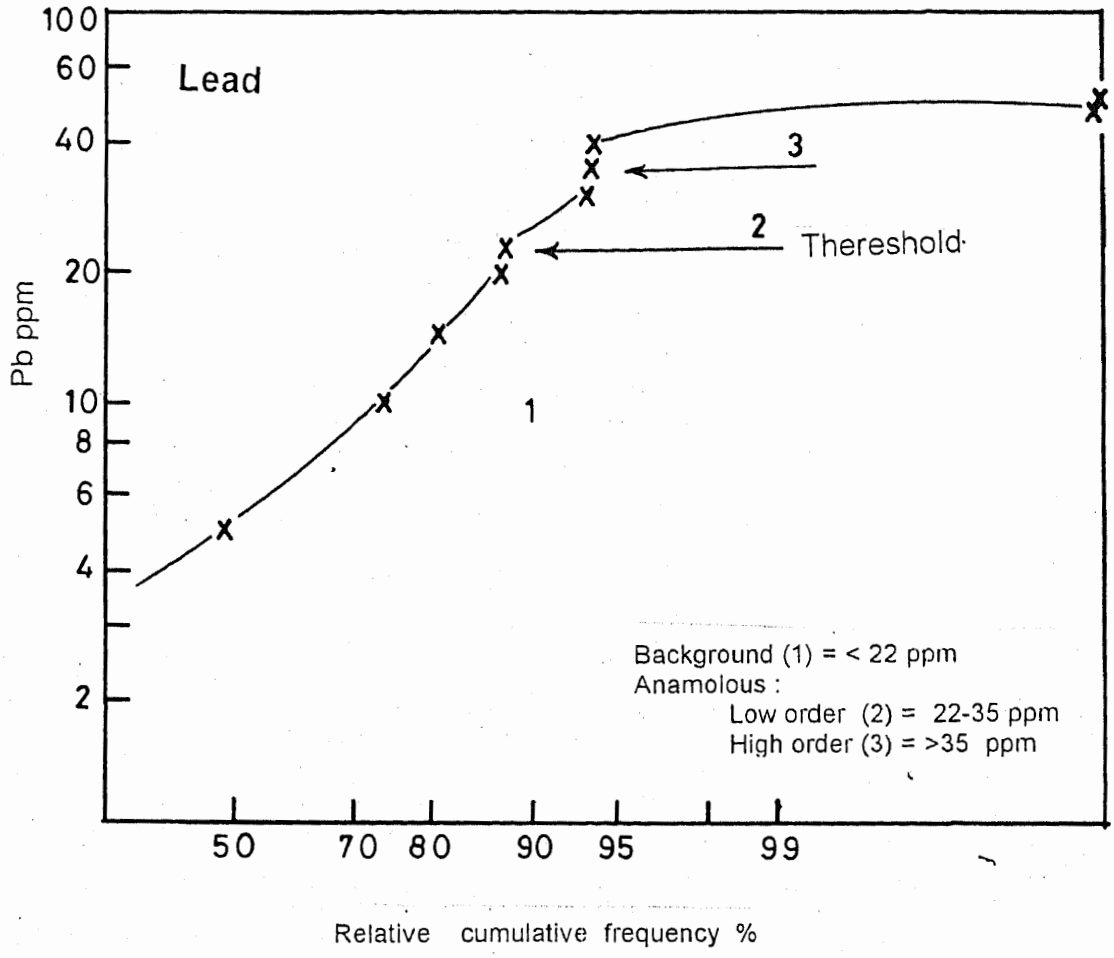

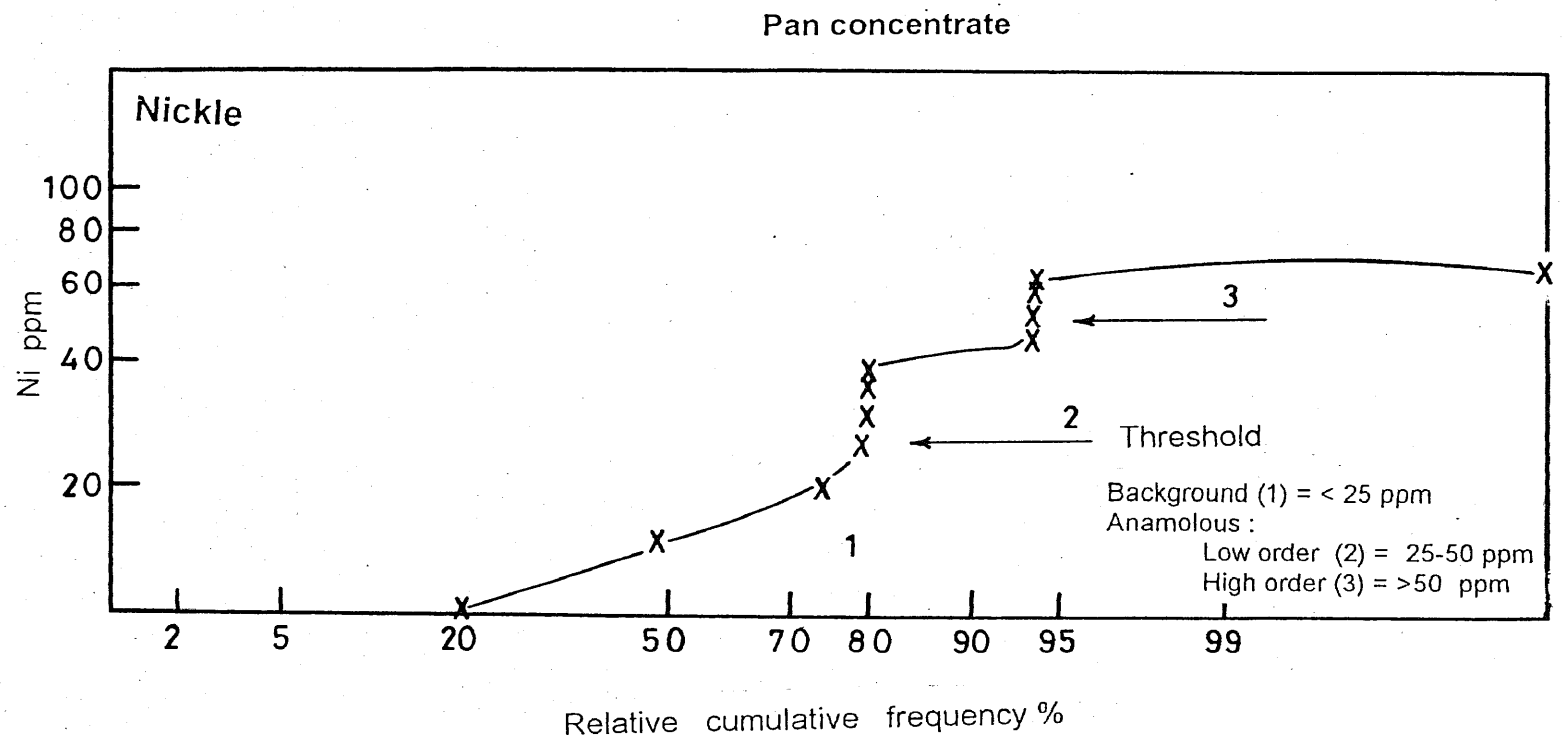
Pan concentrate
Nickle
Ni ppm
100
80
60
40
20
2
5
20
50
70
80
90
95
99
Relative cumulative frequency %
1
2
3
Threshold
Background (1) = < 25 ppm
Anamolous :
Low order (2) = 25-50 ppm
High order (3) = >50 ppm

Pan concentrate

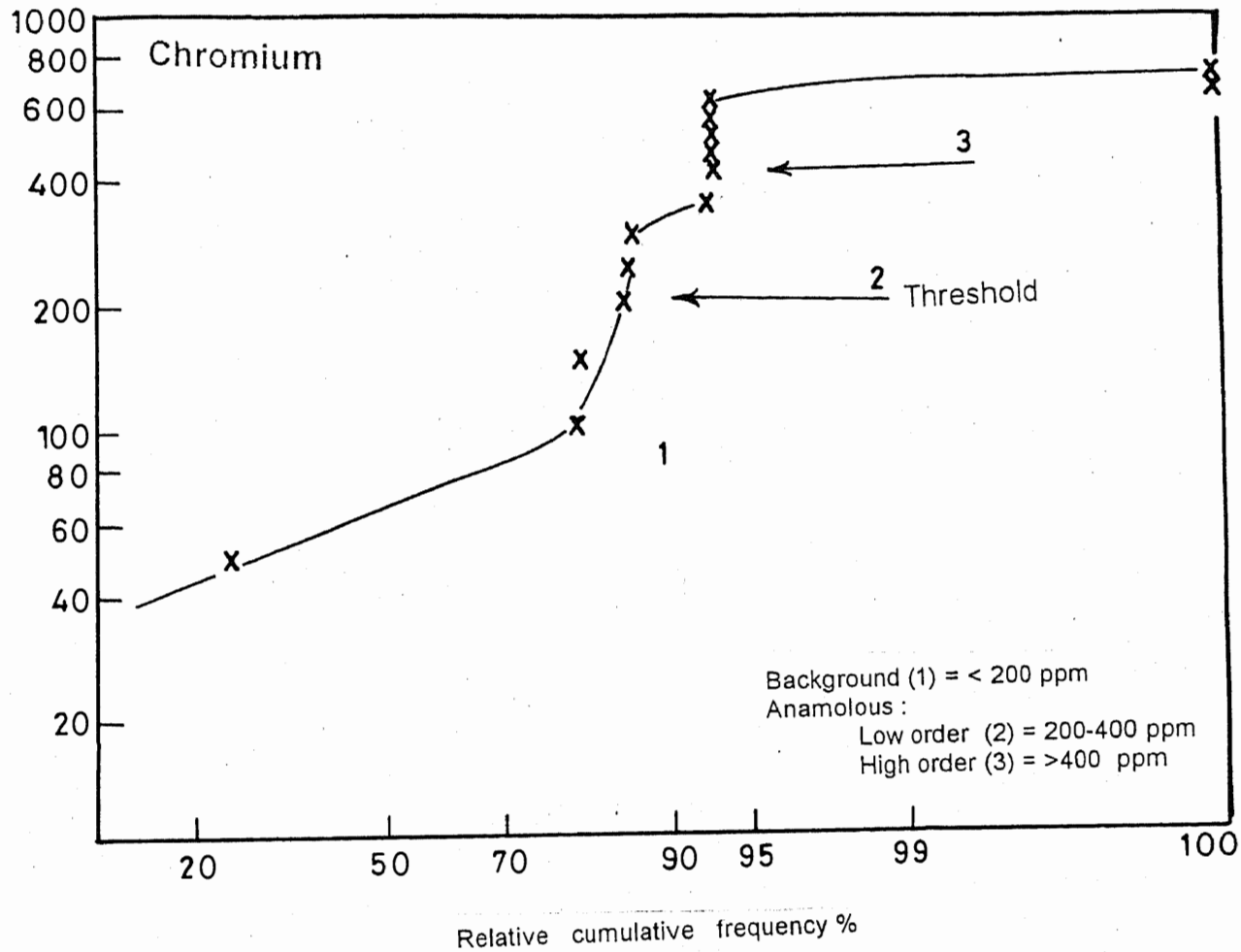

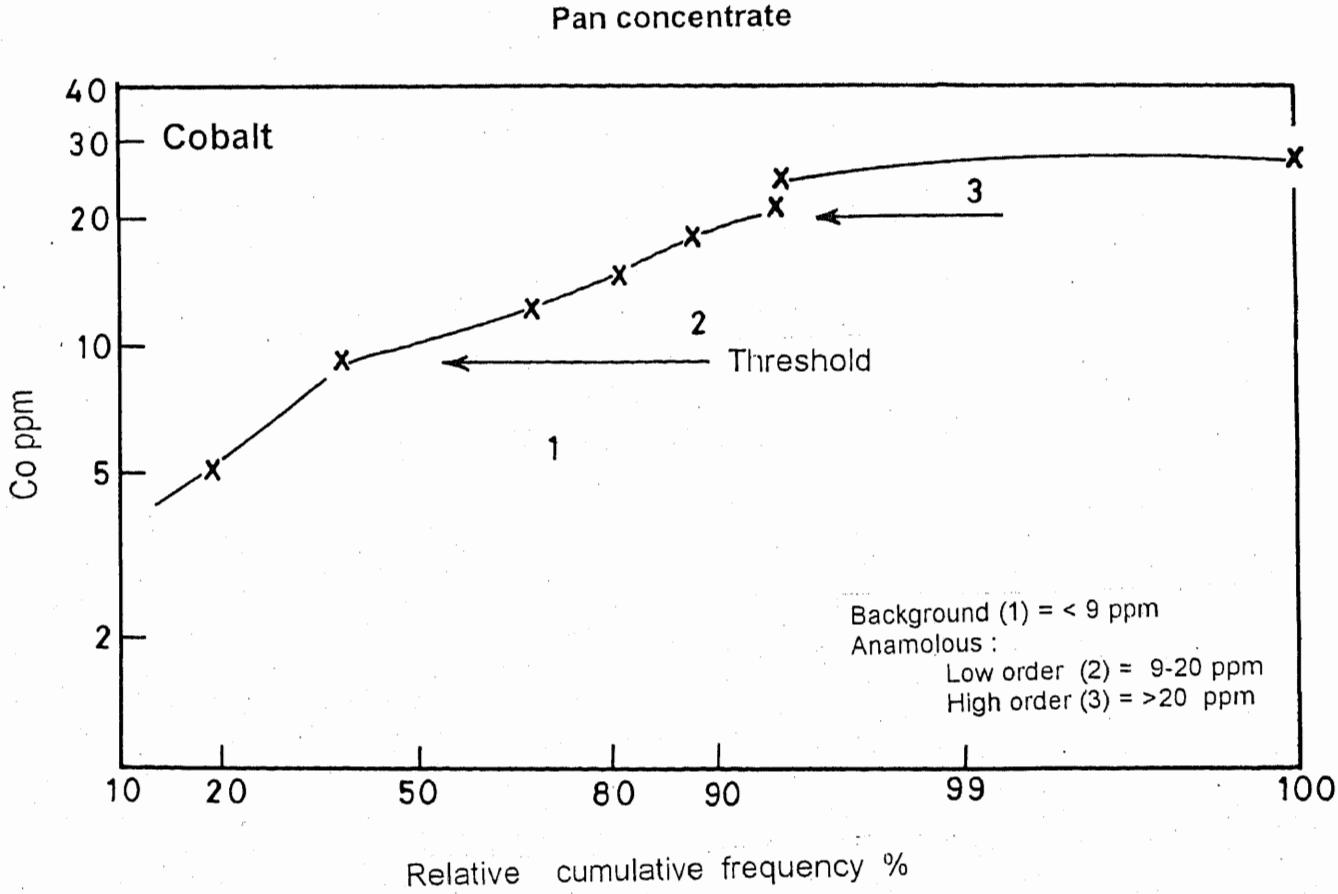
Pan concentrate
Cobalt
Co ppm
40
30
20
10
5
2
3
2
Threshold
1
Background (1) = < 9 ppm
Anamolous :
Low order (2) = 9-20 ppm
High order (3) = >20 ppm
10
20
50
80
90
99
100
Relative cumulative frequency %

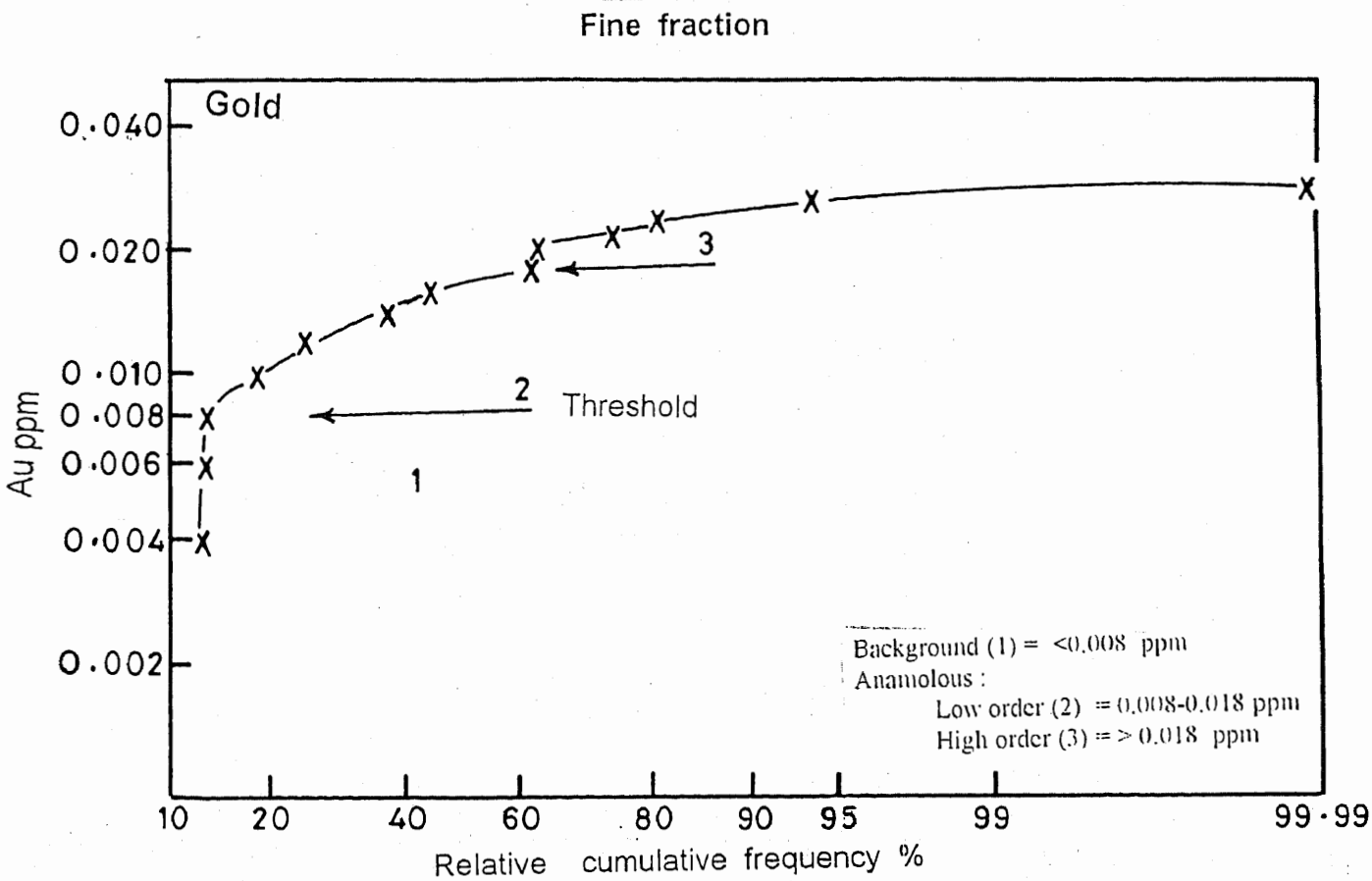

Fig. 8.3. Cumulative frequency curves for Au, Ag, Cu, Zn, Pb, Ni, Cr and Co for the fine fractions of the study area.

Fine fraction

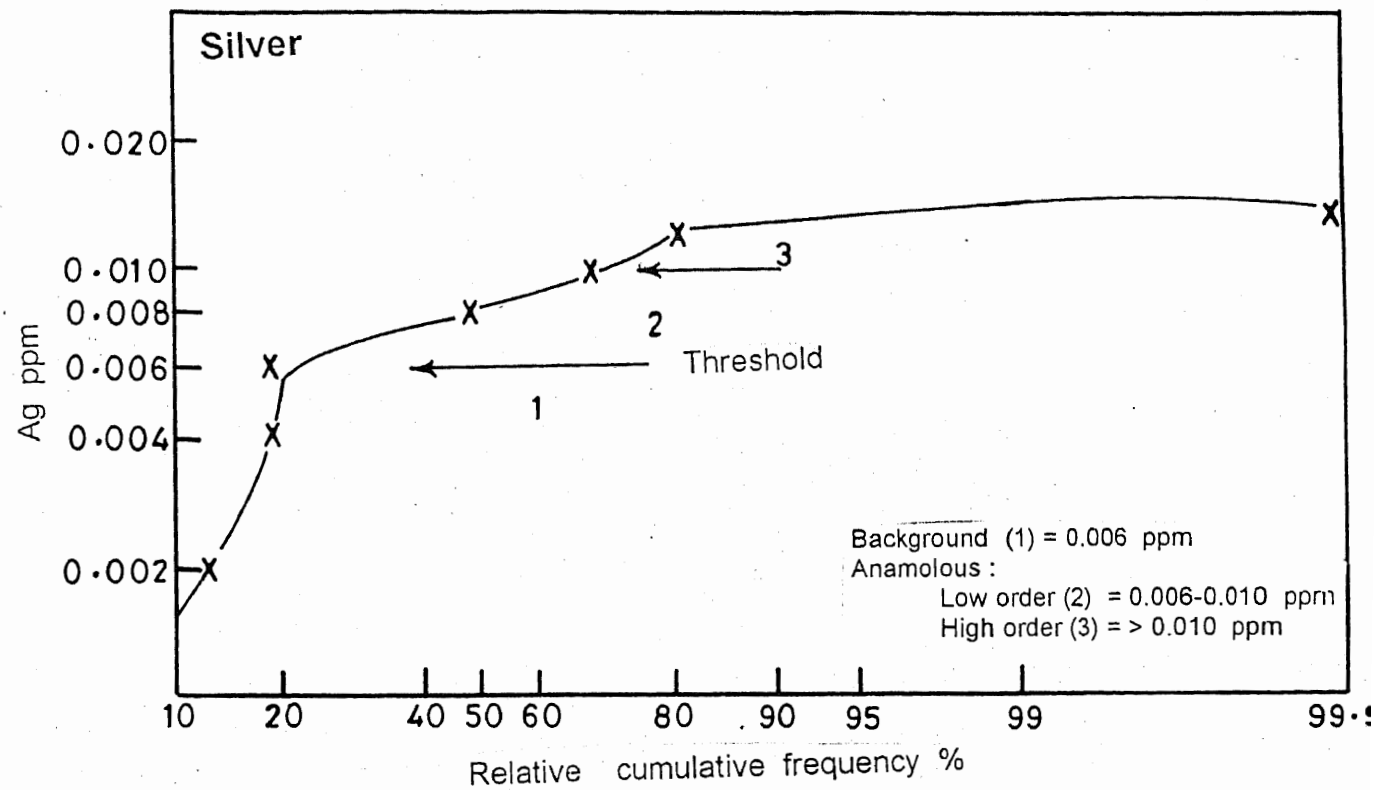

Fine fraction

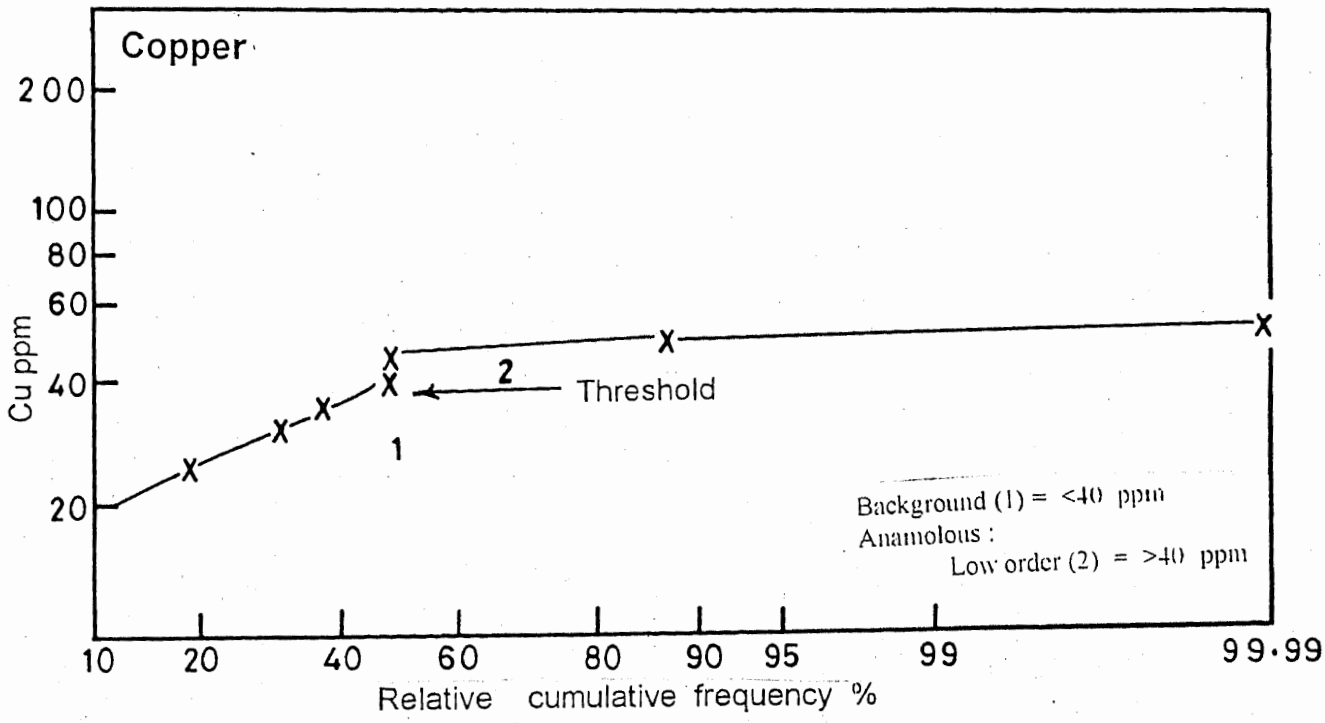

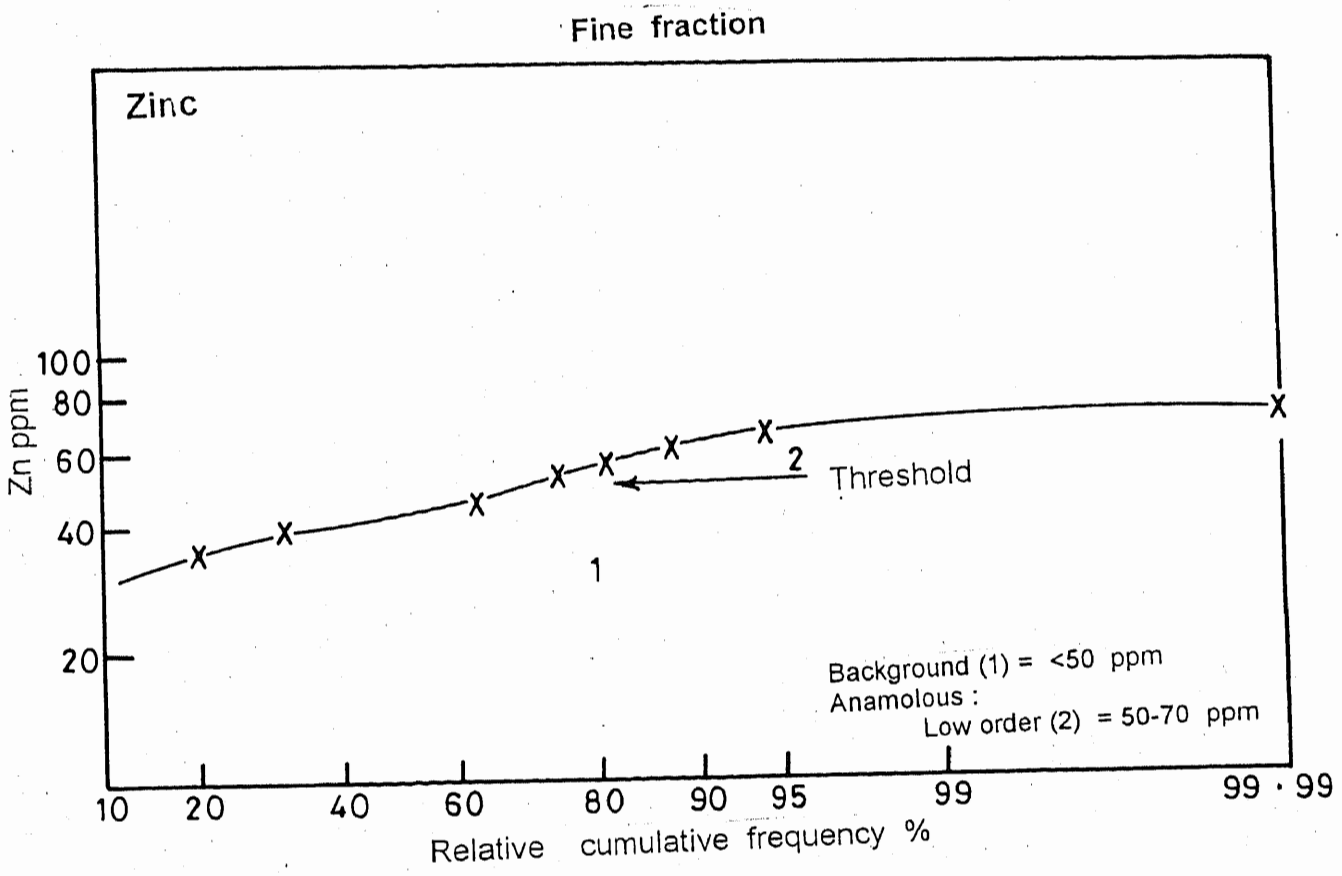
Fine fraction
Zinc
Zn ppm
100
80
60
40
20
Threshold
2
1
Background (1) = <50 ppm
Anamolous :
Low order (2) = 50-70 ppm
10
20
40
60
80
90
95
99
99 · 99
Relative cumulative frequency %

Fine fraction

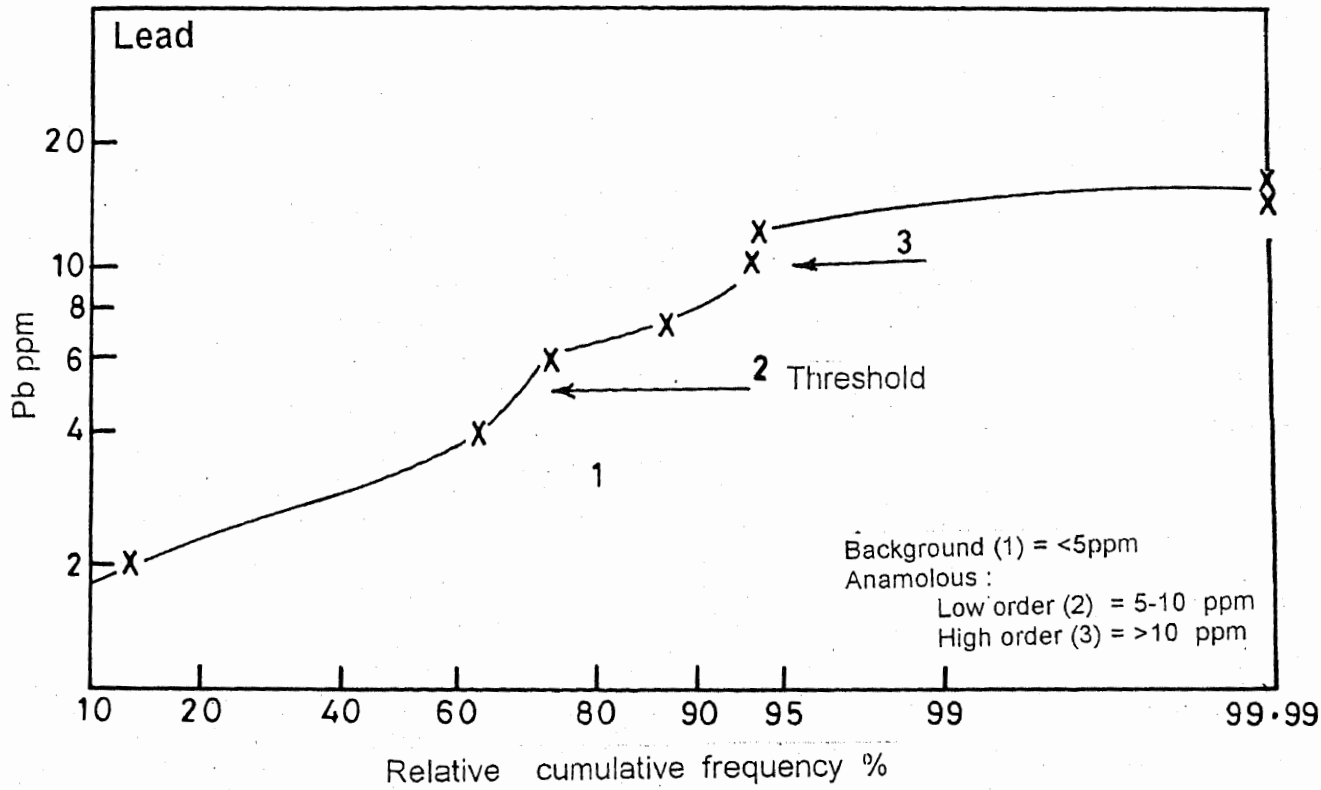

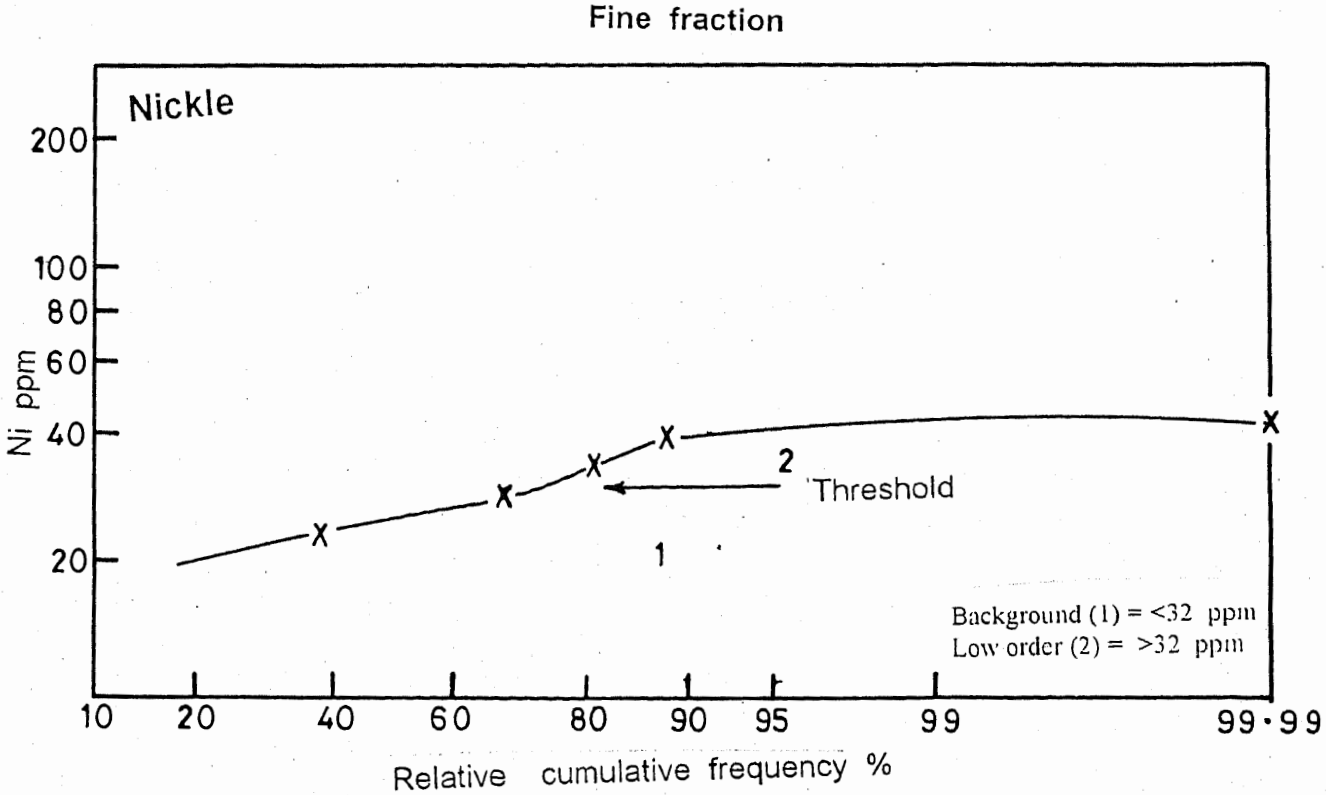
Fine fraction
Nickle
200
100
80
60
40
20
Ni ppm
X
X
X
X
X
2
Threshold
1
Background (1) = <32 ppm
Low order (2) = >32 ppm
10
20
40
60
80
90
95
99
99·99
Relative cumulative frequency %

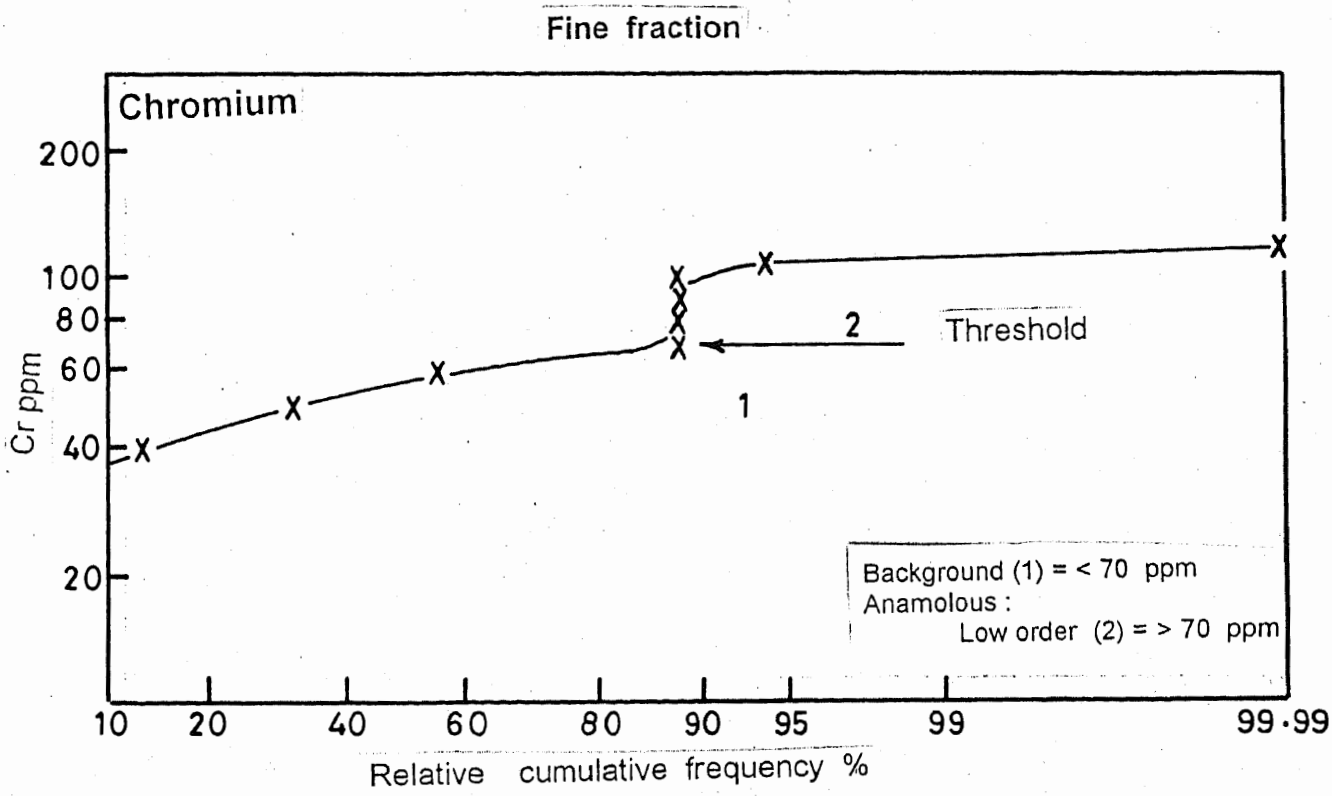
Fine fraction
Chromium
200
100
80
60
40
20
Cr ppm
2
Threshold
1
Background (1) = < 70 ppm
Anamolous :
Low order (2) = > 70 ppm
10
20
40
60
80
90
95
99
99·99
Relative cumulative frequency %

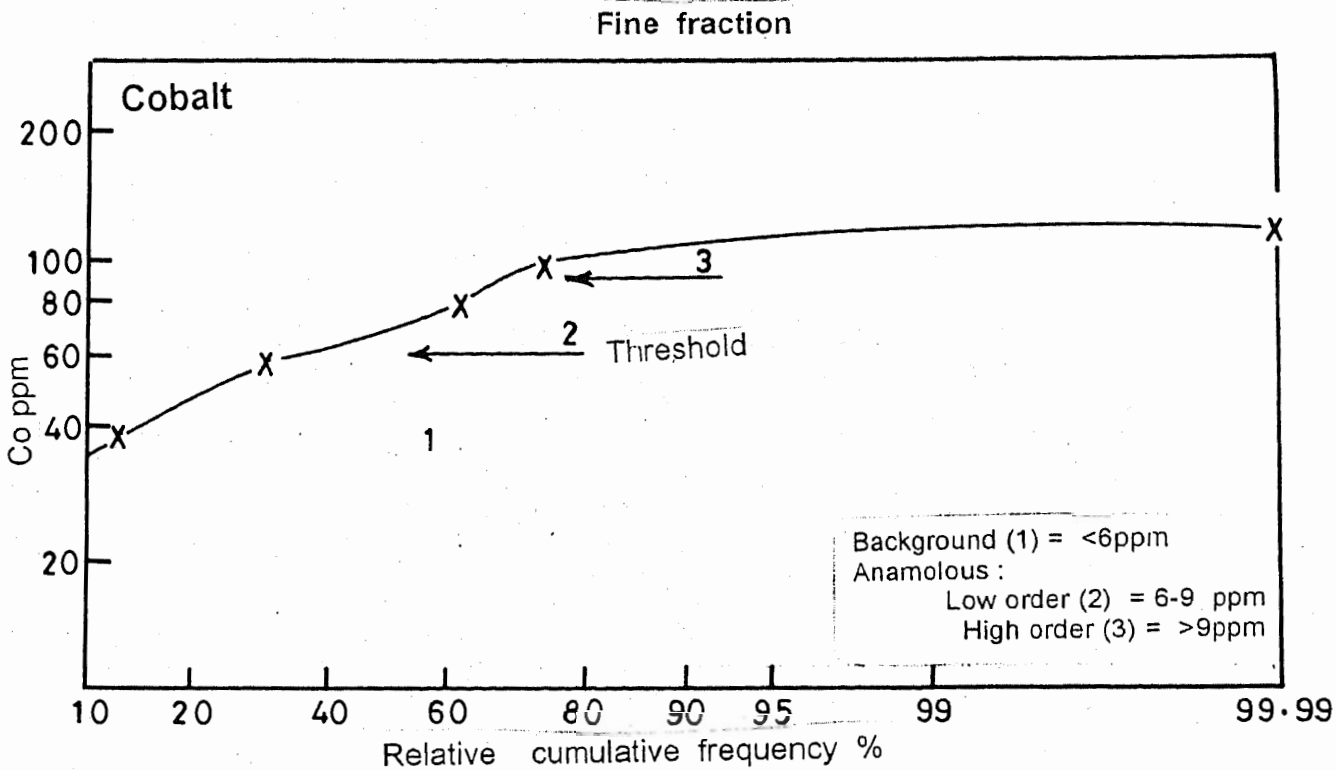
Fine fraction
Cobalt
200
100
80
60
40
20
Co ppm
3
2
Threshold
1
Background (1) = <6ppm
Anamolous :
Low order (2) = 6-9 ppm
High order (3) = >9ppm
10
20
40
60
80
90
95
99
99·99
Relative cumulative frequency %

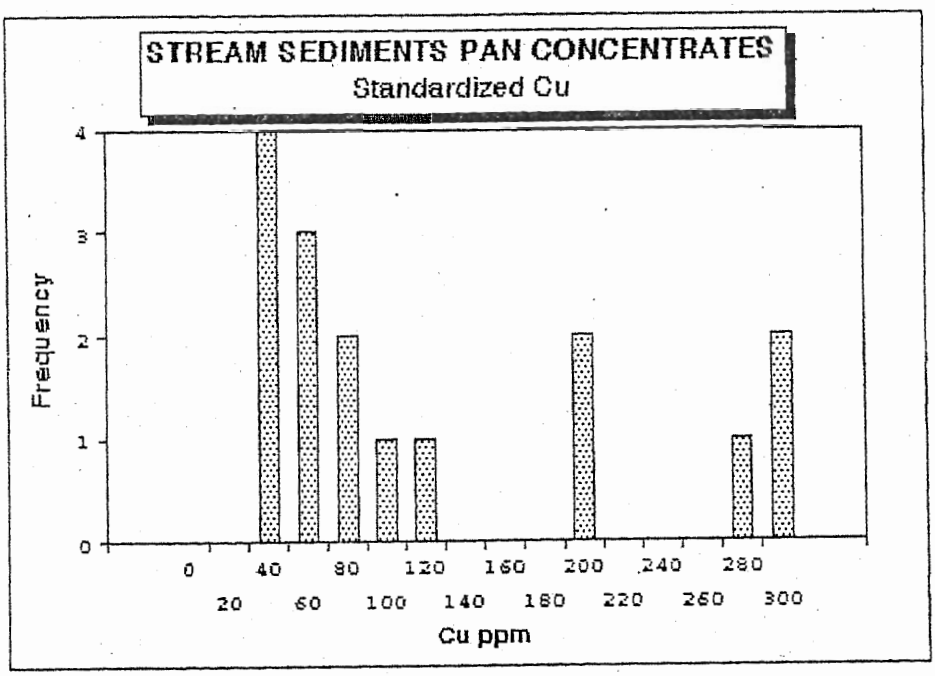

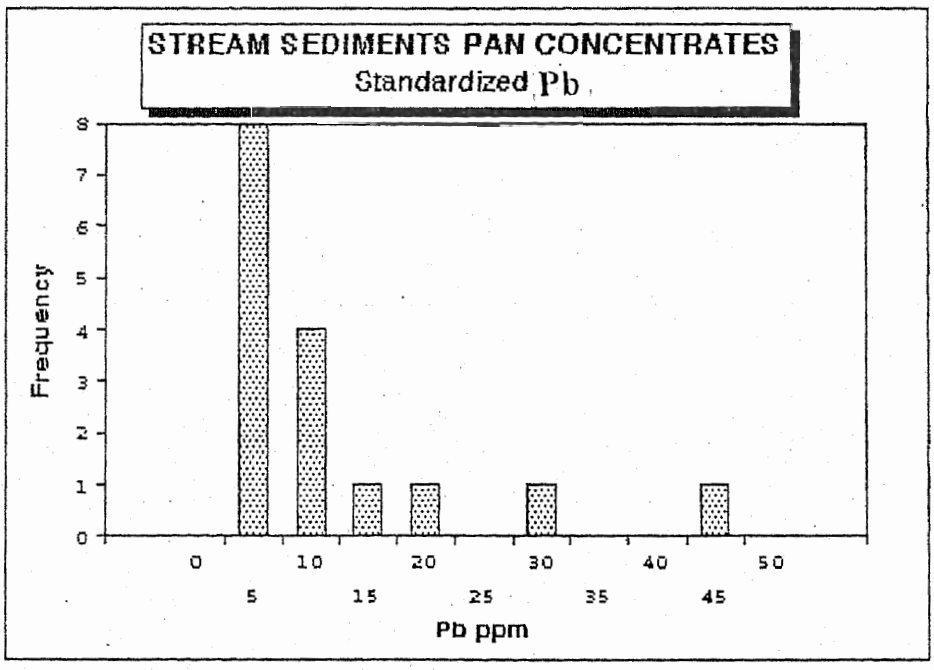

Fig.8.4. Frequency histograms for the pan concentrates of the streams sediments of the study area.

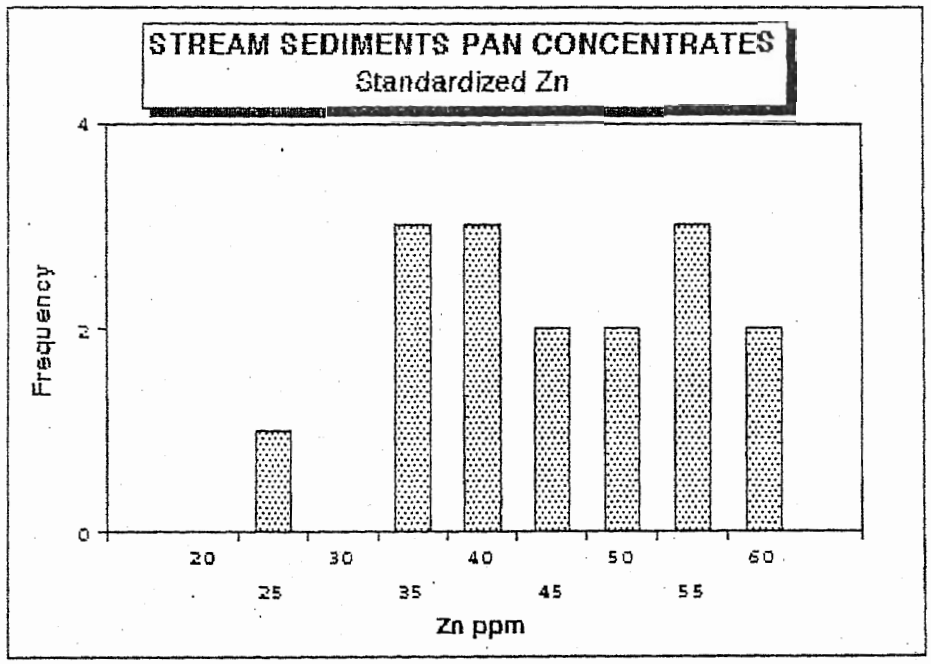
STREAM SEDIMENTS PAN CONCENTRATES
Standardized Zn
Frequency
0
2
4
20
25
30
35
40
45
50
55
60
Zn ppm

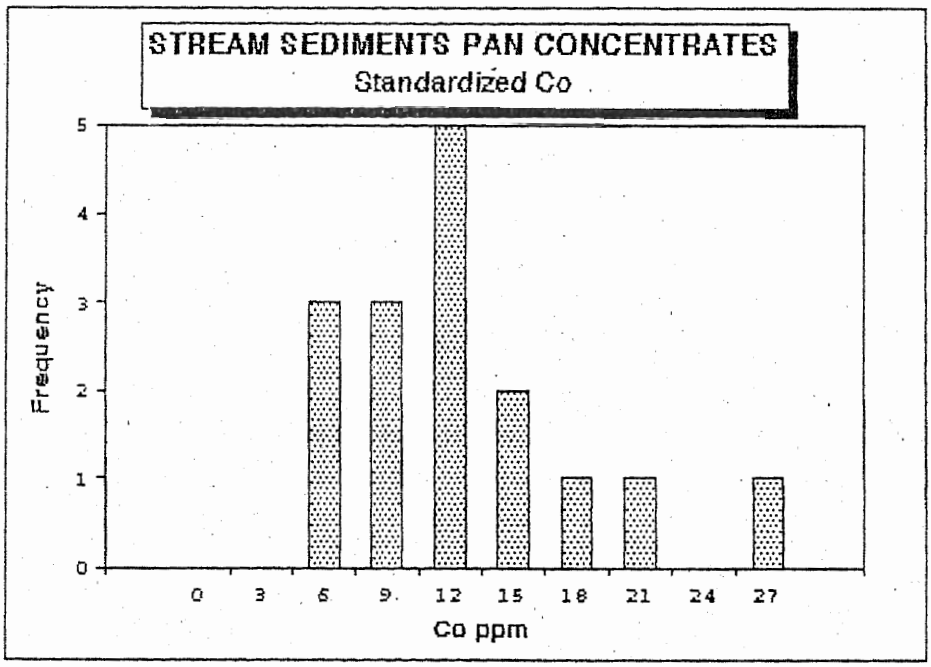
STREAM SEDIMENTS PAN CONCENTRATES
Standardized Co
Frequency
0
1
2
3
4
5
0
3
6
9
12
15
18
21
24
27
Co ppm

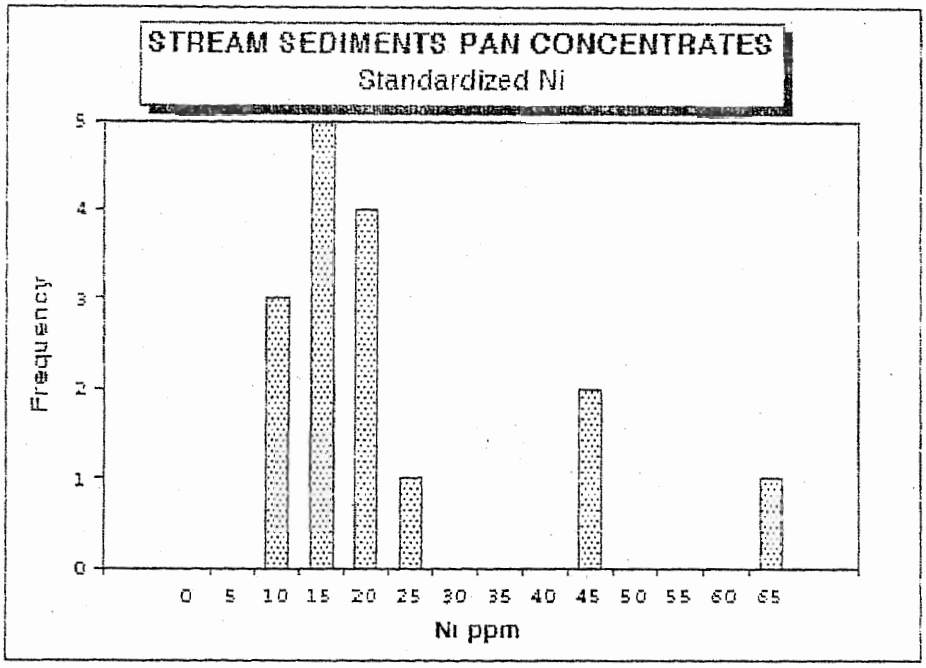
STREAM SEDIMENTS PAN CONCENTRATES
Standardized Ni
Frequency
0
1
2
3
4
5
0 5 10 15 20 25 30 35 40 45 50 55 60 65
Ni ppm

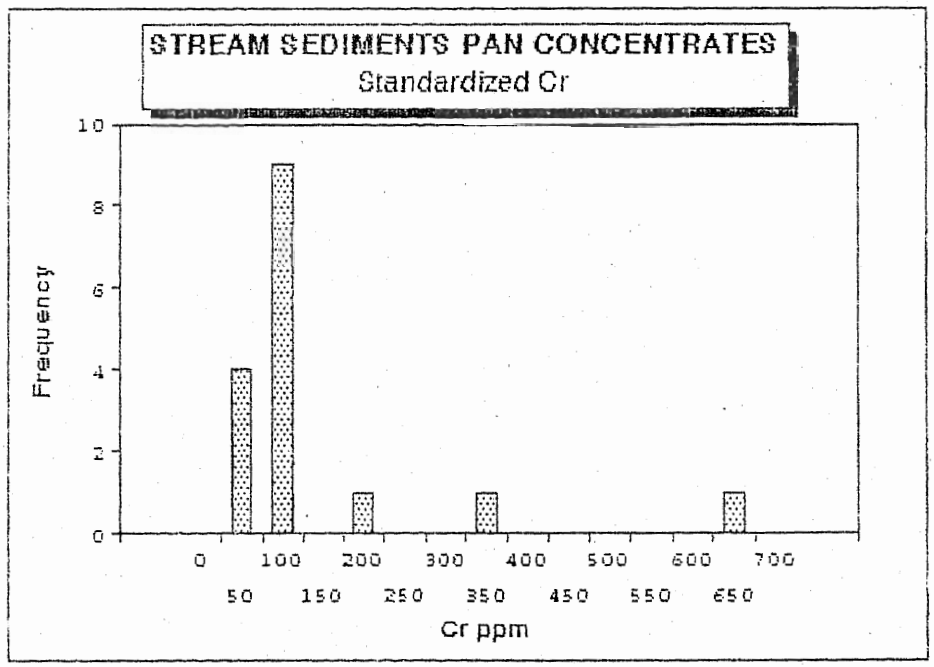
STREAM SEDIMENTS PAN CONCENTRATES
Standardized Cr
Frequency
0
2
4
6
8
10
0 100 200 300 400 500 600 700
50 150 250 350 450 550 650
Cr ppm

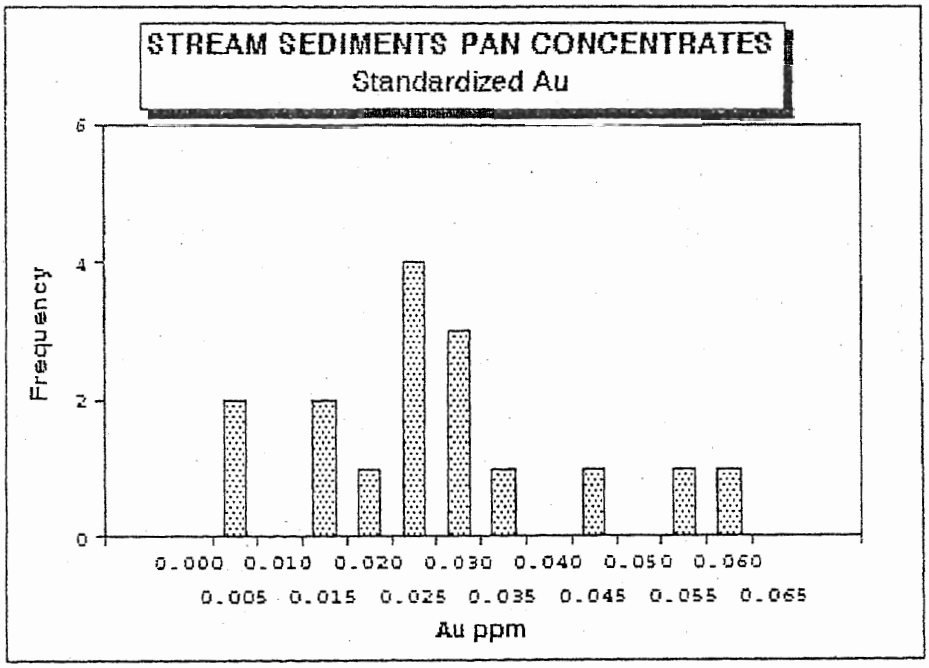
STREAM SEDIMENTS PAN CONCENTRATES
Standardized Au
Frequency
0
2
4
6
0.000 0.010 0.020 0.030 0.040 0.050 0.060
0.005 0.015 0.025 0.035 0.045 0.055 0.065
Au ppm

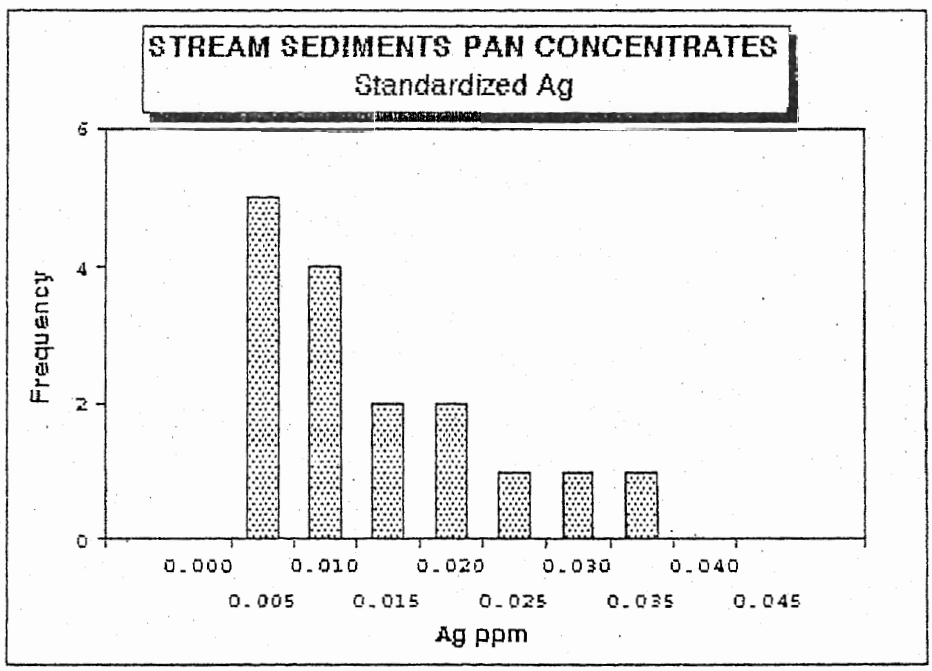
STREAM SEDIMENTS PAN CONCENTRATES
Standardized Ag
Frequency
0
2
4
6
0.000 0.010 0.020 0.030 0.040
0.005 0.015 0.025 0.035 0.045
Ag ppm

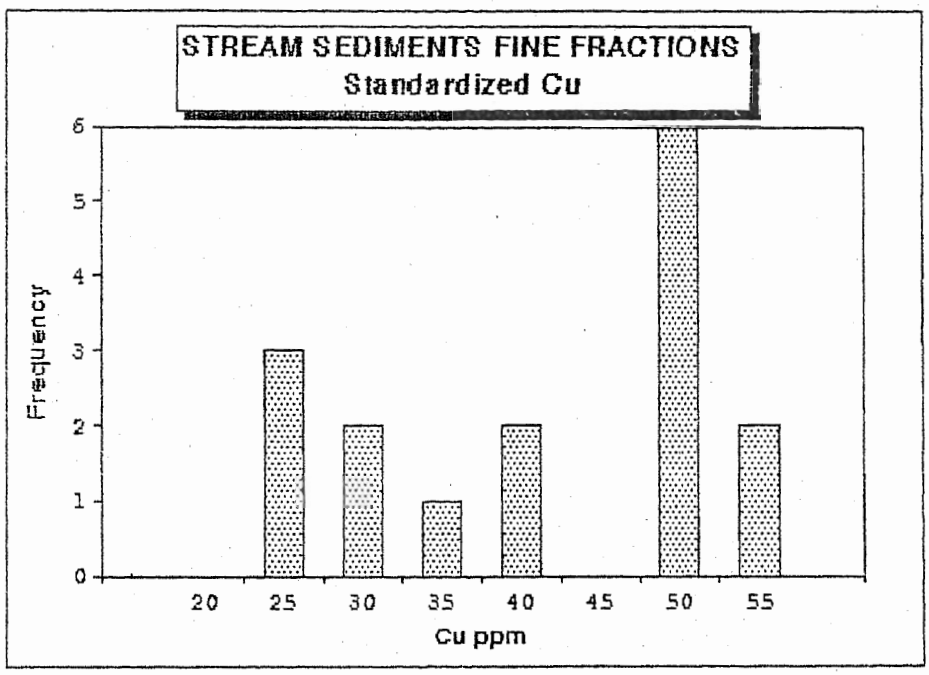

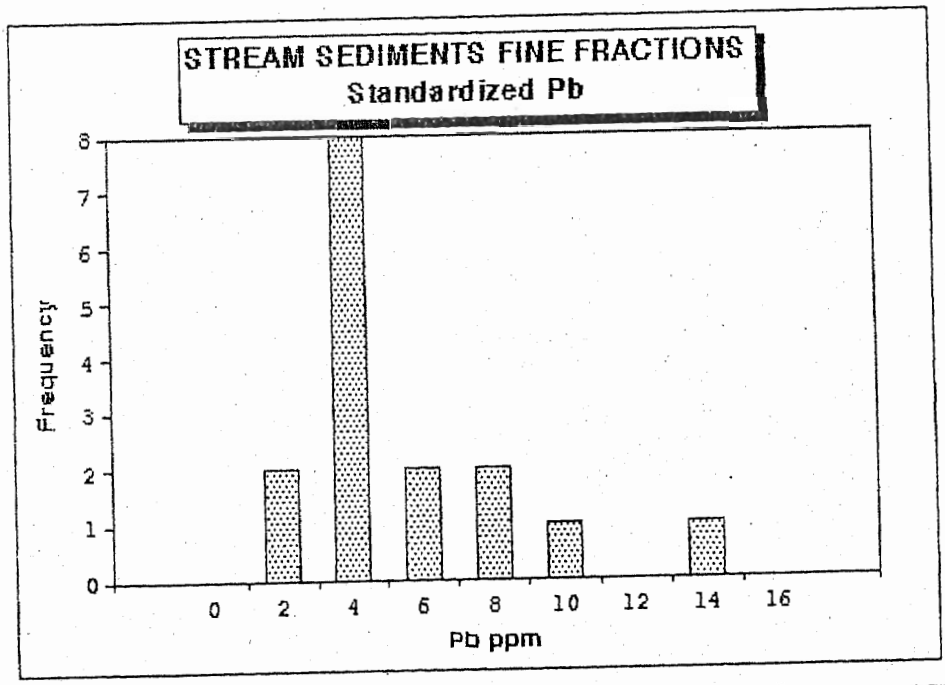

Fig.8.5. Frequency histograms for the fine fractions of the streams sediments of the study area.

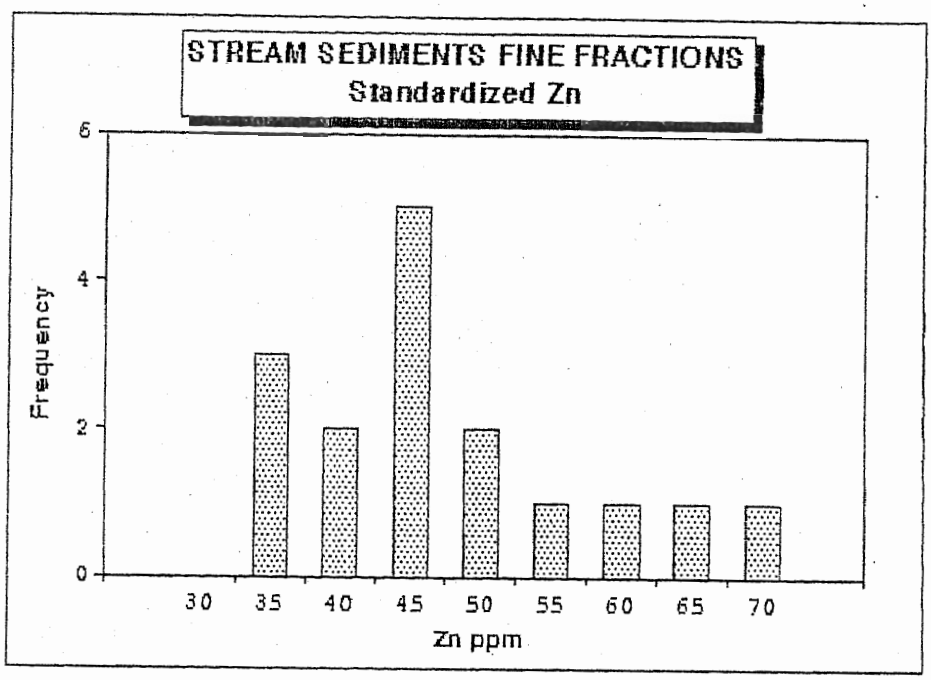
STREAM SEDIMENTS FINE FRACTIONS
Standardized Zn
Frequency
0
2
4
6
30
35
40
45
50
55
60
65
70
Zn ppm

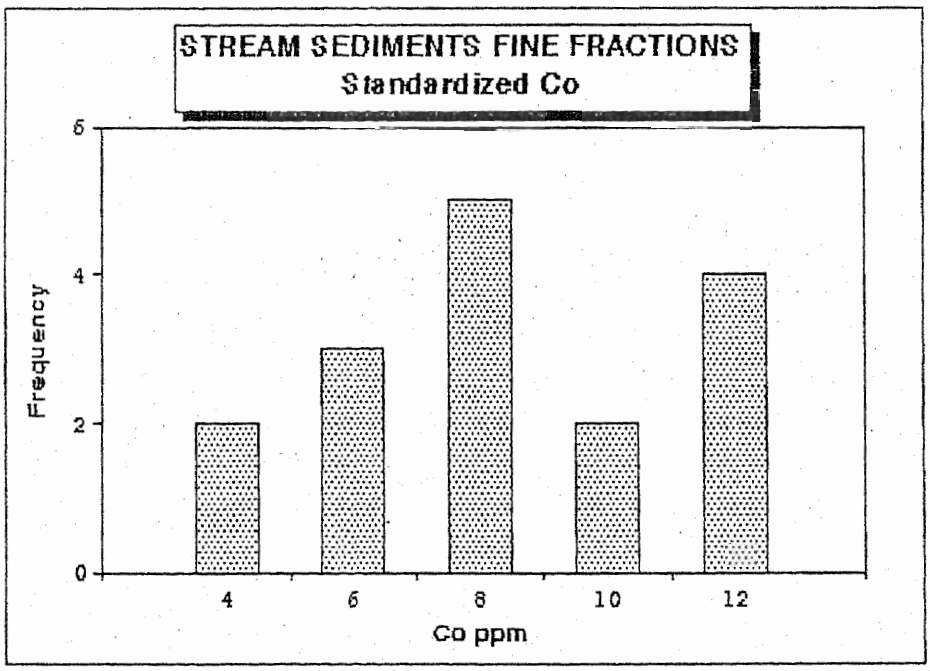
STREAM SEDIMENTS FINE FRACTIONS
Standardized Co
Frequency
0
2
4
6
4
6
8
10
12
Co ppm

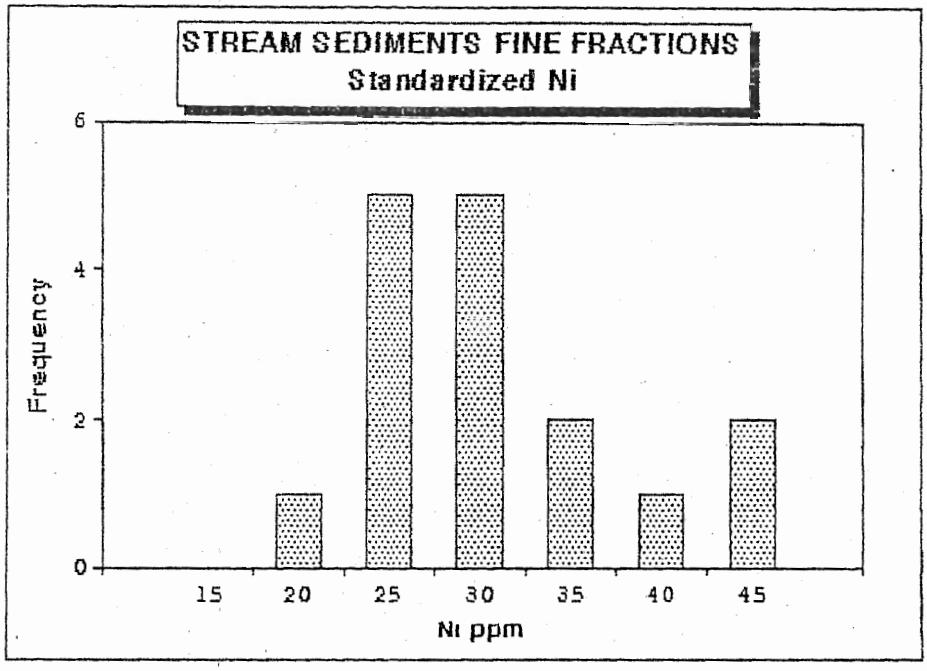
STREAM SEDIMENTS FINE FRACTIONS
Standardized Ni
Frequency
0
2
4
6
15
20
25
30
35
40
45
Ni ppm

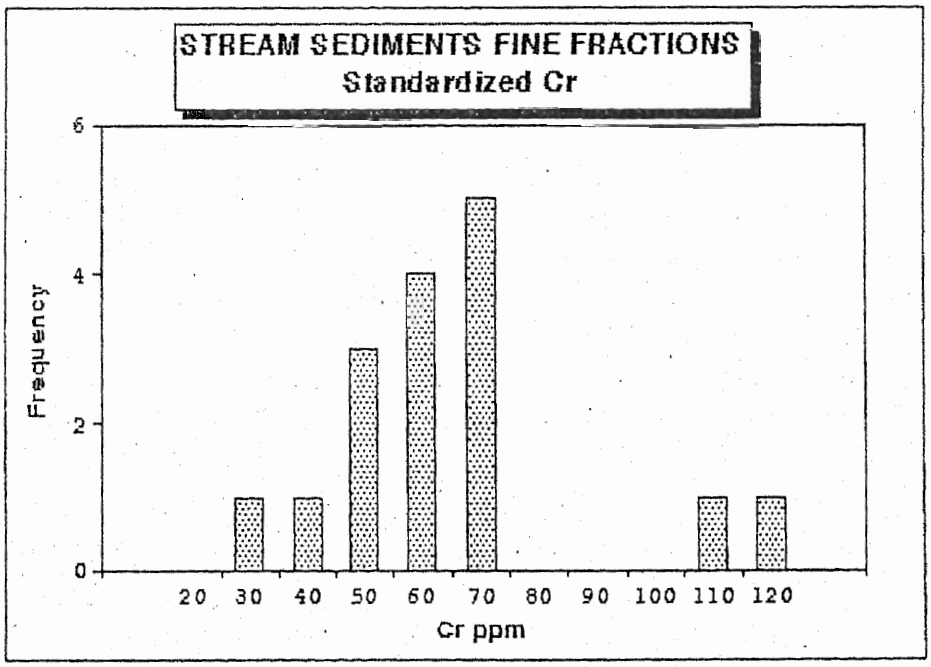
STREAM SEDIMENTS FINE FRACTIONS
Standardized Cr
Frequency
0
2
4
6
20
30
40
50
60
70
80
90
100
110
120
Cr ppm

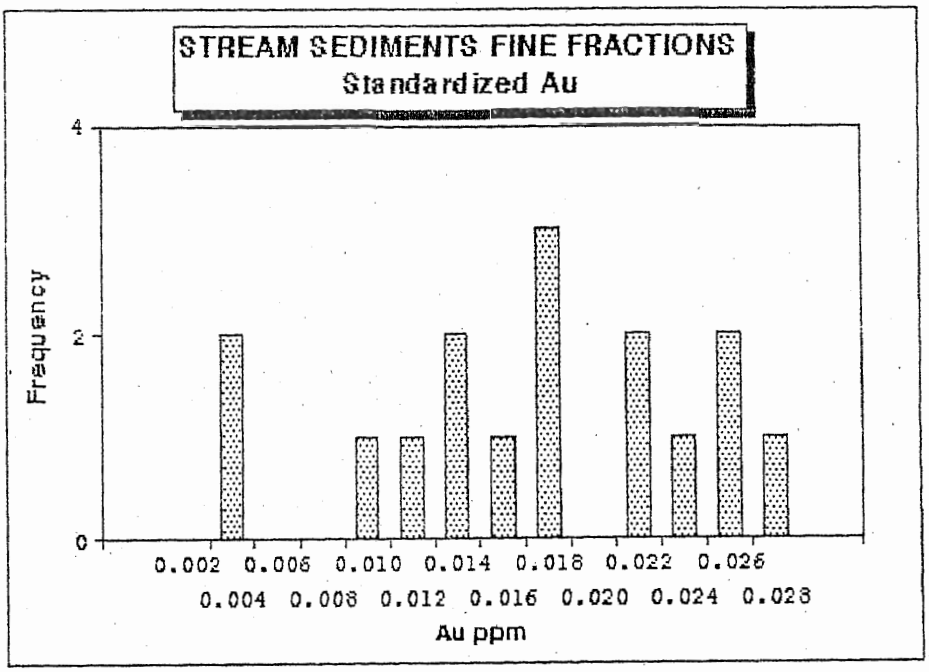
STREAM SEDIMENTS FINE FRACTIONS
Standardized Au
Frequency
4
2
0
0.002 0.006 0.010 0.014 0.018 0.022 0.026
0.004 0.008 0.012 0.016 0.020 0.024 0.028
Au ppm

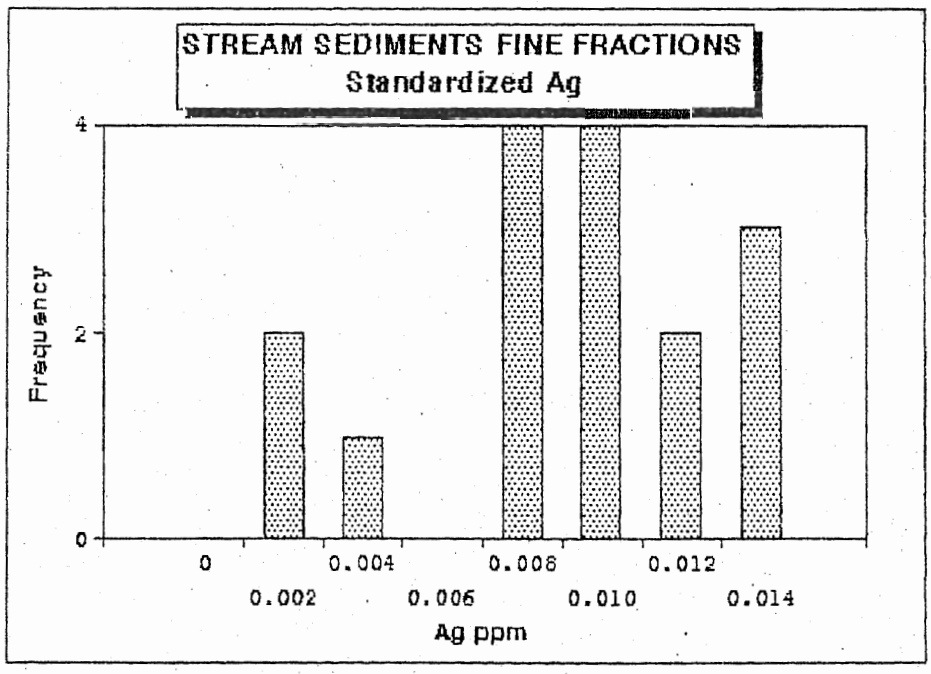
STREAM SEDIMENTS FINE FRACTIONS
Standardized Ag
Frequency
4
2
0
0 0.004 0.008 0.012
0.002 0.006 0.010 0.014
Ag ppm

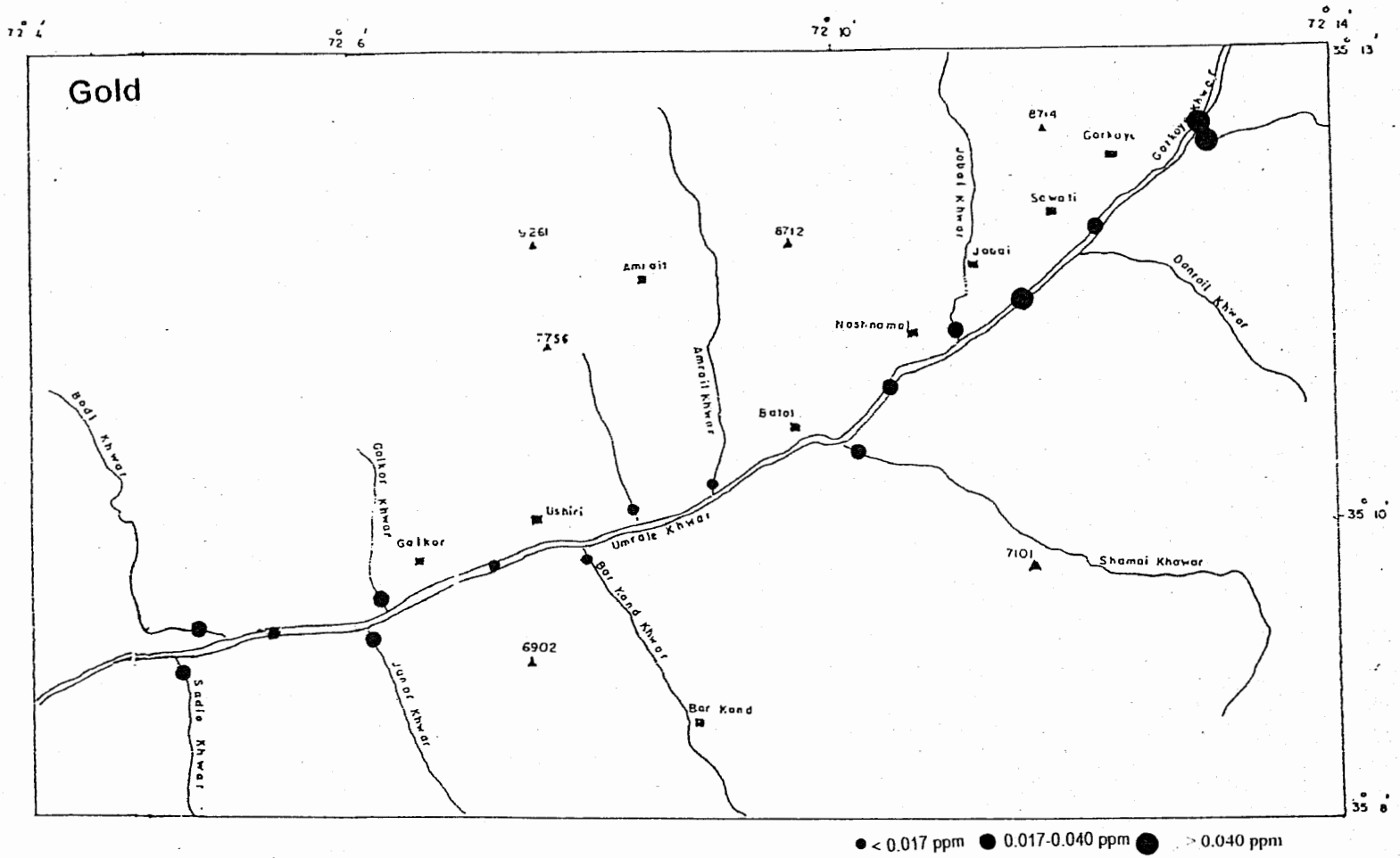

Fig.8.6. Distribution map of Au, Ag, Cu, Zn, Pb, Ni, Cr and Co for the pan concentrates of the study area.

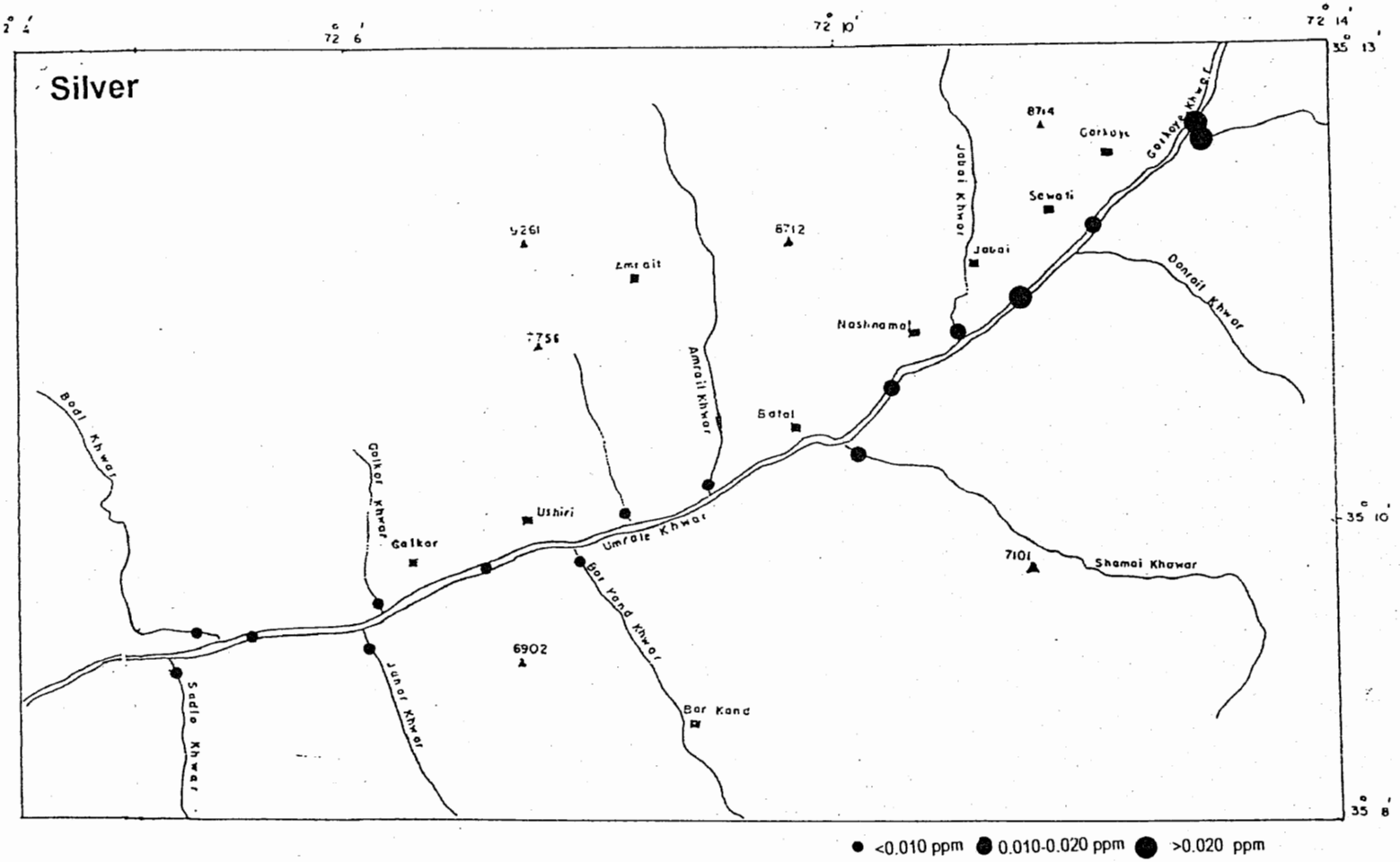
Silver
72° 4'
72° 6'
72° 10'
72° 14'
35° 13'
35° 10'
35° 8'
8714
Gorkuyc
Sewati
Jabai
Jabai Khwar
Gorkuyc Khwar
Dansail Khwar
Nashnamal
6712
5261
Amrail
7756
Amrail Khwar
Batal
Badl Khwar
Galkar Khwar
Galkar
Ushiri
Umrale Khwar
7101
Shamai Khwar
Bar Yand Khwar
Bar Kand
6902
Jurur Khwar
Sadle Khwar
<0.010 ppm
0.010-0.020 ppm
>0.020 ppm

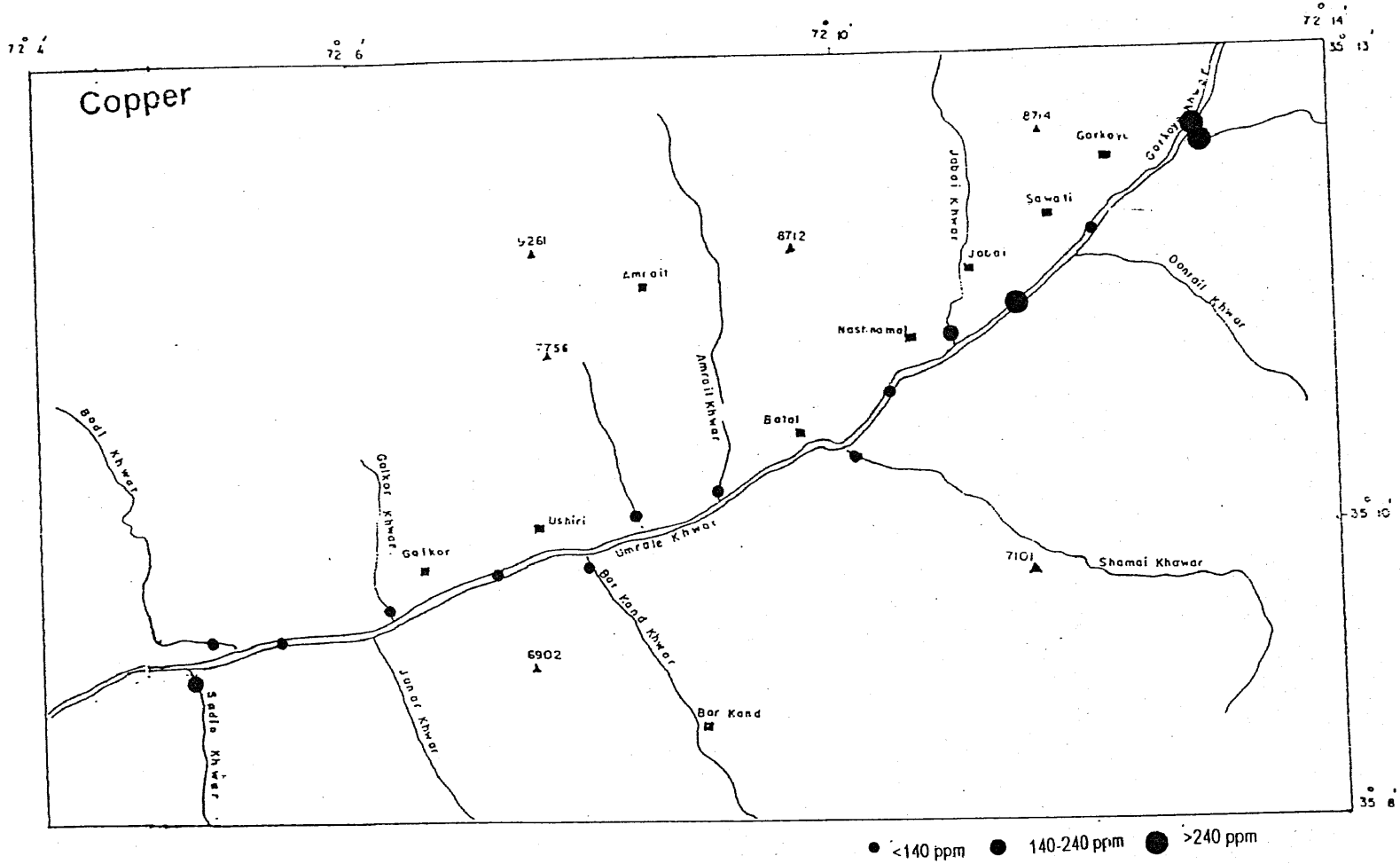
Copper
72° 4'
72° 6'
72° 10'
72° 14'
35° 13'
35° 10'
35° 8'
8714
Garkoyt
Sawati
Jabai Khwar
Jabai
Garkoyt Khwar
8712
9261
Amrait
Oonrait Khwar
Nastnama
7756
Amrait Khwar
Batal
Bodl Khwar
Galkor Khwar
Ushiri
Galkor
Umrale Khwar
7101
Shamai Khawar
Bar Kand Khwar
6902
Jabar Khwar
Bar Kand
Sadle Khwar
<140 ppm
140-240 ppm
>240 ppm

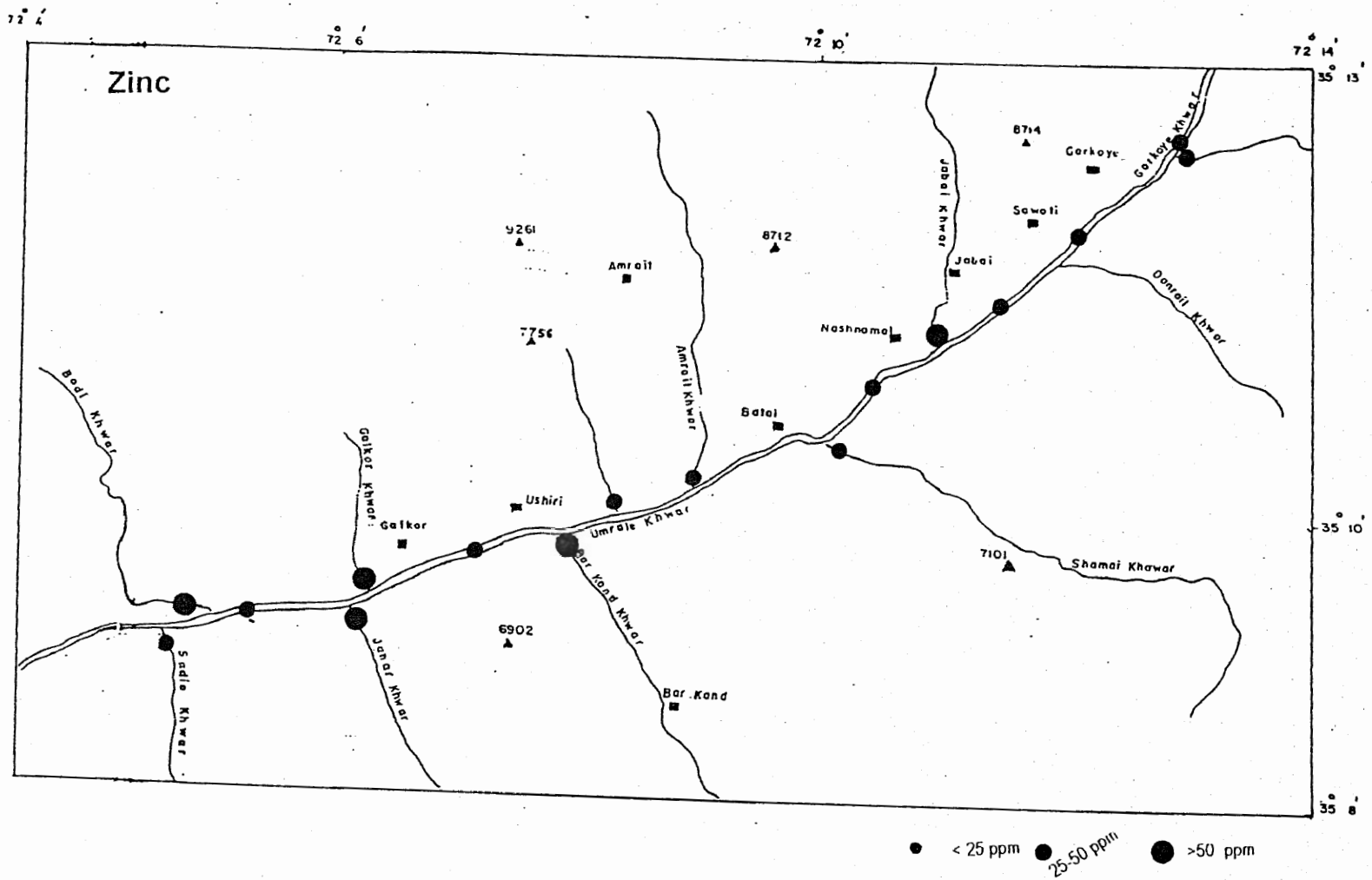
Zinc
72° 4'
72° 6'
72° 10'
72° 14'
35° 13'
35° 10'
35° 8'
8714
Gorkoye
Gorkoye Khwar
Sawati
Jabai Khwar
8712
9261
Amrail
Jabai
Oonrail Khwar
7756
Nashnama
Amrail Khwar
Batai
Badi Khwar
Galkor Khwar
Ushiri
Galkor
Umrale Khwar
7101
Shamai Khwar
Bar Kand Khwar
6902
Spalle Khwar
Janar Khwar
Bar Kand
< 25 ppm
25-50 ppm
>50 ppm

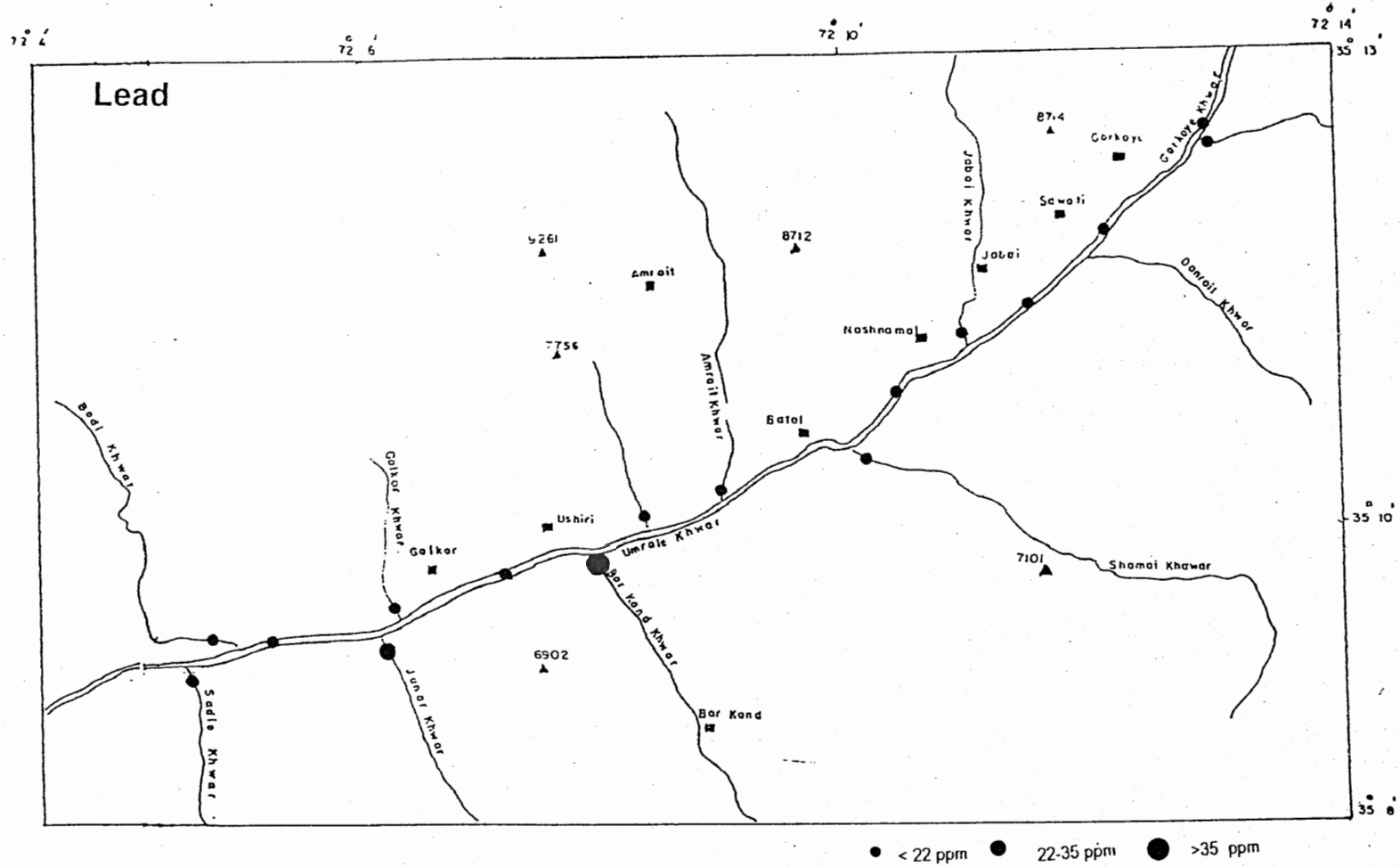
Lead
72° 4'
72° 6'
72° 10'
72° 14'
35° 13'
35° 10'
35° 8'
8714
Gorkoyi
Gorkoyi Khwar
Jabai Khwar
Sawati
8712
9261
Amraii
Jabai
Doorgii Khwar
Nashnamal
7756
Amraii Khwar
Batal
Badi Khwar
Galkar Khwar
Ushiri
Galkar
Umrale Khwar
7101
Shamai Khawar
Bar Kand Khwar
6902
Sadle Khwar
Jandr Khwar
Bar Kand
< 22 ppm
22-35 ppm
>35 ppm

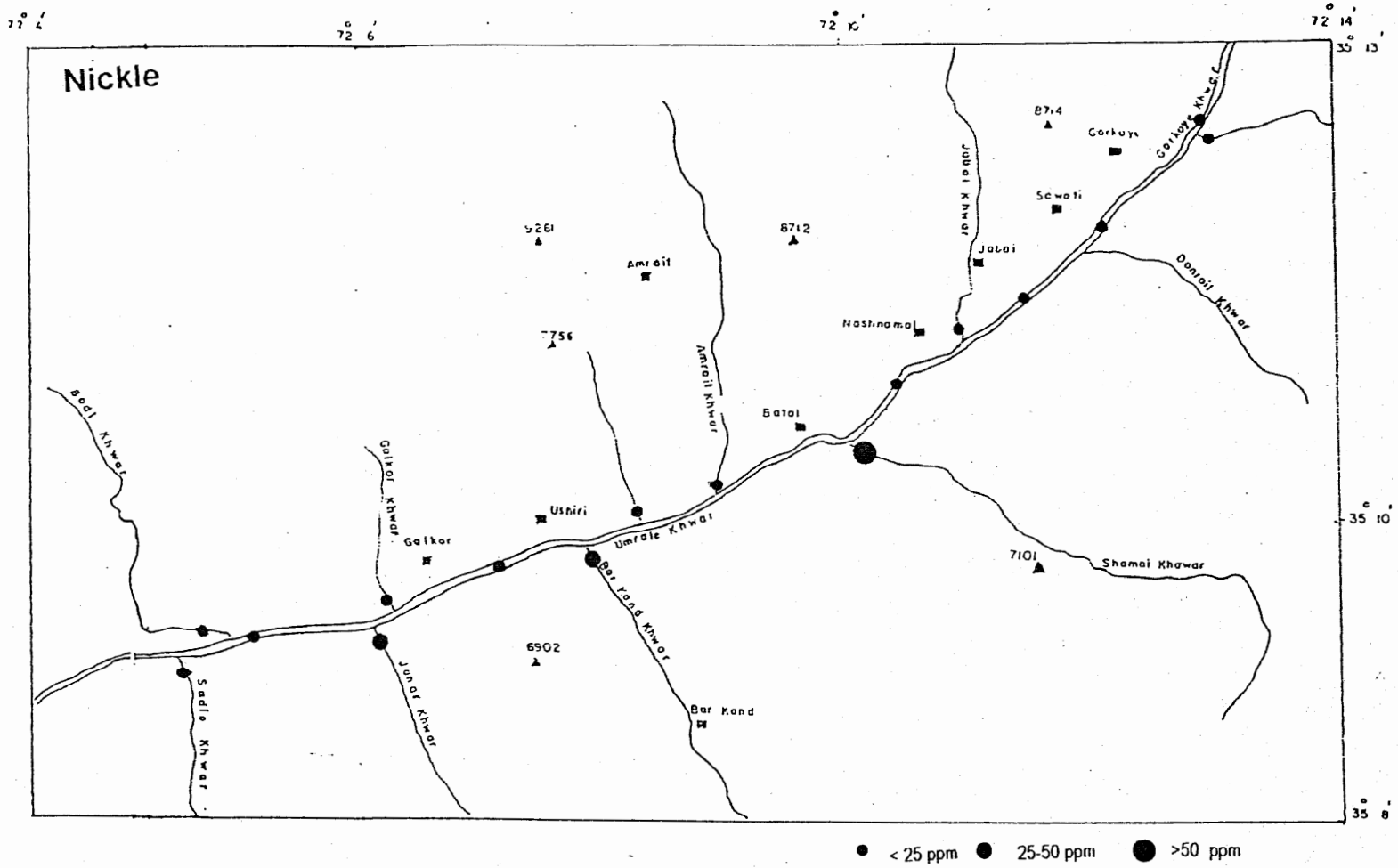
Nickle
72° 4'
72° 6'
72° 8'
72° 14'
35° 13'
35° 10'
35° 8'
8714
Gorkoye
Gorkoye Khwar
Sawati
8712
Jabai
Jabai Khwar
Amrail
Donrail Khwar
Nashnamal
7756
Amrail Khwar
Batal
Badl Khwar
Gaikor Khwar
Ushiri
Gaikor
Umrale Khwar
7101
Shamal Khwar
Bar Kand Khwar
6902
Sadlo Khwar
Jinar Khwar
Bar Kand
< 25 ppm
25-50 ppm
>50 ppm

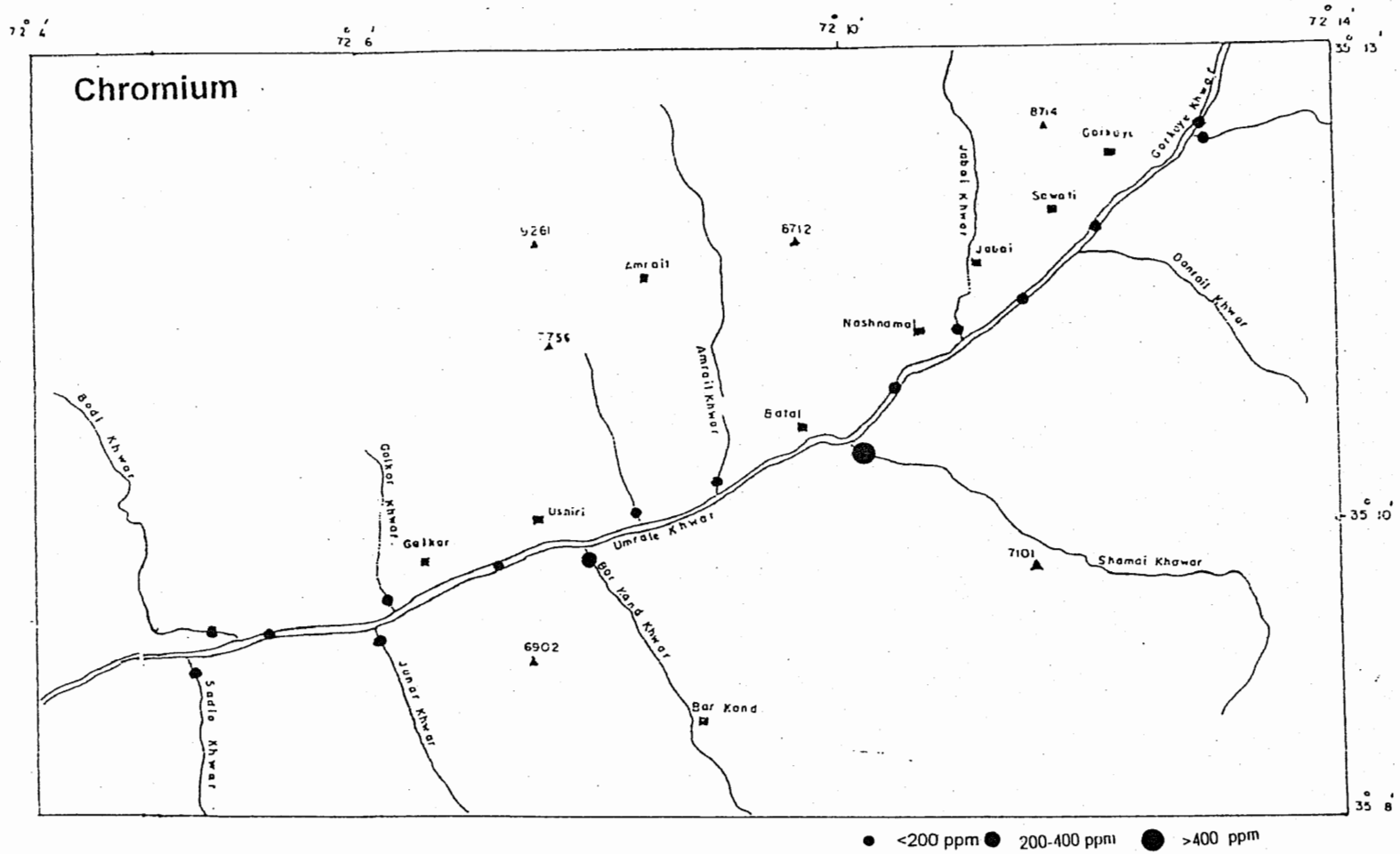
Chromium
72° 4'
72° 6'
72° 10'
72° 14'
35° 13'
35° 10'
35° 8'
8714
Gorkuyo
Gorkuyo Khwar
Sewati
Jabai Khwar
Jabai
9261
8712
Amrail
Oonroli Khwar
Nashnama
7756
Amrail Khwar
Batal
Badi Khwar
Gaikar Khwar
Gaikar
Ushiri
Umrale Khwar
Bar Kand Khwar
7101
Shamai Khawar
6902
Sadlo Khwar
Junar Khwar
Bar Kand
<200 ppm
200-400 ppm
>400 ppm

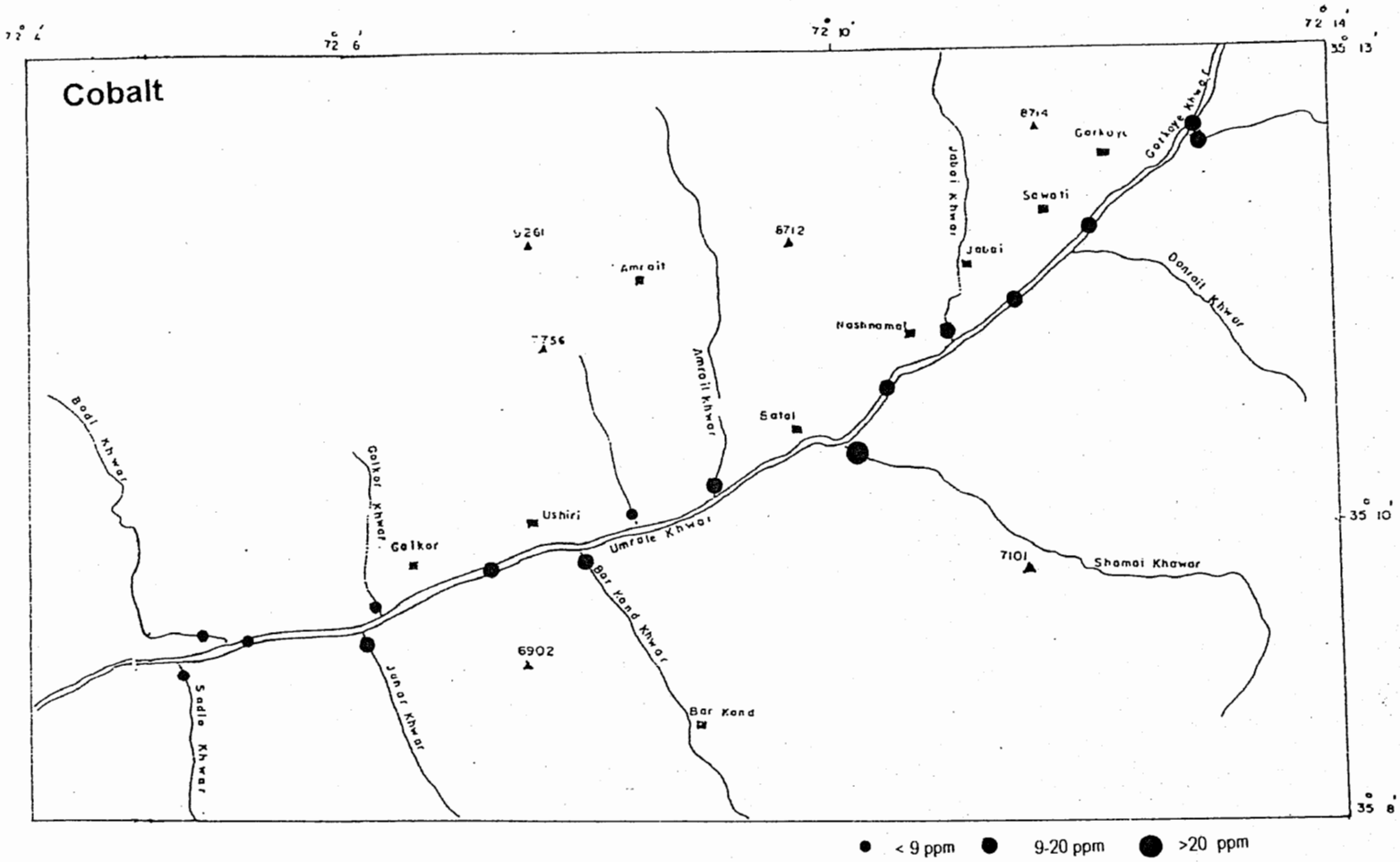
Cobalt
72° 4'
72° 6'
72° 10'
72° 14'
35° 13'
35° 10'
35° 8'
8714
Gorkuri
Gorkuri Khwar
Sawati
Jabai Khwar
Jabai
8712
9261
Amrait
7756
Donrait Khwar
Nashnamal
Amrait Khwar
Satal
Bodi Khwar
Golkor Khwar
Golkor
Ushiri
Umrale Khwar
7101
Shamai Khawar
Bar Kand Khwar
6902
Sadle Khwar
Jandar Khwar
Bar Kand
< 9 ppm
9-20 ppm
>20 ppm

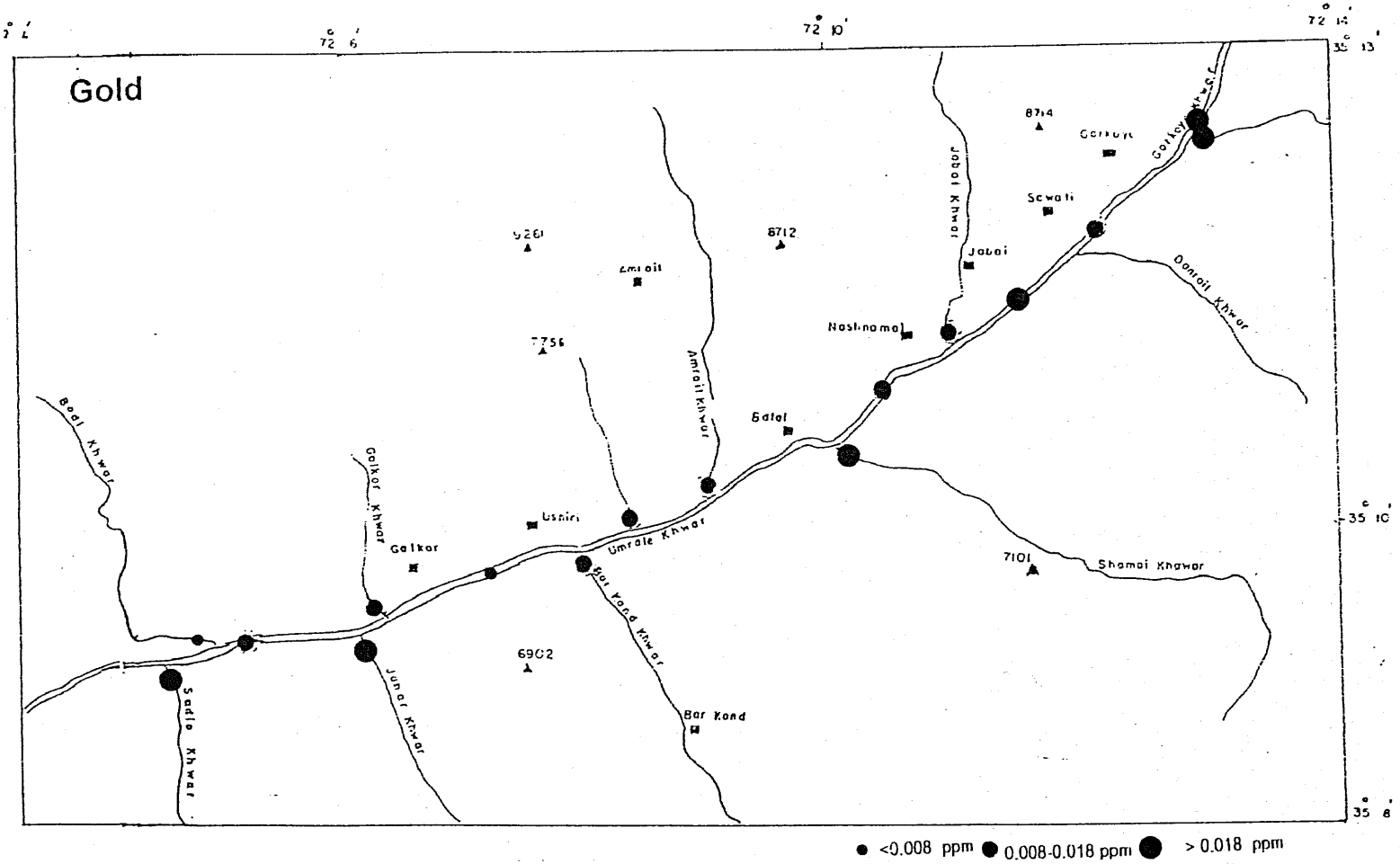

Fig.8.7. Distribution map of Au, Ag, Cu, Zn, Pb, Ni, Cr and Co for the fine fractions of the study area.

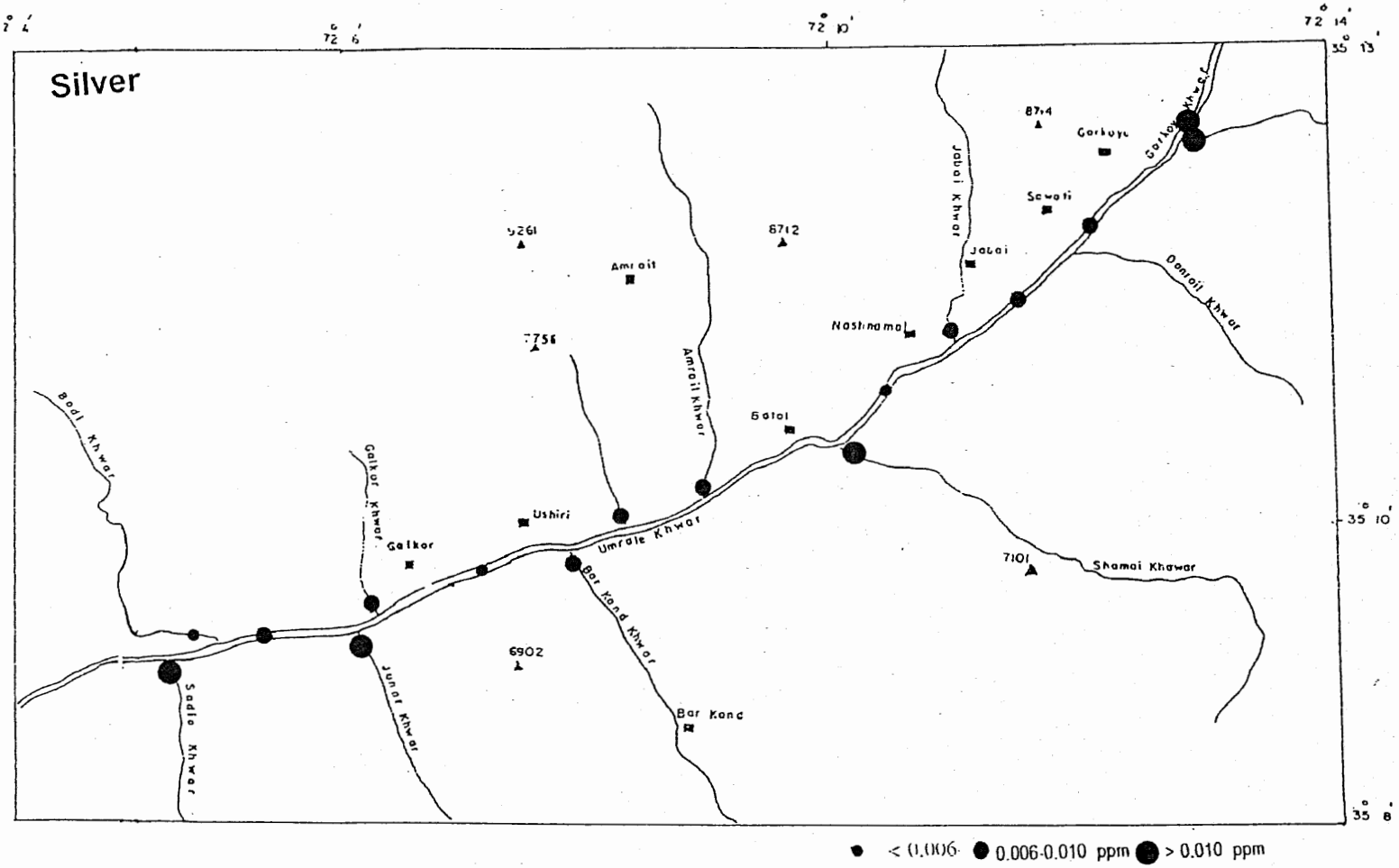
Silver
72° 4'
72° 6'
72° 10'
72° 14'
35° 13'
35° 10'
35° 8'
8714
Gorkuyo
Gorkuyo Khwar
Jabai Khwar
Sawati
8712
9261
Amraii
Jabai
Nashnamal
Deoraii Khwar
7756
Amraii Khwar
Batal
Badi Khwar
Galkor Khwar
Ushiri
Galkor
Umrale Khwar
7101
Shamai Khawar
Bar Kand Khwar
6902
Junar Khwar
Bar Kand
Sadle Khwar
< 0.006
0.006-0.010 ppm
> 0.010 ppm

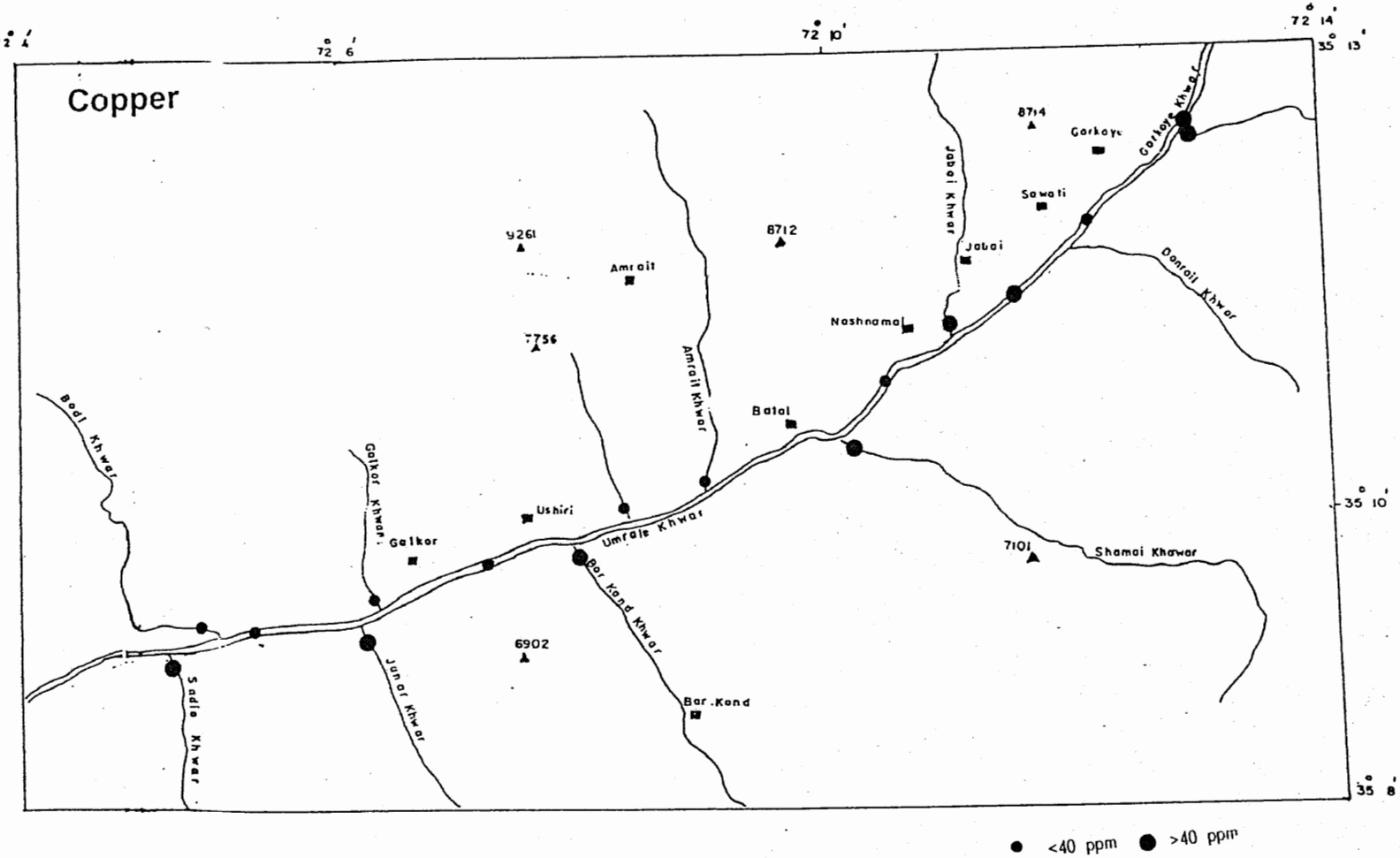
Copper
72° 4'
72° 6'
72° 10'
72° 14'
35° 13'
35° 10'
35° 8'
8714
Gorkoye
Gorkoye Khwar
Sawati
Jabai Khwar
Jabai
Danrail Khwar
8712
9261
Amrait
Nashnamal
7756
Amrait Khwar
Batal
Bodi Khwar
Galkor Khwar
Galkor
Ushiri
Umrale Khwar
7101
Shamai Khawar
Bar Kand Khwar
6902
Sadle Khwar
Jandi Khwar
Bar.Kand
<40 ppm
>40 ppm

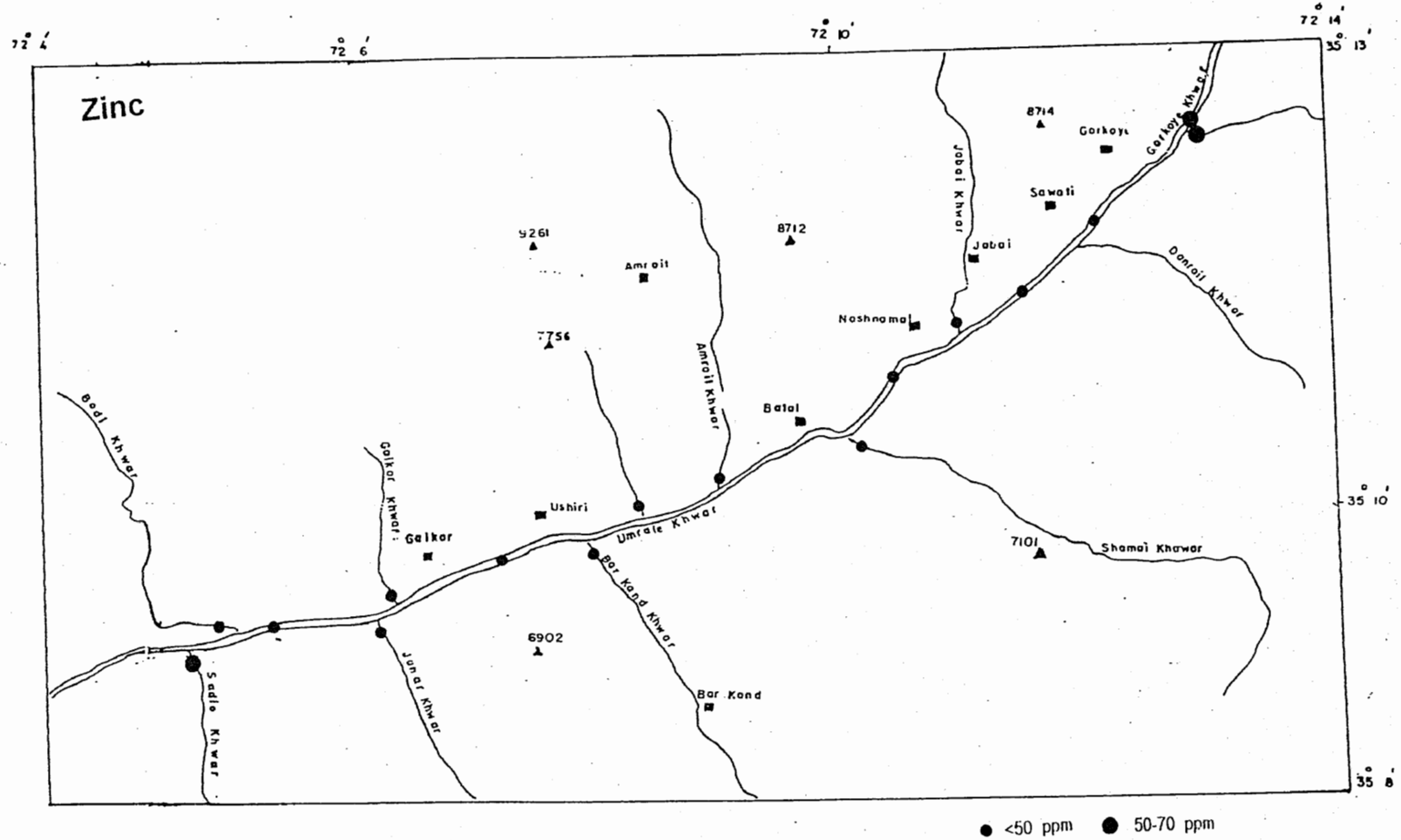
Zinc
72° 4'
72° 6'
72° 10'
72° 14'
35° 13'
35° 10'
35° 8'
8714
Gorkoyt
Gorkoyt Khwar
Sawati
Jabai Khwar
Jabai
8712
9261
Amroit
Donroit Khwar
Noshnama
7756
Amroit Khwar
Batal
Bodi Khwar
Galkor Khwar
Galkor
Ushiri
Umrale Khwar
7101
Shamai Khawar
Bar Kand Khwar
6902
Jarar Khwar
Bar Kand
Sadlo Khwar
● <50 ppm
● 50-70 ppm

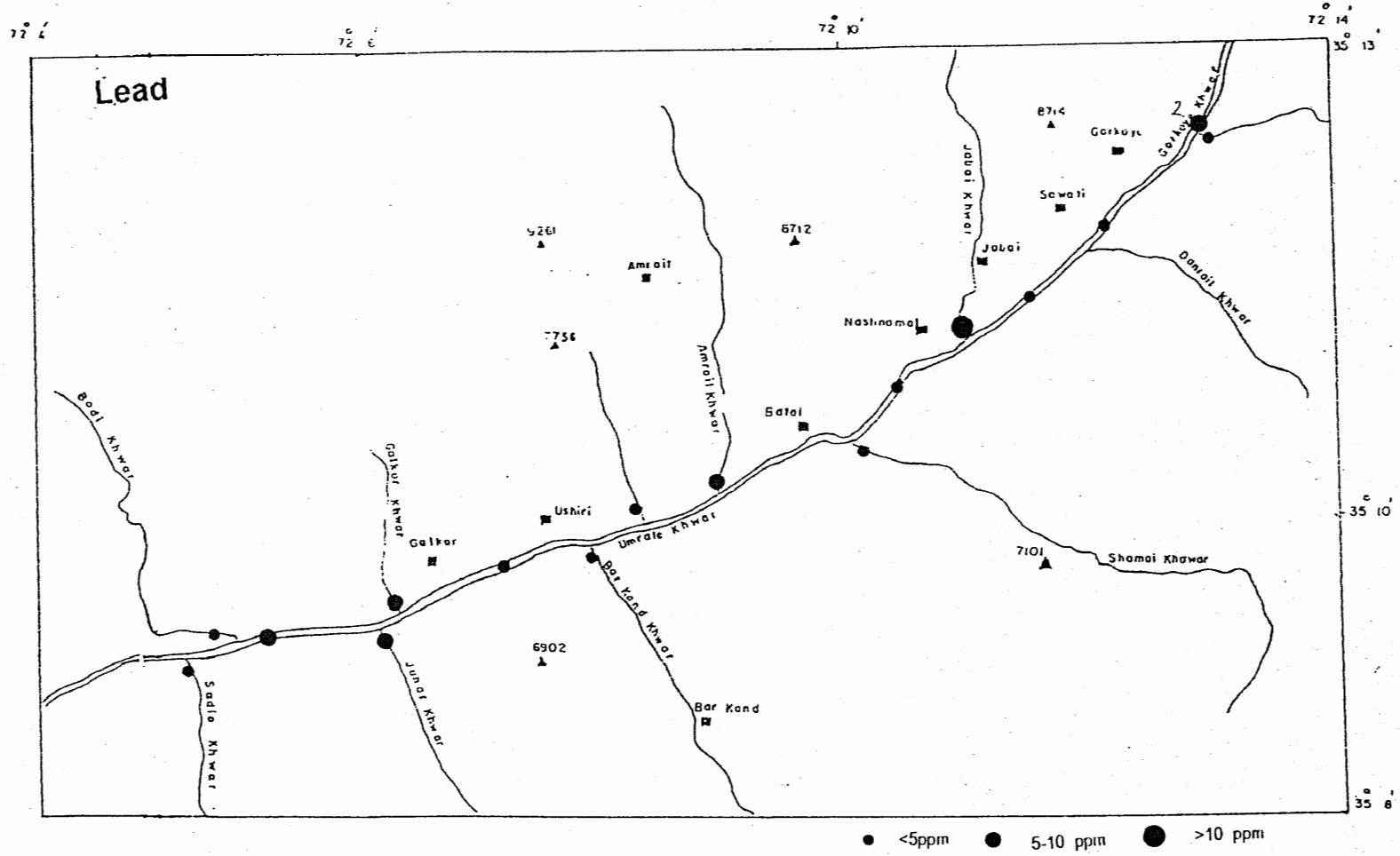
Lead
72° 14'
35° 13'
35° 10'
35° 8'
8714
Gorkoyt
Gorkoyt Khwar
Sewati
Jabai
Jabai Khwar
Danrait Khwar
6712
Amrait
Nashnamal
7756
Amrait Khwar
Batal
Badi Khwar
Ushiri
Galkot Khwar
Galkot
Umrale Khwar
7101
Shamai Khawar
Bar Kand Khwar
6902
Sadio Khwar
Junar Khwar
Bar Kand
<5ppm
5-10 ppm
>10 ppm

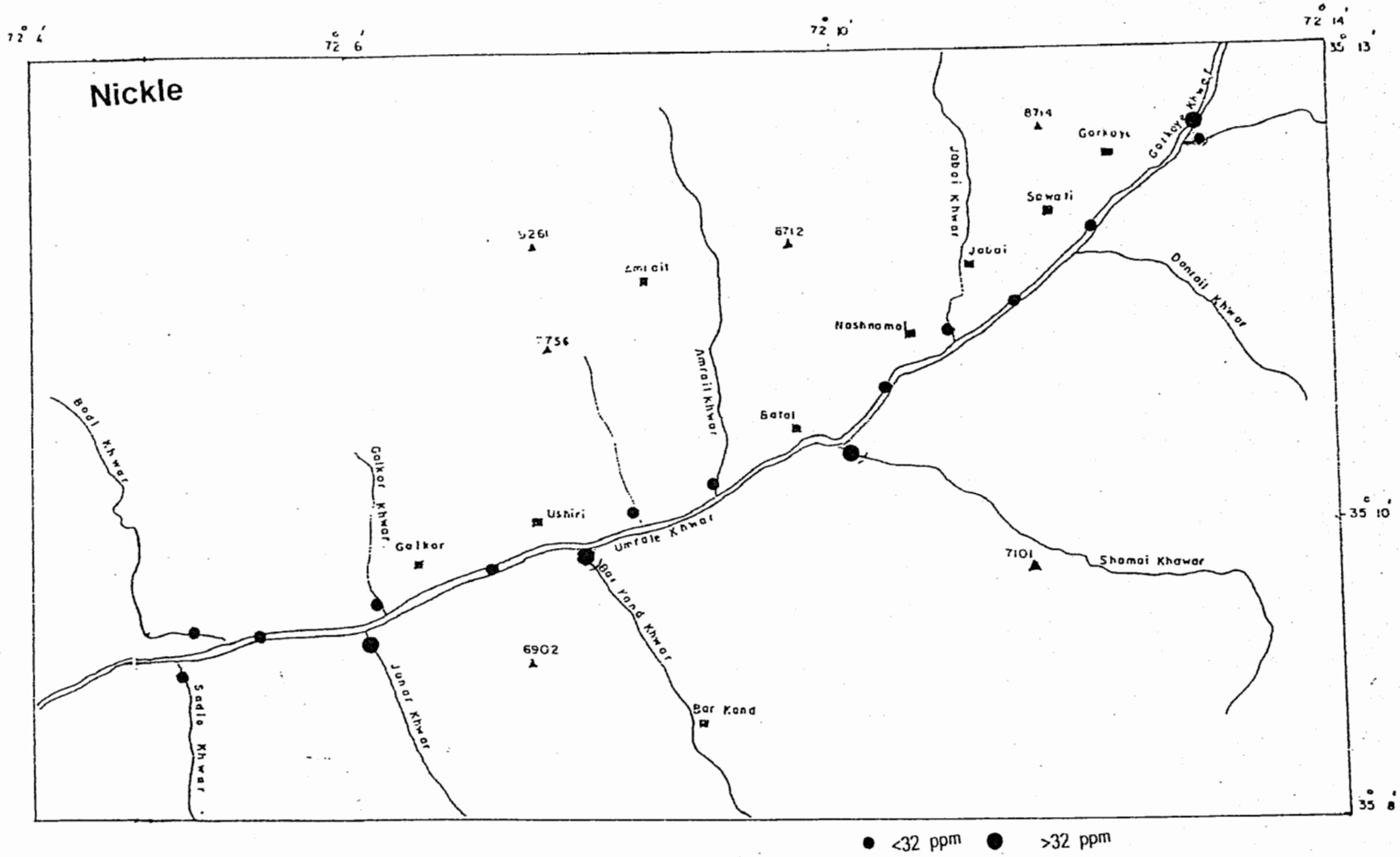
Nickle
72° 4'
72° 6'
72° 10'
72° 14'
35° 13'
35° 10'
35° 8'
8714
Gorkoyk
Gorkoyk Khwar
Jabai Khwar
Sawati
Jabai
Danrali Khwar
5261
Amrail
6712
7756
Nashnamal
Amrail Khwar
Batal
Badal Khwar
Galkor Khwar
Galkor
Ushiri
Umrale Khwar
Bar Kand Khwar
7101
Shamai Khawar
6902
Saplo Khwar
Jurar Khwar
Bar Kand
• <32 ppm
● >32 ppm

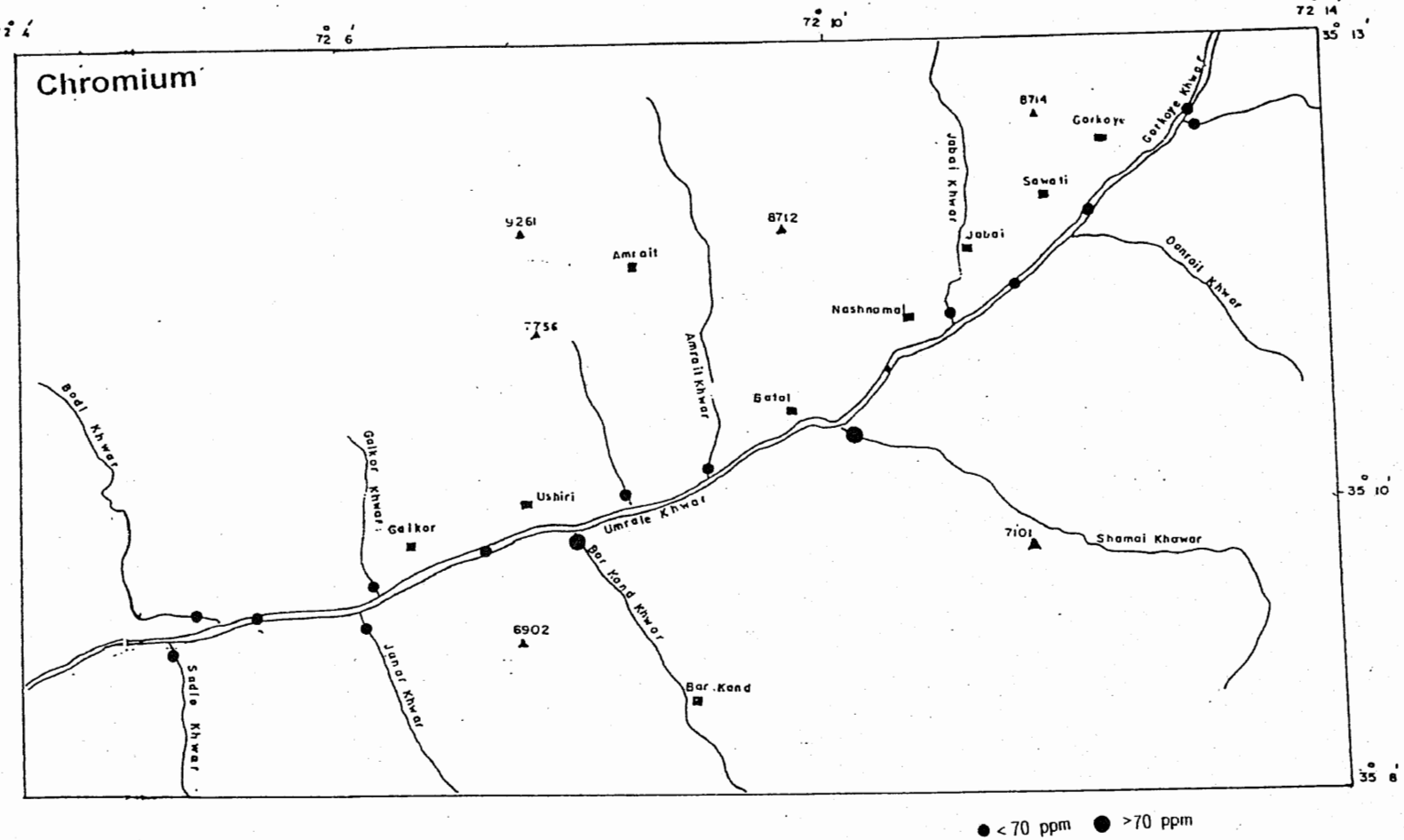
Chromium
72° 4'
72° 6'
72° 10'
72° 14'
35° 13'
35° 10'
35° 8'
8714
Gorkoye
Gorkoye Khwar
Sawati
Jabai Khwar
Jabai
9261
8712
Amrait
Oamrait Khwar
Nashnoma
7756
Amrait Khwar
Batal
Badi Khwar
Galkor Khwar
Ushiri
Galkor
Umrale Khwar
Bar Kand Khwar
7101
Shamai Khawar
6902
Janar Khwar
Sadle Khwar
Bar.Kand
● < 70 ppm
● >70 ppm

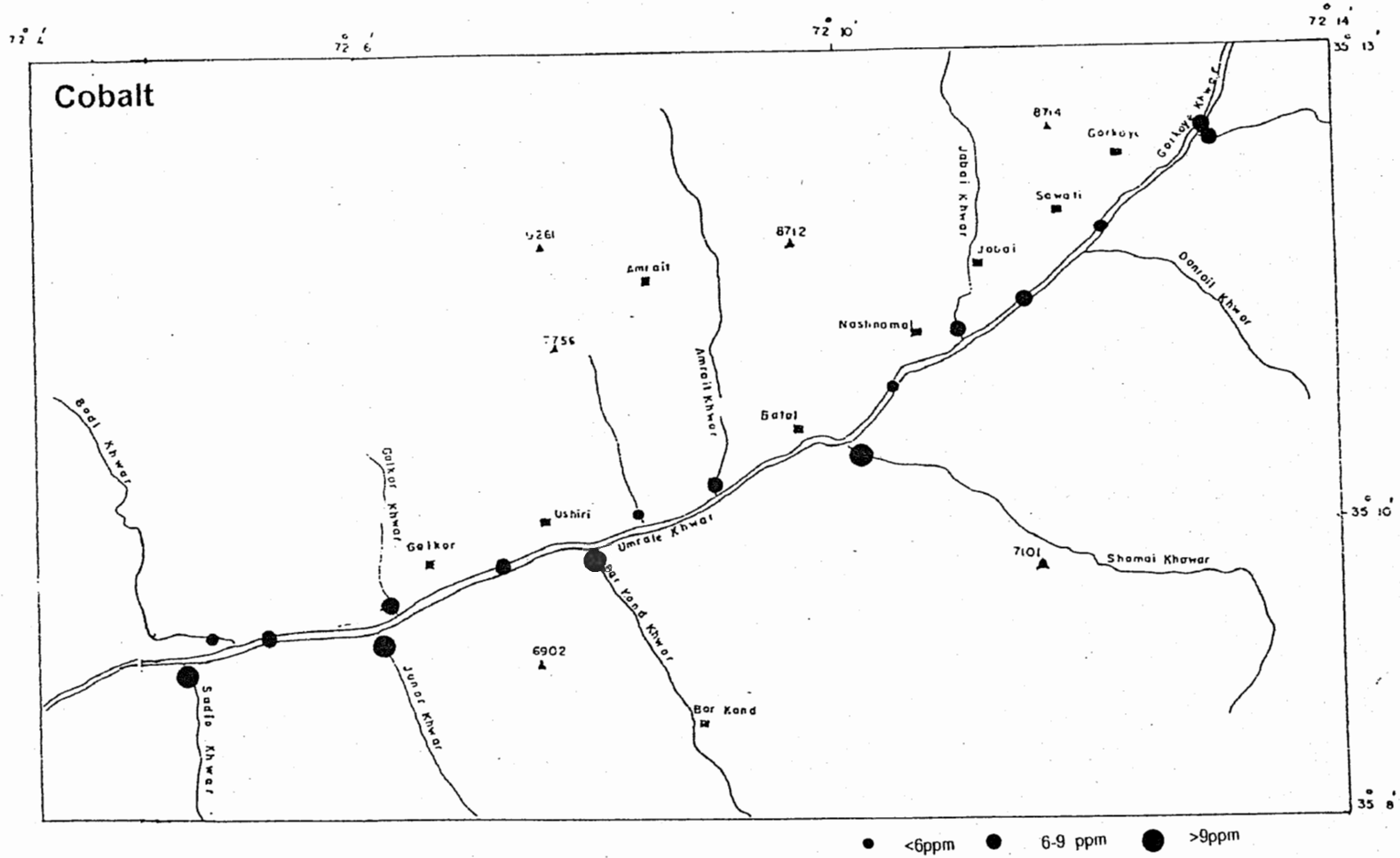
Cobalt
72° 4'
72° 6'
72° 10'
72° 14'
35° 13'
35° 10'
35° 8'
8714
Gorkoyt
Gorkoyt Khwar
Sewati
8712
Jabai Khwar
Jabai
Amrait
Nashnamal
Dantoli Khwar
7756
Amrait Khwar
Batal
Badi Khwar
Gaikor Khwar
Ushiri
Gaikor
Umrale Khwar
Bar Kand Khwar
7101
Shamai Khwar
6902
Jupar Khwar
Sadle Khwar
Bar Kand
<6ppm
6-9 ppm
>9ppm

SUMMARY AND CONCLUSIONS

There could be two possibilities regarding the correlation of the studied amphibolites and hosted gabbro-norites with the main lithological units of the Kohistan island arc:

a) The studied amphibolites and gabbro-norites could be co-related with or considered as a part of the Kamila amphibolite belt of Coward et al., 1982; 1986; and Jan, 1988; Treloar et al., (1996); have distinguished the Kamila amphibolite in to a) Low Ti, High LILE/HFSE and LREE/HREE related to subduction and b) High Ti, Low LILE/HFSE and LREE/HREE not related to subduction. The studied amphibolites and gabbro-norite could be related to the former type.

b) These could also be considered as a part of the Chilas complex of Jan et al. (1984) and Khan et al., (1989). Chilas complex is a massive calc-alkaline gabbro-norite body with layering in places (Khan et al., 1989; 1993). The gabbro-norites are variably deformed and the deformation intensity in the amphibolitized gabbro-norite increases towards south (Treloar et al., 1996). This evidence favour the transformation of studied gabbro-norites to amphibolites as the intensity of deformation and the grade of regional metamorphism increased along shear zones.

In the south-west of the study area, similar rocks (but less amphibolitized) have also been reported by Jan et al. (1983); Jan and Tahirkheli (1990) and Shah et. al. (in press) in Tora Tigga, Samarbagh and Timargara areas. These rocks have been considered as related to Chilas complex.

It is evident from the tectonic discrimination diagrams that both the amphibolites and gabbro-norties have greater affinity with calc-alkaline rocks originated in subduction related environment. Both major and trace element variations of the studied rocks are characteristics of the arc related magmas (see e.g., Green, 1980), such as lack of enrichment of $Fe_2O_3(t)$ and TiO_2, high Al_2O_3 and low TiO_2. This is also illustrated by the calc-alkaline trend in the AFM diagram. However, the formation of these rocks in the continental margins environment can not be ruled out as the calc-alkaline rock can also be formed in continental margin environment.

Whether a part of the Kamila amphibolite belt or Chilas complex, the studied amphibolites and gabbro-norites favour their origination in the subduction related environment within the Kohistan Island arc setting. The falling of data in the field of calc-alkaline rocks related to continental margin is not true. However, to solve this problem and to identify the confirmed relation of studied amphibolites and gabbro-norites either with the rocks of Kamila amphibolite belt or Chilas complex, further detail trace element and REE studies are needed to be done on the studied rocks. These types of gabbro-norites within the northern part of Kamila amphibolites belt of Kohistan island arc are considered as of Chilas complex gabbro-norites elsewhere by Treloar et. al, 1996.

The granitoid rocks (diorite and granodiorite) of the studied area can be correlated with the stage II pluton of Kohistan batholith of Peterson and Windley (1985). These rocks could not be distiguished in the field, however, these are easily distinguished on the basis of petrographic and geochemical studies. The geochemical characteristics of these rocks suggest that these are comagmatic and calc-alkaline in nature. These are originated in the subduction related invironment in the island arc type setting.

The stream sediments survey suggest that the Stream floats are mainly amphibolites, granodiorites, diorites and quartz diorites with subordinate amount of gabbro-norites, quartzites and metasediments. The pan-concentrates have magnetite as the dominant phase while rock fragments, hornblende, zircon, quartz, feldspar, garnet and pyrite occur as minor constituents. No gold in the form of piece, speck and clour has been identified in the pan-concentrates.

The geochemical data of the stream sediments (both pan-concentrates and fine fractions) have been interpreted statistically. It is concluded that all the metals analyzed are not anomalous to the extent which could be related to the significant anomaly associated with the specific mineralization in the area. However, the anomalies of various metals, as depicted by statistical means, could be contributed by the rocks of the area.

REFERENCES

Ahmad, W., 1962. Copper showings in the Ushiri region, Dir, Pakistan. Geol. Surv. Pak. Min. Inf. Circ. No,.8, 14.

Ahmad, Z; & Chaudhry, M. N; 1976. Geology of Babusar area, Diamir district, Gilgit, Pakistan. Geol. Bull. Univ. Punjab 12, 67-78.

Andrews-Speed, C.P. & Brookfield, M.E; 1982. Middle paleozoic to cenozoic geology and tectonic evolution of northwestern Himalaya, Tectonophysics 8, 253-275.

Arbab, M.S.H. & Khan, R.N., 1973. Geology of Dir and Northern part of Timergara Quodranle, N.W.F.P. Pakistan . Geol. Surv. Pak. Inf. Rel. No.49.

Arif, M. & Jan, M. Q; 1993. Chemistry of chromite and associated phases from the shangla ultramafic body in the Indus suture zone of Pakistan. In: Himalayan Tectonics (M.P. Searle & P.J. Treloar, eds.). Geol. Soc. London, Spec. Publ; 74, 101-112.

Barker, E. & Arth, J.J.G., 1976. Generation of trondhjemitic-tonalitic liquids and Archean bimodal trondhjemite-basalt suites. Geology, 4, 596-600.

Butt, K.A., Chaudhry, M.N. & Ashraf, M., 1980. An Interpretation of petrotectonic Assemblage west of western Himalayan syntaxis in Dir District and adjoining Areas in northern Pakistan. Geol. Bull. Univ. Peshawar. 13, 79-86.

Chaudhry, M.N. and Chaudhry, A.G. 1974. Geology of Khagram area, Dir district. Geol. Bull. Punjab Univ. 11, 21-44.

Coward, M.P., Jan, M.Q., Rex, D.C., Terney, J., Tahirwall, M. & Windley, B.F., 1982. Geotectonic framework of the Himalaya of N.W. Pakistan: J. Geol. Soc. London, 139, 299-308.

Coward, M.P., 1986. A section thorugh the Nanga parbat syntexis, Indus valley Kohistan Geol. Bull ,Univ. Peshawar, 18, 147-152.

Cox, K.G., Bell, J.D. & Pankhurst, R.J., 1979. The interpretation of igneous rocks. george Allen and Unwin, London.

Evans, B.K; & Leake, B.E; 1960. The composition and origin of the stripped amphibolites of Cannemara, Irsland. Jour. Petrol, 1, 337-363.

Floyed, P.A. & Winchester, J.A., 1975. Magma-type and tectonic setting discrimation using immobile elements. Earth. Planet. Sci. Lett. 27, 211-218.

Green, T.H., & Pearson, N.J., 1980. Rare-earth element partitioning between sphene and co-existing silicate liquid at high pressure and temperature. Chem. Geol., 55, 105-199.

Hamidullah, S. & Islam, F. & Farooq, M., 1990. Petrology and goechemistry of the

western part of the Dir Ignious complex, Kohsitan island arc. Northern Pakistan. In: Geology and Geodynamic evolulion of the Himalayan collision zone (Sharama, K.K. ed.). Phys. Chem. Earth, 17, 31-46.

Hamidullah, S. & Shah, M.T.; 1993. Textural and mineralogical significance of hornblende from andeiste at Dir, Kohistan arc, N.Pakistan. Geol. Bull. Univ. Peshawar. 26, 45-58.

Hamidullah, S., Shah, M.T., 1993. Textural and minerchemical significance of hornblendes from an andesite at Dir Kohsitan arc, N. Pakistan. Geol. Bull. Univ. Peshawar, 26, 45-58.

Harker, A., 1909. The natural history of igneous rocks, Methuen, London.

Heier, K.S; 1962. The possible origins of amphibolites in an area of high metamorphic grade. Norsk-geol. Tidsskr, 42. 157-65.

Honegger, K., Dietrich. V., Frank, W., Gansser, A., Thani, M. & Trommsdorff. V., 1982 Magmatism and metamorphism in the Ladakh Himalaya (the Indus Tsangpo sutur zone). Earth Planet. Sci. Letters 60, 253-292.

Hyden, H.H., 1915. Notes on the geology of Chitral Gilgit and Pamirs. Geol. Surv. India, 45, 271-335.

Irvine, T.N. & Baragar, W.R.A., 1971. A guide to the chemical classification of the common volcanic rocks. Can. J. Earth. Sci. 8, 523-548.

Ivanac, J.F., Traves, D.M., & King, D., 1956. The Geology of the NW portion of the Gilgit Agency. Rec. Geol. Surv. Pakistan, 3,1-27.

Jan, M. Q; 1988. Geochemistry of amphibolites from the southern part of Kohistan arc, N. Pakistan, Min. Meg., 52, 147-159.

Jan, M.Q. & Tahirkheli, A.Z., 1990. The Tora Tigga complex, southern Dir, NW. Pakistan; an example of mafic ultramafic rocks in the bottom of an island arc. Geol. Bull. Univ. Peshawar, 23, 231-251.

Jan, M.Q., & Howie, R.A., 1981. The mineralogy and geochemistry of the metamorphosed basic and ultrabasic rocks of the Jijal Complex, Kohistan, NW Pakistan. J. Petrolgoy 22, 85-126.

Jan, M.Q., & Windly, B. F., 1990. Chromium spinel-silicate chemistry in ultramafic rocks of the Jijal complex, Northeast Pakistan, J. Petrolgoy, 31, 667-715.

Jan, M.Q., 1979. Petrography of pyroxene granulites from northern Swat and Kohistan. Geol. Bull. Univ. Peshawar, 11, 65-87.

Jan, M.Q., 1988. Geochemistry of amphibolites from the southern part of the Kohistan arc, N Pakistan. Mineral. Mag. 52, 147-159.

Jan, M.Q., Banaras, M., Ghani, A., & Khan, M. A., 1983. The Tora Tigga ultramafic complex, southern Dir District. Geol. Bull. Univ. Peshawar, 16, 11-29.

Jan, M.Q., Kempe, D.R.C. & Tahirkheli, R.A.K., 1969. The Geology of corundum bearing and related rock around Timergara. Geol. Bull. Univ. Peshawar, 4, 82-89.

Jan, M.Q., Khattak, M.U.K., Parvez, M.K., Windley, B.F., 1989. The Chilas stratiform complex: fied and mineralogical aspects. Geol. Bull. Univ. Peshawar, 17, 163-69.

Jan, M.Q; Khattak, M.U.K., Parvez, M.K., and Windley, B.F; 1984. The Chilas stratiform complex: Field and Mineralogical aspects. Geol. Bull. Univ. Peshawar 17, 153-169.

Kakar, S.K., Badshah, M.S., & Khan, J. 1971. The geology of the Jandul valley, western Dir. Geol. Bull. Univ. Peshawar, 6, 54-73.

Kazmi, A.H., Lawrence, R.D; Dewood, H; Snee, L.W. & Hussain, S.S; 1984. Geology of the Indus suture zone in the Mingora-Shangla area of Swat, N.Pakistan. Geol. Bull. Univ. Peshawar 17, 127-144.

Khan, M.A. & Jan, M.Q., & weaver, B.L., 1993. Evolution of the Lower arc crust in Kohistan N. Pakistan: Temporal arc magmatism though early, mature and intra arc rift stages. In: Treloar, P.J., spec. Publ. Geol. Soc. London, 74.

Khan, M.A., Jan, M.Q., Windley, B.F., Tarney, J. & Thrilwall, M.F., 1989. The Chilas ultramafic mafic ignous complex of the Kohstan island arc in the Hamalaya north Pakistan. Geol. Soc. Am. Sp. paper 232, 75-94.

Khan, R.N. & Saleemi, B.A. 1972. Geology of Kotegram and Akhagram Quard range, District Dir and Swat, NWFP Pakistan. Geol. Surv. Pak. Inf. Rel. No.80.

Kloot Wijk, C.T., & Gee, J.S., Pearce, J.W., Smith, G.M., & Mc Fadden, Ph.L, 1992. An early India-Asia contact: Paleo magnetic constraints from Ninetyeast Ridge, OPD leg. 121. Geology 20, 395-398.

Kuno, H., 1968. Differentiation of basalts magmas. In: Hess, H.H. & Poldervaart, A. (eds.), Basalts: The Poldervaart trcatise on rocks of basaltic composition, Vol.2. Interscience, New York, 623-688.

Leak, B.E., 1963. Origin of amphibolites from northwest Adirondacks, New York. Bull. Geol. Soc. Amer. 74, 1193-1202-

Leake, B.E; 1964. The chemical distinction between ortho-and para-amphibolites. Jour. Petrology 15, 238-254.

LeFort, P., Debon, F., & Sonet, J., 1980. The "Lesser Himalaya" cordirite grainite belt; Typology and age of the pluton of Mansehrah, Pakistan; proceedings international Geodynamics confrence. Geol. Bull. Univ., Peshawar, Spec. Issue, 13, 51-61.

Lepeltier, C; 1969. A simplified statistieal treatment of geochemical data by graphical representation. Econ. Geol. 64, 538-550.

Miller, D.J; Louks, R.R. & Ashraf, M; 1991. Platinum group elements mineralization in the Jijal layered mafic-ultramafic complex, Pakistan Himalayas. Econ. Geol; 86,

1093-1102.

Miyashiro, A., 1975. Classification, characteristics, and origin of ophiolites. J. Geol. 83, 249-281.

Miyashiro, a., 1977. Subduction zone ophiolites and island arc ophiolites In: Saxena, S.K. & Bhattachargi, S. (eds.), Energetics of Geological procerses. Spriner-Verlag (N.Y.).

Muenow, D.W., Garcia, M.O., Aggrey, K. E., Bendnarz, U. & Schmincke, H.U., 1990. Volatiles in submarine glasses as a discriminant of tectonic origin: application to the Troodos ophiolite. Nature, 343, 159-161.

Mullen, E.D., 1983. Mno/TiO2/P2O5: a minor element discrimination for basaltic rocks of oceanic environments and its implications for petrogenesis. Earth. Planet. Sci. Lett. 62, 53-62.

Niggli, P; 1954. Rocks and Mineral deposits. Freeman, San Francisco, Calif; 559.

Orville, P.M; 1969. A model for metamorphic differentiation origin of thin layered amphibolites. Amer. J. Sci. 267, 62-86.

Otsu, H., Kubotta, R. & Matsuda, Y., 1984. Partition of statistical frequency distribution of geochemical data. Min. Geol. 34, 51-56 (Japanese with English abstract).

Pearce, J.A. & Cann, J.R., 1971. Ophiolitio origin investigated by discriminaert analysis using Ti, Zr and Y. Earth. Planet. Sci. Lett. 12, 339-349.

Pearce, J.A. & Cann, J.R., 1973. Tectonic setting of basic volcanic rocks determined using trace elements analyses. Earth. Planet. Sci. Lett. 19. 290-300.

Pearce, J.A. & Gale, G.H., 1977. Identification of Ore-deposits environment from trace element geochemistry of associated igneous host rocks. Geol. Soc. Spec. Publ. 7, 14-24.

Pearce, J.A. & Norr, M.J., 1979. Petrogentic implications of Ti, Zr, Y and Nb variations in volcanic rocks. Contrib. Mineral. Petrol. 69. 33-47.

Pearce, J.A. & Norry, M.J., 1979. Petrogenetic implication of Ti, Zr, Y and N b variations in volcanic rocks. Contrib. Mineral. Petrol., 69, 33-47.

Pearce, J.A., 1982. Trace element dearacteristics of lavas from destructive plate bounderies. In: Thorpe, R.S. (ed.), Andesites. Wiley, chichester, 525-548.

Pearce, J.A; 1975. Basalt geochemistry used to investigate past tectonic environments on Cyprus. Tectonophysics 25, 41-67.

Pearce, T.H., Gorman, B.E. & Birkett, T.C., 1975. The TiO_2-K_2O-P_2O_5 diagram: a method of discriminating between occanic and non-oceanic basalt. Earth. Pllanet. Sci. Lett. 24, 419-426.

Pearce, T.H., Gorman, B.E., & Birkett. T.C., 1977. The relationship between major element chemistry and tectonic environment of basic and intermediate volcanic rocks. Earth planet. Sci. Lett. 36, 121-132.

Petterson, M.G. & Windley, B.F. 1985. Rb-Sr dating of the Kohistan arc batholith in the Transhimalayan of of the North Pakistan and tectonic imlications. Earth Planet. Sci. Lett., 74, 45-57.

Petterson, M.g. & Windley, B.F. & Luff, I.W., 1990. The Chalt valcanics, Kohistan, N. Pakistan High-Mg tholeites and low Mg calc-Alkaline volcanism in a cretaceous island arc. In: Geology and Geodynamic evolulion of the Himalayan collision zone (Sharama, K.K. ed.). Phys. Chem. Earth, 17, 19-30.

Powers, H.A., 1955. Compostion and origin of basaltic magma of the Hawaiian islands. Geochim. Cosmochim. Acta, 7, 77-107.

Pudsey, C.J., 1986. The northern suture, Pakistan: margin of a cretaceous island arc. Geol. Mag; 123, 405-423.

Pudsey, C.J., Coward, M.P., Luff, I.W., Shackleton, R.M., Windley, B.F. & Jan, M.Q., 1985. Collision zone between the Kohistan are and the Asian plate in NW Pakistan. Trans. R. Soc. Edinb: Earth Sci. 76, 643-479.

Shah, M.T., 1991.Geochemistry, mineralogy and petrology of the sulfide mineralization and associated rocks in the area around Besham and Dir, Northern Pakistan unpublished. Ph.D. Thesis Univ. S. Carolina, Columbia.

Shah, M.T. & Jan, M.Q., 1996. Review of geochemical characteristics as petrogenetic and palaeotectonic indicators of igneous rocks. Proceed. Pak. Acad. Scie, 33, 73-78.

Shah, M.T., and Majid, M; 1985. Major and trace element variations in the lavos of Shergarh Ser area and their significance with respect to the Kohistan tectonic anomaly. Geol. Bull. Univ. Peshawar, 18, 163-188.

Shah, M.T., Serwar, A. & Khattak, M.U.K., 1996. Geology and geochemistry of the rocks of Timargara and Samarbagh areas, Jandul valley, southern Dir, northern Pakistan, Geol. Bull. Punjab. Univ. 28 (in press).

Shah, M.T., Shervais, J.W. & Ikramuddin, M., 1994. The Dir meta-volcanic sequence: Calcalkaline magmatism in the Kohstan arc terrance, northern Pakistan. Geol. Bull. Univ. Peshawar, 27, 9-27.

Shams, F.A; 1980. An anatectic liquid of granitic composition from Hazara Himalaya. Pakistan and its petrogenetic importance. R.C. Accad. Naz. Lince; vol.68, 207-215.

Shand, S.J; 1922. The problem of the alkaline rocks. Proc. Geol. Soc. S. Afr. xxxv, xix-xxxiii.

Shervais, J.W., 1982. Ti-V plots and the petrogenesis of modern and ophiolitic lavas. Earth planet. Sci. Lett. 59, 101-118.

Simpson, E.S.W; 1954. On the graphical presentation of differentiation trends in igneous rocks. Geol. Mag. 91, 238- 244.

Sinclair, A.J., 1974. Selection of threshold in geochemical data using probability graphs. J. Geochem. Explor. 3, 129-149.

Sinclair, A.J., 1976. "Probability graphs" Assoc. Exploration Geochemists, Spec. Vol. No.4, 95pp.

Sullivan, M.A., Windley, B.F., Saumders, A.D., Haynes, J.r. & Rex. D.C., 1993. A palaeogeographic reconstruction of the Dir group: evidence for magmatic arc migration within Kohistan, N. Pakistan. In: Himalayan tectonics. CP. J. Treloar & M.P. Searl, eds). Spec. Publ. No.74 Geol. Soc. London, 139-160.

Tahirkheli, R.A., 1979. Geology of Kohistan and adjoining eurasian and Indo-Pakistan continents, Pakistan. Geol. Bull. Univ. Peshawar. 11, 1-30.

Tahirkheli, R.A.K., 1982. Geology of Himalaya, Karakoram and Hindukush in Pakistan. Geol. Bull. Univ. Peshawar, 15, 54 pp.

Tahirkheli, R.A.K., 1983. Geological evolution of Kohistan island arc on the southern flank of the Karakoram-Hindukush in Pakistan. Bollettino Geofisica Teorica Applicata 25, 351-364.

Tahirkheli, R.A.K., Mattaure, M; Proust, F., & Tapponnier, P; 1979. The India-Eurasia suture in northern Pakistan: Synthesis and interpretation of data on plate scale. In: Geodynamics of Pakistan (A.Farah, A. & K.A. DeJong, eds.) Geol. Surv. Pakistan, 125-130.

Tennant, C.B. & White, M.L., 1959. Study of the distribution of some geochemical data. Econ. Geol. 54, 1281-1290.

Thornton, C.P. & Tuttle, O.F., 1960. Chemistry of igneous rocks, I. Differentiation index. Amer. J. Sci. 258, 664-684.

Treloar, P.J., Petterson, M.G., Jan, M.Q. & Sullivan, M.A., 1996. Arc-evaluation of the stratigraphy and evolution of the Kohistan arc sequence, Pakistan Himalaya: implications for magmatic and tectonic are building processes. J. Geol. Soc. London. 153, 681-693.

Treloar, P.J., Rex, D.C., Guise, P.G., Coward, M.P., Searle, M.P., Windley, B.F., Petterson, M.g., Jan, M.Q. & Luff, I.W., 1989. K-Ar and Ar-Ar geochronolgoy of the Himalayan collision on NW Pakistan: Constraints on the timing of suturing, deformation, metamorphism and uplift. Tectonics, 8, 881-909.

Wager, L.R. & Deer, W.a., 1939. Geological investigation in East Greenland. Medd. Gronland, 105, 1-352.

Walker, K.R; Joplin, G.A; Lovering, J.F; & Green, R; 1960. Metamorphic and metasomatic convergence of basic igneous rocks and lime-magnesia sediments of the pre-cambrian of north western Queenslend. Jour. Geol. Soc. Australia 6, 149-77.

Weedon, D.S., 1970. The ultrabasic-basic igneous rocks of huntley region, Scott. J. Geol.

16, 26-40.

Wileox, R.E. & Poldervaart, A; 1958. Metadolerite dike swarm in Bakersville-Room mountana area, North Carolina. Bull. Geol. Soc. Amer. 69, 1323-68.

Wood, D.A., 1979. A variable veined sub oceanic upper mentle-genetic significance for mid-ocean ridge basalts from geochemical evidence. Geology, 7, 499-503.

Yoder, H.S., 1969. Calc-alkaline andesites: experimental data bearing on the origin of their assumed characteristics. In: McBirney. A.R.(ed.), proceedings of the Andesite Conference Oregon Dept. Geol. Mineral Industry Bull. 65, 77-89.

Zeitler, P., 1985. Cooling history of the NW Himalaya Pakistan. Tectonics 4, 127-151.

APPENDIX

FIELD AND MICROSCOPIC STUDIES OF STREAM SEDIMENTS

Sample No. 1

Float Geology: Diorite/ granodiorite (90%), Epidote bearing felsic diorite (5%), amphibolite (3%) and quartz vein (2%).

Pan-concentrate mineralogy: It is dominantly composed of magnetite (>65%) with minor amount of quartz, garnet, zircon, pyroxene, and amphibole. No gold is visible.

Sample No. 2

Float geology: Diorite/ granodiorite (95%), Epidote bearing diorite (3%), and amphibolite (2%).

Pan-concentrate mineralogy: It is dominantly composed of magnetite (>70%) and minor amount of garnet, quartz, amphibole, pyroxene, and zircon. No gold is visible.

Sample No. 3

Float geology: Diorite/ granodiorite (90%), Epidote bearing felsic diorite/ granodiorite (3%), amphibolite (5%) and quartz vein (2%).

Pan-concentrate mineralogy: It is dominantly composed of magnetite (>60%) and minor amount of quartz, hornblende, pyroxene and apatite. No gold is visible.

Sample No. 4

Float geology: Diorite (90%), Epidote bearing felsic diorite (2%), amphibolite (5%) and quartz vein (1%) and pyroxene bearing diorite (2%)

Pan-concentrate mineralogy: It is dominantly composed of magnetite (>75%) and minor amount of quartz, feldspar, pyroxene, hornblende and epidote. No gold is visible.

Sample No. 5

Float geology: Diorite (50%), amphibolite (48%) and quartzite (2%)

Pan-concentrate mineralogy: It is dominantly composed of magnetite (>60%) and minor amount of quartz, feldspar, epidote, zircon, hornblende, and tourmaline. No gold is visible.

Sample No. 6

Float geology: Amphibolite (80%), diorite (15%) and quartz vein (5%).

Pan-concentrate mineralogy: It is dominantly composed of magnetite (>60%) and minor amount of garnet, amphibole, pyroxene, zircon and pyrite. No gold is visible.

Sample No. 7

Float geology: : Diorite (60%), Amphibolite (35%), and quartz vein (5%).

Pan-concentrate mineralogy: It is dominantly composed of magnetite (>65%) and minor amount of quartz, pyroxene, hornblende, zircon and epidote. No gold is visible.

Sample No. 8

Float geology: Amphibolite (90%) and quartz vein (10%)

Pan-concentrate mineralogy: It is dominantly composed of magnetite (>60%) and minor amount of quartz, amphibole, garnet, pyroxene, feldspar, and zircon. No gold is visible.

Sample No.9

Float geology: Amphiblite (60%), diorite (20%), quartzite (15%) and quartz vein (5%).

Pan-concentrate mineralogy: It is dominantly composed of magnetite (>65%) and minor amount of amphibole, pyroxene, quartz, zircon, and pyrite. No gold is visible.

Sample No. 10

Float geology: Amphibolite (95%) and quartz vein (5%)

Pan-concentrate mineralogy: It is dominantly composed of magnetite (>75%) and minor amount of feldspar, epidote, zircon, quartz, hornblende, and tourmaline. No gold is visible.

Sample No.11

Float geology: Amphibolite (75%), diorite/granodiorite (20%), matagabbro-norite, (2%), and quartz vein (3%)

Pan-concentrate mineralogy: It is dominantly composed of magnetite (>80%) and minor amount of quartz, feldspar, and hornblende, No gold is visible.

Sample No. 12

Float geology: Amphibolite (60%), diorite (35%) and quartz vein (5%).

Pan-concentrate mineralogy: It is dominantly composed of magnetite (>75%) and minor amount of pyroxene, hornblende, zircon and epidote. No gold is visible.

Sample No. 13

Float Geology: Amphibolite (77%), diorite (15%), quartzite (3%)and quartz vein (5%).

Pan-concentrate mineralogy: It is dominantly composed of magnetite (>70%) with minor amount of garnet, zircon, pyroxene, and amphibole. No gold is visible.

Sample No.14

Float geology: Amphibolite (70%), diorite/granodiorite (25%), matagabbro-norite, (2%), and quartz vein (3%)

Pan-concentrate mineralogy: It is dominantly composed of magnetite (>75%) and minor amount of feldspar, quartz, pyroxene, and hornblende, No gold is visible.

Sample No.15

Float geology: Amphibolite (65%), diorite (30%) and quartz vein (5%).

Pan-concentrate mineralogy: It is dominantly composed of magnetite (>60%) and minor amount of quartz, pyroxene, feldspar, and hornblende, No gold is visible.

Sample No.16

Float geology: Amphibolite (75%), diorite/granodiorite (20%), matagabbro-norite, (2%), and quartz vein (3%)

Pan-concentrate mineralogy: It is dominantly composed of magnetite (>65%) and minor amount of quartz, pyroxene, feldspar, and hornblende, No gold is visible.